



VCU

Virginia Commonwealth University
VCU Scholars Compass

Theses and Dissertations

Graduate School

2012

In vitro methods to predict aerosol drug deposition in normal adults

Renishkumar Delvadia
Virginia Commonwealth University

Follow this and additional works at: <https://scholarscompass.vcu.edu/etd>



Part of the [Pharmacy and Pharmaceutical Sciences Commons](#)

© The Author

Downloaded from

<https://scholarscompass.vcu.edu/etd/314>

This Dissertation is brought to you for free and open access by the Graduate School at VCU Scholars Compass. It has been accepted for inclusion in Theses and Dissertations by an authorized administrator of VCU Scholars Compass. For more information, please contact libcompass@vcu.edu.

© Renishkumar Delvadia 2012
All Rights Reserved

**IN VITRO METHODS TO PREDICT AEROSOL DRUG DEPOSITION IN NORMAL
ADULTS**

A dissertation submitted in partial fulfillment of the requirements for the degree of Doctor of Philosophy at Virginia Commonwealth University.

by

RENISHKUMAR R. DELVADIA, B.PHARM., M.PHARM.
Gujarat University, India
2005

Director: PETER R. BYRON, Ph.D.
Professor & Chair,
Department of Pharmaceutics, School of Pharmacy

Virginia Commonwealth University
Richmond, Virginia
April 2012

DEDICATIONS

*To My Parents
And
My Teachers*

ACKNOWLEDGEMENT

Foremost, I would like to express my heartfelt gratitude to Dr. Peter Byron, who is not only my mentor but also my role model. This thesis would not have been possible without his help, support and patience. With his enthusiasm, inspiration, and great efforts to explain things clearly and simply, he helped to make my PhD research fun for me. Throughout my PhD, he provided sound advice, good teaching and lots of good ideas that helped me to become a good researcher, a better writer and a confident speaker.

I owe my sincere gratitude to my Graduate Committee members for their constant help and support. Special thanks to Dr. Worth Longest, who gave me an opportunity to work with him in the School of Engineering, VCU, and gave me untiring help and direction on the engineering aspects of my PhD. I wish to express my sincere thanks to Dr. Michael Hindle who has immensely contributed towards my PhD work by helping me with all type of technical issues I had. My sincere thanks to Dr. Joanne Peart for her detailed review and valuable advice during the preparation of this dissertation. I am grateful to Dr. Barr for his inputs towards model validation.

My special thanks to Dr. Jurgen Venitz, for his help with the IRB application and statistical analysis and Dr. John Clore for generously serving as medical monitor for my study. I thank my friends Ross and Geng from Department of Mechanical Engineering for their help with airway model construction.

I am thankful to Medical College of Virginia Foundation and School of Pharmacy, VCU for financial support. I would like to acknowledge Pharmaceutics department and Dean's office staff especially Keyetta, Laura, and Karen for management of all my administrative aspects throughout my stay at VCU; they are the best.

I am also grateful to all the former or current ARGers: Dr. Mashahiro Sakagami, Deepika, Swati, Bhawana, Suparna, Megha, Ruba, Sayeed, Min, Xiang, Xiangyin and Yoen-Ju Son. I am particularly thankful to many friends that I have made at VCU, who made my life interesting at Richmond. To name a few: Kumar, Mrugaya, Juni, Kunal, Parth, Lathika, Lokesh, Rati, KJ, Prajakta, Morse, Gopi, Apoorva, Aditi, Matt, Ankit, Ranu, Christine, Li, Clara, Abhishek, Abdullah and Drew. I greatly value their friendship and I deeply appreciate their belief in me.

Finally, I would like to thank my parents for supporting me and encouraging me throughout my life. Without you I would have never achieved this dream. I also like to thank my parents in law for supporting me with their best wishes. I am not able to define in words, the support, care and love I received from my beloved wife, Poonam, throughout my Ph.D. Thank you for being with me dear.

TABLE OF CONTENTS

	Page
ACKNOWLEDGEMENT	iii
LIST OF TABLES	ix
LIST OF FIGURES	xii
ABBREVIATIONS	xv
ABSTRACT	xix
CHAPTER	
1 BACKGROUND AND SIGNIFICANCE	1
2 HYPOTHESES	13
3 SCALING A PHYSICAL MODEL OF THE UPPER AIRWAYS TO PREDICT DRUG DEPOSITION VARIATION IN NORMAL HUMANS	16
3.1 INTRODUCTION	16
3.2 MATERIALS AND METHODS	18
3.2.1 PHYSICAL MODELS OF THE UPPER AIRWAYS.....	21
3.2.2 IN VITRO DEPOSITION TESTING.....	24
3.2.3 ANALYSIS.....	30
3.2.4 IN VITRO-IN VITRO CORRELATIONS (IVIVC).....	30
3.3 RESULTS AND DISCUSSION	31
3.3.1 SCALED PHYSICAL MODELS OF THE UPPER AIRWAYS.....	31
3.3.2 IN VITRO DEPOSITION TESTING AND IVIVC.....	37
3.4 CONCLUSIONS	46
4 IVIVCS FOR DIFFERENT DRY POWDER INHALERS IN NORMAL	

ADULTS	47
4.1 INTRODUCTION	47
4.2 MATERIALS AND METHODS	49
4.2.1 PHYSICAL MODEL OF THE UPPER AIRWAYS AND TEST APPARATUS.....	49
4.2.2 MATERIALS.....	49
4.2.3 IN VITRO DEPOSITION TESTING.....	52
4.3 RESULTS AND DISCUSSION	57
4.4 CONCLUSIONS	65
5 TO PREDICT THE EFFECT OF INHALER INSERTION ANGLE ON AEROSOL DEPOSITION USING IN VITRO AIRWAY MODELS	66
5.1 INTRODUCTION	66
5.2 MATERIALS AND METHODS	68
5.2.1 TEST INHALERS.....	68
5.2.2 PHYSICAL AIRWAY MODELS.....	68
5.2.3 INSERTION ANGLE IN VITRO EXPERIMENTAL SET UP..	70
5.2.4 AERODYNAMIC PARTICLE SIZE DISTRIBUTION DETERMINATION.....	72
5.2.5 ANALYTICAL METHOD.....	72
5.2.6 DATA ANALYSIS METHOD.....	72
5.3 RESULTS	74
5.3.1 EFFECT OF INSERTION ANGLE ON IN VITRO DEPOSITION.....	74

5.3.2	IMPACTOR STUDY.....	80
5.4	DISCUSSION.....	83
5.5	CONCLUSIONS.....	85
6	ASSESSMENT OF INSPIRATORY PROFILES THROUGH DIFFERENT AIRFLOW RESISTANCES AS A FUNCTION OF TRAINING.....	86
6.1	INTRODUCTION.....	86
6.2	INHALATION FLOW CELL.....	88
6.3	CLINICAL STUDY.....	90
6.3.1	SPECIFIC AIMS.....	90
6.3.2	STUDY DESIGN.....	90
6.3.3	EXPERIMENTAL METHODS.....	92
6.3.4	RESULTS.....	98
6.4.5	CONCLUSIONS.....	132
7	SUMMARY AND GENERAL CONCLUSIONS.....	134
	REFERENCES.....	138
	APPENDICES.....	148
	APPENDIX A ORIGINAL DATA SHEETS.....	149
	APPENDIX B REPRESENTATIVE CHROMATOGRAMS, CALIBRATION CURVES AND METHOD VALIDATION RESULTS FOR HPLC METHODS USED IN CHAPTERS 3, 4 AND 5.....	168
	APPENDIX C INHALATION CELL – DESIGN, CONSTRUCTION AND CALIBRATION OF AIRFLOW RESISTANCE TUBES USED IN CLINICAL STUDY.....	179

APPENDIX D CALCULATION OF AIR FLOW RATE LEAVING THE MOUTHPIECE OF INHALATION FLOW CELL.....	187
APPENDIX E DATA FOR FLOW RATE VS TIME FOR INDIVIDUAL VOLUNTEERS INHALING THROUGH THE FLOW CELL.....	192
APPENDIX F PLOTS OF INHALATION VARIABLE(S) OVER TRAINING STATUS FOR ALL VOLUNTEERS, FOR EACH RESISTANCE TUBE EMPLOYED.....	153
APPENDIX G INDIVIDUAL RESULTS FOR ‘COEFFICIENT OF DETERMINATION’ (R SQUARED) OF THE LINEAR REGRESSION PLOTS OF INHALATION VARIABLE(S) VALUES VERSUS DIFFERENTLY TRANSFORMED VALUES FOR AIR FLOW RESISTANCE.....	266
APPENDIX H IRB DOCUMENTS (STUDY – HM-13708).....	274

LIST OF TABLES

	Page
Table 3.1 Actual dimensions of the MT region of our medium, small and large models.....	33
Table 3.2 Luminal diameters (mm) for generation 0 through 3 of MT-TB _{M,S,L}	35
Table 3.3 <i>In vitro</i> and <i>in vivo</i> results for % budesonide deposition from Budelin Novolizers in small, medium and large MT-TB models using inhalation profiles selected to represent the mean and extreme values for PIFR and V of Newman et al.....	39
Table 4.1 Summary of commercial DPIs studied alongside gamma scintigraphy study details in healthy volunteers taken from the literature.....	51
Table 4.2 Summary of <i>in vitro</i> testing conditions.....	53
Table 4.3 Reverse-phase HPLC methods for drug assay.....	56
Table 5.1 Effect of insertion angle on the <i>in vitro</i> albuterol sulfate deposition for the Salbulin Novolizer DPI.....	75
Table 5.2 Effect of insertion angle on the <i>in vitro</i> albuterol sulfate deposition for the drug only Novolizer DPI.....	76
Table 5.3 Effect of insertion angle on the <i>in vitro</i> albuterol sulfate deposition for the Proventil HFA MDI.....	78
Table 5.4 Effect of insertion angle on the <i>in vitro</i> albuterol sulfate deposition for the Respimat SMI.....	79
Table 6.1 Final Subject Demographics (enrolled for Visit 2).....	99

Table 6.2	Summary of subject demographics and screening test results.....	100
Table 6.3	Descriptive results for PIFR by training status and gender for different resistance tubes.....	102
Table 6.4	Descriptive results for the mean ($R*PIFR$) (in $Kpa^{0.5}$) by training status and gender.....	104
Table 6.5	Descriptive results for V (liters) by training status and gender for different resistance tubes.....	108
Table 6.6	Descriptive results for the mean V^* (liters) by training status and gender	111
Table 6.7	Descriptive results for t_{max} by training status and gender for different resistance tubes.....	113
Table 6.8	Descriptive results for the mean t_{max}^* (in seconds) by training status and gender.....	116
Table 6.9	Descriptive results for t_{total} by training status and gender for different resistance tubes.....	118
Table 6.10	Descriptive results for the mean $\left(\frac{t_{total}}{R}\right)$ (in $L/Kpa^{0.5}$) by training status and gender.....	122
Table 6.11	‘r squared’ values from univariate regression analyses performed between the normalized inhalation variable values and demographic data and PFT values, separately for females and males.....	124
Table 6.12	Example of a spreadsheet used to calculate 10 th , 50 th and 90 th percentile flow rate to construct small, medium and large representative inhalation profiles for ‘After formal training’ for Tube 1.....	127
Table 6.13	Descriptive results for inhalation variables in the representative	

	inhalation profiles for ‘After formal training’	129
Table 6.14	Descriptive results for inhalation variables in the representative	
	inhalation profiles for ‘Before formal training’	131

LIST OF FIGURES

		Page
Figure 3.1	Internal appearance of the average or “medium sized” Mouth-throat (MT) according to Xi and Longest with upper airways (trachea-bronchial (TB) segment based on Yeh and Schum.....	20
Figure 3.2	The small, medium and large MT-TB models used in the present study.....	23
Figure 3.3	Diagram of physical test apparatus used to predict deposition of drugs from dry powder inhalers.....	26
Figure 3.4	Simulated air flow rate versus time curves representing ~95% of the range reported by Newman et al for Budelin testing	28
Figure 3.5	The total lung dose from Budelin following <i>in vitro</i> testing at the mean and extremes of flow and volume in each of the 3 MT-TB models following fast, moderate and slow inhalation shown in comparison to median <i>in vivo</i> values.....	41
Figure 3.6	<i>In vitro</i> and <i>in vivo</i> deposition results for Budelin across the test conditions listed in Table 3.3 (A) fast inhalation (B) moderate inhalation and (C) slow inhalation.....	45
Figure 4.1	Simulated ‘average’ flow rate vs. time profiles used in testing different DPIs.....	54
Figure 4.2	Mean % total lung deposition, TLD, for five DPIs following <i>in vitro</i> testing in the medium airway model.....	60
Figure 4.3	Mean % mouth-throat and tracheal drug deposition, (MT + trachea), for	61

	five DPIs following <i>in vitro</i> testing in the medium airway model.....	
Figure 4.4	Values for mean device deposition following <i>in vitro</i> testing in the medium airway model.....	62
Figure 5.1	Novolizer attached to different angled MT models.....	69
Figure 5.2	3D representation of MT-TB geometry in chamber used for <i>in vitro</i> deposition experiments.....	71
Figure 5.3	Size distributions for the Novolizer drug-excipient and micronized drug aerosols.....	81
Figure 5.4	(A) MT and impactor albuterol sulfate deposition (% of delivered dose) and (B) % difference in the deposition on the various impactor stages at the MT deposition extremes shown in Figure 5.3 (+10° angle in comparison to -20°).....	82
Figure 6.1	Inhalation flow cell design (A; schematic) and (B; photograph), and (C; photograph of the top and the side views of the resistance tubes with identical external but different internal dimensions).....	89
Figure 6.2	Inhalation written instructions.....	94
Figure 6.3	Illustration of inhalation profile.....	96
Figure 6.4	Linear regression of Mean (R*PIFR) – After training 2 and Mean (R*PIFR) – After training 1.....	105
Figure 6.5	Normal-Quantile plot for residuals of repeated measures ANOVA for mean (R*PIFR) in males and females combined.....	106
Figure 6.6	Linear regression of mean V* – After training 2 and mean V* – After training 1.....	110

Figure 6.7	Normal-Quantile plot for residuals of repeated measures ANOVA for mean V^*	111
Figure 6.8	Linear regression of mean t_{\max}^* – After training 2 and mean t_{\max}^* – After training 1.....	115
Figure 6.9	Normal-Quantile plot for residuals of repeated measures ANOVA for mean t_{\max}^*	116
Figure 6.10	Linear regression of mean $\left(\frac{t_{\text{total}}}{R}\right)$ – After training 2 and mean $\left(\frac{t_{\text{total}}}{R}\right)$ – After training 1.....	120
Figure 6.11	Normal-Quantile plot for residuals of repeated measures ANOVA for mean $\left(\frac{t_{\text{total}}}{R}\right)$	121
Figure 6.12	Representative inhalation profiles for different resistance tubes, ‘After formal training’	128
Figure 6.13	Simulated small, medium and large inhalation profiles used for the <i>in vitro</i> deposition studies from Budelin in comparison with the representative small, medium and large inhalation profiles for the inhalation flow cell containing Tube 4.....	129
Figure 6.14	Figure 6.13: Representative inhalation profiles for different resistance tubes, ‘Before formal training’	130

ABBREVIATIONS

®	registered trademark
μ	Micro
2D	two dimensional
3D	three dimensional
ANOVA	analysis of variance
API	active pharmaceutical ingredient
AT	after training
BS	breath simulator
BT	before training
CAD	computer assisted design
CFD	computational fluid dynamics
CI	confidence interval
cm	centimeter
COPD	chronic obstructive pulmonary disease
CT	computed tomography
CV	coefficient of variation
DMF	deviation from normal
DPI	dry powder inhaler
e.g.	for example
et al	and others
F	females

FEF	forced expiratory flow rate
FET	forced expiratory time
FEV1	forced expiratory volume in one second
FR	flow rate
FVC	forced vital capacity
HFA	hydrofluoroalkane
HPLC	high performance liquid chromatography
i.e.	that is
IVIVC	<i>in vitro</i> - <i>in vivo</i> correlation
K	degrees Kelvin
kg	kilogram
kPa	kilopascal
L	liter
LL	left lower
LLN	lower limit of normal
LOQ	limit of quantification
LU	left upper
M	males
mbar	millibar
min	minute
MRI	magnetic resonance imaging
MT	mouth-throat
NGI	Next generation impactor

°C	degrees Celsius
P	peripheral
PDD	pulmonary drug delivery
PEF	peak expiratory flow rate
PFT	pulmonary function test
PIFR	peak inhalation flow rate
pMDI	pressurized metered dose inhaler
R	air flow resistance
RL	right lower
RM	right middle
RM-ANOVA	repeated measures analysis of variance
RSD	relative standard deviation
RT	respiratory tract
RU	right upper
s	second
SD	standard deviation
SMI	SoftMist inhaler
TB	tracheo-bronchial
TLD	total lung deposition
™	trade mark
t_{\max}	time to reach PIFR
t_{total}	total inhalation time
USP	United States Pharmacopeia

V	inhalation volume
vs.	versus
w/v	weight per volume
yr	year

ABSTRACT

IN VITRO METHODS TO PREDICT AEROSOL DRUG DEPOSITION IN NORMAL ADULTS

By Renishkumar R. Delvadia, B. Pharm., M.Pharm.

A dissertation submitted in partial fulfillment of the requirements for the degree of Doctor of Philosophy at Virginia Commonwealth University.

Virginia Commonwealth University, 2012

Major Director: Peter R Byron, Ph.D.
Professor & Chair, Department of Pharmaceutics
School of Pharmacy

This research was aimed at the development and validation of new *in vitro* methods capable of predicting *in vivo* drug deposition from dry powder inhalers, DPIs, in lung-normal human adults.

Three physical models of the mouth, throat and upper airways, MT-TB, were designed and validated using the anatomical literature. Small, medium and large versions were constructed to cover approximately 95% of the variation seen in normal adult humans of both genders. The models were housed in an artificial thorax and used for *in vitro* testing of drug deposition from

Budelin Novolizer DPIs using a breath simulator to mimic inhalation profiles reported in clinical trials of deposition from the same inhaler. Testing in the model triplet produced results for *in vitro* total lung deposition (TLD) consistent with the complete range of drug deposition results reported *in vivo*. The effect of variables such as *in vitro* flow rate were also predictive of *in vivo* deposition. To further assess the method's robustness, *in vitro* drug deposition from 5 marketed DPIs was assessed in the "medium" MT-TB model. With the exception of Relenza Diskhaler, mean values for %TLD_±SD differed by only $\leq 2\%$ from their literature *in vivo*.

The relationship between inhaler orientation and *in vitro* regional airway deposition was determined. Aerosol drug deposition was found to depend on the angle at which an inhaler is inserted into the mouth although the results for MT deposition were dependent on both the product and the formulation being delivered. In the clinic, inhalation profiles were collected from 20 healthy inhaler naïve volunteers (10M, 10F) before and after they received formal inhalation training in the use of a DPI. Statistically significant improvements in Peak Inhalation Flow Rate (PIFR) and Inhalation Volume (V) were observed following formalized training. The shapes of the average inhalation profiles recorded in the clinic were found to be comparable to the simulated profiles used in the *in vitro* deposition studies described above.

In conclusion, novel *in vitro* test methods are described that accurately predict both the average and range of aerosol airway drug deposition seen from DPIs in the clinic.

CHAPTER 1

BACKGROUND AND SIGNIFICANCE

From the launch of the pressurized metered dose inhaler (pMDI) about six decades ago research on pulmonary drug delivery (PDD) has expanded rapidly. Indeed, it is possible that we may see PDD as a potential platform not only for treatment of airway problems but also for systemic diseases (Yang et al, 2008). Reduced dose, rapid onset of action and targeted drug delivery are some of the important advantages associated of the lung as a route of delivery (Yang et al, 2008). Currently there are three main types with device available for aerosol drug delivery on the market; nebulizers, pMDIs, and DPIs. While pMDIs have proven to be most popular amongst the three, with chlorofluorocarbon propellant replacement, propellant-free DPIs have become mainstay treatments for pulmonary disease.

Performance and drug delivery efficiency of DPIs rely on formulation characteristics, dispersion mechanisms, and the interaction between them (Frijlink & De Boer, 2004; Islam & Gladki, 2008). One of the important advantages of DPIs over pMDIs is that DPIs can potentially deliver much larger drug doses with less variation in the lung dose compared to pMDIs (Newman & Peart, 2009a). The typical DPI formulation is either an adhesive blend of

micronized drug particles with larger carrier particles like lactose, or spherical aggregates of micronized particles with or without micronized lactose (Telko & Hickey, 2005). These formulations offer better flow properties compared to the unprocessed micronized drug, that make it easy to fill into blisters or meter from a DPI reservoir with accuracy and precision (Newman & Peart, 2009a; Telko & Hickey, 2005). However, in order to enable drug penetration into the lungs and show therapeutic activity, drug particles must either be detached from the carrier or dispersed from the aggregate before leaving the device during a patient's inhalation. For this reason DPIs are usually equipped with some type of dispersion mechanism that utilizes the inspiration of the patient as an energy source to disperse the drug particles (Atkins, 2005; Newman & Peart, 2009a). Some of the common dispersion mechanisms include the use of turbulent airflow path(s), vortex chamber(s), grids or screens, and cyclone separators (Atkins, 2005; Newman & Peart, 2009a). It is largely the dispersion unit in a DPI that determines the inhaler's airflow resistance. Depending on the airflow resistance, DPIs can be broadly classified into high, medium or low resistance groups. Notably, however, no standard method for classification exists.

In spite of recent advances in DPI design and formulation strategies, most currently marketed DPIs are low efficiency devices, showing lung drug delivery of drug values of 30% or less with respect to the nominal or loaded dose in the device (Cass et al, 1999; Newman et al, 2000; Newman et al, 2000c; Pitcairn et al, 1994). Of course, it is also possible to question whether the lung deposition of inhaled medication has any pharmacological relevance. The answer may depend on several factors; among these are the drug, the dose and its purpose (Newman et al, 2000c). It is quite possible that increasing the dose of a β -agonist drug depositing

in the lungs may not always increase the therapeutic effect but may overdose the patient and produce adverse events (Pritchard, 2001); this because dose-response curves are often sigmoidal and it is only when the lung dose produces a response below the maximal plateau level that we expect enhancements in efficacy with higher TLD. Nevertheless, for topically acting compounds it is generally believed that similar regional distribution of the TLD will lead to similar efficacy while the quotient $TLD/(\text{Loaded Dose})$ is usually thought of as a measure of an inhaler's delivery efficiency.

High MT deposition is a major factor responsible for the poor efficiency of currently marketed DPIs. There are three main mechanisms that govern aerosol deposition in the airway and thus the deposition of drugs from aerosols delivered from inhalers: inertial impaction, diffusion and sedimentation (Gonda, 2004). Well documented evidence suggests that inertial impaction is the primary mechanism for deposition of pharmaceutical aerosols in the upper airway that consists, from the point of view of oral inhalation, of MT and trachea (Hickey, 2004). Aerosols traveling further into the lung experience much slower air velocities causing deposition in the more peripheral airways to occur increasingly due to sedimentation and diffusion (Gonda, 2004). Drug deposited in the MT region get swallowed and usually do not contribute to local therapeutic activity in the airways; moreover, that part of a dose may produce undesirable effects. MT deposition from inhalers may be dependent on inhaler design, airflow resistance, dispersion mechanisms as well as the properties of the generated aerosol such as aerosol momentum, particle density, and plume dynamics (Longest et al, 2009; Xi & Longest, 2008; Yeh et al, 1976). Perhaps it is most important to recognize that aerosol that fails to pass the MT region, cannot penetrate the lung. For example, MT deposition of aerosol by inertial impaction

increases with increase in particle velocity or particle size and this is purported to be the reason that slow jet inhalers such as Respimat[®], a softmist inhaler (SMI), shows considerably less MT deposition compared to high velocity inhalers, such as pMDIs and some DPIs (Longest & Hindle, 2009; Newman et al, 2000c). It is usually recommended therefore, to inhale slowly through SMIs and pMDIs (to minimize MT deposition). For DPIs, however, where the patient provides the energy for aerosol creation, slow inhalation usually also results in less drug dispersion. When compared to fast inhalation through a DPI, this effect often overcomes any reduced impaction gains made from inhaling slowly. For example, in a study by Newman et al, the authors reported gains in median TLD of budesonide from ASTA Medica's DPI (now Budelin[®] Novolizer[®] 200 µg budesonide/dose). TLD values of 19.5%, 25.5% and 32.1 % were reported when adult healthy volunteers inhaled with mean peak inspiratory flow rates, PIFR, of 54, 65 and 99 L/min, respectively (Newman et al, 2000). Novolizer is a low variability powder inhaler, containing a blend of micronized drug (<5µm) with coarse (>60 µm) lactose monohydrate carrier particles. Its dry particle flow path involves "Air Classifier Technology (ACT)" that works on the principle of cyclone separation and results in better drug detachment from carrier particles when patients inhale fast. In fact, Novolizer is designed in such a way that it delivers drug only when the patient achieves a certain flow rate. De Boer et al. investigated the effect of formulation, some features of ACT design and various *in vitro* testing conditions on the performance of Novolizer and has described the inhaler in detail (de Boer et al., 2006).

The variability associated with airway deposition must also be considered. The literature suggests that inhalers with high MT, or oropharyngeal deposition also show large variability in TLD (Borgstrom et al, 2006). The primary cause for this type of variability appears to be associated with the patient-inhaler interaction that is governed by two major physiological

variables, the airway geometry and the inhalation maneuver (Clark & Egan, 1994; Finlay & Martin, 2008). Studies have shown that variations in the oropharyngeal volume can significantly alter the oropharyngeal deposition of some inhaled medications (Burnell et al, 2007; Ehtezazi et al, 2010; Grgic et al, 2004). Furthermore, because the oropharyngeal region also undergoes continuous dynamic changes during the inhalation cycle, this can also result in intra-subject variability in the geometry of the aerosol path to the lungs (Burnell et al, 2007; Grgic et al, 2004). Indeed, a major source of the intra-subject variability of MT deposition has been shown to be the variable tongue position during inhalation (Ehtezazi et al, 2004; Fadl et al, 2007). Ehtezazi et al has reported that significant amounts of aerosol drug deposits on the front part of the tongue, when the tongue is pulled back, and on the posterior portion of the mouth, when tongue is pulled forward. Changes in the cross sectional areas of the airways or changes in aerosol trajectories may also produce intra- and inter-subject variations in deposition (Fadl et al, 2007). The shape of the airway geometry may also be dependent on the airflow resistance of the inhaler (Ehtezazi et al, 2005; McRobbie, 2005). For example, Ehtezazi et al have found that cross sectional areas and mean volumes of the oral cavity, oropharynx and larynx decrease with increases in the air flow resistance of the device through which a subject is asked to inhale (Ehtezazi et al, 2005). Similar to MT, TB caliber and geometry may also differ between persons and within persons (Montaudon et al, 2007). For example, evidence in the literature suggests that chronic obstructive pulmonary disease (COPD) sufferers may have significantly altered airway luminal cross-sectional areas compared to healthy subjects (Brillet et al, 2008). Surprisingly, no study has been reported that specifically looked at the effect of this geometric variability in the TB region on the regional deposition of inhaled medications.

Another aspect of DPIs is the demand for thorough patient education in the use of the chosen inhaler to ensure its efficacy (Broeders et al, 2009). There are several devices available commercially to help physicians train patients on how to inhale “correctly” through DPIs. Most of these devices provide feed-back on whether or not a patient is achieving a “desirable” or “minimally effective” PIFR (Lavorini et al, 2010). Despite substantial efforts from physicians, nurses and pharmacists however, recent surveys suggest that many patients do not use their inhalers in the “correct way” (Rootmensen et al, 2010; van Beerendonk et al, 1998). Inhalation at sub-optimal flow rates, shallow inhalation, poor co-ordination and incorrect inhaler orientation are some of the common mistakes reported (Rootmensen et al, 2010). If inhalers are not used in the recommended way a poor and/or variable lung dose may result (van Beerendonk et al, 1998), although this is probably inhaler-dependent. In addition to PIFR, inhalation volume, V , may also play a significant role in explaining deposition variability. Importantly PIFR and V through inhalers show tremendous variability between subjects due to differences in age, sex, race, height, and disease while intra-subject variability also occurs because of improper patient training (Cegla, 2004; de Boer et al, 1996; Pellegrino et al, 2005).

In the past, numerous *in vivo* studies have attempted to understand the regional fractionation of aerosols from inhalers. Most involved either radio-imaging techniques or pharmacokinetic (PK) approaches. While radio-imaging techniques can extract details of regional deposition, they are the most challenging to perform practically. Radio-imaging also has risks of exposing humans to the radiation and is expensive, variable and time-consuming, chiefly because the (radio)label must be shown to accompany the drug (Newman et al, 2009b). PK approaches, in contrast, are safe and drug specific but do not always produce results that provide

information on the drug's regional deposition in the lung, for example because especially significant ciliary clearance coinciding with slow lung absorption may significantly alter distribution in the airways during the period when drug absorption occurs. Therefore, PK approaches, if not used with caution, can lead to incorrect conclusions on regional drug deposition (Newman et al, 2009b).

These limitations of the methods used *in vivo* have driven the development of faster, less expensive, *in vitro* models to predict deposition of inhaled drug particles, a topic that is explored in detail in this thesis. Currently cascade impactor testing methods are widely used *in vitro* to characterize the aerosol drug output from DPIs. They provide information on the aerodynamic particle size distribution of the drug in the aerosol cloud emitted from the inhaler under the test conditions employed. Efforts have been made to correlate the size distribution data obtained from such studies with the regional drug deposition results obtained in clinic (Mitchell et al, 2007). However, this has met with limited success and the approach is often criticized for not being a good predictor of either total or regional drug deposition in the human airways. Most importantly, by focusing only on aerosol size such methods neglect the way that aerosol cloud characteristics and deposition depend on each patient's unique respiratory maneuver and airway geometry (Jaafar-Maalej et al, 2009). Also, it is not possible to assess the deposition variability as a function of variability in airway geometry using impactors. Because of the above mentioned limitations of cascade impactor methods, substantial efforts have been made to find alternatives, especially to characterize the deposition from DPIs. At present, three alternative approaches have been used widely; computational fluid dynamic (CFD) modeling, mathematical modeling based

on earlier empirical deposition data, and *in vitro* drug deposition studies in physical airway models.

CFD and *in vitro* studies using physical models are presently most popular because of their versatility (Housiadas & Lazaridis, 2010) and the ease with which we can now create models of the airways and study flow patterns within them. It should be noted that the prediction accuracy of a CFD model is highly dependent on how the model is designed and its underlying assumptions (Housiadas & Lazaridis, 2010). Also, it may often be tedious and challenging to build a CFD model to predict drug deposition and delivery from a complex system like a DPI, as a function of each patient's unique inhalation maneuver. *In vitro* deposition studies in physical models on other hand, work on minimal assumptions once the models have been created and these may facilitate the study of aerosol deposition as function of flowrate profiles and airway geometry and, help to validate CFD models designed to mimic their results. These advantages of *in vitro* testing in physical airway models make the approach a good choice for regional aerosol deposition characterization of inhalers, especially for DPIs.

Physical airway models representing MT and TB regions of adults have been used in many studies to characterize deposition of environmental aerosol and inhaled medications (Anderson et al, 1995; DeHaan & Finlay, 2001). Many of these airway models were developed from casts made from human cadavers. The cast based models offers the unique advantage that they preserve the small anatomical details of the airway. However, they usually overestimate the airway diameters due to tissue shrinkage following death. Additionally, the cadaver casting method involves a step of pouring a dense casting liquid resin into the airway that tends itself to

widen the airspace by creating hydrostatic pressure in the airway lumen (Yeh & Schum, 1980). For these reasons, the dimensions of cast-based models are often corrected for lumen enlargement, in order to match with the volumetric lung capacity of the living human (Yeh & Schum, 1980).

Fortunately, with advancements in imaging technology such as computed tomography, CT, or magnetic resonance imaging, MRI, it is now possible to obtain accurate anatomical details of living human airway models that can be used to develop improved physical airway models (Grgic et al, 2004; Pritchard & McRobbie, 2004). Unlike cadaver casting, imaging the living person excludes the overestimation of parameters such as airway diameter due to tissue shrinkage or casting material. Another advantage is that models can also be constructed that account for dynamic changes in the airway during inhalation from different devices (Ehtezazi et al, 2004; Grgic et al, 2004). There are, however, also limitations to imaging techniques. Dimensional accuracy of the model developed from the CT or MRI images greatly relies on the resolution of the images. Of course, the higher the resolution, the better the accuracy [Longest 2009, personal communication] but to improve image resolution, longer scanning is required that may extend to several minutes (Burnell et al, 2007; McRobbie, 2003). In this situation, MRI may be superior compared to CT due to the associated risk of X-ray radiation with CT. (McRobbie, 2003; Pritchard & McRobbie, 2004). Moreover, it is clearly impossible for a person to forcefully inhale for several minutes. Also, images of complex geometries such as those in the MT region must often be processed manually, increasing the chances of manual errors and subjective data interpretation.

It has become a common practice to develop airway models by combining information obtained from human casts, CT and/or MRI images alongside anatomical information from the literature (Stapleton et al, 2000; Xi & Longest, 2007). Once these models have been created accurately ‘in silico’, using computer aided design (CAD) software, it is possible to construct physical models made from different polymers to represent the minute details of airway anatomy using rapid prototyping techniques. More recently, geometrically simplified or idealized physical airway models are becoming more popular for the study of drug deposition from pharmaceutical inhalers (Longest & Hindle, 2009; Stapleton et al, 2000; Xi & Longest, 2007). Geometries of idealized models are developed by modifying the actual geometries obtained from different sources, aimed to preserve the important anatomical details yet allow easy reproducible construction. However, apart from the (potentially high) resolution of the ‘in silico’ geometry, the geometric accuracy of the airway model so produced may also depend on the resolution of the prototyping instrument used to produce it. Rapid prototyping also requires smoothing of the minor geometric details, something that may result in a model with slightly different geometries than intended.

Most physical airway models used for drug deposition studies at this time have been limited to realistic geometric models of the MT region. In these studies, TLD is calculated as the amount of drug that escapes the inhaler yet passes through (penetrates) the MT region as an aerosol. Unfortunately, the approach ignores the need to assess the TLD within the lung itself. Nevertheless, the MT models in the literature have been used to study the effects of MT airway geometry on aerosol deposition from inhalers and to understand aerosol deposition mechanisms in the upper airways (Anderson et al, 1995; Burnell et al, 2007; DeHaan & Finlay, 2001;

Rahmatalla et al, 2002). However, there is evidence in the literature that suggests that realistic MT models may accurately predict *in vivo* MT deposition when experiments are correctly designed (Olsson et al, 2008).

Many deposition studies have been reported that involve the use of trachea-bronchial, TB, models to understand the deposition of monodispersed aerosols. Most TB models used in these studies were developed from mathematical lung models as simplified descriptions of the geometries seen in lung casts from living humans or human cadavers. One such lung model, the Weibel A model, is very popular and has been used most frequently for aerosol deposition studies. It is a symmetrical lung model where the airway branches have similar bifurcation patterns, with each generation possessing the same diameter, cross sectional area and length (Weibel, 1963). Although this Weibel model is widely used because of its simplicity, it is often criticized for the same reason. In this context, in 1980, Yeh and Schum developed a “Typical Path Lung Model” which defined geometric parameters of the human airways in which airway diameters, lengths, angles relative to the direction of gravity and branching angles were all defined separately for each lobe of the lungs and also for the whole of each lung (Yeh & Schum, 1980). Yeh and Schum’s model is considered more realistic as it also represents the asymmetry of the human airway. Unfortunately, while these models offer a place to start, they do not provide a systematic approach to airway modeling for differently sized humans.

Most *in vitro* drug deposition studies in MT or TB models have been performed using constant flow rate conditions that fail to represent the inhalation maneuvers of individuals using inhalers (Anderson et al, 1995; Anderson et al, 1999; Grgic et al, 2004; Rahmatalla et al, 2002).

It is evident from the clinical literature that significant intra- and inter-subject variability in inhalation profiles exists. Because airway geometry and the inhalation profiles used by patients play a significant role in defining regional aerosol deposition, most especially from DPIs, a method that can characterize the drug deposition from inhalers as a function of both of these variables would be useful.

This research therefore, was aimed to develop and evaluate *in vitro* methods to characterize drug deposition from powder inhalers in several, carefully designed physical models of the mouth, throat, upper TB airways and the remaining lung, as a function of different, but typical, patient inhalation profiles. Using these novel *in vitro* methods, the drug deposition from different inhalers was studied in airway geometries believed to apply to different human subsets. The *in vitro* deposition results were compared to those reported in the clinical literature, to both validate the *in vitro* methods and to make airway drug deposition predictions for certain clinically relevant alterations in patient use, based upon the *in vitro* test data. In addition, inhalation profiles of healthy volunteers, before and after formal training, were documented in order to improve our understanding of the inter- and intra subject variability due to the inhalation maneuvers commonly used during the use of today's dry powder inhalers.

CHAPTER 2

HYPOTHESES

The goal of this research was to develop *in vitro* methods to predict regional aerosol drug deposition from DPIs in normal adult airways. Overall, it was hypothesized that for powder inhalers aerosol drug deposition was mainly dependent on airway geometry and the inhalation maneuver used by the individual subject. Therefore, the project was first aimed to develop *in vitro* methods to use realistic physical airway models representing the mouth, throat, and upper airways in which drug deposition could be characterized regionally, when these models were used to ‘inhale’ drug from a DPI according to typical, but different, flowrate vs. time profiles. Once methods were developed, *in vitro* deposition results were measured and compared to those reported in the clinical literature, in order to create and validate IVIVCs. A final part of the project was aimed to document and understand the way people inhale through different marketed DPIs as a result of different forms of “training”. The research was designed to test the following six hypotheses:

1. Small, medium and large *in vitro* realistic physical airway models of the mouth, throat, and upper airways (MT-TB models) can be developed geometrically, and constructed physically,

that represent approximately 95% of the anatomical variation seen in the normal adult human population.

2. Once constructed, these MT-TB airway models, partnered with carefully selected inhalation flow rate vs. time profiles, can be used to study and predict the ‘average’ as well as the observed variability seen *in vivo* for drug deposition in the lungs of trained healthy adults using commercially manufactured DPIs.
3. Robustness of the new *in vitro* methods can be demonstrated by assessing the accuracy with which ‘average’ regional drug deposition can be predicted across a range of commercially available DPIs, irrespective of inhaler variables such as device design, dispersion mechanism(s), powder formulation and the magnitude of each inhaler’s resistance to air flow.
4. The novel *in vitro* methods can be used to study other sources of aerosol drug deposition variability such as the effect of inhaler orientation on regional drug deposition resulting from use of different inhalers.
5. The average and range of flow rate versus time profiles used by inhaler-naïve adults inhaling in accord with both written and oral directions can be collected by asking a group of human subjects to inhale through an instrumented drug-free inhalation flow cell and analyzing the resultant data.

6. Statistically different inhalation profiles (inhalation flow rate versus time curves with statistically different properties) are expected to result from different forms of patient training; in particular, exposure to the written instructions that usually accompany a DPI product were expected to produce suboptimal inspiratory maneuvers when compared to personal training in device usage by a health professional

In Chapter 3, the methods used to develop different airway models are described alongside the experimental set up that was used to study regional airway deposition from DPIs and test hypotheses 1 and 2 above. Accordingly, that chapter also describes the *in vitro* study that was performed to assess and validate regional deposition variation from a specific inhaler and compare the results to literature values found in the clinic. Chapter 4 describes the effort to demonstrate the robustness of the new *in vitro* method across inhalers (hypothesis 3) while Chapter 5 deals with one example of method application to understand other possible sources of drug deposition variability (hypothesis 4). Chapter 6 describes the clinical study aimed to document the variability of inhalation profiles used by inhaler-naïve adults during their use of DPIs with different airflow resistances as well as the effects of training (hypotheses 5 and 6) Chapter 7 summarizes the findings of the research described in this thesis.

CHAPTER 3

SCALING A PHYSICAL MODEL OF THE UPPER AIRWAYS TO PREDICT DRUG DEPOSITION VARIATION IN NORMAL HUMANS

3.1 INTRODUCTION

Lung deposition in different human subjects is often highly variable, even for a single inhaler (Borgstrom et al, 2006). Because of this, collecting proof of equivalent deposition between inhalers or inhaler prototypes is challenging because it demands clinical trials with the power to discriminate between devices; large variability demands large trials. Unfortunately, expensive trials constrain product development by precluding inhaler device changes once Phase 2 clinical trials begin (Byron et al, 2010a). As a result IVIVC discussions are frequent in regulatory circles, as these correlations may provide a way to predict and improve device performance without repeating large trials in different human cohorts (Byron et al, 2010b).

To be useful to the industry and its regulators, IVIVCs need to relate *in vitro* test results not only to mean data from human clinical trials, but also to the small and large extremes in a population that are best represented by lower and upper 95% confidence limits. Because the magnitude of the deposition variance seen *in vivo* from a given inhaler has not been well-

correlated to morphologic measurements of the upper airways (mouth-throat, trachea and upper bronchi), this Chapter describes the development and initial validation of new *in vitro* methods that seek to provide this information. Three airway models are described that can be partnered with realistic inhalation profiles to provide *in vitro* estimates of the mean and 95% limits of *in vivo* deposition seen in normal human volunteers of both genders. Scaled models are described with reference to the existing literature on normal human airway dimensions. These have been constructed and used to collect drug deposition results for a marketed powder inhaler. To create and validate an IVIVC, *in vitro* results are compared to the clinical deposition results for the same inhaler, Novolizer. The approach that was used was similar to one described by Olsson et al (Olsson et al, 2008).

3.2 MATERIALS AND METHODS

3.2.1 PHYSICAL MODELS OF THE UPPER AIRWAYS

An existing physical model of the mouth-throat and upper airways (Figure 3.1) (Byron et al, 2010a) was scaled in accord with the literature describing the regional morphometry of the respiratory tract (RT) to produce the hollow tube models shown in Figure 3.2. As an initial hypothesis, we assigned the dimensions of the model shown in Figure 3.1 to those of an average RT or “medium-sized” model representing the upper oral airways of an averagely sized normal human of either gender. The total internal volume of this “average RT model” was 100.6 cm^3 comprised of at least two distinct sections: $\text{MT} = 61.6 \text{ cm}^3$ and $\text{TB} = 39.0 \text{ cm}^3$. The hypothesis, that this was a “medium - sized” RT model was backed by considerable preliminary data (Burnell et al, 2007; Cherng et al, 2002; Leader et al, 2004; Montaudon et al, 2007) and efforts to develop an *in vitro* test that successfully employed the model to predict drug deposition from inhalers when coupled to a breath simulator (Byron et al, 2010b; Delvadia et al, 2010). Notably, the model (Figure 3.1) incorporates mouth-throat, MT (including the larynx), and trachea and upper bronchi, TB; the latter section includes the trachea (generation 0) extending through the upper bronchi (generation 3). The MT geometry was based on Xi and Longest (Xi & Longest, 2007) while TB was designed using the classic morphometric data of Yeh and Schum (Yeh & Schum, 1980) and described in the studies of Tian et al. (Tian et al, 2011a; Tian et al, 2011b). Unlike the symmetrical branching described by Weibel (Weibel, 1963), the TB model contains asymmetric branching angles, tube dimensions and more realistic angles of inclination to gravity (Yeh & Schum, 1980). To prevent the model reaching a physical size that would make *in vitro* testing impractical, the number of tracheo-bronchial generations was limited. Nevertheless, the TB airways extend to the approximate point of entry to each lung lobe (right upper, middle and

lower, left upper and lower, or RU, RM, RL, LU, LL, respectively). To generate similar pressures at the model outlets in the experiments, three bifurcations were used in each branching pathway. As a result, the model contained eight outlets with two outlets extending into the LU, LL, and RU lobes and one outlet extending into the RM and RL lobes (Figure 3.1).

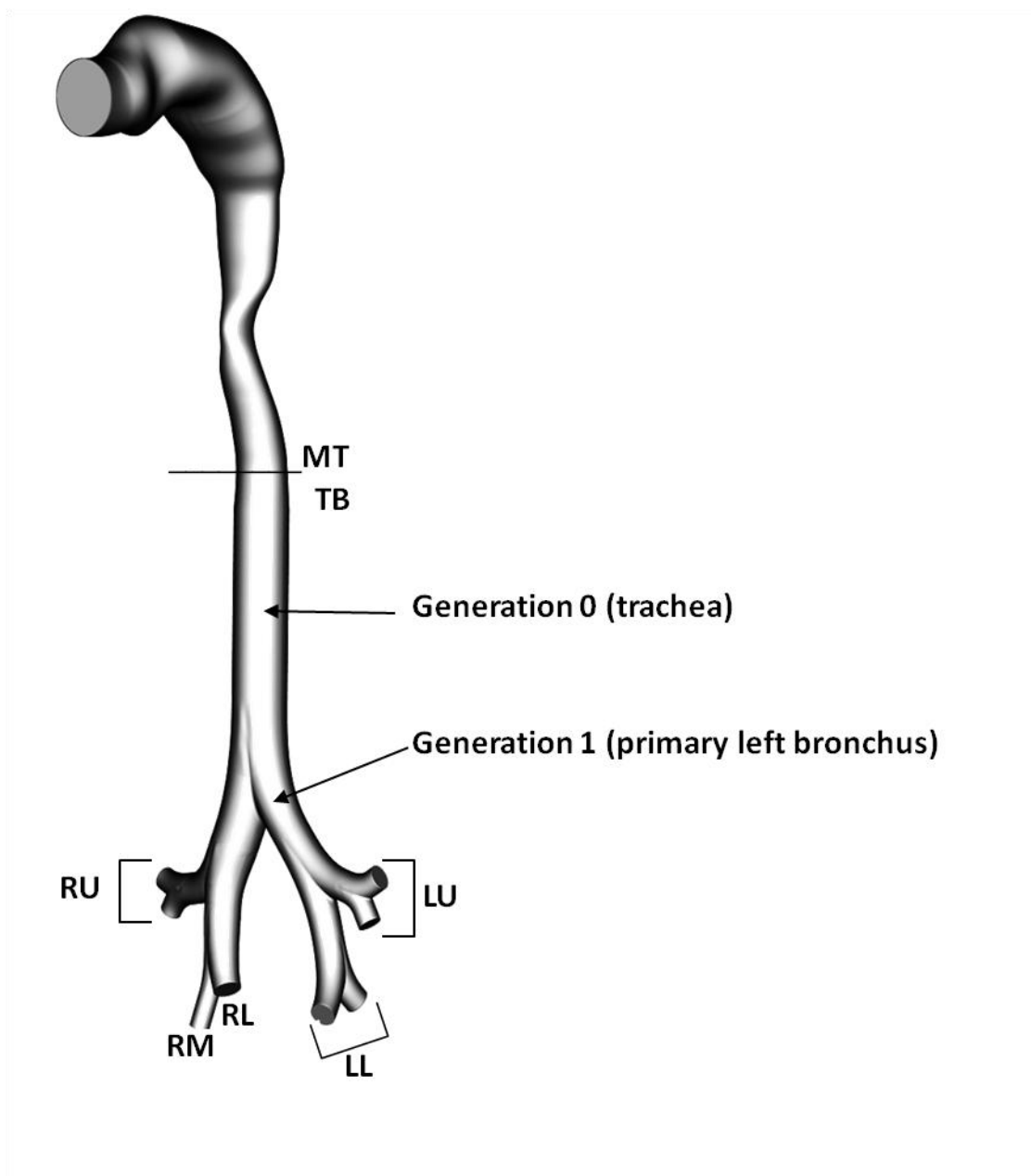


Figure 3.1: Internal appearance of the average or “medium sized” Mouth-throat (MT) according to Xi and Longest (Xi & Longest, 2007) with upper airways (tracheo-bronchial (TB) segment based on Yeh and Schum (Yeh & Schum, 1980). Scaled hollow models were constructed with an integral mouthpiece to fit Budelin inhalers as described in Figure 3.2. These were subdivided for drug analysis at various locations using airtight, friction-fit junctions; RU, RM, RL, LU, LL represents right upper, middle and lower, left upper and lower lung lobes, respectively.

3.2.1.1 Scaling the airway model to represent small and large humans

Large and small geometry models were scaled to represent the upper and lower 95% confidence limits for the MT and TB regions based on literature reports of their dimensions in different adult populations. The MT geometry of Figure 3.1 was scaled volumetrically by adding and subtracting 37.8 cm^3 to the original “medium sized” volume (65 cm^3) of Xi and Longest (Xi & Longest, 2007). In practice, this was accomplished by multiplying each linear dimension of the model by length scale factors of 1.165 (e.g. $[102.8 \text{ cm}^3/65 \text{ cm}^3]^{0.333}$) and 0.748, respectively. The value of 37.8 cm^3 was assigned based on 2 x the standard deviation of the average MT volume reported by Burnell et al (Burnell et al, 2007), a working assumption that this volume was normally distributed across a mixed – gender, adult population and the statistical generalization that the mean value $\pm 2\text{SD}$ should embrace >95% of the population. The circular inlet diameter shown in Figure 3.1 was then adapted to fit the Novolizer mouthpiece. This resulted in the medium MT volume of 61.6 cm^3 and adaptor volume of 5.4 cm^3 (see Table 3.1) reported in this study.

Similarly, the “medium sized” TB geometry shown in Figure 3.1 was derived from Yeh and Schum (Yeh & Schum, 1980) after first following their advice to scale the model to a lung volume of interest. Their limiting dimensions describe a geometry corresponding to total lung capacity, TLC, of “standard sized man” (5.6 Liters) ("Chapter 3 Physiological data for reference man," 1975). We created our “medium sized” TB model to correspond to a lung volume of 3.5L (e.g. a lung volume between functional residual capacity and TLC seen typically during inhaler use by males and females; (Byron et al, 2010a; Clark & Hollingworth, 1993; Delvadia et al, 2010). Thus, dimensions reported in Yeh and Schum were multiplied by a length scale of 0.855 ($[3.5/5.6]^{0.333}$) to create a medium - sized TB geometry; this was paired with the “medium – sized

MT” to produce MT-TB_M (Figure 3.1). Small and large TB geometries, for pairing with small and large MT models were designed by scaling the medium sized TB model using the same factors that were used for MT, to represent the 95% confidence limits in the normal adult population. A literature validation of these models was performed by comparing their physical dimensions to data in the literature for normal human adults.

3.2.1.2 Model Construction

Small, medium and large three-dimensional (3D) airway geometries were constructed in SolidWorks[®] computer assisted design (CAD) software (SolidWorks, Concord, MA) by pairing MT and their companion TB geometries. These designs were constructed as hollow plastic MT-TB models (Accura 60, 3D System, Valencia, CA) using a rapid prototyping process (Viper SLA, 3D Systems). MT models were made to snap fit on top of their companion TB models to form MT-TB_S, MT-TB_M and MT-TB_L, where subscripts represent small, medium, and large, respectively (Figure 3.2); in practice, similar airtight snap-fit junctions can be created elsewhere, when deposition in different regions is of interest.



Figure 3.2: The small, medium and large MT-TB models used in the present study. Complete dimensional description is available at <http://www.rddonline.com/resources/tools/models.php>. Models were constructed of Accura 60 (3D System, Valencia, CA) using rapid prototyping (Viper SLA, 3D Systems). MT models were made to snap fit (at arrow) on top of companion TB models to form MT-TB_S, MT-TB_M and MT-TB_L with internal volumes of MT = 26.6, 61.6, 96.1 and TB = 16.3, 39.0, 61.6 cm³, respectively. The integral Budelin mouthpiece adapter added an additional volume of 5.4 cm³ to all models.

3.2.2 IN VITRO DEPOSITION TESTING

Each airway model was installed in an identical custom-built cylindrical Plexiglas housing (internal diameter and height were 13.9 and 12.6 cm, respectively; volume was 1.9 L) with minimal dead space (Figure 3.3). To evaluate drug deposition in this setup in a relatively small number of experiments and to compare the resulting *in vitro* deposition with estimated lung deposition in the clinic, a marketed powder inhaler was selected that possessed reproducible dosing paired with good quality published airway deposition data; the latter in a group of trained normal humans inhaling at different, but well - defined flow rates. Novolizer was used as the multi-dose powder inhaler with reproducible dosing (Weda et al, 2004; Fenton et al, 2003). Budelin Novolizers (budesonide 200 µg) were purchased from the supplier (Meda Pharmaceuticals, Bishops Stortford, UK). The deposition of radiolabeled budesonide from Budelin Novolizers was assessed previously in 13 healthy volunteers by Newman et al (Newman et al, 2000). The authors described the deposition of single 200 µg doses of budesonide from the inhaler at peak inspiratory flow rates, PIFR, of 99 ± 13 , 65 ± 3 , and 54 ± 7 L/min paired with mean inhalation volumes, V, of 3.13 ± 1.01 , 2.96 ± 0.83 , and 2.77 ± 0.63 L, respectively (note that the Asta Medica device referred to by Newman et al is marketed by Meda Pharmaceuticals as Budelin in the EU). Before formally testing Budelin in our models, we confirmed that delivered doses of budesonide from test inhalers fell within USP limits when tested by withdrawal of 4L air at 83 L/min (corresponding to a 4kPa pressure drop across the inhaler) ("USP. General Chapter <601> Aerosols, Nasal Sprays, Metered Dose Inhalers, and Dry Powder Inhalers," 2009). Single metered dose deposition testing in each of the MT-TB models was then performed after priming each Novolizer and inserting it into a mouth opening designed and manufactured to fit the inhaler mouthpiece (Figure 3.3). Airtight seals between the inhaler mouthpiece, MT and

TB models were maintained in all cases. During simulated inhalations, air was drawn through the inhaler and airway model through a low resistance filter (Pulmoguard II[®], SDI Diagnostics, MA, USA) capable of retaining all aerosolized drug that passed through the model. The filter was connected to a computer programmed breath simulator (ASL 5000, IngMar Medical, Pittsburgh, PA, USA) equipped with digital recording software (LabVIEW[®]) to vary and record the rate and volume of air drawn through the set-up. In all experiments, the internal surfaces of the MT - TB models were coated with a silicone spray (Dow Corning[®] 316 Silicone Release Spray, Dow Corning Corp., Midland, Michigan, USA) followed by solvent evaporation before each experiment. Powder aerosols were collected as unit doses following each simulated inhalation. Drug deposited in the inhaler mouthpiece, MT, TB, and Plexiglas housing plus filter (the latter designated as “peripheral deposition”; P) was recovered and analyzed by HPLC after each dose, meaning that each experiment or experimental replicate began with equipment that was clean and drug-free.

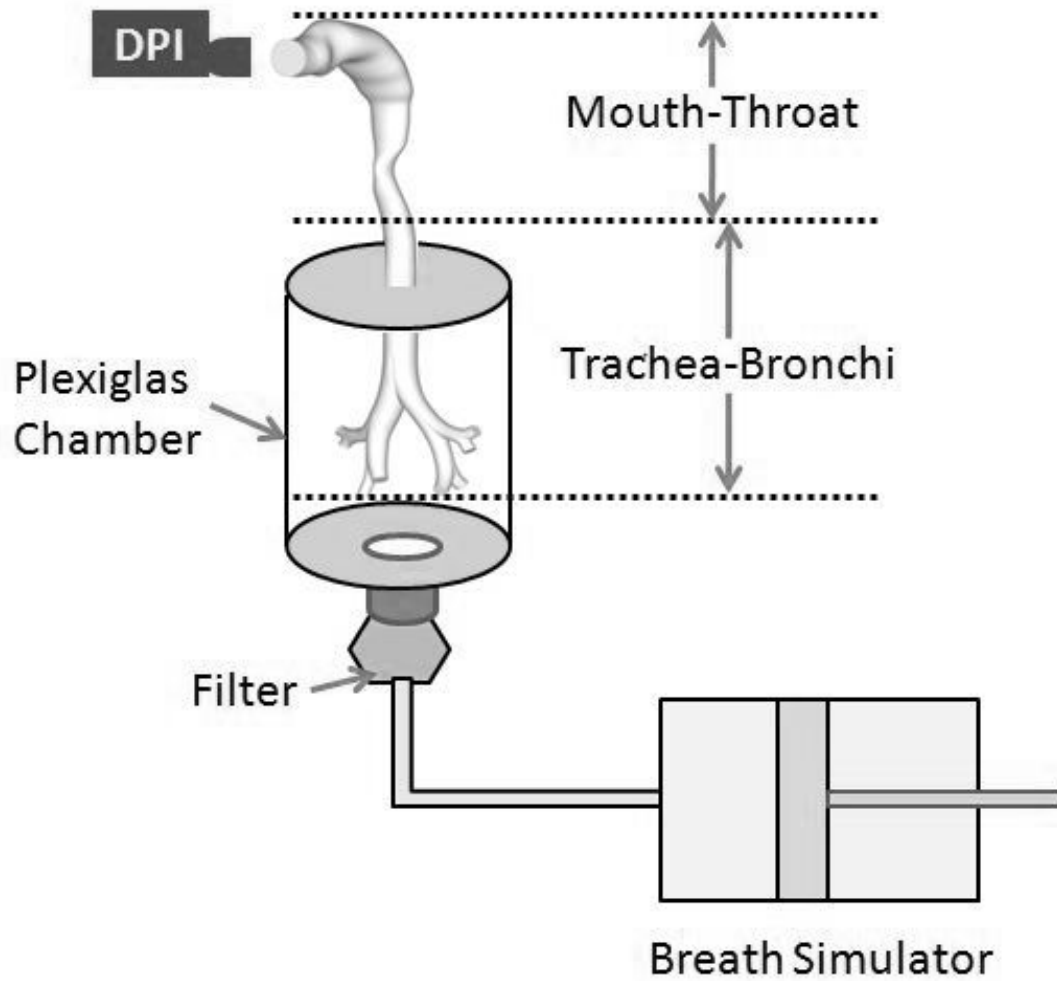


Figure 3.3: Diagram of physical test apparatus used to measure deposition of drugs from dry powder inhalers (DPIs). The externalized MT region is connected to TB through generation 3. Differently scaled versions are shown in Figure 3.2. Drug retained in the Plexiglas chamber and filter is designated P (peripheral deposition) following actuation of the breath simulator to withdraw air according to a known flow rate vs. time profile.

A randomized experimental design was used to study the *in vitro* effects of different inspiratory maneuvers and airway geometries. Values for PIFR and V were chosen to correspond to the mean \pm 2SD values used by Newman et al in the clinic (Newman et al, 2000) for use in the 3 airway geometries MT-TB_S, MT-TB_M and MT-TB_L (Figure 3.2). Precise values, selected to mimic the *in vivo* study are shown, alongside the *in vitro* and clinical deposition results (Newman et al, 2000), in Section 3.3 below. To illustrate and clarify the selection of air flow rate versus time curves used *in vitro*, profiles chosen for the low flow rate arm of this study are shown in bold in Figure 3.4.

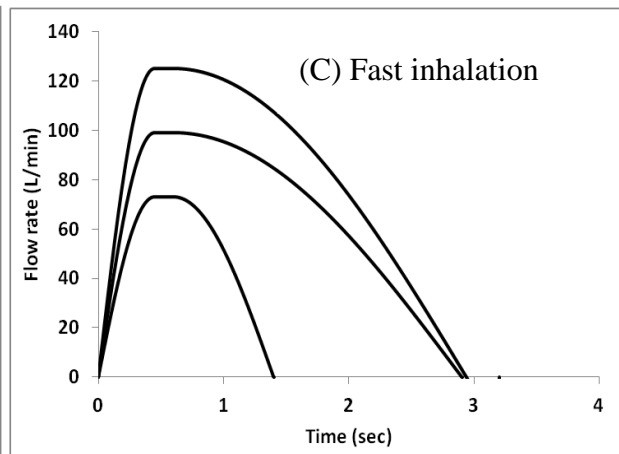
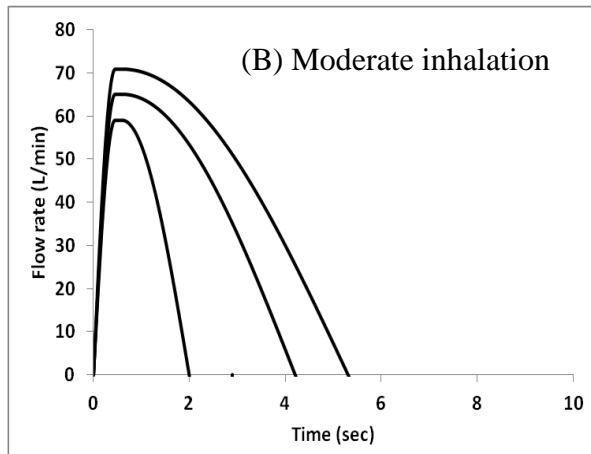
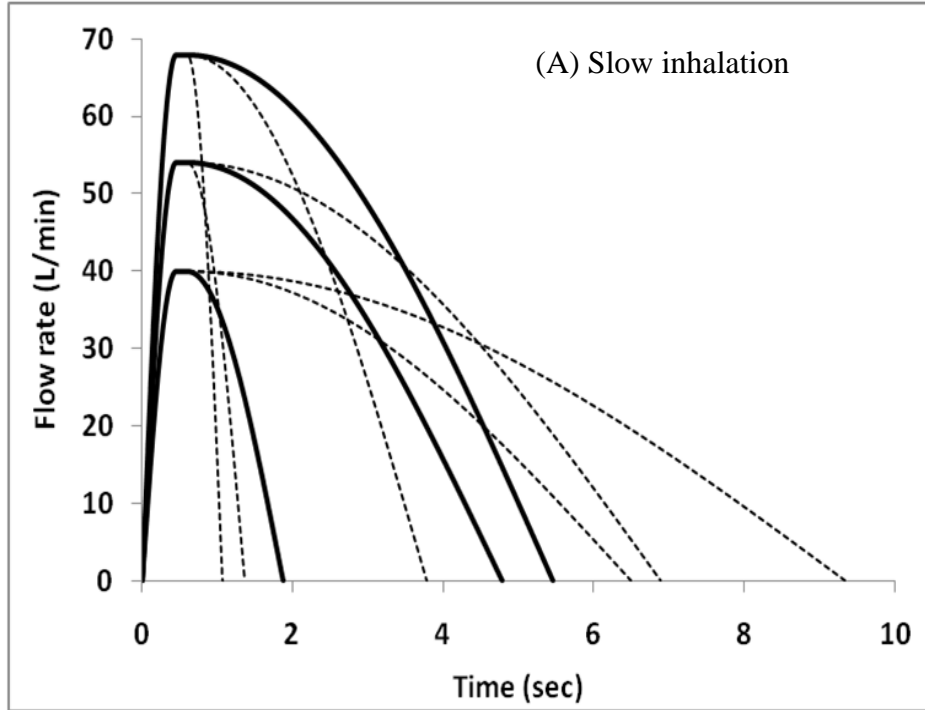


Figure 3.4: Simulated air flow rate versus time curves representing ~95% of the range reported by Newman et al for the Budelin testing (Newman et al, 2000) for **(A) Slow inhalation arm:** Reported values for PIFR and V (54 ± 7 L/min and 2.77 ± 0.97 L, respectively) were processed to yield *in vitro* flow rates at t_{\max} of 40, 54 and 68 L/min (mean ± 2 SD). Small, medium and large values for V were calculated similarly (0.83, 2.77, 4.77 L) except V_{large} was held constant at 4L, the maximum feasible value for *in vitro* testing with the breath simulator. Only bold profiles were used *in vitro* where small, medium and large volumes were paired with small, medium and large flow rates to provide an estimate of the expected deposition variations corresponding to 95% of Newman et al's clinical population (Newman et al, 2000). Using the similar method described above the simulated airflow profiles to represent for **moderate** and **fast inhalations** arms were generated and are shown in **Figure 3.4 (B)** and **3.4 (C)**, respectively.

In all experiments, the calibrated piston in the breath simulator was programmed to increase air flow rate through the apparatus over an acceleration phase to the chosen value for PIFR at $t_{max} = 0.45s$ according to

$$FR(t) = PIFR \times \sin\left(\frac{\pi}{2} \frac{t}{t_{max}}\right) \quad (\text{Eq.3.1})$$

At $t > t_{max} < 0.6s$, FR was held constant at PIFR, after which flow rate was decreased to zero according to

$$FR(t) = PIFR \times \cos\left(\frac{\pi}{2} \times \frac{t-(t_{max}+0.15)}{t_{total}-(t_{max}+0.15)}\right) \quad (\text{Eq. 3.2})$$

The value for t_{total} , the time for completion of an inspiratory maneuver, was varied so that V, the total volume inhaled (or the area under each FR vs. time curve; Figure 3.4), corresponded to either the mean or mean \pm 2SD reported in the clinical deposition study for Budelin by Newman et al (Newman et al, 2000).

In vitro experiments were randomized with respect to the selection of paired values of PIFR and V (see Table 3.3) and the choice of model. Each *in vitro* experiment was performed 5 times and the average (\pm SD) and absolute range of data for mass of drug retained in different sections of the apparatus determined by chemical analysis.

3.2.3 ANALYSIS

Budesonide was recovered from the different sections of the apparatus with a mixture of 30 parts 0.1%v/v acetic acid in water plus 70 parts methanol by volume. This solvent system was the same as the mobile phase used for budesonide analysis by HPLC method described in Chapter 4, Section 4.2. Drug amounts were calculated from the products of concentration x volume.

3.2.4 IN VITRO-IN VITRO CORRELATIONS (IVIVC)

The results for % drug deposition in each *in vitro* region were compared to those from *in vivo* gamma scintigraphic studies on Budelin Novolizers in normal adult volunteers of both genders by Newman et al (Newman et al, 2000). Inhalation profiles were chosen *in vitro* to represent both the average and extreme inhalation maneuvers used in the clinic to follow drug deposition of single 200 µg doses of radio-labeled budesonide.

3.3 RESULTS AND DISCUSSION

3.3.1 SCALED PHYSICAL MODELS OF THE UPPER AIRWAYS

A literature validation of the small, medium and large sized MT-TB models was performed by comparing their physical dimensions to data reported for normal human adults of both genders. Table 3.1 shows the internal dimensions of the MT used in this study alongside the means and relative standard deviations reported by Burnell et al following their analysis of the MRI scans of 20 adult volunteers using 4 different inhalers (Burnell et al, 2007). While small differences in the dimensions of the different regions were noted, the internal areas, volumes and angles of the MT_M used in this study were close to the mean values reported by Burnell et al. (Burnell et al, 2007) and the range of dimensions in our models fell within the reported 95% confidence intervals with the exception of 2 outliers (Table 3.1). While the starting point for the “medium sized” model employed here was a simplified elliptical version of the MT taken from a cast of an average sized human (Xi & Longest, 2007), Burnell et al used MRI scanning from subjects actually using inhalers. Furthermore, they reported that the single most influential variable affecting drug retention in their models was throat model volume. That feature (mean and variance in volume) showed close agreement to the scaled models described in the present study in large part because our volumetric dimensions were scaled to broadly correspond to the confidence limits described by Burnell et al (Burnell et al, 2007). Until very recently Burnell’s models were not publically available, although this situation has now been partly remedied by the publication of the details of a single model, purported to be of those used in the study by Olsson et al (Olsson et al, 2008). The geometric characteristics of the physical models described here can be downloaded as shown in Figure 3.2. Notably also, the MT models described by

O'Callaghan's group show a mean volume of 61.86 cm^3 , comparable to the value of 61.6 cm^3 for our medium sized model (Ehtezazi et al, 2010). Thus, it appeared that our mouth-throat models were a reasonably accurate representation of the upper airway encountered by inhaled aerosols across both genders in a normal adult population in a future study it is intended to perform more systemic comparison of our MT_M model dimensions with that made available recently by the industry consortium. Notably, the length scale factors of 1.165 (e.g. $[102.8 \text{ cm}^3/65 \text{ cm}^3]^{0.333}$) and 0.748, respectively that we have used here differ from those advocated by Finlay et al of 1.3 and 0.7 (Finlay et al, 2010). Furthermore, while our models presently fail to account for dynamic changes that result from inhalation effort (Byron et al, 2010b; Ehtezazi et al, 2004), it is not yet known how much such changes in volume actually affect airway drug deposition *in vivo*.

Table 3.1: Actual dimensions of the MT region of the medium, small and large models (without mouthpiece adapter; Figure 3.2) in comparison with the mean (2*SD) data of Burnell et al (Burnell et al, 2007). Outliers (values in which the small or large models had dimensions outside of Burnell’s 95% CI) are bold and underscored. The volumes of the TB regions are not included in this Table.

Parameters[#]	MT-TB_S	MT-TB_M	MT-TB_L	Burnell et al.
MT volume (cm ³)	26.6	61.6	96.1	60.7 (37.8)
Buccal volume (cm ³)	15.0	33.9	52.3	35.1 (28.0)
Angle bcd	340	340	340	350 (10.5)
Angle cda	260	260	260	251(18.6)
Amin (mm ²)	228	408	554	293 (328)
Amax (mm ²)	344	614	833	1032 (908)
Bmin (mm ²)	140	251	340	272 (277)
Bmax (mm ²)	297	531	<u>720</u>	368 (294)
Cmin (mm ²)	47	84	114	127 (109)
Cmax (mm ²)	117	209	284	431 (276)
Dmin (mm ²)	58	104	141	133 (96)
Dmax (mm ²)	<u>105</u>	188	255	263 (95)
Length ad (mm)	17.2	23	26.8	27.1 (19.9)

[#]Terms describing dimensions (e.g. Bmin, Dmax etc) were defined in Table 2 and Figure 3 of Burnell et al., 2007

Table 3.2 shows the internal luminal dimensions of TB used in this study, alongside the values and variations reported in the literature for adults of both genders. All dimensions are for normal adults. As described earlier, the “medium sized” TB geometry was scaled from Yeh and Schum (Yeh & Schum, 1980) to a lung volume = 3.5L and paired with the “medium – sized MT” to create MT-TB_M. Small and large TB geometries, for pairing with the small and large MT models described above, were derived from TB_M using the same factors and methods used to produce the scaled versions of the MT. This resulted in models that showed close agreement with dimensions for normal adults in the literature; in particular, dimensional variations reported as two standard deviations by Montaudon et al (Montaudon et al, 2007) agreed well with luminal diameters of our MT-TB_L and MT-TB_S models (Table 3.2).

Table 3.2: Luminal diameters (mm) for generation 0 through 3 (Figures 3.1 and 3.2) of MT-TB_{M,S,L} (shown in bold type) in comparison with values reported in the literature.

Generation	0 (trachea)	1	2	3
MT-TB_M	17.2	13.4	9.92	7.2
Montaudon: mean (Montaudon et al, 2007)	18.5	13.9	10.4	6.8
Nikiforov: mean (Nikiforov & Schlesinger, 1985)	-	14.2	9.10	6.3
Weibel: mean (Weibel, 1964)	18	12	8.3	5.6
Horsfield and Cumming: mean (Horsfield & Cumming, 1968)	16	12.0(R), 11.1(L)	-	-
Raabe et al.: mean (Raabe et al, 1976)	20.1, 23.5	17.5(R), 13.8(L) 18.5(R), 14.5(L)	-	-
MT-TB_L	20.0	15.6	11.5	8.4
Montaudon: mean+2SD (Montaudon et al, 2007)	21.7	16.7	12.2	8.4
MT-TB_S	12.9	10.0	7.4	5.4
Montaudon: mean-2SD (Montaudon et al, 2007)	15.3	11.1	8.6	5.2

R, L = Right and left lung; SD = standard deviation

We reviewed several additional dimensions in a similar way to that described above and in Table 3.2. For example, we compared values for the cross-sectional areas and the length and variability of different airway generations in our models to those from the airways of adults in the literature (Cherng et al, 2002; Montaudon et al, 2007; Vock et al, 1984). While dimensional values taken from the literature were comparable to those of our models, it became apparent that this approach was data heavy and unrealistic. Furthermore, because the literature used different methods and our models were simplified in several respects (e.g. tracheal rings are omitted and circular connecting segments are assumed in our models; Figure 3.1 and 3.2) for the purpose of an overall comparison, internal volumetric comparisons, like that for MT, were thought to be best. Internal tracheal volumes for our small, medium and large TB models were 9.5, 22.7 and 36.0 cm³ respectively. These were very similar to the mean tracheal volume ($\pm 2SD$) as reported by Leader et al of 22.6 (7.2 to 38.0) cm³ (Leader et al, 2004). However, because luminal volume *in vivo* was difficult to define precisely (length depends on the way that the position of bifurcation is defined and variations in diameter and cross sectional shape are reported to occur with length and inspiratory flow rate (Fouke et al, 1981; Osmanliev et al, 1982), even these comparisons are challenging. Thus, because our aim was to relate variations in regional drug deposition to airway geometries seen across a population of normal adults, we hypothesized that our models were valid for this purpose. To test that hypothesis we built the models and sought to determine whether they were able to predict clinical variations seen in drug deposition. In short, only if the models described in Figure 3.2 failed to predict clinical deposition data did we plan to incorporate further physical details. If the models proved to be predictive however, we planned to use them and vary, test and report the effect of certain usage variables such as inhaler insertion angle, depth of insertion, etc.

3.3.2 IN VITRO DEPOSITION TESTING AND IVIVC

While several *in vivo* imaging methods are possible to define the deposition of radio-labeled drug aerosols (Newman, 2009b) two dimensional gamma scintigraphy has become the most popular technique for studying this topic *in vivo* (Scheuch et al, 2010). While efforts continue to standardize the details of the method (Scheuch et al, 2010; Newman, 2009b), Newman and his colleagues have led this field for some time and are an accepted source of inhaler scintigraphy data. Accordingly, we selected their study of Novolizer (Newman et al, 2000) as a data-rich source of drug deposition information with which to compare our *in vitro* results; while many aerosol deposition studies can be criticized for providing only meager details of the method used, theirs' is the one that offers some important details. Their study of budesonide deposition contained descriptions of the inspiratory maneuvers used by 13 trained adult volunteers. Each volunteer was trained to inhale at fast, moderate and slow flow rates through Novolizer containing ^{99m}Tc labeled budesonide in a cross over study (Newman et al, 2000). Comparative *in vitro* particle size analyses showed that radioactive counting and drug assay produced statistically comparable data, showing that the ^{99m}Tc label was a valid drug marker and that the labeling process did not perturb aerosol emissions from the inhaler (Newman et al, 2000). Such a proof of similarity between the APSD of the drug from a DPI tested under standard conditions and the radiolabel plus drug of a labeled inhaler is now recognized as an essential step if gamma scintigraphic deposition studies are to be accepted as evidence of drug deposition in a clinical study. In some cases, this step is lacking, leading to frail conclusions concerning drug deposition *in vivo* (to be discussed in Chapter 4). Total and regional lung deposition, oropharyngeal deposition and inhaler mouthpiece retention were quantified as % total radioactive counts, following standard corrections for quenching and radioactive decay. Because

of the overlay of the esophagus and the trachea in 2D scintigraphy, *in vivo* lung deposition is often expressed without including the trachea as part of the lung and this was the method used in the scintigraphic evaluation of Budelin (Newman et al, 2000) [Newman, SP: Personal Communication, 2009]. Because of this anatomical inaccuracy, we assayed tracheal deposition separately *in vitro* and included it with drug deposited in the mouth-throat (Table 3.3).

Table 3.3: *In vitro* and *in vivo* results for % budesonide (Mean (SD); n= 5) deposition from Budelin Novolizers in small, medium and large MT-TB models using inhalation profiles selected to represent the mean and extreme values for PIFR and V of Newman et al (Newman et al, 2000).

MT-TB Model ^a	PIFR (L/min) ^b	V (L) ^b	Device ^c	MT ^d	TLD (TB+P-trachea) ^e	<i>In vivo</i> TLD ^f
Fast inhalation						
MT-TB _S	73	1.11	48.36 (4.27)	40.08 (5.98)	11.55 (1.97) (9.72-13.99)	Lower limit=9.4
MT-TB _M	99	3.13	14.14 (2.47)	55.95 (2.92)	29.92 (1.35) (29.02-31.78)	Median 32.1
MT-TB _L	125	4.00	13.26 (1.65)	48.58 (2.83)	38.20 (1.73) (35.94-40.44)	Upper limit=41
Moderate inhalation						
MT-TB _S	59	1.30	49.48 (4.27)	40.09 (5.51)	10.43 (1.92) (8.03-13.15)	Lower limit=12.1
MT-TB _M	65	2.96	16.08 (4.97)	62.24 (5.84)	21.68 (1.32) (20.38-23.81)	Median 25
MT-TB _L	71	4.00	14.35 (1.81)	58.88 (1.95)	26.71 (1.93) (23.48-28.69)	Upper limit=37.4
Slow inhalation						
MT-TB _S	40	0.83	55.43 (11.37)	39.12 (12.06)	5.45 (1.23) (4.82-7.51)	Lower limit=8.8
MT-TB _M	54	2.77	23.45 (5.60)	61.08 (4.93)	15.52 (1.96) (13.88-18.61)	Median 19.9
MT-TB _L	68	4	12.65 (1.33)	62.28 (1.41)	25.07 (2.46) (22.86 – 27.97)	Upper limit=26.6

^aMT-TB_S , MT-TB_M or MT-TB_L ; ^bmean±2SD reported by Newman as shown in Figure 3.4; ^cmouthpiece and dosing chamber/air classifier; ^dMT includes trachea; ^eTotal lung dose and experimental range (**bold**=*in vitro* values differ from clinical estimate); ^f% deposition values from Table 3 in Newman et al. (Newman et al, 2000)

Results for total lung deposition *in vivo* and *in vitro* are compared head-to-head in Table 3.3 and Figure 3.5. Clearly, the *in vitro* results for TLD (the drug recovered from TB (minus trachea) and P (artificial thorax and filter)) were associated with the inhaler test conditions as well as the MT-TB models chosen to span 95% of the range of airway geometries. While some of the clinical values fell outside of the *in vitro* range (shown in bold in Table 3.3), the overall similarity between lung deposition values reported by Newman et al (Newman et al, 2000) and the *in vitro* estimates was remarkable. With the exception of MT-TB_L at moderate flow and 4L volume, low, mean and high deposition values predicted in each model were close to the clinical results throughout (Newman et al, 2000), implying that our *in vitro* method produced meaningful results.

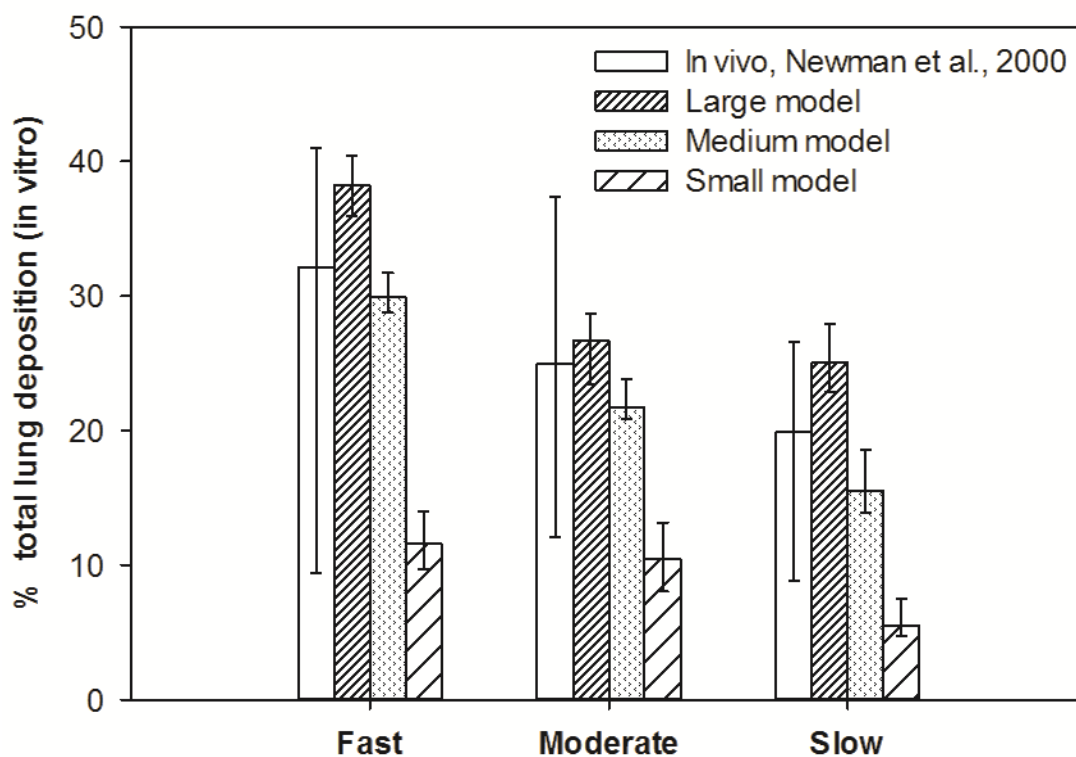


Figure 3.5: The total lung dose (TLD; Table 3.3) from Budelin following *in vitro* testing at the mean and extremes of flow and volume in each of the 3 MT-TB models following fast, moderate and slow inhalation shown in comparison to median *in vivo* values reported by Newman et al (Newman et al, 2000). Error bars show the entire deposition range in all cases.

The agreement shown in Table 3.3 between *in vivo* and *in vitro* results also appeared to support the way in which *in vitro* testing extremes were chosen in the present study, to minimize the number of *in vitro* tests required while still reflecting and predicting the overall deposition variations seen in the clinic. In practice, we first selected a powder inhaler that emptied reliably (Delvadia et al, 2010), avoiding the need to deal with dosage form variability as a significant source of additional variance in the present study. Then, we studied the effect of 3 separate test conditions and three major variables (model geometry, PIFR and V). However, out of a possible 3^3 experimental matrix, we studied the subset of cases described in Table 3.3. To reduce the size of the matrix we hypothesized that in each of Newman's cross over study arms [in each arm, the same 13 adults, (with different geometries) were instructed to inhale at low, moderate or high flow rates], upper and lower flow rate extremes (e.g. 40 and 68 L/min at the low flow condition; Figure 3.4) were coupled with the extreme small and large lung volumes (e.g. 0.83 and 4.77 L; Figure 3.4). We also coupled small, medium and large profiles to S, M, and L models; the assumption, that the extremes of each inhalation maneuver, studied over the range of geometries seen across a normal male and female adult population, should describe the vast bulk of the variation seen in drug deposition in the clinic. The agreement between the *in vitro* results and the variations seen in budesonide deposition are shown most dramatically in Figure 3.5. *In vitro* variance in TLD for a given model under a given set of test conditions was small, reflecting the reproducibility of this inhaler when tested *in vitro*. However, the mean and the range of results *in vivo* was entirely predictable when the tested variations were created by coupling different breathing maneuvers and different airway geometries based on their ranges displayed in this mixed gender adult population; this in spite of the *in vitro* models' inability to account for dynamic changes resulting from inhalation effort (Byron et al, 2010a; Ehtezazi et al, 2004). Our

findings were also consistent with the results reported by Olsson et al (Olsson et al, 2008) in their IVIVC for inhaled budesonide. In that study, total drug dose *in vitro* was evaluated pharmacokinetically, after oral absorption was prevented using charcoal-block technique (Olsson et al, 2008).

Budesonide retention in the (Novolizer) device, MT (including trachea) and TB+P (TLD) for all *in vitro* test conditions (Table 3.3) is shown in Figure 3.6 in comparison with the *in vivo* results reported by Newman et al (Newman et al, 2000). Most deposition was either in the device, MT or the peripheral *in vitro* compartment (Plexiglas container and filter). While this statement was true for all models, and TB deposition from Budelin (in the absence of the model trachea) was <1% of the total recovered dose for all tested inhalation profiles, results for other inhalers to be reported elsewhere, shows that TB deposition *in vitro* depends on the choice of inhaler, drug and formulation. Notably, and consistent with our *in vitro* results for Budelin, Newman reported significant peripheral deposition *in vivo* and no change in the central/peripheral distribution ratio as a function of slow, moderate or fast inhalation (Newman et al, 2000). One significant disagreement between the *in vitro* and *in vivo* results in Figure 3.6 appeared to be for inhaler device retention in the case of the small model at low flow and volume extremes (Device; cross hatched bars; Figure 3.6); deposition or retention in the inhaler *in vitro* appeared to overestimate the *in vivo* determination (Newman et al, 2000). Our current explanation for this discrepancy for Novolizer, a powder inhaler whose emptying is known to be affected by volume and flow rate (low volumes and low flow results in incomplete emptying) (Byron et al, 2010a; Weda et al, 2004) relates to the necessary but unrealistic test conditions used during *in vivo* investigations (radio-labeled powder is loaded and emptied, dose by dose to minimize risk); furthermore, validation of radiolabeling in *in vivo* study was only performed at

the ‘medium inhalation flow condition’; in short, we believe that our *in vitro* determinations (Figure 3.6) for the commercial product are broadly correct, because these involve the device’s self-metering capabilities, with its cartridge-packed powder reservoir in place (Weda et al, 2004).

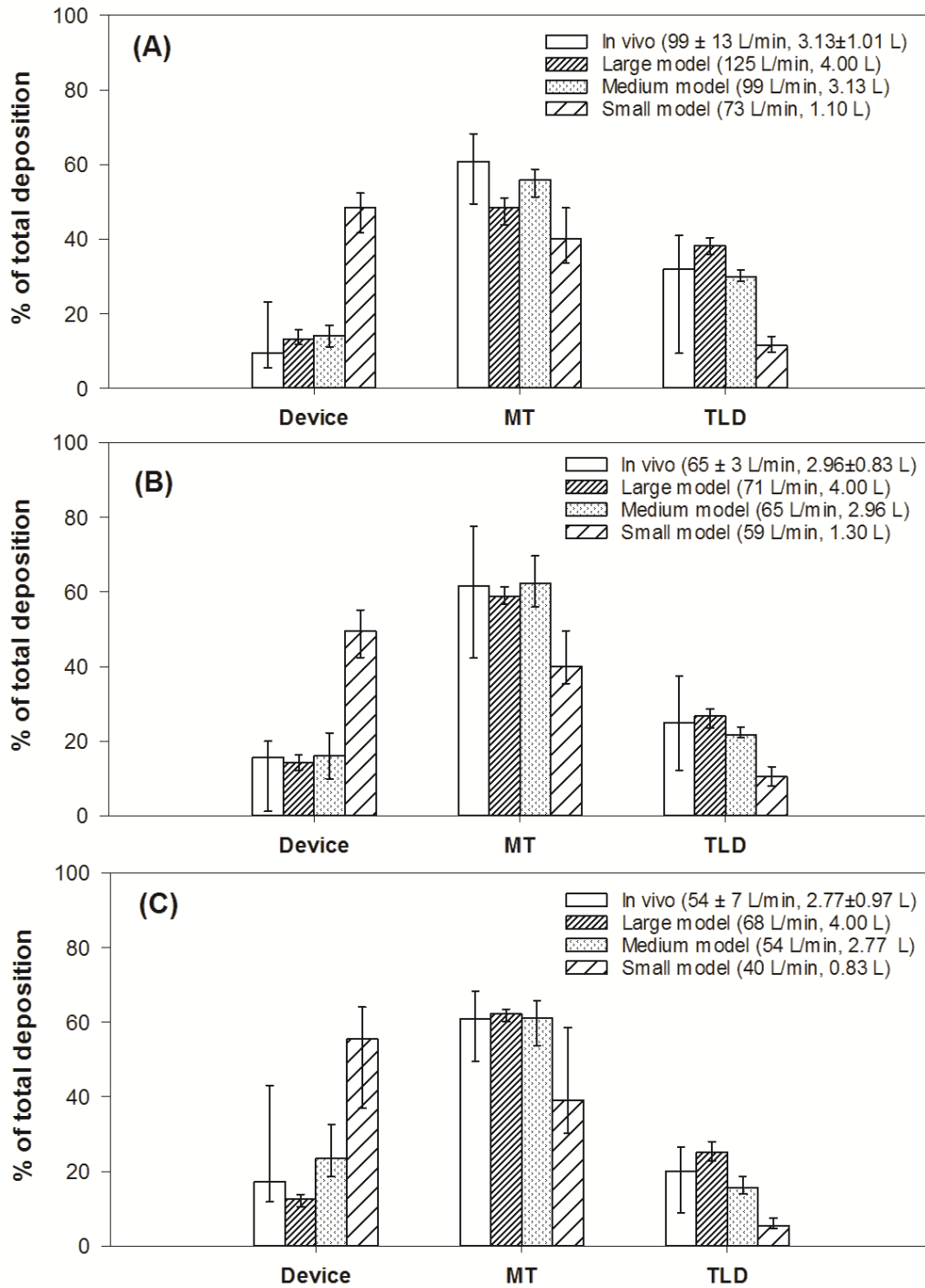


Figure 3.6: *In vitro* and *in vivo* deposition results for Budelin across the test conditions listed in Table 3.3 (A) fast inhalation (B) moderate inhalation and (C) slow inhalation. MT includes the trachea; TLD excludes the trachea *in vitro* and *in vivo*.

3.4 CONCLUSIONS

In conclusion, we have described new physical models that, when partnered with appropriate inhalation flow rate vs. time profiles provide excellent predictions of the median and range of lung deposition results *in vivo* for a trained normal population using a marketed powder inhaler. It is clear from the results that the bulk of *in vivo* variance in deposition across a trained population of normal volunteers was explained by variations in airway morphology and the way that the inhalation maneuver was performed. In the case of Budelin Novolizer, there was little additional variance in drug delivery due to the device or formulation and the present physical airway models appeared to offer the means to predict the *in vivo* results; in short, the reported IVIVC appears to be valid for this inhaler. With the goal of adding further weight to these test methods, we have reported the results for other powder inhalers, for which *in vivo* results are also available in the literature, in Chapter 4.

CHAPTER 4

IVIVCS FOR DIFFERENT DRY POWDER INHALERS IN NORMAL ADULTS

4.1 INTRODUCTION

Dry powder inhalers (DPIs) are often judged on the efficiency and reproducibility with which they deliver drug to the lungs (Newman & Chan, 2008). Hence, *in vitro* methods that can predict the regional deposition pattern and fractionation of the aerosol drug dose from inhalers are of interest to clinicians, inhaler developers and regulatory agencies. To be accepted as surrogates for *in vivo* studies, these *in vitro* methods should be accurate and precise. While it is a separate challenge to develop such methods for pMDIs and inhalers that create drug aerosols in the absence of the patient's inspiratory effort, dry powder inhalers must take into account the DPI-patient interaction (Byron et al, 2010b). Moreover, because variability in DPI design and formulation is considerable, any useful *in vitro* method must be able to demonstrate that its results are predictive across a wide range of products and that the method is unbiased.

In our previous study (Chapter 3), we described different airway models of the mouth - throat, trachea and upper bronchi that, after scaling could create small, medium, and large versions (MT-TB_S, MT-TB_M, MT-TB_L) that together spanned 95% of the geometric variation

seen in the upper airways of normal human adults of both genders. When these models were parsed with the simulated inhalation maneuvers (and used in the equipment setup shown in Figure 3.3) it proved possible to predict median lung deposition and its 95% confidence limits, in differently trained healthy adults, from Budelin Novolizer. To extend our previous findings, the present study was aimed to assess the robustness of these *in vitro* methods for predicting ‘average’ *in vivo* deposition patterns in normal adult humans across a range of different DPIs. Airway drug deposition patterns from five marketed DPIs were determined *in vitro* and compared to literature values reported following gamma scintigraphy studies in healthy volunteers to evaluate the *in vitro* – *in vivo* correlation stoichiometry across inhalers from different manufacturers.

4.2 MATERIALS AND METHODS

4.2.1 PHYSICAL MODEL OF THE UPPER AIRWAYS AND TEST APPARATUS

An anatomically accurate airway model of the mouth-throat, trachea and upper generations of the bronchial tree (MT-TB) was used to assess aerosol drug deposition from 5 different marketed DPIs. This model and the methods used to study airway drug deposition from inhalers have been described in detail previously in Chapter 3. The complete geometry of the MT-TB_M model that was used for *in vitro* testing is the same as that described as the “medium” model in the previous study. Briefly, the model consisted of a characteristic MT geometry developed by Xi and Longest (Xi & Longest, 2007), the trachea, and the first three bifurcations of the upper TB airways based on the data of Yeh and Schum (Yeh & Schum, 1980) scaled to approximately adult medium-size dimensions (Tian et al, 2011a, Tian et al, 2011b). The MT-TB_M model was constructed from laser cured resin (Accura 60, 3D System, Valencia, CA) using rapid prototyping (Viper SLA, 3D Systems), housed in a Plexiglas chamber with the mouth throat (MT) section exposed for attachment to different inhalers (Figure 3.3). Suitable mouthpiece adaptors were created to connect the mouthpiece of each inhaler to the mouth inlet of the model so that air could be drawn through the assembly according to breath-simulator defined flow profiles (Figure 4.1). The MT-TB model and a sample mouthpiece adapter as used in this study are freely available for download from the RDD Online website (Longest, 2011).

4.2.2 MATERIALS

The commercial DPIs used in this study are shown in Table 4.1. DPIs were chosen based on the availability of gamma scintigraphy studies in the literature performed in normal adults for which inspiratory profile information was either reported or could be reasonably deduced. All

inhalers were obtained from pharmacy outlets in either the USA or UK. Chemicals and solvents used in the study were HPLC grade obtained from Fisher Scientific (Pittsburgh, PA). Drug analysis employed reverse-phase HPLC analysis with a Waters HPLC separations module and photo-diode array detector (Waters models 2690 and 2996, Waters Corporation, Milford, MA, USA). Separation columns and assay conditions are shown in Table 4.3.

Table 4.1: Summary of commercial DPIs studied alongside gamma scintigraphy study details in healthy volunteers taken from the literature (Borgstrom et al, 1994; Brand et al, 2007; Cass et al, 1999; Meyer et al, 2004; Vidgren et al, 1994).

DPI	Formulation	R [#]	N (MF)	Inhalation Training	D	PIFR (L/min)	V (L)
Spiriva [®] HandiHaler [®]	18 µg tiotropium and lactose	0.0467	5 (3,2)	trained using product information	2	NR	NR
Foradil [®] Aerolizer [®]	12 µg formoterol fumarate and 25 mg lactose	0.0176	10 (6,4)	trained using product information	2	84.5 (30- 130)*	NR
Salbutamol Easyhaler [®]	200 µg salbutamol sulfate and lactose	0.0435	8 (7,1)	trained to inhale “rapidly and forcefully”	1	57.8±15.9	NR
Pulmicort [®] Turbuhaler [®]	“pelletized” 200 µg budesonide	0.0352	10 (5,5)	trained to inhale at PIFR = 60 L/min	4	58 (53–64)	2.90 (2.07– 4.97)
Relenza [®] Diskhaler [®]	5 mg zanamivir and 20 mg lactose	0.0198	13 (5,8)	NR	2	84.8±16.2 83.2±17.7	2.71±1.02 2.84±1.06

apparent airflow resistance of test inhaler ($\text{kPa}^{0.5} \cdot \text{L}^{-1} \cdot \text{min}$) based on linear regression of pressure drop^{1/2} versus flow rate profile. D: number of doses inhaled; PIFR: Reported Peak Inhalation Flow Rate; V: Reported Inhalation Volume (experimental ranges and \pm SD are shown as reported ; NR: not reported; N: total number of healthy volunteers, M: Male, F: Female; * estimated from Figure 1 of reference (Meyer et al, 2004)

4.2.3 IN VITRO DEPOSITION TESTING

The general method used to assess *in vitro* regional deposition from the different inhalers has been described in detail previously in Chapter 3. The ‘medium’ airway model was installed in a purpose-built airtight Plexiglas[®] housing (artificial thorax) connected to a programmable breath simulator capable of pulling air at variable flow rates as shown in Figure 3.3. Before each deposition experiment, internal surfaces of the model were coated with either glycerol: methanol mixture (1:2) or silicone fluid (Dow Corning[®] 316 Silicone Release Spray, Dow Corning Corp., Midland, Michigan, USA) to prevent re-entrainment after particle deposition. When activated, the breath simulator pulled air, through the inhaler, model, chamber housing and filter using a flowrate profile typical of inhaler use *in vivo* (Table 4.2 and Figure 4.1). Simulated inhalation flow rate versus time profiles used for the *in vitro* studies are shown in Figure 4.1. Simulated profiles were created and replicated by the breath simulator (ASL 5000, IngMar Medical, Pittsburgh, PA, USA) as described in detail previously in Chapter 3. Values for PIFR and V (Figure 4.1) were chosen based on the inhalation parameters reported in the literature for trained normal adults as described in Table 4.1 except for Handihaler[®] (Borgstrom et al, 1994; Cass et al, 1999; Chodosh et al, 2001; Meyer et al, 2004; Newman et al, 2001; Vidgren et al, 1994). For Handihaler values for PIFR and V were chosen based on the mean values reported in patients as shown in Table 4.2 and Figure 4.1. In all cases, inhalation flow profiles were chosen that were specific to the inhaler and the reported or likely inspiratory profile used by subjects during gamma scintigraphic deposition studies (Table 4.1).

Table 4.2: Summary of *in vitro* testing conditions. PIFR and V values that comprised the “average” air flow profiles (Figure 4.1) were either derived from clinical reports in Table 4.1 or, when these were not reported, they were estimated (shown in **bold**) based on (a) Newman et al (Newman et al, 2001) (Easyhaler) or (b) values reported in the literature for inhalers with comparable resistances (Aerolizer[®] and Handihaler[®] (Chodosh et al, 2001; Meyer et al, 2004).

Inhaler	PIFR (L/min)	V (L)	Actuation ^a	Drug Solvent used for recovery
Spiriva [®] Handihaler [®]	30	2.62	Two doses/ one inhalation per dose	ammonium formate buffer (20mM, pH 3.4)
Foradil [®] Aerolizer [®]	84.5	2.78	One dose/ two inhalations	deionized water
Salbutamol Easyhaler [®]	57.8	2.62	One dose/one inhalation	deionized water
Pulmicort [®] Turbuhaler [®]	58	2.90	One dose/ one inhalation	31% acetic acid (0.1% v/v) + 69% methanol
Relenza [®] Diskhaler [®]	84	2.78	One dose/ one inhalation	deionized water

^aActuation represents the numbers of doses inhaled/ number of inhalations per dose.

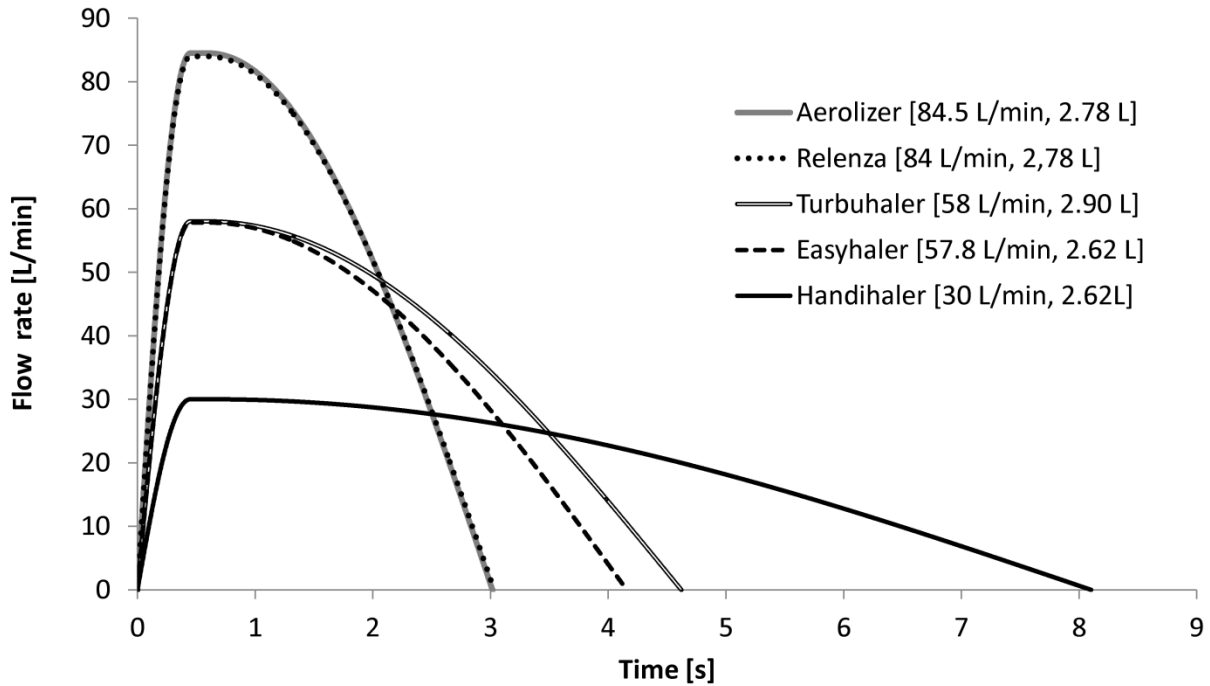


Figure 4.1: Simulated ‘average’ flow rate vs. time profiles used in testing different DPIs. Profiles were generated using methods described in detail previously in Chapter 3 to represent reported or estimated values for PIFR and V from clinical testing of DPIs in normal human volunteers. PIFR was held constant between $T = 0.45$ and 0.6 s in each case. Values for inhaled volume, V, for Aerolizer[®] and Handihaler[®] were not reported in the literature (Table 4.1); test values for those inhalers (Table 4.2 and here) were estimated from reports for Relenza[®] and Easyhaler[®] (based on their comparable airflow resistances).

Drug deposited in the various regions of the model and the DPI device was recovered using appropriate volumes of solvent as listed in Table 4.2. Total drug recovery was calculated by adding the drug deposited in the device, MT (including the trachea) and total lung (bronchi + chamber + filter) as described previously in Chapter 3. Regional deposition results were expressed as % of total drug recovery. Inhalers were tested as if they were being used in practice according to their package inserts; thus, for 3 of the 5 of the inhalers single doses were actuated once while for Aerolizer, each capsule was actuated using two separate flow rate versus time profiles to ensure good device emptying. Also, in the case of Handihaler, two capsules were used for each *in vitro* deposition experiment to achieve drug concentrations well within the quantification range of the analytical method (Handihaler package insert; Aerolizer clinical study (Brand et al, 2007) and personal communication). Before testing, each HPLC method (see summaries in Table 4.3) was validated according to ICH guidelines ("International Committee for Harmonization Q2B: Validation of Analytical Procedures: Methodology,") and shown to have inaccuracy and imprecision values below 3% in all cases (Appendix B). Each *in vitro* deposition experiment was performed five times.

In order to further assess the validity of deposition predictions based on these methods, results for mean % drug deposition in each *in vitro* region were compared to those from the *in vivo* gamma scintigraphy studies listed in Table 4.1 (Borgstrom et al, 1994; Brand et al, 2007; Cass et al, 1999; Meyer et al, 2004; Vidgren et al, 1994) for each of the inhalers investigated.

Table 4.3: Reverse-phase HPLC methods for drug assay. All methods employed Waters 2690 HPLC separations modules and a Waters 2996 PDA detector (Waters Corporation, Milford, MA). HPLC conditions and columns were as shown.

Drug	Mobile Phase	Column	Flow (mL/min)	Detection wavelength (nm)	Linear calibration Range (µg/mL)
Tiotropium bromide	25% ammonium formate buffer (20mM, pH 3.4) + 75% methanol in water	Restek PFP propyl (3.2 x 150 mm, 5 µm; Restek, Bellefonte, PA, USA)	0.75	236	0.05-2.50
Formoterol fumarate (Akapo & Asif, 2003)	65% ammonium acetate buffer (50mM, pH 5.0) + 35% methanol in water	Symmetry C ₁₈ (4.0 x 100 mm, 3.5 µm; Waters Corporation, Milford, MA, USA)	1.00	242	0.10-1.0
Albuterol sulfate	30% ammonium formate buffer (20mM, pH 3.4) + 70% methanol in water	Restek PFP propyl (3.2 x 150 mm, 5 µm; Restek, Bellefonte PA, USA)	0.75	276	0.10-10
Budesonide (Martin et al, 2002)	31% acetic acid (0.1% v/v) + 69% methanol in water	Symmetry C ₁₈ (4.0 x 100 mm, 3.5 µm; Waters Corporation, Milford, MA, USA)	1.00	245	0.20-10.00
Zanamivir (Kamiya et al, 2009)	50% phosphate buffer (35mM, pH 2.5) + 50% acetonitrile in water	Partisil 10 SCX (4.6 x 250 mm, 10 µm; Whatman Inc., Piscataway, NJ, USA)	1.20	238	5.00-100.00

4.3 RESULTS AND DISCUSSION

The five DPIs used in this study differed in many respects. The drug, drug formulation, metered and delivered doses, aerosol dispersion mechanisms (Islam & Gladki, 2008; Newman & Peart, 2009a; Son & McConville, 2008) and air flow resistances all varied markedly (Table 4.1). The labeled drug dose across inhalers ranged from 12 μg (Foradil Aerolizer) through 5 mg (Relenza Diskhaler). The inhalers also covered the range of airflow resistances that is typical across all commercial DPIs that are presently available. Relenza and Aerolizer are examples of low resistance inhalers; Handihaler and Easyhaler have high resistances, while Turbuhaler fell between these extremes (Table 4.1). Even though our previous work in Chapter 3 implied that our *in vitro* tests were good predictors of *in vivo* drug deposition and that a 1:1 IVIVC was possible we performed this study with the inhalers in Table 4.1 to further challenge the predictivity of our methods across products with a range of different properties.

Unfortunately, published *in vivo* deposition studies on inhalers are rarely as well designed or described as those of Newman et al. with the Budelin Novolizer, which described both the subjects and the multiple ways in which those subjects were trained to inhale (Newman et al, 2000). Based on this data, it was possible to study the performance of the newly described *in vitro* methods in small, medium and large MT-TB models across a range of reported *in vivo* air flow profiles as described Chapter 3. This approach was used to create an IVIVC to show the median and the likely 95% confidence limits of drug deposition from Budelin in the lung. Because of the way that the *in vivo* drug deposition studies for inhalers shown in Table 4.1 were executed and reported such a thorough approach involving confidence limits was not possible. Instead, the present study was designed to evaluate the “average” drug deposition predictions for different inhalers *in vitro*, following the use of the medium airway model (MT-TB_M) coupled

with inhalation profiles based on those used *in vivo*. These *in vitro* deposition results were compared to the “average” *in vivo* values from scintigraphy in normal volunteers to create and evaluate IVIVCs for different products (Borgstrom et al, 1994; Brand et al, 2007; Cass et al, 1999; Meyer et al, 2004; Vidgren et al, 1994).

It is important to recognize that the *in vitro* determinations were performed by direct drug assay following the use of “in date” commercially-produced inhalers that had been subjected to regulatory inspection and quality control. In the selected *in vivo* studies from the literature, volunteers inhaled ^{99m}Tc radio-labeled drug formulations and the label, not the drug, was used to assess deposition (Borgstrom et al, 1994; Brand et al, 2007; Cass et al, 1999; Meyer et al, 2004; Vidgren et al, 1994). In the selected studies the labeling process was reported to produce comparable aerodynamic particle size distributions (APSD) to the unlabeled drug products by impingement/impactor testing under constant flow conditions. Notably however, radio-labeling techniques that are routinely used to prepare these physical admixtures of label and the dry powder drug formulation are rarely without problems. For example, due to short radioactive half life concerns, APSDs are usually only checked for formulations that are not actually administered to volunteers while those doses that are administered are prepared and used in “one-off” experiments following radiolabeling procedures that are far from robust (Dolovich, 2004). To create the correlations described here, the gamma camera counts are reported from different regions after correction for radioactive decay, tissue attenuation and scattering. With the exception of Easyhaler, in which all the results were expressed as a % of the delivered radioactivity (measurement of DPI device retention was impractical), corrected counts from the DPI device, lungs (trachea is omitted as described previously in Chapter 3, the mouth-throat (MT; including the gastro-intestinal and tracheal region) and exhalation filter, were each reported

as a percentage of the total count from each experiment. Percent counts in each region were considered to be an indirect measure of the percentage of drug deposited in the different sites. Because tracheal deposition was separately reported for the antiviral Relenza (Cass et al, 1999), *in vivo* data for that device was adapted to conform to the definitions used for all other inhalers.

Figures 4.2, 4.3 and 4.4 show the observed drug deposition *in vitro* and *in vivo* for each different DPI. The literature values from the clinical scintigraphy studies are for healthy adults of both genders in each of the small studies summarized in Table 4.1. *In vitro* regional drug deposition results were a function of the inhalation profiles (Figure 4.1) used for testing and the number of actuations per dose shown in Table 4.2. These waveforms were chosen carefully based on the literature descriptions of the *in vivo* studies and our inhalation profile simulation methods described in detail previously in Chapter 3. Total lung (Figure 4.2), MT (Figure 4.3) and DPI device retention (Figure 4.4) are presented as % of total drug recovery *in vitro* in comparison with % of total counts *in vivo* (Borgstrom et al, 1994; Brand et al, 2007; Cass et al, 1999; Meyer et al, 2004; Vidgren et al, 1994).

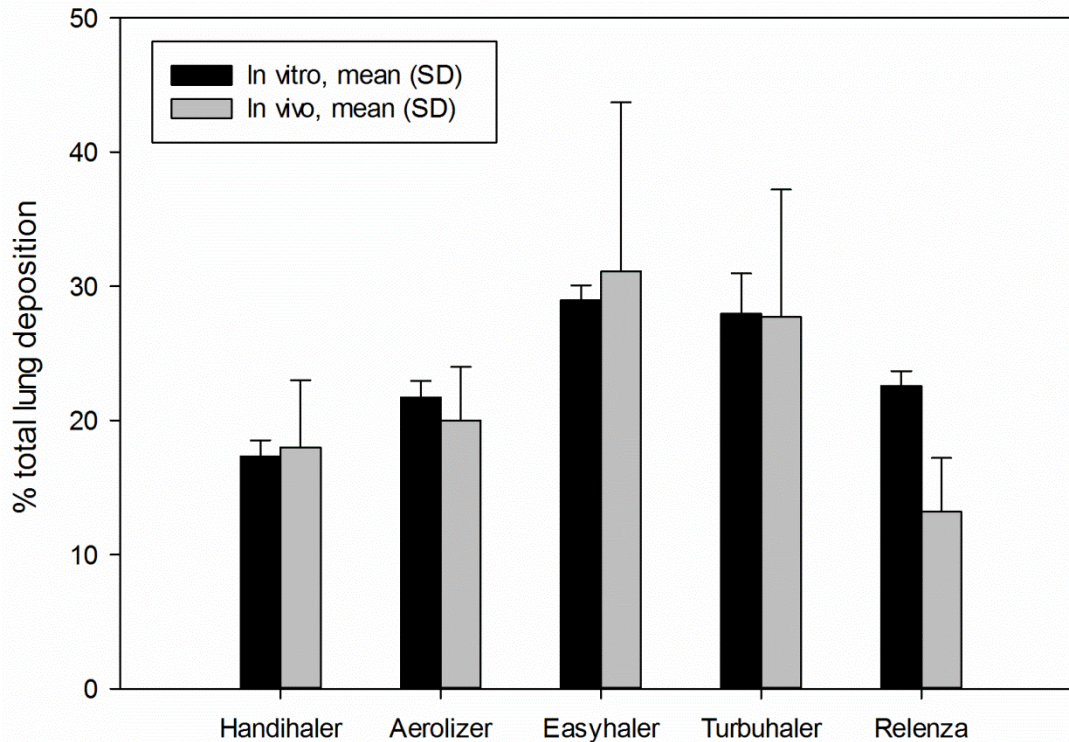


Figure 4.2: Mean % total lung deposition, TLD, for five DPIs following *in vitro* testing (n=5) in the medium airway model. Tests employed the ‘average’ flow rate profiles shown in Figure 4.1 in all cases. Results are shown in comparison to mean (SD) *in vivo* values reported in the literature (Borgstrom et al, 1994; Brand et al, 2007; Cass et al, 1999; Meyer et al, 2004; Vidgren et al, 1994). Error bars are standard deviations.

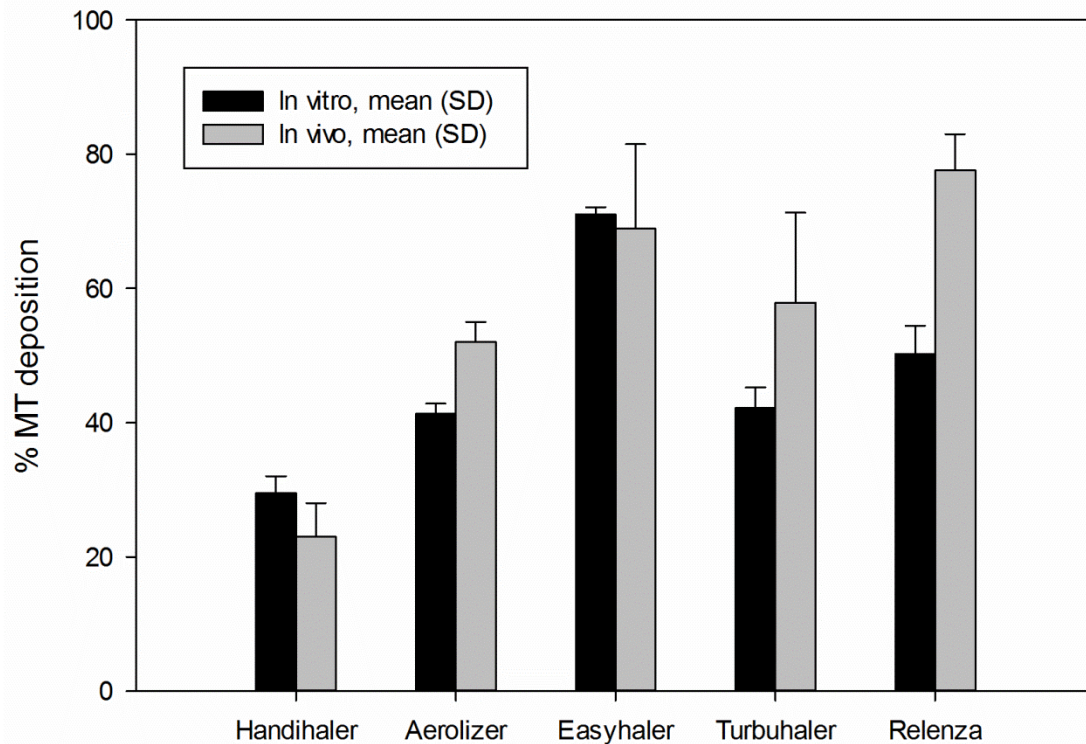


Figure 4.3: Mean % mouth-throat (including tracheal deposition) drug deposition for five DPIs following *in vitro* testing (n=5) in the medium airway model. Tests employed the ‘average’ flow rate profiles shown in Figure 4.1 in all cases results are shown in comparison to mean (SD) *in vivo* values reported in the literature (Borgstrom et al, 1994; Brand et al, 2007; Cass et al, 1999; Meyer et al, 2004; Vidgren et al, 1994). Error bars are standard deviations.

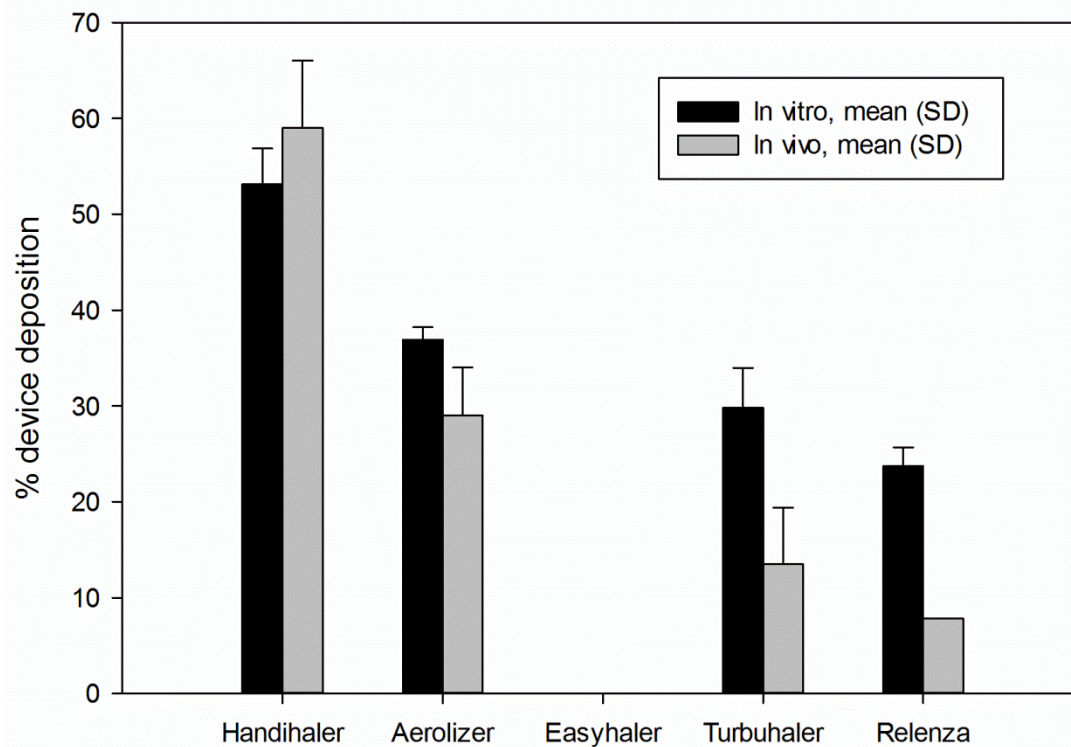


Figure 4.4: Values for mean device deposition following *in vitro* testing (n=5) in the medium’ airway model, using air flow profiles shown in Figure 4.1, in comparison to mean (SD) *in vivo* reported in the literature (Borgstrom et al, 1994; Brand et al, 2007; Cass et al, 1999; Meyer et al, 2004; Vidgren et al, 1994). Error bars are standard deviations. Easyhaler was not assessed.

Figure 4.2 shows clearly that mean *in vitro* deposition was comparable to that seen *in vivo* with the exception of Relenza where the *in vitro* results apparently over-estimated the average lung deposition of the antiviral drug, zanamivir, from Diskhaler. The IVIVCs in Figure 4.2 (except Relenza) showed a 1:1 comparison between *in vitro* and *in vivo* results with an absolute %TLD difference of 2 % or less for all the DPIs. This finding is significant because it shows that our *in vitro* method appears capable of accurately predicting the ‘average’ *in vivo* lung deposition across a variety of DPI devices and formulations, even when the latter is collected in small numbers of mixed gender normal human adults using methods that are commonly believed to be quite variable (Newman & Chan, 2008; Newman et al, 2000c). As expected, variance *in vitro* was much smaller than the variance seen in each *in vivo* study (Figures 4.3 – 4.5) showing that the *in vitro* methods and the DPI devices were more robust than the *in vivo* techniques. In the case of Relenza, a high drug dose DPI, we took care to avoid the powder re-entrainment possibilities seen previously with this device during cascade impaction studies (Kamiya et al, 2009). In this case it appeared that the disparity between the *in vitro* and *in vivo* results for Relenza are most likely due to the poor labeling validation in the *in vivo* study resulting in differences in deposition patterns between the radio-label and the drug. This supposition is supported by the values for device retention in the *in vivo* study (Figure 4.4), where Relenza shows unrealistically good device emptying in the clinic that in practice leads to overestimates for both MT and TLD (Figures 4.4 and 4.3, respectively); inference is supported by independent reports of Relenza device retention (Kamiya et al, 2009).

Figure 4.3 shows good agreement between the values for MT deposition *in vitro* and *in vivo*. With the exception of Relenza, the means were comparable; In the case of Turbuhaler and Aerolizer, a slight tendency to under-estimate *in vivo* MT deposition was observed.

Explanations for inconsistencies in the *in vivo* deposition estimates for Relenza may be related to the common practice in scintigraphy studies, to compare *in vitro* APSDs of drug and radiolabel based only on the dose collected in the impactor rather than the complete metered dose (Cass et al, 1999). This “powder sampling” practice is likely to lead to false conclusions of “valid labeling” if device retention plus the “large particle fractions” of the labeled dose that fail to enter the impactor become incomparable due to poor labeling techniques. In fact, considering the invasive nature of the radio-labeling techniques most often employed for *in vivo* DPI deposition estimates (these involve “dampening” the powder to be aerosolized with label in an organic solvent) (Dolovich, 2004), it seems quite likely that the size distributions of the complete radiolabel dose and the unaltered drug dose may differ. For example, Borgstrom et al., in their radio-labeling method validation studies for Pulmicort Turbuhaler, reported that mouthpiece retention of radiolabel was almost half compared to non-labeled budesonide deposition (Borgstrom et al, 1994).

4.4 CONCLUSIONS

From this study we concluded that our *in vitro* methods using a “medium” geometry MT-TB model coupled with an appropriately simulated inhalation profile was capable of predicting the average values for total lung deposition, mouth-throat deposition, and drug retention in the DPI device across a broad range of differently designed inhalers used by normal human volunteers of both genders. The predictability of the method was found to be independent of inhaler variables such as the dispersion mechanism, the magnitude of each inhaler’s resistance to air flow and/or the precise design of the formulation. Indeed, we believe that the *in vitro* methods described here and in Chapter 3 are robust and often superior, for powder inhaler assessments, to the techniques used commonly in the clinic requiring the use of invasive radio-labeling techniques.

CHAPTER 5

TO PREDICT THE EFFECT OF INHALER INSERTION ANGLE ON AEROSOL DEPOSITION USING IN VITRO AIRWAY MODELS

5.1 INTRODUCTION

Studies using monodispersed aerosols have shown that MT deposition changed as a function of the entry angle (Fadl et al, 2007). However, the aerosol particle size considered for these studies was significantly larger than traditional pharmaceutical aerosols. Therefore, there are a number of open questions related to the effect of inhaler insertion angle on MT drug deposition. It is reasonable to assume that most inhalers are frequently used at angles between +/- 10° relative to a horizontal axis extending from the mouth inlet; usage at +/- 20° is also likely. Considering this potential range of angles, it is unclear if DPIs or MDIs are more sensitive to insertion angle effects. The high velocity jets of some DPIs with small aerosol exit channel make it likely that the insertion angle is an important factor in MT deposition. Because MT deposition occurs before any deposition in the lung, this Chapter focused on whether MT deposition was inhaler orientation dependent. Notably also, the magnitude of this orientation effect on regional deposition could also be formulation dependent for DPIs. In addition, it is not clear if removing the larger carrier lactose particles and producing a more monodispersed aerosol will make MT

deposition more or less sensitive to the insertion angle for DPIs. Similarly for MDIs, the inhaler insertion angle may affect the spray momentum associated with the aerosol formation and alter MT drug deposition. In contrast, considering SMIs, spray momentum is greatly reduced compared with MDIs. A better understanding of insertion angle effects will allow these questions to be addressed with the intent of potentially improving delivery efficiency and reducing dose variability to the lungs.

A study was performed to determine the effect of inhaler insertion angle on aerosol deposition using an *in vitro* airway model. Physical airway models were constructed and used to simulate the airway of an adult inhaling through a DPI, MDI and SMI, respectively. The inhalers were inserted at a series of different angles relative to a horizontal axis extending from the mouth inlet.

5.2 MATERIALS AND METHODS

5.2.1 TEST INHALERS

The MDI used in this study was the Proventil[®] HFA MDI which delivers 120 µg albuterol sulfate per actuation from the valve (Schering-Plough, USA). The SMI was the Respimat[®] SoftMist[®] inhaler (Boehringer Ingelheim, Germany). For Respimat aerosol generation, a solution formulation (0.6% w/v albuterol sulfate in water) was loaded into an empty formulation canister. The DPI was Novolizer[®] (Meda Pharma GmbH & Co. KG, Germany) which was used with two formulations. Firstly, the Salbulin commercial formulation which delivers 120µg albuterol sulfate/dose as a drug / lactose blend. Secondly, a micronized drug only formulation of albuterol sulfate, which delivers 1000 µg albuterol sulfate/dose.

5.2.2 PHYSICAL AIRWAY MODELS

Physical airway models used in this study were similar to the ‘medium’ airway model described in Chapter 3 and 4. The MT region of the model was based on the elliptical MT geometry defined by Xi and Longest (Xi & Longest, 2007), while TB geometry (extended to 3 generations considering trachea as generation 0) was developed from the Yeh and Schum lung model (Yeh & Schum, 1980) by scaling it to match TB geometry of an average adult as described by Tian et al (Tian et al, 2011a). The only difference from the previously used MT-TB_M model was 5 mm inhaler insertion depth addition in MT model described in Chapters 3 & 4, and minor geometric changes to assure connectivity as shown in Figure 5.1. This allowed the inhalers to be attached at zero degrees to the horizontal plane of the MT model and the effect of inhaler orientation, studied by customizing the mouth inlet for each of the three inhalers to

produce airtight connections to produce insertion angles of -20, -10, 0, +10, and +20 degrees relative to a horizontal axis extending from the mouth inlet. Figure 5.1 illustrates the Novolizer attached to the different angled MT models.

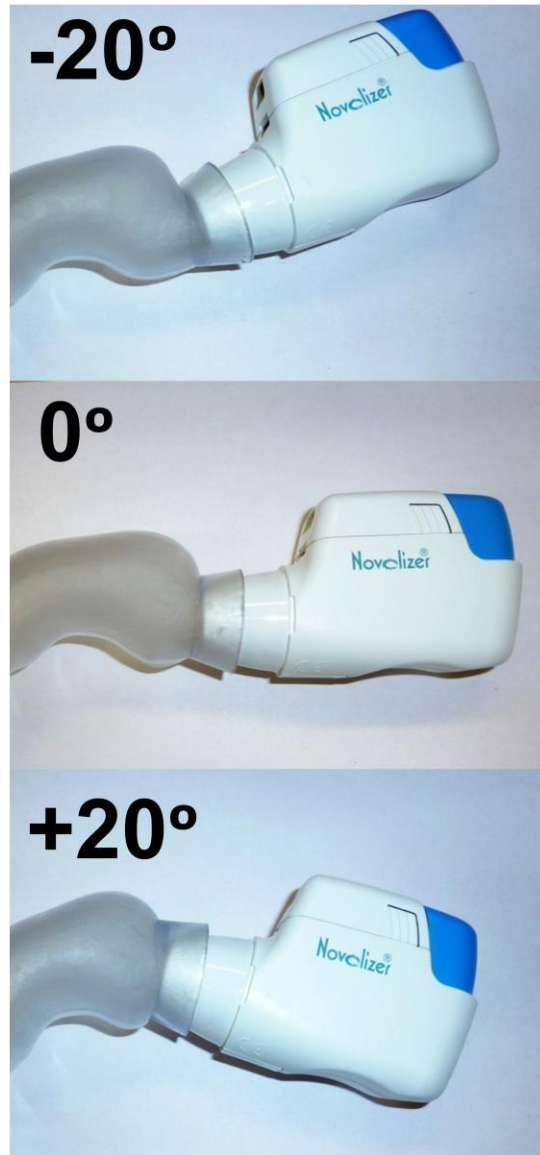


Figure 5.1: Novolizer attached to different angled MT models.

5.2.3 INSERTION ANGLE IN VITRO EXPERIMENTAL SET UP

Figure 5.2 shows the experimental set-up employed to measure the *in vitro* aerosol deposition from the different inhalers; previous studies in Chapter 3 and 4 have described the development and validation of this methodology. The TB region of the airway model was enclosed into an airtight Plexiglas chamber that was connected to a vacuum pump via a low resistance microbial filter. The internal surfaces of the airway model were coated with glycerol-methanol (1:2) or silicone (Dow Corning® 316 Silicone Release Spray, Dow Corning Corp., Midland, Michigan, USA) to prevent particle bounce and re-entrainment. Single doses were actuated from the inhalers attached to the model using the following flow rate – time protocols; Proventil HFA MDI and Respimat SMI: 30 L/min for 10 s, Novolizer DPI: 75 L/min for 3.2 s. In the case of the Novolizer DPI – drug only formulation study, the MT model was connected directly to the filter; the TB region and Plexiglas chamber were excluded from the set up. Following each inhalation, albuterol sulfate retained in the device and deposited in the MT, TB and Plexiglas chamber + filter regions of the model were recovered using appropriate volumes of deionized water; In this Chapter, TLD was defined as drug entering the Plexiglas chamber and filter; TB was not included as part of TLD, unlike the case in Chapters 3 and 4. For each inhaler, four replicate experiments were performed for each of the insertion angles.

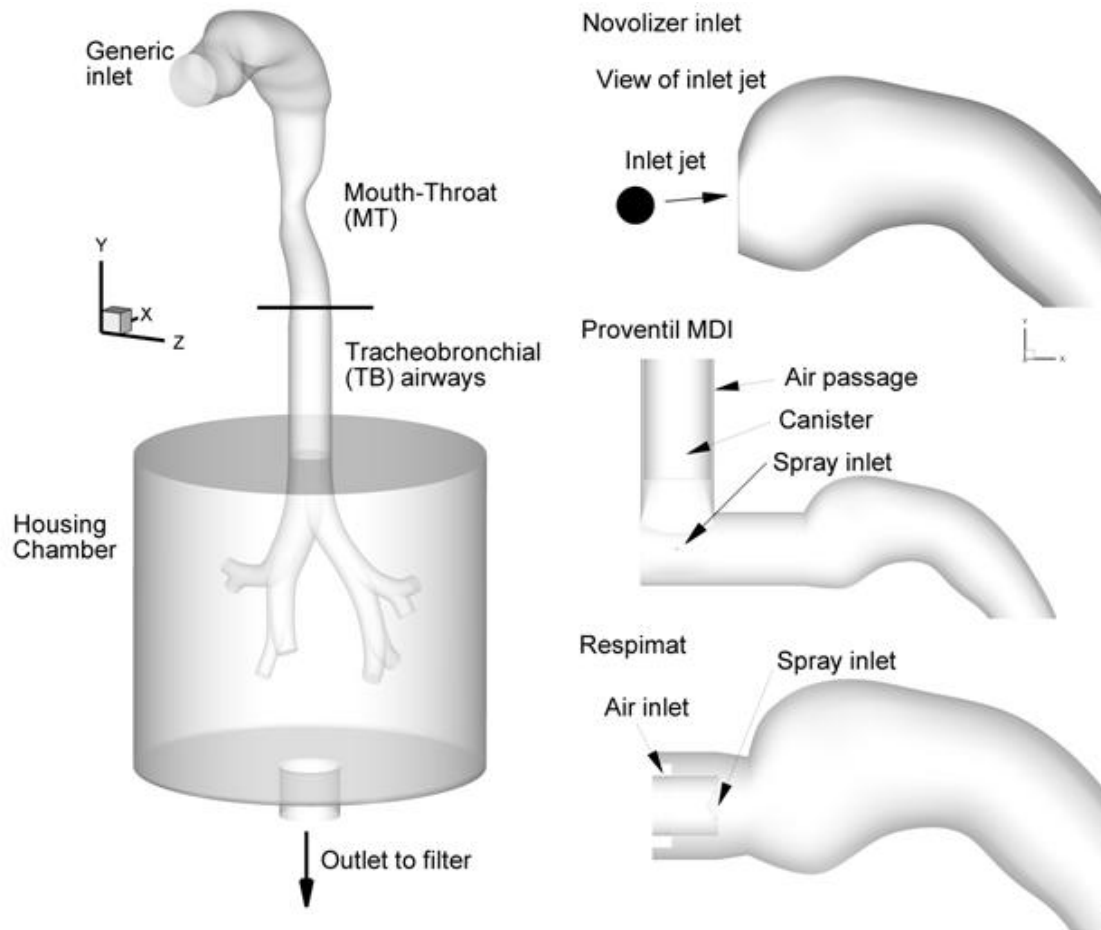


Figure 5.2: 3D representation of MT-TB geometry in chamber used for *in vitro* deposition experiments.

5.2.4 AERODYNAMIC PARTICLE SIZE DISTRIBUTION DETERMINATION

The aerodynamic particle size distributions of the two Novolizer formulations used in this study were determined using Next Generation Impactor (NGI; MSP Corp., Shoreview, MN). The impactor was held in the horizontal orientation and the primed Novolizer was attached directly to the pre-separator. The inhaler was actuated using a constant flow rate of 75 L/min for 3.2 s (4L volume). Impactor stages were coated with silicone spray (Dow Corning® 316 Silicone Release Spray, Dow Corning Corp., Midland, Michigan, USA) to prevent re-entrainment of aerosolized particles. Albuterol sulfate deposited on the impactor stages was recovered using deionized water and quantified using a validated HPLC method. Each experiment was performed for four times.

In a separate study, the aerodynamic particle size distribution of the aerosol exiting the -20 and +10° MT model was determined using the NGI for the Novolizer DPI – drug only formulation. In this study, the MT model was connected to the pre-separator and the DPI was actuated using a flow rate of 75 L/min for 3.2 s.

5.2.5 ANALYTICAL METHOD

Albuterol sulfate recovered from the different regions of the models, inhalers and impactor stages were analyzed using a validated isocratic HPLC assay method described in Chapter 4, Section 4.2.2.

5.2.6 DATA ANALYSIS METHOD

Total drug recovery was calculated as the sum of the individual amounts of drug deposited on the different regions of the model and retained in the device after actuation. Drug deposition in the device, MT, TB and lung regions (TLD) were expressed as a percentage of the

total drug recovery [(drug deposited in region/total drug recovered) x 100]. Statistical analysis of the overall effect of inhaler insertion angle on *in vitro* drug deposition was performed using one-way ANOVA. Post hoc Tukey's Honest Significant Difference (HSD) test was used to compare the individual angles. Student t-test was used to compare the regional deposition between the different devices. JMP 8 was used for statistical analysis. A significance level of $P < 0.05$ was used in all cases.

5.3 RESULTS

5.3.1 EFFECT OF INSERTION ANGLE ON IN VITRO DEPOSITION

Tables 5.1 and 5.2 show the effect of inhaler insertion angle on the *in vitro* aerosol deposition from the Novolizer DPI with the Salbulin and drug only formulations, respectively. Device retention differed significantly between the two formulations (student t-test, $p < 0.05$) using the Novolizer. For the Salbulin formulation, device retention was low, about 4%, however there was high MT deposition; the drug recoveries were all more than 90% of the nominal dose. In contrast, using the drug only formulation about 25% of the dose was retained in the device and this was accompanied by lower MT deposition. For the Salbulin formulation, one-way ANOVA analysis showed no significant difference in device, MT and TB and total lung deposition using the different insertion angles [$p > 0.05$]. The lowest and highest MT depositions for the Salbulin formulation were observed at +20 and -20 degrees, respectively, with the nominal absolute, but insignificant difference of 4.28%. In contrast, for the drug only Novolizer DPI, there was a significant effect of insertion angle on the MT and total lung deposition [one-way ANOVA, $p < 0.0001$]. More specifically, there were significant reductions in MT deposition when the Novolizer was inserted at the -20 and -10 degree angles compared to the 0 degree angle (Tukeys HSD). However, when the DPI was inserted at + 10 and +20 degrees there was no significant change in MT deposition over the horizontal (0 degrees). For the drug only Novolizer DPI, the lowest and highest MT deposition was observed at +10 and -20 degree insertion angles, respectively, with a significant absolute difference of 8.79%.

Table 5.1: Effect of insertion angle on the *in vitro* albuterol sulfate deposition for the Salbulin Novolizer DPI (mean (SD), n=5).

Angle (degree)	% of total recovery			
	Device	MT	TB	TLD
-20	4.24 (0.22)	68.28 (1.26)	0.77 (0.16)	26.72 (1.20)
-10	3.71 (0.46)	66.73 (2.63)	0.74 (0.09)	28.82 (3.07)
0	3.92 (0.72)	64.71 (3.20)	0.82 (0.17)	30.55 (3.55)
+10	4.02 (0.49)	64.95 (2.33)	0.78 (0.17)	30.25 (2.85)
+20	4.13 (0.57)	64.10 (1.53)	0.81 (0.12)	30.96 (1.88)

Table 5.2: Effect of insertion angle on the *in vitro* albuterol sulfate deposition for the drug only Novolizer DPI (mean (SD), n=5).

Angle (degree)	% of total recovery#		
	Device	MT*	TLD*
-20	24.02 (0.80)	34.95 (0.92)**	41.04 (0.86)**
-10	25.04 (1.55)	32.58 (0.75)**	42.38 (1.77)**
0	25.63 (1.84)	27.60 (1.28)	46.77 (0.72)
+10	25.07 (1.74)	26.16 (0.88)	48.77 (1.40)
+20	25.22 (0.92)	27.07 (1.06)	47.71 (0.94)

MT model was connected directly to the filter; the TB region and Plexiglas chamber were excluded from the set up

* P<0.05 Significant effect of insertion angle on MT and TLD deposition (One-way ANOVA).

** Significant effect of insertion angle MT and TLD deposition compared 0 degrees (Post hoc Tukey HSD).

Table 5.3 shows the effect of inhaler insertion angle on the *in vitro* aerosol deposition from the Proventil HFA MDI; the drug recoveries were all more than 95% of the nominal dose. Device retention on the MDI was about 15 % of the dose and was not affected by insertion angle. MT deposition was lower for the Proventil MDI compared to the Salbutin Novolizer DPI for all insertion angles (student t test, $p < 0.05$). However, there was a significant effect of insertion angle of the MDI on the MT and total lung deposition. Post hoc analysis revealed a significant increase in MT deposition for the -10 and -20 insertion angles compared to 0 degree. This trend was similar to the results observed for the drug only Novolizer DPI. In the case of Proventil HFA MDI, the lowest and highest % MT depositions were observed at +10 and -20 degree angles, respectively, with a significant absolute difference of 11.34 %.

Table 5.4 shows the effect of inhaler insertion angle on the *in vitro* aerosol deposition from the Respimat SMI. Drug deposition was less than 20% of the recovered dose on both the device and MT, respectively, which resulted in a high pulmonary fraction compared to the MDI and DPI. There was no significant change in % deposition in any region with change in Respimat SMI insertion angle [one-way ANOVA, $p > 0.05$]. The lowest and highest MT depositions for Respimat were observed at -10 and +10 degrees, respectively, with the non-significant absolute difference of just 2.47%.

Table 5.3: Effect of insertion angle on the *in vitro* albuterol sulfate deposition for the Proventil HFA MDI (mean (SD), n=5).

Angle (degree)	% of total recovery#		
	Device	MT*	TLD*
-20	16.35 (2.73)	47.11 (2.40)**	36.53 (1.75)**
-10	15.96 (0.60)	42.68 (1.33)**	41.35 (0.89)**
0	15.33 (0.63)	38.05 (2.18)	46.62 (1.96)
+10	15.46 (1.14)	35.77 (1.45)	48.77 (1.11)
+20	17.48 (2.55)	38.31 (2.22)	44.21 (0.98)

#TB deposition was below LOQ (below 1% of the nominal dose)

* P<0.05 Significant effect of insertion angle on MT and TLD deposition (One-way ANOVA).

** Significant effect of insertion angle MT and TLD deposition compared 0 degrees (Post hoc Tukey HSD).

Table 5.4: Effect of insertion angle on the *in vitro* albuterol sulfate deposition for the Respimat SMI (mean (SD), n=5).

Angle (degree)	% of total recovery			
	Device	MT	TB	TLD
-20	16.67 (4.78)	11.62 (2.71)	2.23 (0.34)	69.48 (4.45)
-10	17.35 (7.76)	9.27 (2.81)	2.19 (0.70)	71.19 (5.26)
0	17.04 (7.84)	11.01 (4.29)	2.46 (0.76)	69.49 (3.70)
10	15.57 (6.57)	11.74 (6.86)	2.18 (0.33)	70.52 (6.89)
20	13.32 (3.13)	10.40 (1.03)	2.79 (1.33)	73.49 (1.85)

5.3.2 IMPACTOR STUDY

Figure 5.3 shows the mass fraction of albuterol sulfate deposited on the impactor stages for aerosols generated from the Novolizer DPI using the Salbulin formulation and drug only formulations.

Figure 5.4(a) compares the mass fraction of albuterol sulfate deposited in MT and impactor from 'drug only' Novolizer inserted at -20 and +10 degree angles; extreme %MT depositions were observed for these two angles. There was a significant difference in % deposition at impactor stages 2, 3, 4 and 5 (student t-test, $p < 0.05$). Figure 5.4(b) depicts the % difference in the impactor deposition (% delivered dose) between +10° and -20° angles that was calculated from

$$\% \text{ difference} = \frac{(\% \text{deposition for } +10^{\circ} \text{ MT} - \% \text{deposition for } -20^{\circ} \text{ MT}) * 100}{\% \text{deposition for } -20^{\circ} \text{ MT}}$$

%difference increased with increase in particle size indicating a change in the impaction deposition with change in angle.

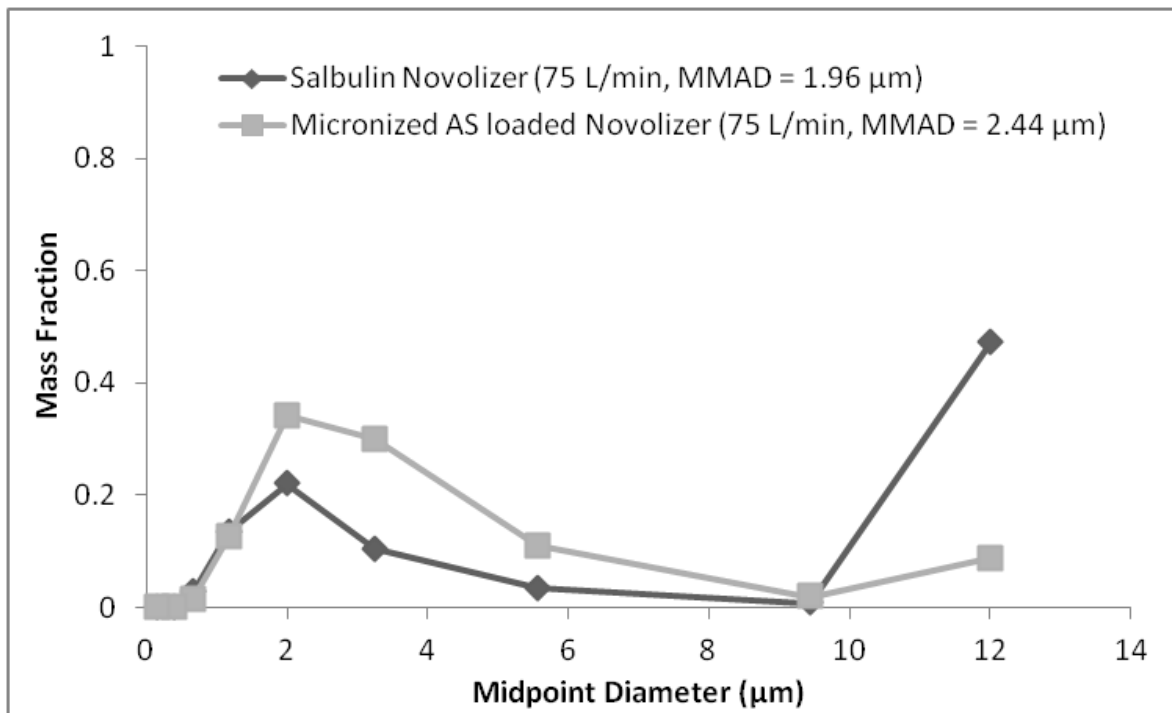


Figure 5.3: Size distributions for the Novolizer drug-excipient (Salbulin) and micronized drug only formulation aerosols following their actuation directly into the NGI preseparator.

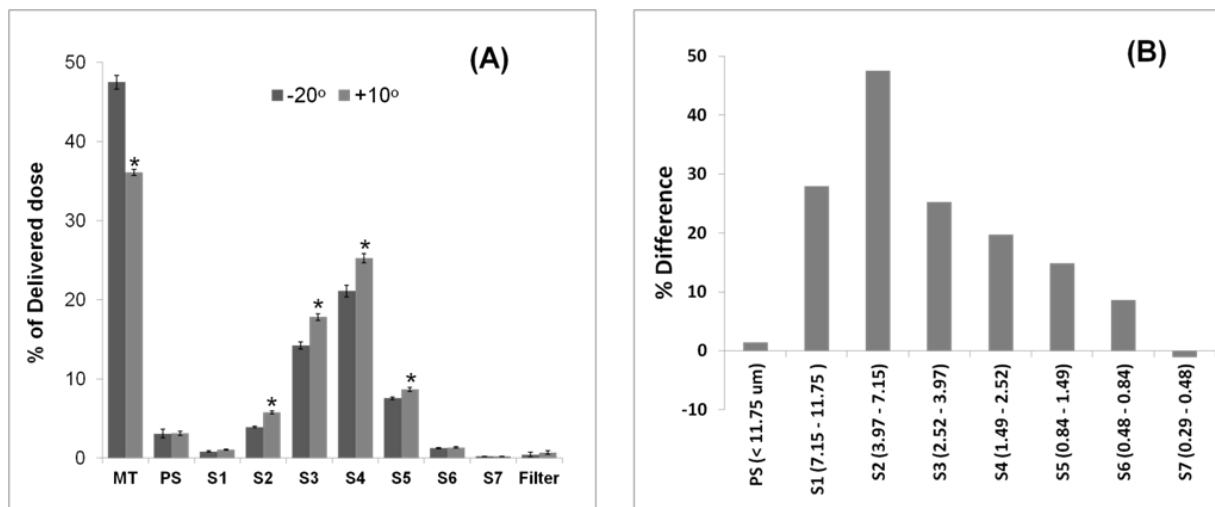


Figure 5.4: (A) MT and Impactor albuterol sulfate deposition (% of delivered dose) (n=5) and (B) % difference in the deposition on the various impactor stages at the MT deposition extremes shown in Figure 5.3 (+10 degree angle in comparison to -20 degree) for the drug only Novolizer tests in which MT was connected directly to the NGI preseparator.

5.4 DISCUSSION

In this study, the effect of inhaler insertion angle on *in vitro* drug deposition in an airway model was investigated. The airway model was employed using experimental techniques to gain further insight into the critical factors controlling MT deposition for a DPI, MDI and SMI. A secondary study, to be published by Longest et al, on CFD aerosol deposition prediction was initiated based on these results and is presently in progress.

Inhaler insertion angle appeared to be critical for the Proventil HFA MDI and the drug only Novolizer DPI. For the Proventil MDI, inserting the inhaler at negative angles relative to horizontal caused an increase in MT deposition probably because the aerosol was directed towards the tongue. This was likely due to the high velocity of the aerosol delivered through Proventil HFA that makes the aerosol deposition more dependent on the aerosol trajectory. A similar observation was reported by Fadl et al. for monodispersed aerosols delivered from MDIs (Fadl et al, 2007). This argument was further supported by the results for Respimat SMI, that product delivers aerosol at almost one tenth the exit velocity of Proventil MDI (Longest et al, 2009).

For the drug only Novolizer DPI, a significant effect of insertion angle was observed. In contrast, despite the use of the same device, the Salbutamol Novolizer DPI, which had the highest MT deposition, but showed no effect of insertion angle on MT deposition. This observation suggested that not only the velocity of the aerosol but also the formulation in the DPI plays an important role in whether or not MT deposition from a given DPI will be orientation dependent. Even though the exact mechanism for this observation is not clear at present, for ‘drug only’ formulation, the particle size distribution data of the aerosol exiting the MT model (-20 and +10

degree) did provide further insight. Figure 5.4 (b), shows that larger particles were most affected by the orientation change, implied change in impaction deposition with change in angle.

It may be possible that inserting each the three inhalers in a downward position (+20 case) results in additional aerosol deposition on the tongue while inserting the inhalers in an upward direction result in more deposition on back of the throat likely due to the reduced distance from inhaler mouthpiece to the first impaction site when inhalers were held at negative angles. Interestingly, for all inhalers being studied, changes in MT drug deposition due to orientation were not always accompanied by a corresponding change in the TB deposition. Also, changing the angles from +10 to +20 degree didn't significantly change MT deposition for any the inhalers. Possible reasons for this may be explained by CFD modeling in future. The method described here enables investigation of these effects simply and reproducibly.

It was evident from this study that, for some inhalers, the correct inhaler orientation can reduce not only inter-subject but also intra-subject variability. In this regard, it is important to recognize that inhaling at the optimal flow rate alone does not maximize lung dose and it is equally important to educate patients about the correct way to hold the inhaler during inhalation. This finding is of significance given the fact that most patients do not appreciate the need for holding the inhaler at correctly.

5.5 CONCLUSIONS

From this study we concluded that the change in the angle at which an inhaler is inserted into the mouth may have profound effect on aerosol behavior within the mouth-throat region, particularly on aerosol travel path and that this may result in changes in the lung dose. The magnitude of the inhaler orientation effect on regional deposition appeared to be dependent on aerosol velocity; higher when the aerosol is delivered as a high velocity jet as in the case of MDIs and some DPIs. The magnitude of the orientation effect from DPIs was also formulation dependent. This study demonstrated that inhaling at an optimal flow rate alone does not guarantee drug delivery; it was equally important to educate patients to hold the inhaler correctly during inhalation. Future studies will seek to build and validate CFD predictions of aerosol deposition in the physical models and to extend the assessment of user variables or drug delivery from various inhalers.

CHAPTER 6

ASSESSMENT OF INSPIRATORY PROFILES THROUGH DIFFERENT AIRFLOW RESISTANCES AS A FUNCTION OF TRAINING

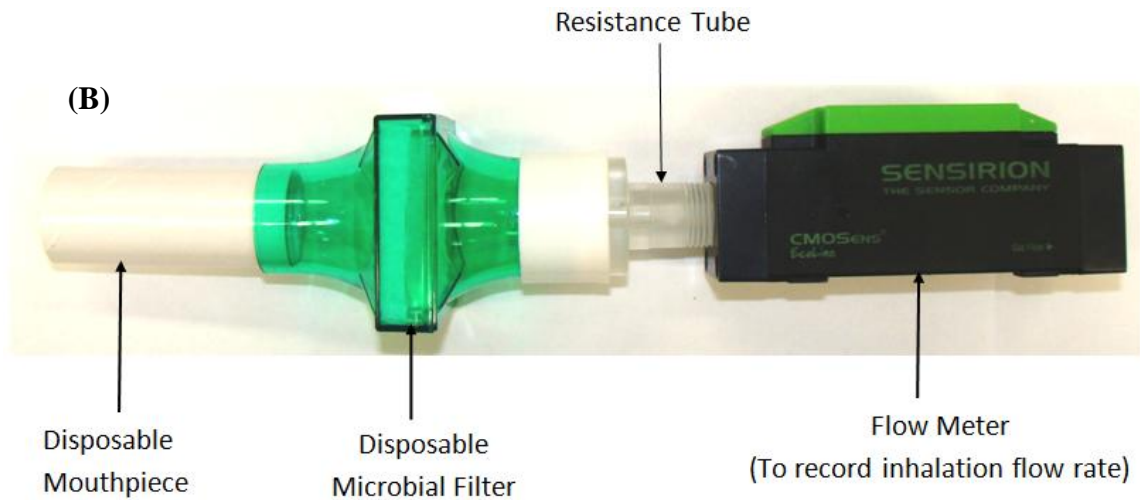
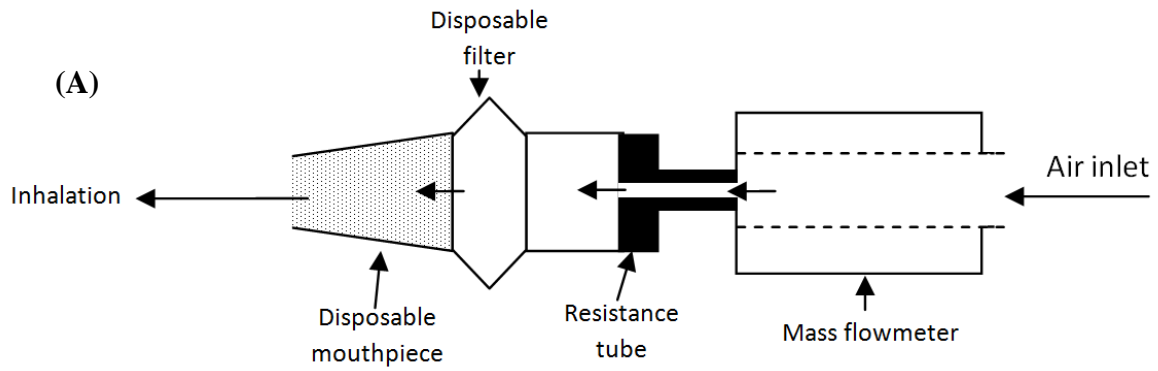
6.1 INTRODUCTION

It is well known that performance of DPIs often depends on the way that patients use them. While this can be influenced by instruction leaflets, personal training and of course, the subject's lung function, DPI design is still in the rudimentary phase. In large part, this is because of poor *in vitro* performance testing that fails to concern itself with the way that patients actually inhale through each device. Reports of > 94% of the patients failing to use DPIs correctly are common so that failure to exhale before inhalation, failure to inhale rapidly and deeply as well as incorrect mouthpiece positioning (Broeders et al, 2009; van Beerendonk et al, 1998) may all have a significant influence on regional drug deposition and clinical outcome. At this stage it is imperative that we document and characterize the inhalation profiles commonly used by healthy volunteers before and after they are trained in the use of DPIs, in part to assess the difference between device performance in a clinical trial (in which patients are usually trained to use an inhaler) and device performance following initial prescription pick up from the pharmacy, where

frequently, patients are left to find out for themselves how to use their new inhaler with the aid of an instruction leaflet. This study was designed to ensure that the simulation techniques that were described and employed in Chapters 3 and 4 to mimic patient profiles *in vitro* using a programmable breath simulator were actually representative of those that are used by human volunteers both before and after training in a clinical setting while also assessing the likely inter-subject variability in the inhalation profiles of normal adults of both genders while using DPIs with different resistances. By selecting inhaler-naïve subjects from the general population we also sought to understand whether formal training helps to improve inhalation technique.

6.2 INHALATION FLOW CELL

An inhalation flow cell with variable air flow resistance was constructed as shown in Figure 6.1. The purpose of this cell was to record the flow rate vs. time profiles of volunteers inhaling through a mouthpiece attached to various air flow resistances, corresponding to those of typical powder inhalers, as if the whole cell was a DPI. Upon inhalation from the mouthpiece, air was drawn through the mass flowmeter (Mass Flow Meter EM1, Sensirion Inc., CA, USA) followed by a resistance tube containing a channel with different diameters, a low resistance microbial filter and a disposable mouthpiece. The flow rate vs. time profile generated by the in line flowmeter can be recorded for each inhalation digitally (SensiViewer, Sensirion Inc., CA, USA) using a computer. The resistance tubes with different orifice diameters were fabricated and inserted in the inhalation flow cell to generate different air flow resistances in such a way that, along with the cell itself, they produce total air flow resistances comparable to those reported for different marketed DPIs as listed in Table 4.1 and Novolizer. Resistance tubes were designed, constructed and calibrated as described in Appendix C; the diameters of resistance tubes named Tube 1, Tube 2, Tube 3, Tube 4, Tube 5 and Tube 6 were 3.6, 3.8, 4.2, 5.2, 5.8, and 6.5 mm respectively; these tubes produced airflow resistance similar to Handihaler, Easyhaler, Turbuhaler, Novolizer, Diskhaler, and Aerolizer, respectively, when inserted in inhalation flow cell (Appendix C).



(C)

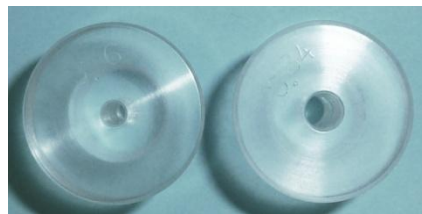


Figure 6.1 Inhalation flow cell design (A; schematic) and (B; photograph). Photographs in C show the top and the side views of the resistance tubes with identical external but different internal dimensions.

6.3 CLINICAL STUDY

6.3.1 SPECIFIC AIMS

The goal of this study was to document the range of inhalation flow rate versus time profiles used by normal subjects inhaling through resistances typical of those seen in DPIs. Specifically, we wanted to collect pilot data from 20 volunteers without lung disease and use the data to:

1. Document the inhalation flow rate versus time curves for adults inhaling through different air flow resistances (using the inhalation flow cell shown in Figure 6.1).
2. Compare the profiles in the same subjects before and after their having received both written and practical training in the inhalation techniques most commonly associated with DPIs and DPI package inserts.
3. Document the intra- and inter- subject variations in flow rate vs. time when specific air flow resistances are employed.
4. Propose representative inhalation profiles for future use with the *in vitro* inhaler test methods that are described in Chapters 3 and 4.

6.3.2 STUDY DESIGN

This protocol was designed to document the inhalation profiles commonly used by healthy volunteers who are 1) trained in DPI use solely by reading a typical package insert, and 2) formally trained in DPI use by a health professional, such as a pharmacist. The objective was to collect a range of typical flow rate versus time profiles for subjects inhaling through different air flow resistances designed to mimic those seen in DPIs. To collect the needed information,

however, subjects were not exposed to any drug; rather data was collected to show the likely inter-subject variability in the inhalation profiles of adults inhaling through different air flow resistances representative of the DPIs in Table 4.1 and Novolizer.

Twenty study subjects were recruited from the general Richmond population through advertisements. An initial telephone interview was conducted with each interested participant to determine his/her eligibility (Inclusion and exclusion criteria were as described in Section 6.3.3.1). If the subject appeared to be qualified for the study, they were invited to the Aerosol Research Lab, School of Pharmacy, VCU for a screening visit to be followed up by a second visit for inhalation profile collection.

On the first visit, potentially eligible subjects were informed about the study. If they were willing to participate, formal informed consent was obtained after all questions had been asked and answered. Each volunteer was asked to provide demographic data, namely age, gender and health information such as medical and smoking history, medication history and present medications. Vital signs (blood pressure, pulse rate), height and weight measurements were taken. An initial spirometric screen was used to ensure normal pulmonary function (FEV1 >predicted Lower Limit of Normal (LLN); (Marion, 2001; Marion et al, 2001; Miller et al, 2005)).

If deemed eligible by the Medical Monitor, the subjects were invited to participate in the second phase of the study. On the second visit, inhalation profiles were collected from healthy male (n=10) and female (n=10) adults. Approximately 18 inhalation profiles were collected from each eligible subject.

6.3.3 EXPERIMENTAL METHODS

6.3.3.1 Study Population

Twenty eligible subjects were enrolled in this pilot study (between 18 and 65 years old).

Subjects conforming to the following criteria were considered eligible.

Must be healthy as determined by a health questionnaire (Appendix H)
Must have never used or been trained to use a DPI,
Must not be currently pregnant (self reported)
Must not have symptoms of an obstructive or restrictive lung disease or be suffering from allergies or congestion at the time of testing
Must have FEV1 >LLN predicted
Must be medically stable with no evidence of acute medical or psychiatric illness,
Must not be currently using any inhaler, nasal spray or drug known to affect lung function, Bronchodilators and decongestants in any form are excluded
Must be at least 4 feet 10 inch tall,
Must weigh at least 110 pounds (50 kg) and be no more than 264 pounds (120kg)
Must not currently, or in the past year, have used tobacco products

6.3.3.2 Collection of inhalation profiles

Inhalation flow rate, FR. vs. time profiles of each eligible volunteer inhaling through an inhalation flow cell were recorded as the volumetric air flow rate vs. time profiles for air exiting the mouthpiece of the calibrated inhalation cell after the following instructions were provided to each volunteer in sequence.

Instruction A: Written instructions that were believed to summarize the typical patient leaflet directions for how to inhale when using the marketed DPIs were employed. Volunteers were each given a set of written instructions to read (Figure 6.2). After reading the instructions volunteers were asked to inhale through the inhalation flow cell (as if they were using a powder inhaler and believing they were conforming to the instructions). Inhalation profiles were

recorded for each of six different resistance tubes placed in the inhalation flow cell in random order (e.g. each volunteer received the cells loaded with different resistances in different order). The results from these experiments were used to provide information on the type and range of inspiratory maneuvers to be expected when inhaler-naïve subjects were not formally trained in the use of DPIs except by having been provided an instruction leaflet; data for flow rate vs. time for each subject and each resistance were analyzed separately and called ‘Before training’.

Instruction B: Verbal instructions and a practical demonstration of how to use a powder inhaler correctly was then offered to the volunteer (this was delivered by a trained pharmacist and referred to as ‘formal training’). Following formal training, volunteers were asked to inhale through the inhalation flow cell in accord with this additional training. Profiles were recorded for each of six different resistance tubes placed in the inhalation flow cell, once again, in random order. Each experiment (instruction B only with each resistance) was repeated once and data for flow rate vs. time for each subject and each resistance was calculated separately and called ‘After training 1’ and ‘After training 2’. The results from these experiments were also used to define the types and range of inspiratory maneuvers used by normal volunteers.

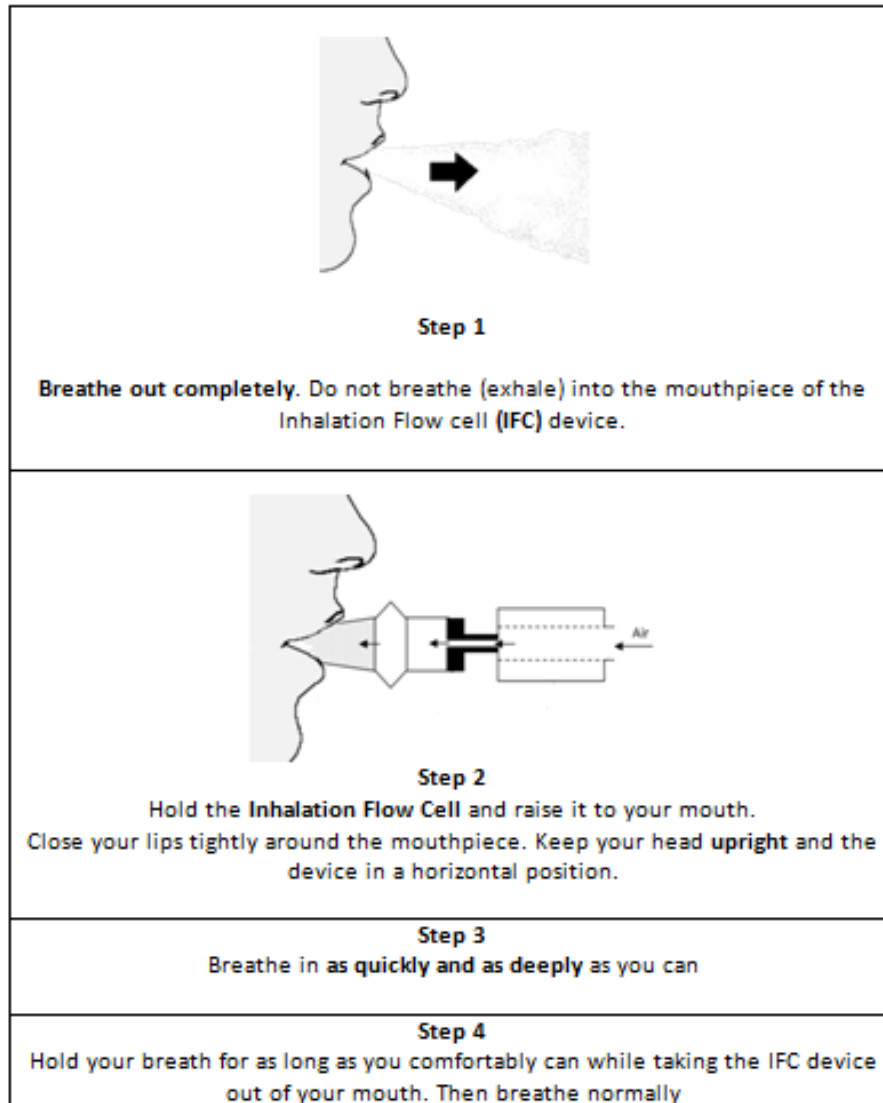


Figure 6.2: Inhalation written instructions (Artwork in the figure was adapted from the HandiHaler patient leaflet instruction).

6.3.3.3 Data analysis plan – primary variables

Individual FR vs. time profiles were analyzed in order to determine commonly used inhalation variables as follows:

1. PIFR - Maximum volumetric flow rate value recorded in each volunteer's inhalation profile (e.g. the largest numerical value in the digital record)
2. V - Area under the curve, AUC, of the inhalation profile (calculated trapezoidally, by addition of the AUC per 5 msec time increment),
3. t_{\max} - Time required to reach PIFR from the start of inhalation maneuver
4. t_{total} - Total inhalation time

Figure 6.3 illustrates these inhalation variables graphically.

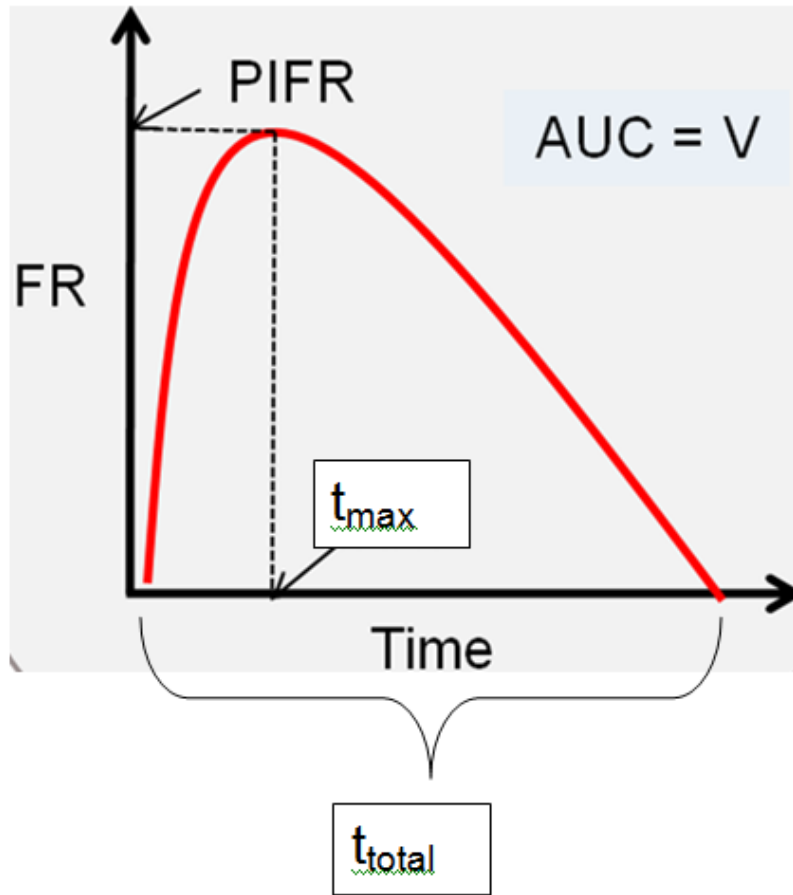


Figure 6.3 Illustration of inhalation profile.

6.3.3.4 Statistical analysis

Descriptive statistics: Descriptive statistics, mean, median, standard deviation, minimum and maximum values, coefficient of variation ($CV (\%) = 100 \times \text{standard deviation} / \text{mean}$) were estimated for each of the inhalation variables, i.e., PIFR, V, t_{\max} , and t_{total} ; both, *by* gender and *across* gender.

Inferential statistics: For each individual dataset from a given volunteer, the quantitative relationship between each primary inhalation variable and the corresponding air flow resistance (R) was assessed by linear regression analysis (inhalation variable(s) vs. R, 1/R, LogR and $R^{0.5}$), separately, for each training status. Best fit was selected based on the coefficient of determination (r squared) value where the largest 'r squared' value indicated the best fit. In cases where significant relationships existed between the inhalation variable and the air flow resistance, the inhalation variables were normalized by resistance and averaged across all resistances in order to obtain a secondary, resistance-independent, normalized, inhalation variable. In case of insignificant relationships between a variable and R, the inhalation variables were averaged across resistances, without normalization, also to obtain a secondary, resistance-independent, inhalation variable. The effect of formal training on the secondary inhalation variables was assessed using repeated-measures ANOVA; gender was added as covariate in the model, as well as the interaction between training status and gender. The level of significance was preset at 0.05. Normality of the residuals was judged by Normal Quantile Plots and visual inspection of the distribution of the residuals. If the residuals were not normally distributed, the ANOVA model was repeated, using instead the log-transformed secondary inhalation variable data. JMP 8.0. (SAS Corp, RTP, NC) was used for all statistical analyses.

6.3.4 RESULTS

6.3.4.1 Subject Demographics

A total of 22 subjects were qualified after successfully passing the initial telephone interview. Two subjects were disqualified, one due to overweight and another due to recent smoking history. The remaining 20 subjects, 10 males and 10 females, successfully completed the screening tests and qualified for visit 2. All 20 subjects enrolled successfully completed the study. Final subject demographics are shown in Table 6.1. A summary of subject demographics and pulmonary function test results are depicted in Table 6.2. The mean age of females and males were 31.1 and 34.0 years, respectively.

Table 6.1 : Final Subject Demographics (enrolled for Visit 2).

Patient ID	Gender	Race	Height [cm]	Weight [kg]	Age [yrs]
HM-13708-01	Male	Indian	177	66	23
HM-13708-02	Female	Caucasian	164	64	25
HM-13708-03	Male	Caucasian	169	67	19
HM-13708-04	Female	Asian	147	50	23
HM-13708-05	Female	Caucasian	158	60	48
HM-13708-07	Female	African	163	63	30
HM-13708-08	Male	Caucasian	186	98	52
HM-13708-09	Female	Hispanic	158	57	34
HM-13708-10	Male	Caucasian	179	91	31
HM-13708-11	Male	Caucasian	177	90	40
HM-13708-12	Male	Asian	172	64	30
HM-13708-13	Female	African	163	62	27
HM-13708-14	Male	African	182	91	41
HM-13708-15	Female	Caucasian	168	62	45
HM-13708-16	Female	African	166	76	42
HM-13708-17	Male	Caucasian	169	68	22
HM-13708-18	Male	Indian	174	70	28
HM-13708-19	Female	Indian	161	62	28
HM-13708-20	Female	Asian	170	51	38
HM-13708-21	Male	Caucasian	181	112	25

Table 6.2: Summary of subject demographics and screening test results (mean±SD).

	Males	Females	Overall
Total	10	10	20
Caucasian	6	3	9
African	1	3	4
Asian	1	2	3
Hispanic	0	1	1
Others	2	1	3
Age [yrs]	31.1 ± 10.31	34.0 ± 8.81	32.6±9.23
Height [cm]	176.6 ± 5.64	161.8 ± 6.49	169.2±9.40
Weight [kg]	81.7 ± 16.75	60.7 ± 7.29	71.2±16.16
<u>PFT</u>			
FVC [L]	5.02 ± 0.60	3.31 ± 0.35	4.15±0.98
FEV1 [L]	4.23 ± 0.41	2.81 ± 0.32	3.51±0.80
FEV1/FVC	0.84 ± 0.04	0.85 ± 0.06	0.85±0.05
FEF 25-75% [L/s]	4.72 ± 0.70	3.29 ± 0.87	3.99±1.03
PEF [L/s]	10.08 ± 1.28	7.12 ± 0.77	9.15±1.92
FET [s]	6.46 ± 1.01	6.91 ± 3.77	6.69±2.63

PFT = Pulmonary function tests

6.3.4.2 PIFR

The descriptive results for PIFR are shown in Table 6.3. Visual inspection of the data indicated that males had higher mean PIFR compared to females across different resistances. Both, males and females, showed increased mean PIFR with a decrease in air flow resistance, irrespective of the subject's training status. The data also indicated that, following formal training (After training 1 and 2), the volunteers inhaled faster and showed lower inter-subject variability in PIFR (based on SD and CV values) compared to the results designated as "Before training". This occurred in both, males and females. As seen in Table 6.3, overall CV values were similar for all the resistance tubes which indicated that inter-subject variability of PIFR appeared to be independent of the airflow resistance of DPI; it should be noted however, that the absolute SD values of PIFR increased with decrease in airflow resistance. Also, % change in mean PIFR following the formal training (with respect to PIFR before training) was independent of airflow resistance indicating that the effect of formal training in PIFR was independent of airflow resistance.

Table 6.3: Descriptive results for PIFR by training status and gender for different resistance tubes; air flow resistance of the tubes ($\text{kPa}^{0.5} \cdot \text{L}^{-1} \cdot \text{min}$) are described in parentheses along with the Tube number.

		Female			Male			Overall		
		Before	After 1	After 2	Before	After 1	After 2	Before	After 1	After 2
Tube (R in $\text{kPa}^{0.5} \cdot \text{L}^{-1} \cdot \text{min}$)		PIFR [L/min]	PIFR [L/min]	PIFR [L/min]	PIFR [L/min]	PIFR [L/min]	PIFR [L/min]	PIFR [L/min]	PIFR [L/min]	PIFR [L/min]
Tube1 (0.0462)	Mean	48.6	55.3	57.1	61.5	70.8	68.2	55.1	63.1	62.6
	SD	11.1	6.4	7.6	15.1	7.5	7.0	14.5	10.5	9.1
	Min	24.3	47.1	43.0	26.3	59.3	59.3	24.3	47.1	43.0
	Max	66.5	69.0	71.7	77.8	80.8	80.4	77.8	80.8	80.4
	CV	22.8	11.6	13.4	24.5	10.5	10.3	26.3	16.6	14.6
	Median	49.3	54.3	57.2	62.9	70.6	69.1	53.6	60.6	60.5
Tube2 (0.0432)	Mean	47.7	62.3	62.0	68.9	76.7	75.4	58.3	69.5	68.7
	SD	13.0	7.8	8.3	15.1	5.1	6.6	17.5	9.8	10.0
	Min	26.2	53.0	51.3	32.8	68.3	63.2	26.2	53.0	51.3
	Max	65.7	78.9	78.9	86.5	82.5	82.7	86.5	82.5	82.7
	CV	27.3	12.5	13.3	22.0	6.7	8.8	30.1	14.1	14.6
	Median	48.5	61.0	60.9	68.3	77.6	77.4	63.2	69.5	68.2
Tube3 (0.0344)	Mean	52.6	71.2	69.4	79.0	87.1	84.3	65.8	79.1	76.9
	SD	15.5	9.9	10.2	16.0	9.5	8.5	20.4	12.5	11.9
	Min	23.2	55.4	47.5	52.0	70.8	75.6	23.2	55.4	47.5
	Max	70.6	93.2	85.2	106.9	101.9	97.5	106.9	101.9	97.5
	CV	29.4	14.0	14.7	20.2	11.0	10.1	31.1	15.8	15.5
	Median	53.7	70.5	69.5	77.3	89.1	82.0	67.1	78.5	75.8
Tube4 (0.0241)	Mean	77.3	96.0	93.3	99.6	121.0	114.1	88.5	108.5	103.7
	SD	19.4	13.6	17.6	25.5	14.2	13.3	24.9	18.6	18.6
	Min	35.7	80.7	61.6	35.7	98.4	91.2	35.7	80.7	61.6
	Max	101.7	121.7	126.1	127.0	141.7	135.8	127.0	141.7	135.8
	CV	25.1	14.2	18.9	25.6	11.7	11.7	28.1	17.2	17.9
	Median	79.5	94.7	94.6	103.9	124.3	113.3	92.9	107.2	103.6
Tube5 (0.0200)	Mean	83.7	111.2	108.0	118.3	142.9	138.8	101.0	127.1	123.4
	SD	26.2	15.9	14.0	32.0	15.7	14.0	33.6	22.4	20.9
	Min	33.3	86.3	83.0	57.5	118.6	110.7	33.3	86.3	83.0
	Max	131.6	141.5	136.1	154.5	159.8	153.6	154.5	159.8	153.6
	CV	31.3	14.3	13.0	27.1	11.0	10.1	33.2	17.6	16.9
	Median	83.0	110.4	107.2	125.2	147.7	139.0	101.8	123.2	122.9
Tube6 (0.0179)	Mean	95.9	121.6	121.7	134.7	157.3	150.0	115.3	139.5	135.8
	SD	24.4	13.5	17.0	36.8	17.9	17.8	36.3	23.9	22.3
	Min	43.8	95.5	102.2	59.2	117.2	125.0	43.8	95.5	102.2
	Max	129.3	138.7	155.8	177.9	176.9	170.1	177.9	176.9	170.1
	CV	25.5	11.1	14.0	27.3	11.4	11.9	31.5	17.2	16.4
	Median	97.2	124.9	121.2	131.9	162.6	156.0	109.7	136.4	133.8

(A) PIFR and R relationship:

Relationships between PIFR values and R were assessed. The results showed that $1/R$ gave the best fit for PIFR among the four transformations investigated. Table G.1 shows 'r squared' values of the plots of PIFR vs. differently transformed values for air flow resistance (Appendix G). Values for 'r squared' shown in the table clearly indicated that a better correlation was obtained with $1/R$ as the independent variable. Notably, this procedure was repeated with other inhalation variables as described above. Residuals in plots of PIFR vs. $1/R$ were also randomly distributed, without any systematic pattern. The observed positive linear relationship between PIFR and $1/R$ is consistent with the physiological literature where the slope of the regression line of PIFR vs. $1/R$ plot gives the square root of maximum pressure drop across the inhaler achieved by a given volunteer, that reportedly stays approximately constant for a range of air flow resistances typical of those seen in marketed DPIs (Smutney et al, 2009).

One of the primary hypotheses of this Chapter was that “formal training significantly improves PIFR”. Since the inhalation profiles and hence, PIFR values were documented for six different air flow resistances presented randomly to each subject, a separate statistical analysis would have been required to formally test this hypothesis at each resistance level. Therefore, a secondary variable, namely mean normalized PIFR value, was calculated from the six PIFR values per subject per training state (one per each air flow resistance), using the following steps.

1. Each PIFR value was multiplied by its corresponding R value (because PIFR and $1/R$ were linearly related). This resulted in six different $R*PIFR$ values for each training status (Before training, After training 1, After training 2) per subject.
2. Means of each set of six $R*PIFR$ values were calculated. This way, the total numbers of PIFR values per volunteer were reduced from eighteen (6 resistances * 3 training status) to three mean

(R*PIFR) values (one value per each training status). A summary of the results for mean (R*PIFR) values are compiled in Table 6.4.

Table 6.4: Descriptive results for the mean (R*PIFR) (in kPa^{0.5}) by training status and gender.

	Female			Male			Overall		
	Before	After 1	After 2	Before	After 1	After 2	Before	After 1	After 2
	Mean (R*PIFR)	Mean (R*PIFR)	Mean (R*PIFR)	Mean (R*PIFR)	Mean (R*PIFR)	Mean (R*PIFR)	Mean (R*PIFR)	Mean (R*PIFR)	Mean (R*PIFR)
Mean	1.895	2.402	2.381	2.619	3.029	2.920	2.257	2.715	2.650
SD	0.432	0.287	0.316	0.589	0.259	0.235	0.625	0.417	0.387
Min	0.893	2.012	1.900	1.291	2.529	2.510	0.893	2.012	1.900
Max	2.507	3.009	3.033	3.391	3.376	3.287	3.391	3.376	3.287
CV	22.8	11.9	13.3	22.5	8.5	8.1	27.7	15.4	14.6
Median	1.879	2.375	2.372	2.654	3.053	2.920	2.244	2.661	2.583

(B) Comparison of After training 1 versus After training 2 results for PIFR:

The regression analysis indicated that there was a significant positive linear relationship between mean (R*PIFR)-After training 1 and mean (R*PIFR)-After training 2 [$p < 0.0001$, r squared = 0.948] (Figure 6.4). The slope of the regression line was 0.91 [95% CI = (0.80, 1.01)]; the slope was not significantly different from 1.00 because 95% CI includes 1.00, indicating that the difference between mean (R*PIFR)-After training 1 and -After training 2 was insignificant, statistically. Since mean (R*PIFR)-After training 1 and -After training 2 values were not significantly different, both values were grouped together as a single statistical category described as ‘After training’ instead of categorizing and testing each separately as ‘After training 1’ and ‘After training 2’. This procedure resulted in one value of mean (R*PIFR) for ‘Before training’ and two mean (R*PIFR) values for ‘After training’ per volunteer.

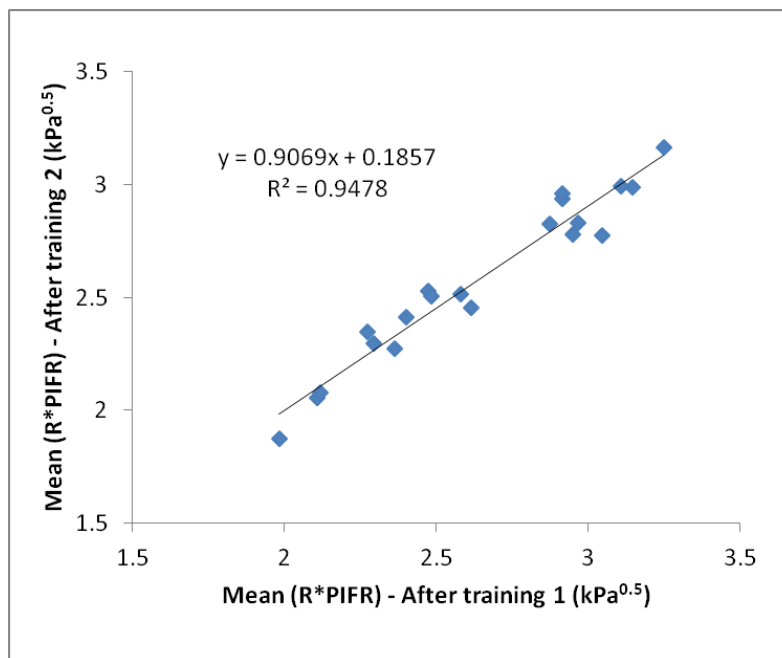


Figure 6.4: Linear regression of Mean (R*PIFR) – After training 2 and Mean (R*PIFR) – After training 1; 95% CI of the regression line slope (0.80, 1.01) also included 1.00 indicating that slope was not significantly different from 1.00.

(C) Primary analysis for PIFR – Effects of training and gender:

Repeated-measures ANOVA indicated that there was no evidence of a significant interaction between gender and training status for mean (R*PIFR) [$p = 0.386$]. Hence, effects of gender and training on mean (R*PIFR) were evaluated independently. A significant improvement of $0.426 \text{ kPa}^{0.5}$ in mean (R*PIFR) was observed after formal training in the whole subject population [$n=20$; $p < 0.0001$]. Also, a significant effect of training by gender was observed with respect to mean (R*PIFR) [$p < 0.0001$] where males had larger PIFR*R values on average than females. Also, based on Normal-Quantile plots, the residuals of repeated measures ANOVA model appeared to be normally distributed as shown in Figure 6.5

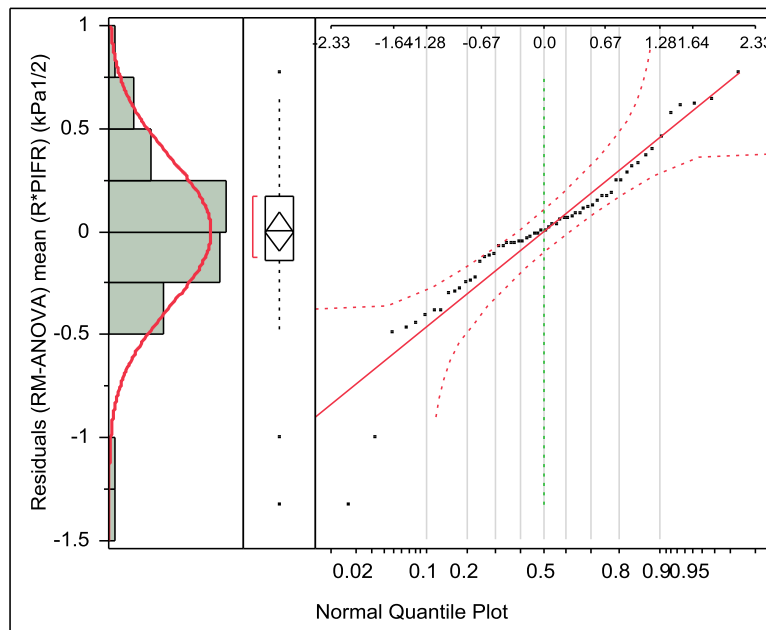


Figure 6.5: Normal-Quantile plot for residuals of repeated measures ANOVA for mean (R*PIFR) in males and females combined.

6.3.4.3 Inhalation Volume, V

The descriptive results for inhalation volume are presented in Table 6.5. Visual inspection of this data indicated that males inhaled more air compared to females, irrespective of the air flow resistance employed or the subject's training status. Mean values for V however, showed only small changes due to air flow resistance. Nevertheless, it appeared that formal training caused volunteers to inhale more deeply than they did 'Before training'. Also, formal training helped to reduce the inter-subject variability in inhalation volume (based on SD and CV values) in both genders. As can be seen in Table 6.5, overall CV values are similar for all the resistance tubes which indicated that inter-subject variability of V was independent of the airflow resistance of DPI; also, unlike PIFR, SD value of V didn't change with change in airflow resistance..

Table 6.5: Descriptive results for V (liters) by training status and gender for different resistance tubes; air flow resistance of the tubes ($\text{kPa}^{0.5} \cdot \text{L}^{-1} \cdot \text{min}$) are described in parentheses below the Tube number.

		Female			Male			Overall		
		Before	After 1	After 2	Before	After 1	After 2	Before	After 1	After 2
Tube (R in $\text{kPa}^{0.5} \cdot \text{L}^{-1} \cdot \text{min}$)		V [L]	V [L]	V [L]	V [L]	V [L]	V [L]	V [L]	V [L]	V [L]
Tube1 (0.0462)	Mean	1.517	1.870	1.993	2.780	3.632	3.711	2.148	2.751	2.852
	SD	0.602	0.392	0.406	1.054	0.742	0.830	1.057	1.073	1.087
	Min	0.863	1.197	1.204	1.720	2.835	2.598	0.863	1.197	1.204
	Max	2.701	2.489	2.436	5.455	5.264	5.429	5.455	5.264	5.429
	CV	39.7	21.0	20.4	37.9	20.4	22.4	49.2	39.0	38.1
	Median	1.396	1.893	2.044	2.460	3.563	3.583	2.184	2.662	2.517
Tube2 (0.0432)	Mean	1.463	1.889	2.035	2.796	3.836	3.779	2.129	2.862	2.907
	SD	0.749	0.479	0.413	1.010	0.745	0.770	1.103	1.170	1.078
	Min	0.631	1.260	1.361	1.602	3.134	2.536	0.631	1.260	1.361
	Max	2.790	2.644	2.728	5.167	5.571	5.300	5.167	5.571	5.300
	CV	51.2	25.4	20.3	36.1	19.4	20.4	51.8	40.9	37.1
	Median	1.223	1.887	2.087	2.547	3.651	3.932	2.077	2.889	2.632
Tube3 (0.0344)	Mean	1.375	1.981	2.081	2.785	3.788	3.742	2.080	2.885	2.912
	SD	0.514	0.456	0.378	1.079	0.831	0.878	1.095	1.133	1.076
	Min	0.604	1.315	1.628	1.739	2.751	2.583	0.604	1.315	1.628
	Max	2.463	2.606	2.701	5.393	5.649	5.522	5.393	5.649	5.522
	CV	37.4	23.0	18.2	38.7	21.9	23.5	52.7	39.3	37.0
	Median	1.279	1.930	2.032	2.473	3.730	3.752	1.923	2.679	2.642
Tube4 (0.0241)	Mean	1.632	2.069	2.173	3.197	3.819	3.797	2.414	2.944	2.985
	SD	0.580	0.504	0.383	1.003	0.780	0.808	1.131	1.102	1.036
	Min	0.806	1.079	1.593	2.079	3.022	2.833	0.806	1.079	1.593
	Max	2.743	2.655	2.691	5.564	5.743	5.596	5.564	5.743	5.596
	CV	35.5	24.4	17.6	31.4	20.4	21.3	46.9	37.4	34.7
	Median	1.460	2.234	2.174	3.116	3.689	3.770	2.257	2.838	2.762
Tube5 (0.0200)	Mean	1.765	2.098	2.086	3.370	3.913	3.943	2.568	3.006	3.015
	SD	0.540	0.427	0.433	0.789	0.803	0.824	1.054	1.122	1.148
	Min	1.207	1.553	1.345	2.340	2.836	2.833	1.207	1.553	1.345
	Max	2.868	2.873	2.837	5.020	5.743	5.557	5.020	5.743	5.557
	CV	30.6	20.3	20.8	23.4	20.5	20.9	41.0	37.3	38.1
	Median	1.547	2.096	2.017	3.308	3.755	3.771	2.389	2.855	2.835
Tube6 (0.0179)	Mean	1.617	2.242	2.234	3.127	3.696	3.787	2.372	2.969	3.011
	SD	0.610	0.462	0.372	0.959	0.861	0.872	1.101	1.004	1.030
	Min	0.466	1.373	1.514	2.248	3.019	2.733	0.466	1.373	1.514
	Max	2.600	2.852	2.741	5.493	5.600	5.522	5.493	5.600	5.522
	CV	37.7	20.6	16.6	30.7	23.3	23.0	46.4	33.8	34.2
	Median	1.690	2.331	2.307	2.696	3.354	3.698	2.294	2.936	2.737

(A) V versus R relationship:

Relationship between V and R was assessed in a similar way to PIFR versus R. Regression analyses indicated that in most of the cases there was no significant relationship between V or any of the R transforms investigated (Table G.2, Appendix G). These observations confirmed that inhalation volume did not significantly depend on air flow resistance, i.e., no normalization was required.

Since there was no relationship between V and R, mean V*, values were calculated by taking averages of each set of six values of V per volunteer, per training status. This resulted in three mean V* values per volunteer ['Before training', 'After training 1' and 'After training 2']. Note that the asterisk (*) used in mean V* differentiates this variable from the mean values of V reported in Table 6.5. A summary of the mean V* values are compiled in Table 6.6.

(B) Comparison of After training 1 and After training 2 mean V* :

Regression analysis indicated a significant positive relationship between mean V*-After training 1 and mean V* -After training 2 [$p < 0.0001$, $r \text{ squared} = 0.962$]. The slope of the regression line was 0.97 [95% CI = (0.87, 1.06)] (Figure 6.6); the slope was not significantly different from 1.00 indicating that there was no significant difference between mean V* After training-1 and After training-2. Thus, mean V* -After training 1 and -After training 2 values were grouped together to form a single statistical category 'After training' instead of categorizing and testing each separately as 'After training 1' and 'After training 2'. This procedure resulted in one value of mean V* for 'Before training' and two mean V* values for 'After training' per volunteer.

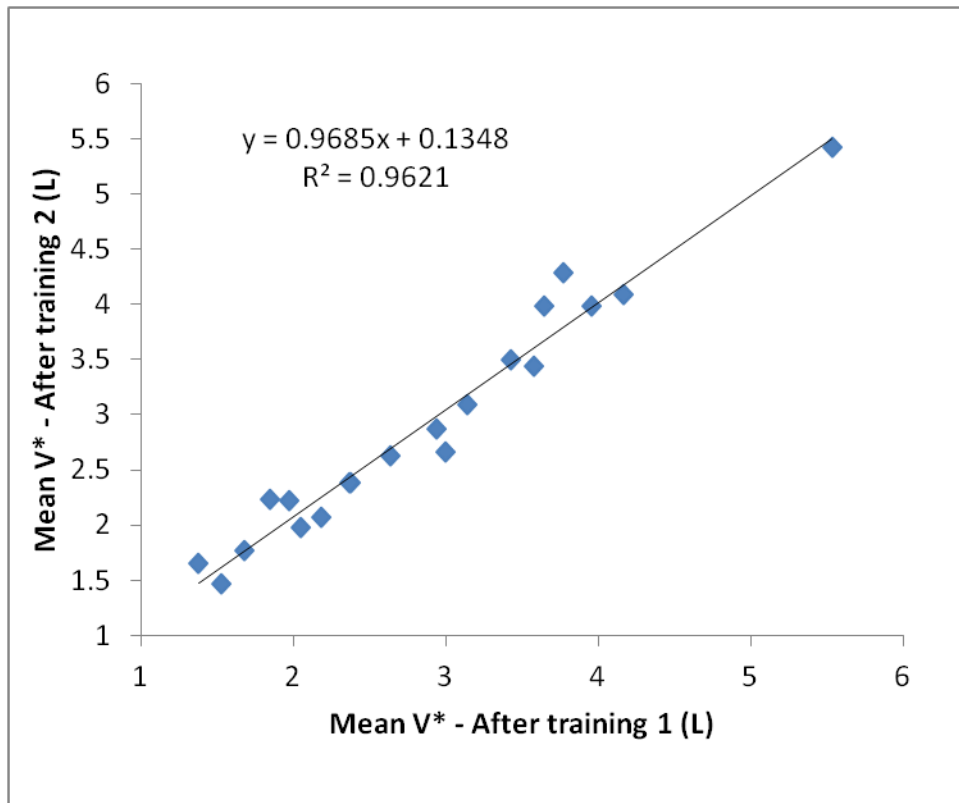


Figure 6.6: Linear regression of mean V* – After training 2 and mean V* – After training 1; 95% CI of the regression line slope (0.87, 1.06) also included 1.00 indicating that slope was not significantly different than 1.00.

(C) Primary analysis for mean V* – Effects of training and gender:

The repeated measures ANOVA model indicated that there was no evidence of a significant interaction between gender and training status for mean V* [$p = 0.122$]. Hence, the effects of gender and training on mean V* were evaluated independently. A statistically significant improvement = 0.64 L in mean V* was observed after formal training across gender ($n=20$) compared to mean V* observed before training [$p < 0.0001$]. Also, a significant gender difference in mean V* was observed across the training status [$p < 0.0001$]; overall, males ($n=10$) inhaled 1.586 L more compared to females ($n=10$), as expected, based on the fact that males have higher total lung capacity (Hankinson et al, 1999). Following construction of

Normal-Quantile plots (Figure 6.7), residuals of the repeated measures ANOVA model were found to be non-normally distributed. When the analysis was repeated using log transformed data for mean V* the conclusion was the same (data not described).

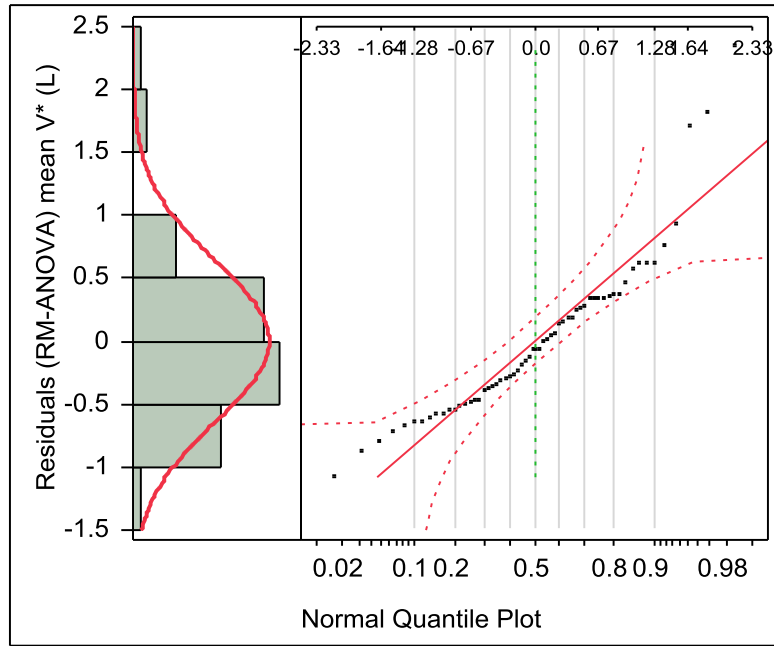


Figure 6.7: Normal-Quantile plot for residuals of repeated measures ANOVA for mean V*.

Table 6.6: Descriptive results for the mean V* (liters) by training status and gender.

	Female			Male			Overall		
	Before MeanV*	After 1 MeanV*	After 2 MeanV*	Before MeanV*	After 1 MeanV*	After 2 MeanV*	Before MeanV*	After 1 MeanV*	After 2 MeanV*
Mean	1.562	2.025	2.100	3.009	3.781	3.793	2.285	2.903	2.947
SD	0.532	0.410	0.370	0.925	0.758	0.814	1.044	1.078	1.064
Min	1.065	1.393	1.486	2.366	2.982	2.713	1.065	1.393	1.486
Max	2.484	2.687	2.679	5.349	5.595	5.488	5.349	5.595	5.488
CV	34.0	20.2	17.6	30.7	20.0	21.5	45.7	37.2	36.1
Median	1.384	2.031	2.167	2.620	3.688	3.799	2.384	2.834	2.696

6.3.4.4 t_{\max}

The descriptive results for t_{\max} are presented in Table 6.7. Based on the visual inspection of the data, it appeared that mean (t_{\max}) was largely unaffected by changes in air flow resistance, irrespective of the training status of the volunteers. The data also indicated that following formal training, volunteers took shorter time to reach PIFR than they took 'Before training'. However, unlike the cases of V and PIFR, formal training did not appear to systematically reduce the inter-subject variability in values for t_{\max} .

Table 6.7: Descriptive results for t_{\max} by training status and gender for different resistance tubes; air flow resistance of the tubes ($\text{kPa}^{0.5} \cdot \text{L}^{-1} \cdot \text{min}$) are described in parentheses below the Tube number.

		Female			Male			Overall		
		Before	After 1	After 2	Before	After 1	After 2	Before	After 1	After 2
Tube (R in $\text{kPa}^{0.5} \cdot \text{L}^{-1} \cdot \text{min}$)		t_{\max} [s]	t_{\max} [s]	t_{\max} [s]	t_{\max} [s]	t_{\max} [s]	t_{\max} [s]	t_{\max} [s]	t_{\max} [s]	t_{\max} [s]
Tube1 (0.0462)	Mean	0.799	0.621	0.581	0.953	0.574	0.591	0.876	0.597	0.586
	SD	0.446	0.340	0.305	0.461	0.215	0.321	0.448	0.278	0.305
	Min	0.265	0.215	0.355	0.440	0.190	0.240	0.265	0.190	0.240
	Max	1.570	1.155	1.360	2.060	0.860	1.175	2.060	1.155	1.360
	CV	55.8	54.7	52.5	48.3	37.5	54.4	51.2	46.5	52.1
	Median	0.658	0.548	0.470	0.910	0.585	0.430	0.708	0.585	0.445
Tube2 (0.0432)	Mean	0.828	0.558	0.608	0.909	0.664	0.545	0.869	0.611	0.577
	SD	0.690	0.211	0.261	0.611	0.328	0.224	0.636	0.274	0.239
	Min	0.320	0.195	0.255	0.460	0.220	0.270	0.320	0.195	0.255
	Max	2.590	0.865	1.050	2.560	1.250	0.950	2.590	1.250	1.050
	CV	83.3	37.9	42.9	67.2	49.3	41.0	73.2	44.8	41.4
	Median	0.513	0.548	0.583	0.728	0.568	0.515	0.705	0.568	0.558
Tube3 (0.0344)	Mean	0.846	0.410	0.452	0.831	0.701	0.562	0.839	0.555	0.507
	SD	0.619	0.123	0.152	0.475	0.388	0.331	0.537	0.318	0.257
	Min	0.260	0.175	0.215	0.365	0.240	0.315	0.260	0.175	0.215
	Max	1.955	0.580	0.705	1.550	1.695	1.450	1.955	1.695	1.450
	CV	73.2	30.0	33.6	57.1	55.4	59.0	64.0	57.2	50.7
	Median	0.663	0.438	0.470	0.608	0.658	0.475	0.625	0.488	0.470
Tube4 (0.0241)	Mean	0.915	0.470	0.559	0.937	0.598	0.598	0.926	0.534	0.579
	SD	0.633	0.168	0.274	0.660	0.290	0.266	0.629	0.240	0.263
	Min	0.365	0.180	0.240	0.460	0.230	0.220	0.365	0.180	0.220
	Max	2.210	0.710	1.195	2.575	1.230	1.075	2.575	1.230	1.195
	CV	69.1	35.8	49.0	70.4	48.6	44.4	67.9	45.0	45.5
	Median	0.648	0.500	0.500	0.620	0.530	0.593	0.623	0.513	0.523
Tube5 (0.0200)	Mean	0.795	0.472	0.442	0.896	0.643	0.543	0.845	0.557	0.492
	SD	0.360	0.097	0.228	0.647	0.195	0.305	0.512	0.174	0.268
	Min	0.425	0.350	0.230	0.515	0.305	0.225	0.425	0.305	0.225
	Max	1.690	0.650	1.030	2.660	0.920	1.330	2.660	0.920	1.330
	CV	45.2	20.6	51.7	72.3	30.3	56.3	60.6	31.1	54.4
	Median	0.723	0.488	0.388	0.653	0.630	0.453	0.688	0.520	0.433
Tube6 (0.0179)	Mean	0.633	0.452	0.535	0.958	0.507	0.650	0.796	0.479	0.592
	SD	0.368	0.212	0.235	0.714	0.219	0.608	0.577	0.212	0.453
	Min	0.200	0.215	0.215	0.455	0.165	0.150	0.200	0.165	0.150
	Max	1.340	0.945	0.855	2.335	0.940	2.310	2.335	0.945	2.310
	CV	58.1	47.0	44.0	74.6	43.2	93.6	72.6	44.2	76.4
	Median	0.505	0.390	0.490	0.650	0.473	0.455	0.595	0.458	0.460

(A) Relationship between t_{\max} and R:

Relationships between t_{\max} and R were explored similarly. Regression analyses indicated that in most cases there was no significant correlation between t_{\max} and any R transform (Table G.3, Appendix G). In short, normalization of values for t_{\max} was unnecessary.

Mean t_{\max}^* values were calculated by taking averages of each set of six t_{\max} values per volunteer, per training status; resulting in three mean t_{\max}^* values per volunteer [one from each training status]. Note that the asterisk (*) used in mean t_{\max}^* differentiates this variable from the mean values of t_{\max} reported in Table 6.7. Summary of mean t_{\max}^* values are compiled in Table 6.8.

(B) Comparison of After training 1 and After training 2 mean t_{\max}^* :

Regression analysis indicated a significant positive relationship between mean t_{\max}^* -After training 1 and mean t_{\max}^* -After training 2 [$p < 0.0001$, $r^2 = 0.610$]. The slope of the regression line was 1.04 [95% CI = (0.63, 1.46) (Figure 6.8)]; the slope was not significantly different from 1.00 indicating that there was no significant difference between mean t_{\max}^* After training-1 and t_{\max}^* After training-2. Thus, mean t_{\max}^* -After training 1 and t_{\max}^* After training 2 values were grouped together to form a single statistical category called 'After'. This procedure resulted in one value of mean t_{\max}^* for 'Before training' and two mean t_{\max}^* values for 'After training' per volunteer.

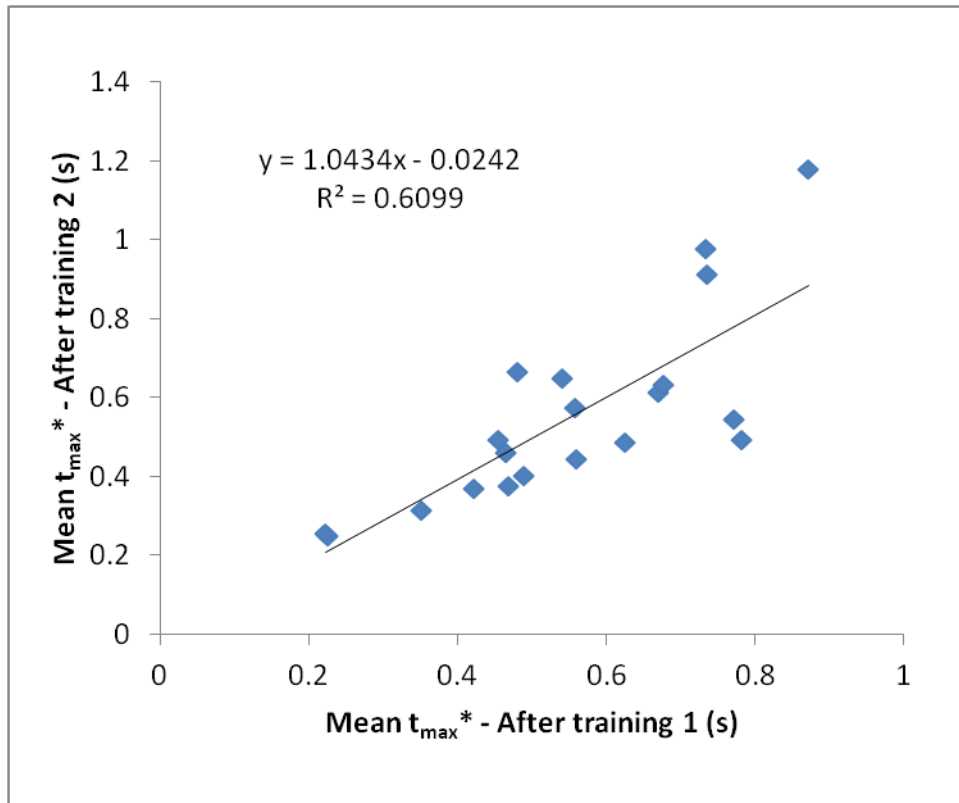


Figure 6.8: Linear regression of mean t_{\max}^* – After training 2 and mean t_{\max}^* – After training 1; 95% CI of the regression line slope (0.63, 1.46) also included 1.00 indicating that the slope was not significantly different from 1.00.

(C) Primary analysis for t_{\max} – Effects of training and gender

Repeated measures ANOVA indicated that there was no evidence of significant interaction between gender and training status for mean t_{\max}^* [$p = 0.850$]. Hence, effects of gender and training on mean t_{\max}^* were evaluated independently. A significant reduction of 0.303 seconds in mean t_{\max}^* was observed after formal training in the whole subject population [$p < 0.0001$]. No significant effect of gender on mean t_{\max}^* was observed, across the training status [$p = 0.364$]. Following construction of Normal-Quantile plots (Figure 6.9), residuals of the repeated measures ANOVA model were found to be non-normally distributed. When the analysis was

repeated using log transformed data for mean t_{\max}^* , the conclusion was the same (data not shown).

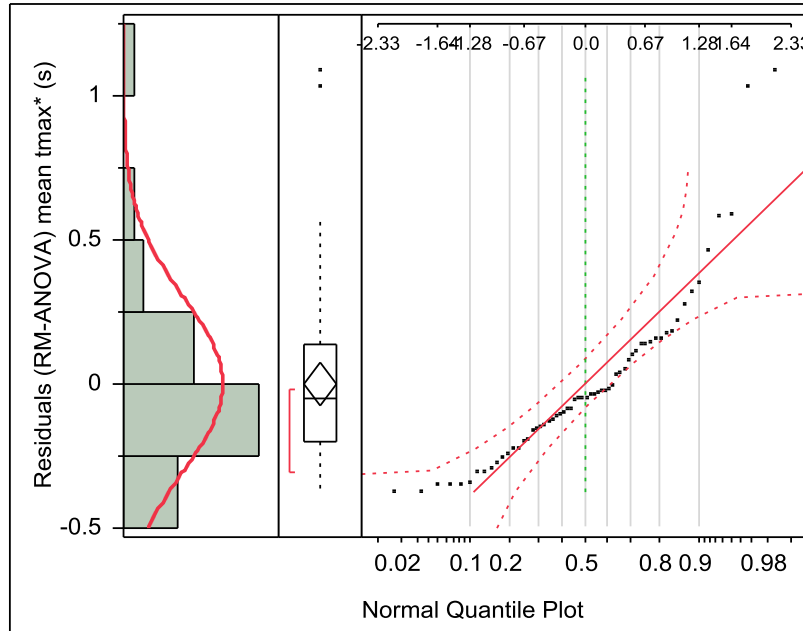


Figure 6.9: Normal-Quantile plot for residuals of repeated measures ANOVA for mean t_{\max}^* .

Table 6.8: Descriptive results for the mean t_{\max}^* (in seconds) by training status and gender.

	Female			Male			Overall		
	Before	After 1	After 2	Before	After 1	After 2	Before	After 1	After 2
Mean	0.803	0.497	0.529	0.914	0.614	0.582	0.858	0.555	0.555
SD	0.447	0.153	0.210	0.456	0.192	0.275	0.443	0.179	0.240
Min	0.453	0.222	0.255	0.540	0.225	0.250	0.453	0.222	0.250
Max	1.893	0.734	0.978	1.944	0.872	1.179	1.944	0.872	1.179
CV	55.7	30.8	39.6	49.9	31.3	47.3	51.7	32.3	43.2
Median	0.667	0.473	0.491	0.744	0.619	0.520	0.683	0.550	0.495

6.3.4.5 t_{total}

The descriptive results for t_{total} are presented in Table 6.9. Visual inspection of this data indicated that males inhaled longer than females, irrespective of the air flow resistance employed or the subject's training status. Both, males and females, showed a decreased mean t_{total} with a decrease in air flow resistance, irrespective of the subject's training status. This was apparently because low air flow resistance allowed faster inhalation resulting in smaller total inhalation times. It also appeared that formal training slightly increased t_{total} especially in cases of high air flow resistance. Formal training also reduced inter-subject variability of t_{total} in both genders. As can be seen in Table 6.3, overall CV values are similar for all the resistance tubes which indicated that inter-subject variability of t_{total} was independent of the airflow resistance of DPI.

Table 6.9: Descriptive results for t_{total} by training status and gender for different resistance tubes; air flow resistance of the tubes ($\text{kPa}^{0.5} \cdot \text{L}^{-1} \cdot \text{min}$) are described in parentheses along with the Tube number.

		Female			Male			Overall		
		Before	After 1	After 2	Before	After 1	After 2	Before	After 1	After 2
Tube (R in $\text{kPa}^{0.5} \cdot \text{L}^{-1} \cdot \text{min}$)		t_{total} [s]	t_{total} [s]	t_{total} [s]	t_{total} [s]	t_{total} [s]	t_{total} [s]	t_{total} [s]	t_{total} [s]	t_{total} [s]
Tube1 (0.0462)	Mean	2.841	3.207	3.227	4.313	4.862	5.223	3.577	4.034	4.225
	SD	0.886	0.738	0.690	2.306	1.200	1.392	1.860	1.289	1.480
	Min	1.620	2.170	2.145	2.200	3.545	3.610	1.620	2.170	2.145
	Max	4.030	4.605	4.160	9.555	7.535	8.290	9.555	7.535	8.290
	CV	31.2	23.0	21.4	53.5	24.7	26.6	52.0	31.9	35.0
	Median	2.990	3.248	3.313	3.783	4.638	4.818	3.355	3.700	3.835
Tube2 (0.0432)	Mean	2.719	2.992	3.112	3.946	4.959	4.834	3.332	3.975	3.973
	SD	1.069	0.783	0.787	2.038	1.089	1.090	1.704	1.368	1.279
	Min	1.440	1.820	1.810	1.925	3.520	3.135	1.440	1.820	1.810
	Max	4.880	4.555	4.640	8.565	7.490	7.100	8.565	7.490	7.100
	CV	39.3	26.2	25.3	51.7	22.0	22.5	51.2	34.4	32.2
	Median	2.695	3.030	3.238	3.458	4.683	4.913	2.883	3.755	3.693
Tube3 (0.0344)	Mean	2.524	2.718	2.850	3.499	4.248	4.201	3.011	3.483	3.525
	SD	0.896	0.619	0.623	1.373	1.219	0.955	1.234	1.225	1.047
	Min	1.205	2.055	2.025	1.935	2.775	2.640	1.205	2.055	2.025
	Max	4.240	4.085	3.850	5.920	7.195	5.920	5.920	7.195	5.920
	CV	35.5	22.8	21.9	39.2	28.7	22.7	41.0	35.2	29.7
	Median	2.513	2.508	2.875	2.805	4.223	4.403	2.745	3.223	3.233
Tube4 (0.0241)	Mean	2.107	2.187	2.350	3.188	3.354	3.376	2.647	2.770	2.863
	SD	0.659	0.542	0.654	1.978	0.937	0.930	1.538	0.956	0.943
	Min	1.185	1.225	1.590	1.835	2.305	2.355	1.185	1.225	1.590
	Max	3.300	2.885	3.780	8.395	5.620	5.085	8.395	5.620	5.085
	CV	31.3	24.8	27.8	62.0	27.9	27.6	58.1	34.5	32.9
	Median	2.105	2.270	2.325	2.513	3.200	3.060	2.255	2.688	2.608
Tube5 (0.0200)	Mean	2.182	2.010	1.838	2.786	2.960	3.007	2.484	2.485	2.422
	SD	0.534	0.485	0.329	1.094	0.752	0.684	0.893	0.786	0.795
	Min	1.435	1.280	1.105	1.635	1.945	1.905	1.435	1.280	1.105
	Max	2.930	2.780	2.200	5.560	4.795	4.195	5.560	4.795	4.195
	CV	24.5	24.1	17.9	39.3	25.4	22.7	36.0	31.6	32.8
	Median	2.158	1.935	1.885	2.528	2.810	3.058	2.278	2.595	2.188
Tube6 (0.0179)	Mean	1.789	1.821	1.938	2.404	2.581	2.748	2.096	2.201	2.343
	SD	0.626	0.417	0.419	1.195	0.748	0.963	0.981	0.706	0.834
	Min	0.440	1.210	1.100	1.460	1.595	1.745	0.440	1.210	1.100
	Max	2.585	2.300	2.480	5.215	4.265	4.560	5.215	4.265	4.560
	CV	35.0	22.9	21.6	49.7	29.0	35.0	46.8	32.1	35.6
	Median	1.783	1.918	1.985	2.030	2.495	2.358	1.810	2.140	2.208

(A) t_{total} and R correlation:

The relationship between t_{total} and R was assessed in a similar way to relationships between PIFR and R. The results showed that R gave the best fit for t_{total} among the four R transforms investigated (Appendix G). Residuals in plots of t_{total} vs. R were randomly distributed, without showing any systematic pattern.

Each t_{total} value (minutes) was divided by its corresponding R value (because plots of t_{total} vs. R were linear). This resulted in six different $\left(\frac{t_{\text{total}}}{R}\right)$ values for each training status (Before training, After training 1, After training 2), per subject. A mean $\left(\frac{t_{\text{total}}}{R}\right)$ value was calculated by taking the mean of each set of six t_{total}/R values. This data processing step produced three mean $\left(\frac{t_{\text{total}}}{R}\right)$ values per volunteer [one value for each training status]. A summary of the results for mean $\left(\frac{t_{\text{total}}}{R}\right)$ values are compiled in Table 6.10.

(B) Comparison of After training 1 and After training 2 values for t_{total} :

Regression analysis indicated a significant negative linear relationship between mean $\left(\frac{t_{\text{total}}}{R}\right)$ -After training 1 and mean $\left(\frac{t_{\text{total}}}{R}\right)$ -After training 2 [$p < 0.0001$, r squared = 0.924] (Figure 6.10). The slope of the regression line was 0.97 [95% CI = (0.84, 1.11)]; the slope was not significantly different from 1.00, indicating the difference between mean $\left(\frac{t_{\text{total}}}{R}\right)$ -After training 1 and After training 2 was statistically insignificant. Since mean $\left(\frac{t_{\text{total}}}{R}\right)$ -After training 1 and -After training 2 values were not significantly different, both values were grouped together as a single statistical category described as ‘After training’ instead of categorizing and testing each separately as ‘After training 1’ and ‘After training 2’. This procedure resulted in one value of

mean $\left(\frac{t_{\text{total}}}{R}\right)$ values for ‘Before training’ and two mean $\left(\frac{t_{\text{total}}}{R}\right)$ values for ‘After training’ per volunteer.

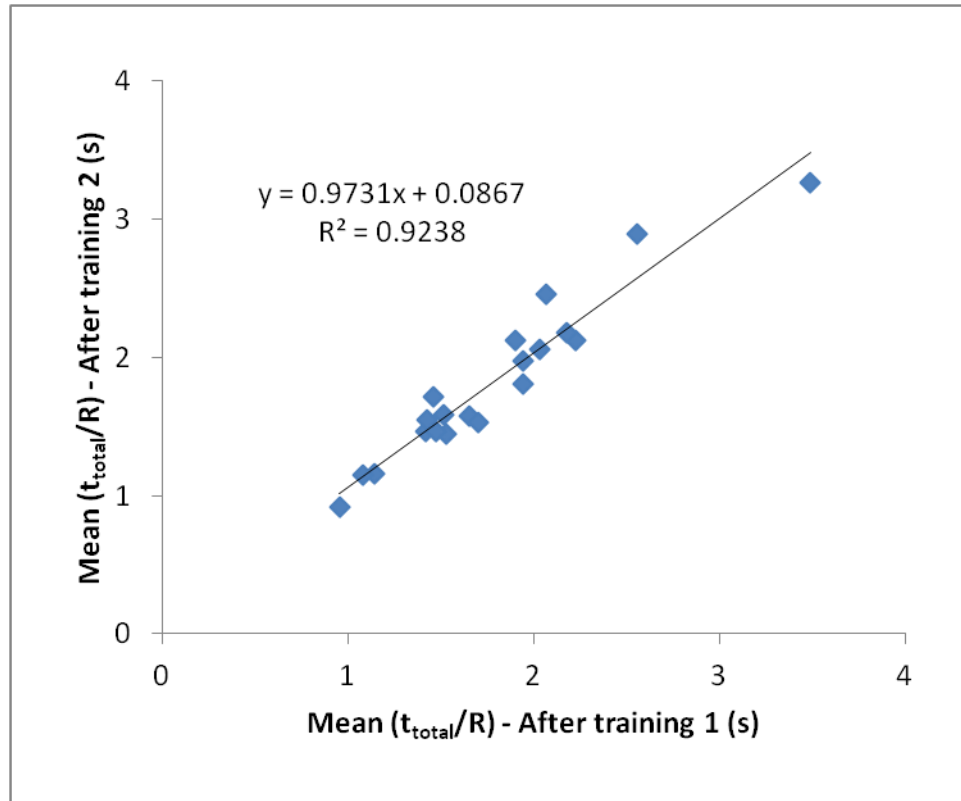


Figure 6.10: Linear regression of mean $\left(\frac{t_{\text{total}}}{R}\right)$ – After training 2 and mean $\left(\frac{t_{\text{total}}}{R}\right)$ – After training 1; 95% CI of the regression line slope (0.84, 1.11) also included 1.00 indicating that slope was not significantly different than 1.00.

(C) Primary analysis for t_{total} – Effects of training and gender:

Repeated measures ANOVA indicated that there was no evidence of significant interaction between gender and training status for mean $\left(\frac{t_{\text{total}}}{R}\right)$ [p = 0.314]. Hence, effects of gender and training on mean $\left(\frac{t_{\text{total}}}{R}\right)$ were evaluated independently. No significant change in mean $\left(\frac{t_{\text{total}}}{R}\right)$ was observed following formal training compared to ‘Before training’ [p = 0.101].

On other hand, a significant difference in mean $\left(\frac{t_{\text{total}}}{R}\right)$ was observed between males and females [$p = 0.006$]; males inhaled for longer compared to females. Following construction of a Normal-Quantile plot, residuals of repeated measures ANOVA model were found to be non-normally distributed (Figure 6.11). When the analysis was repeated using log transformed data for mean $\left(\frac{t_{\text{total}}}{R}\right)$ the conclusion was the same (data not shown).

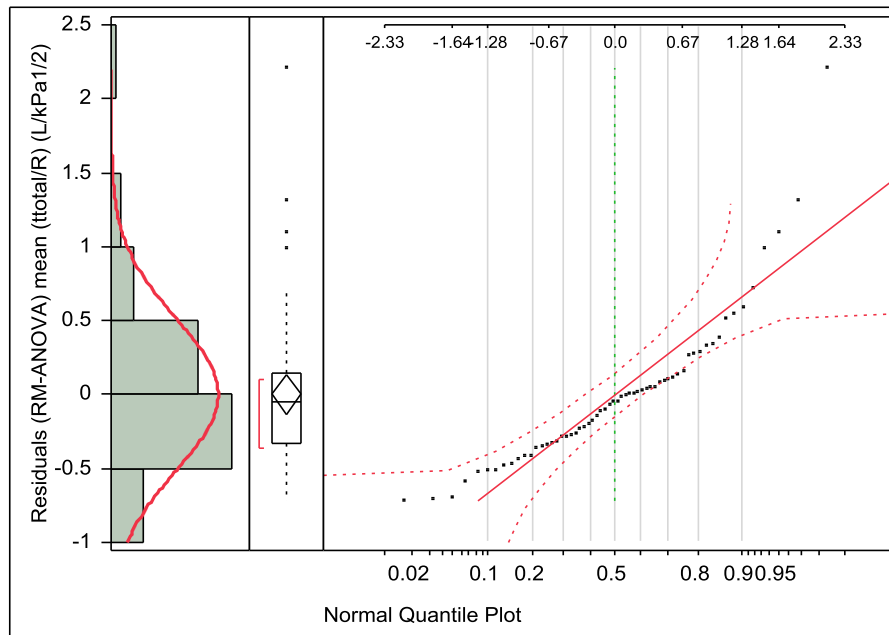


Figure 6.11: Normal-Quantile plot for residuals of repeated measures ANOVA for mean $\left(\frac{t_{\text{total}}}{R}\right)$.

Table 6.10: Descriptive results for the mean $\left(\frac{t_{total}}{R}\right)$ (in L/kPa^{0.5}) by training status and gender.

	Female			Male			Overall		
	Before	After 1	After 2	Before	After 1	After 2	Before	After 1	After 2
	Mean $\left(\frac{t_{total}}{R}\right)$	Mean $\left(\frac{t_{total}}{R}\right)$	Mean $\left(\frac{t_{total}}{R}\right)$	Mean $\left(\frac{t_{total}}{R}\right)$	Mean $\left(\frac{t_{total}}{R}\right)$	Mean $\left(\frac{t_{total}}{R}\right)$	Mean $\left(\frac{t_{total}}{R}\right)$	Mean $\left(\frac{t_{total}}{R}\right)$	Mean $\left(\frac{t_{total}}{R}\right)$
Mean	1.373	1.418	1.451	1.923	2.152	2.197	1.648	1.785	1.824
SD	0.349	0.295	0.307	0.903	0.557	0.557	0.723	0.575	0.582
Min	0.940	0.957	0.916	1.207	1.477	1.465	0.940	0.957	0.916
Max	1.959	1.947	1.979	4.132	3.491	3.270	4.132	3.491	3.270
CV	25.4	20.8	21.2	46.9	25.9	25.4	43.9	32.2	31.9
Median	1.366	1.443	1.502	1.588	2.048	2.125	1.506	1.676	1.652

6.3.4.6 Relationship of the inhalation variables according to subject demography data and PFT values

Relationships between each of the normalized ‘After training 1’ inhalation variable values with demographic data and PFT values were explored using univariate linear regression analysis; ‘r squared’ values for each univariate analysis are shown in Table 6.11. The results indicated that volunteers’ height, weight or age were not significantly correlated with any of the normalized inhalation variables, except for a mild, but statistically significant, correlation between female age and the mean $\left(\frac{t_{\text{total}}}{R}\right)$ value (Table 6.11). Similarly, except for FVC vs. mean t_{max}^* in females, and FEV1 vs. mean (R*PIFR) in males, FVC and FEV1 were not significantly correlated with any other normalized inhalation variable. The absence of significant relationships may well be due to small sample size.

Table 6.11: ‘r squared’ values from univariate regression analyses performed between the normalized inhalation variable values and demographic data and PFT values, separately for females and males.

	Mean (R*PIFR)		Mean V*		Mean t _{max} *		Mean ($\frac{t_{total}}{R}$)	
	Females	Males	Females	Males	Females	Males	Females	Males
Height	<0.10	0.13	0.28	0.33	<0.10	0.20	0.30	0.17
Weight	<0.10	<0.10	0.34	0.21	<0.10	<0.10	0.42**	<0.10
Age	<0.10	0.32	<0.10	0.38	0.25	0.311	<0.10	0.28
FVC	<0.10	0.36	<0.10	0.33	0.47**	<0.10	<0.10	0.33
FEV1	<0.10	0.46**	<0.10	0.25	0.38	<0.10	0.17	0.37

** Significant correlation (p<0.05)

6.3.4.7 Selection of inhalation profile:

Three representative inhalation profiles for ‘After formal training’ (small, medium, and large) were selected based on a statistical assessment of all the recorded profiles following formal training. These profiles were created to represent inter- and intra-subject variations in the recorded inhalation maneuvers that can be expected in normal volunteers, and used for potential *in vitro* regional deposition studies in future. The profiles were derived using the following steps

1. As shown in Table 6.12, volumetric flow rate (leaving the inhalation cell mouthpiece) vs. time data of each volunteer following formal training (After training 1 and After training 2) were compiled; Table 6.12 shows an example for Tube 1.
2. The 10th, 50th and 90th percentile flow rate at each time point was calculated across the entire time domain of 10 s.
3. The small, medium and large inhalation profiles were generated by plotting 10th, 50th and 90th percentile flow rate vs. time, respectively.

Representative inhalation profiles for ‘After formal training’ for other air flow resistances were created in the same way as that described for Tube 1. The small, medium and large representative inhalation profiles of different air flow resistances (Tubes 1-6) are shown in Figures 6.12 (A-F) (represented as “Actual” profiles) together with the small, medium and large simulated inhalation profiles; the “simulated” inhalation profiles were generated using the method described in Section 3.2.2 in Chapter 3. The PIFR and V values used to create the sine-wave simulated profiles were taken from those reported for corresponding representative profiles’ values shown in Table 6.13 while t_{\max} was held at 0.45 s for all the simulated profiles. As can be seen from the Figure 6.12 (A-F), the simulated profiles closely matched the

representative profiles from the analysis of the clinical data. This observation is of great importance because it validates our use of sine-wave simulated profiles for the deposition studies described in Chapters 3 and 4. Similarly, representative inhalation profiles for ‘Before formal training’ were constructed as for ‘After formal training’; The small, medium and large representative inhalation profiles for ‘Before formal training’ of different air flow resistances (Tubes 1-6) are shown in Figures 6.14 (A-F); the “simulated” inhalation profiles were generated using the PIFR and V values shown in Table 6.14 while t_{\max} was held at 0.45 s for all the simulated profiles. Figure 6.13 compares the simulated small, medium and large inhalation profiles used for the *in vitro* deposition studies from Budelin Novolizer (Fast inhalation arm, Figure 3.2 (B)) shown in Chapter 3 with the representative small, medium and large inhalation profiles after training for Tube 4, The airflow resistance of the inhalation flow cell was the same as that of Novolizer when Tube 4 was inserted. The PIFR and t_{\max} values of simulated profiles (derived using $\text{mean} \pm 2\text{SD}$ values reported by Newman et al. 2000) were comparable to those observed for the representative profiles. However, the inhalation volume of the large simulated profile (4.0 L) was smaller than the representative inhalation profile (4.6 L) because of the limited maximum volume capacity of the breath simulator (4L)

Table 6.12: Example of a spreadsheet used to calculate 10th, 50th and 90th percentile flow rate to construct small, medium and large representative inhalation profiles for ‘After formal training’ for Tube 1; AT1 – After training 1 and AT2 – After training 2.

Volunteer (Training)	Time (s) --> -----> -----> ----->					
	0.000	0.005	0.010 0.500..... 2.00010.000
1 (AT1)	0.0	2.4	3.0.....79.1..... 68.9...	0.0
2 (AT1)	0.0	0.6	3.0.....68.8..... 30.2...	0.0
3 (AT1)	0.0	0.6	1.8.....71.4..... 67.0...	0.0
4 (AT1)	0.0	1.2	1.2.....60.3..... 43.1...	0.0
5 (AT1)	0.0	1.2	2.4.....86.0..... 46.9...	0.0
7 (AT1)	0.0	1.2	1.2.....68.9..... 33.5...	0.0
8 (AT1)	0.0	1.2	4.9.....51.4..... 44.5...	0.0
9 (AT1)	0.0	0.6	1.8.....60.4..... 30.1...	0.0
10 (AT1)	0.0	0.6	1.2.....76.4..... 69.1...	0.0
11 (AT1)	0.0	0.6	1.2.....71.6..... 74.0...	0.0
12 (AT1)	0.0	1.2	1.2.....71.2..... 51.3...	0.0
13 (AT1)	0.0	0.6	1.2.....54.7..... 28.1...	0.0
14 (AT1)	0.0	0.6	2.4.....71.5..... 62.7...	0.0
15 (AT1)	0.0	2.4	2.4.....40.7..... 9.5...	0.0
16 (AT1)	0.0	1.2	2.4.....64.7..... 21.3...	0.0
17 (AT1)	0.0	0.6	1.2.....89.7..... 58.4...	0.0
18 (AT1)	0.0	1.2	1.8.....79.2..... 60.4...	0.0
19 (AT1)	0.0	1.2	1.8.....68.9..... 43.1...	0.0
20 (AT1)	0.0	1.2	1.8.....69.1..... 38.3...	0.0
21 (AT1)	0.0	0.6	1.2.....86.1..... 69.0...	0.0
1 (AT2)	0.0	2.4	3.6.....70.2..... 60.3...	0.0
2 (AT2)	0.0	0.6	1.2.....66.0..... 17.8...	0.0
3 (AT2)	0.0	0.6	1.2.....78.0..... 64.3...	0.0
4 (AT2)	0.0	1.2	1.2.....56.5..... 46.0...	0.0
5 (AT2)	0.0	1.2	1.2.....74.9..... 46.0...	0.0
7 (AT2)	0.0	0.6	1.8.....64.2..... 28.9...	0.0
8 (AT2)	0.0	1.8	1.8.....66.3..... 58.6...	0.0
9 (AT2)	0.0	0.6	1.2.....58.4..... 40.0...	0.0
10 (AT2)	0.0	0.6	1.2.....75.1..... 66.2...	0.0
11 (AT2)	0.0	0.6	1.8.....70.6..... 68.5...	0.0
12 (AT2)	0.0	0.6	1.8.....70.2..... 53.2...	0.0
13 (AT2)	0.0	0.6	3.6.....64.3..... 9.4...	0.0
14 (AT2)	0.0	1.2	2.4.....75.2..... 51.7...	0.0
15 (AT2)	0.0	1.2	1.8.....43.6..... 42.4...	0.0
16 (AT2)	0.0	0.6	2.4.....62.3..... 19.5...	0.0
17 (AT2)	0.0	1.8	2.4.....83.7..... 46.0...	0.0
18 (AT2)	0.0	0.6	2.4.....72.5..... 53.2...	0.0
19 (AT2)	0.0	1.2	1.8.....70.2..... 44.8...	0.0
20 (AT2)	0.0	1.8	1.2.....58.6..... 28.9...	0.0
21 (AT2)	0.0	0.6	2.4.....64.2..... 66.1...	0.0
10 th %tile	0.0	0.6	1.2.....56.7..... 22.0...	0.0
50 th %tile	0.0	1.0	1.8.....69.4..... 46.0...	0.0
90 th %tile	0.0	1.8	3.0.....79.2..... 68.3...	0.0

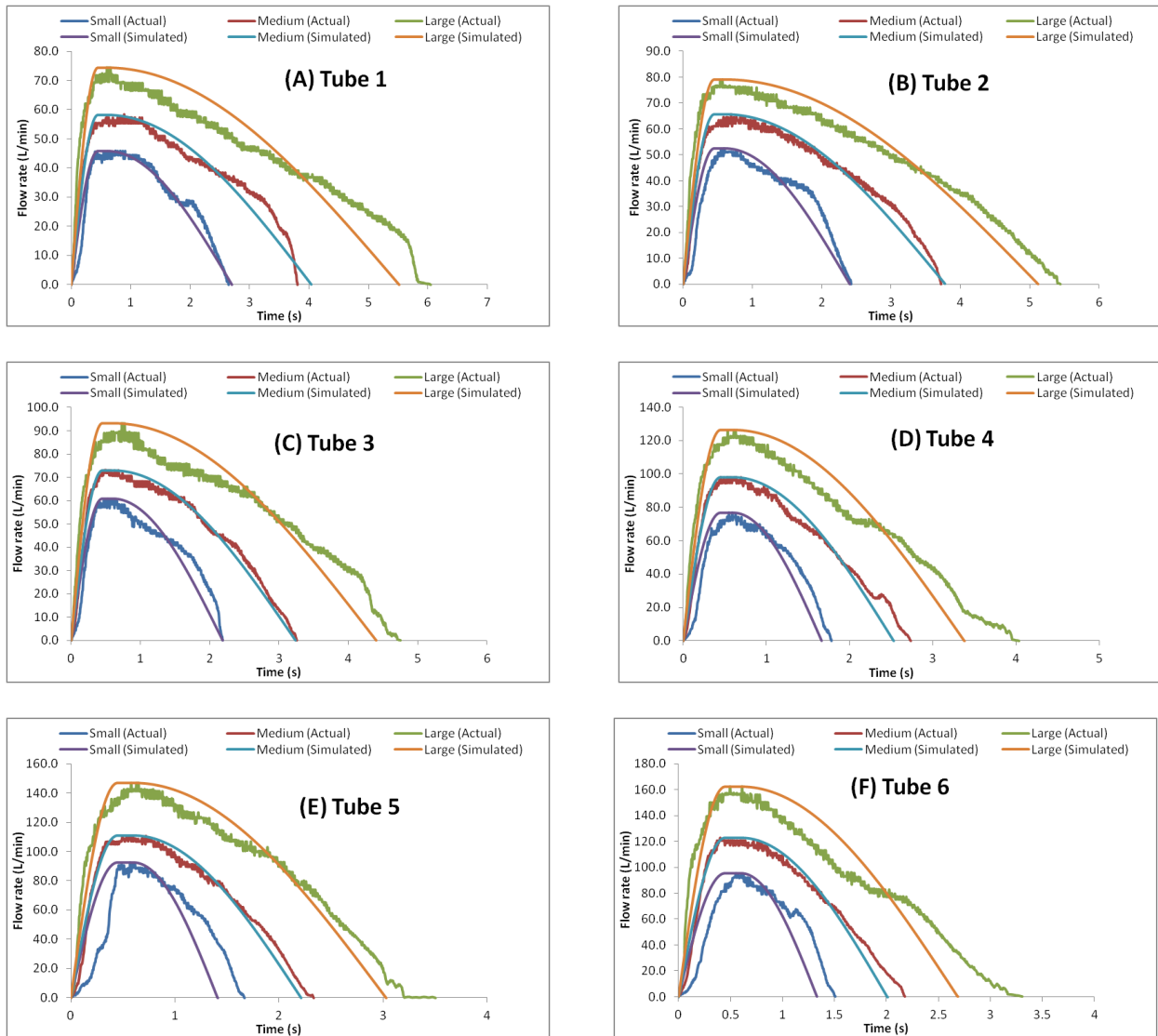


Figure 6.12: Representative inhalation profiles for different resistance tubes, ‘After formal training’, in comparison with the inhalation profiles simulated using the methods described in Chapter 3, Section 3.2.2.

Table 6.13: Descriptive results for inhalation variables in the representative inhalation profiles shown in Figure 6.12 (A-F) for ‘**After formal training**’, for different resistance tubes; air flow resistance of the tubes ($\text{kPa}^{0.5} \cdot \text{L}^{-1} \cdot \text{min}$) are described in parentheses below the name of the tube.

Tube (R in $\text{kPa}^{0.5} \cdot \text{L}^{-1} \cdot \text{min}$)	Inhalation profile	PIFR (L/min)	V (L)	t_{\max} (s)	t_{total} (s)
Tube1 (0.0462)	Small	45.8	1.352	0.745	2.645
	Medium	58.3	2.557	0.890	3.805
	Large	74.5	4.432	0.600	6.045
Tube2 (0.0432)	Small	52.6	1.389	0.595	2.425
	Medium	65.6	2.694	0.690	3.720
	Large	79.0	4.369	0.565	5.445
Tube3 (0.0344)	Small	60.8	1.466	0.525	2.190
	Medium	73.1	2.575	0.490	3.260
	Large	93.3	4.428	0.730	4.750
Tube4 (0.0241)	Small	76.9	1.430	0.550	1.785
	Medium	98.2	2.723	0.450	2.735
	Large	126.2	4.640	0.610	4.040
Tube5 (0.0200)	Small	92.5	1.469	0.570	1.670
	Medium	110.8	2.700	0.560	2.330
	Large	147.2	4.862	0.650	3.505
Tube6 (0.0179)	Small	95.3	1.435	0.555	1.510
	Medium	122.9	2.733	0.400	2.175
	Large	162.3	4.773	0.610	3.305

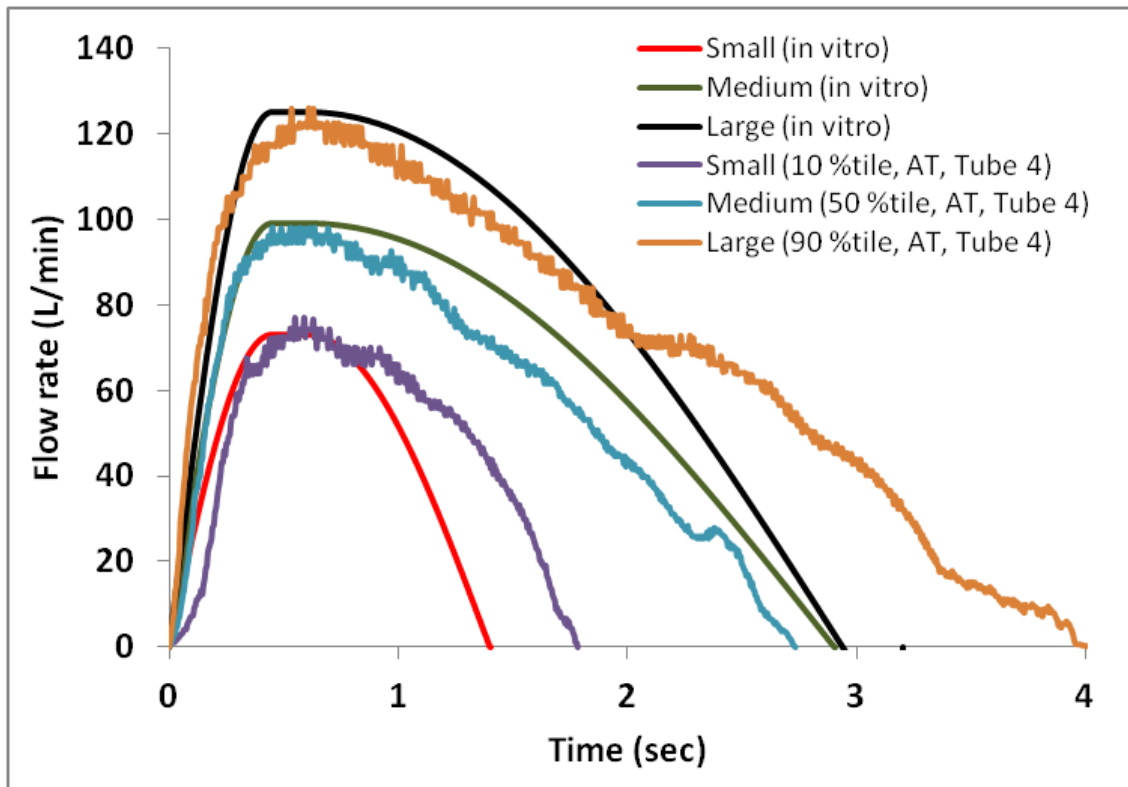


Figure 6.13: Simulated small, medium and large inhalation profiles used for the *in vitro* deposition studies from Budelin Novolizer (Fast inhalation arm, Figure 3.2 (B)) shown in Chapter 3 in comparison with the representative small, medium and large inhalation profiles for the inhalation flow cell containing Tube 4 (designed to have the same resistance as Novolizer), ‘After formal training (AT)’.

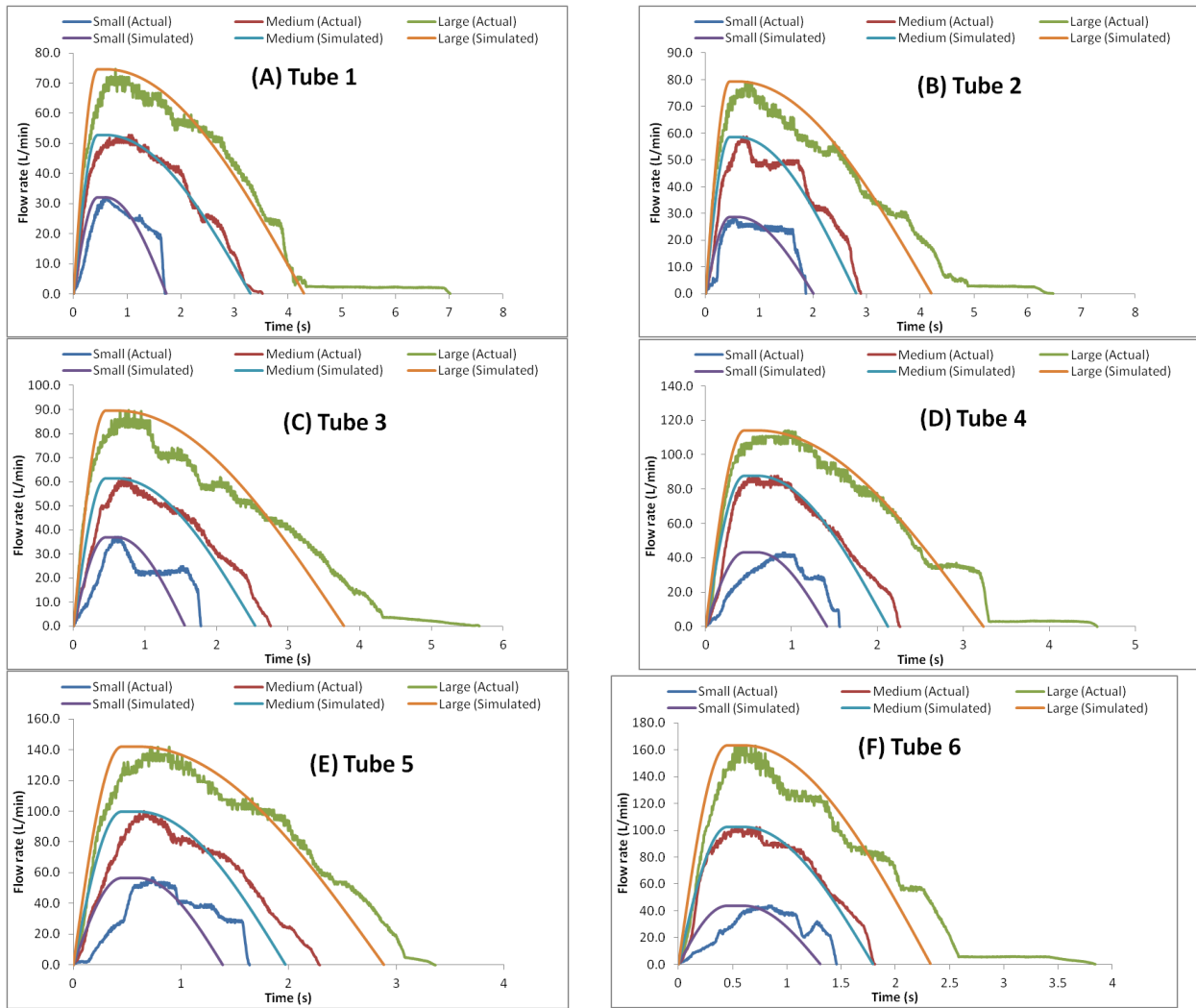


Figure 6.14: Representative inhalation profiles for different resistance tubes, ‘**Before formal training**’, in comparison with the inhalation profiles simulated using the methods described in Chapter 3, Section 3.2.2.

Table 6.14: Descriptive results for inhalation variables in the representative inhalation profiles shown in Figure 6.14 (A-F) for ‘**Before formal training**’, for different resistance tubes; air flow resistance of the tubes ($\text{kPa}^{0.5} \cdot \text{L}^{-1} \cdot \text{min}$) are described in parentheses below the name of the tube.

Tube (R in $\text{kPa}^{0.5} \cdot \text{L}^{-1} \cdot \text{min}$)	Inhalation profile	PIFR (L/min)	V (L)	t_{\max} (s)	t_{total} (s)
Tube1 (0.0462)	Small	32.1	0.620	0.595	1.705
	Medium	52.7	1.889	1.030	3.525
	Large	74.6	3.469	0.780	7.015
Tube2 (0.0432)	Small	28.6	0.635	0.545	1.865
	Medium	58.7	1.802	0.705	2.895
	Large	79.4	3.618	0.780	6.470
Tube3 (0.0344)	Small	36.9	0.642	0.610	1.780
	Medium	61.4	1.713	0.680	2.755
	Large	89.7	3.676	0.770	5.670
Tube4 (0.0241)	Small	43.2	0.689	0.900	1.560
	Medium	87.6	2.051	0.760	2.260
	Large	114.1	4.021	0.925	4.560
Tube5 (0.0200)	Small	56.6	0.884	0.730	1.635
	Medium	99.9	2.182	0.655	2.285
	Large	141.9	4.468	0.730	3.360
Tube6 (0.0179)	Small	43.6	0.644	0.840	1.460
	Medium	102.4	2.039	0.530	1.815
	Large	163.2	4.171	0.580	3.845

6.4.5 CONCLUSIONS

This study described the method and results of a clinical study designed to document the inhalation profiles commonly used by differently trained normal human adults of both genders during the use of DPIs of variable resistances, without using DPIs themselves and without administering drugs to the volunteers. The study showed that volunteers inhale faster and deeper when they are trained using written instructions in combination with formal training from a health professional, such as a pharmacist, compared to the use of written instructions alone. The study also indicated that formal training helps to reduce inter-subject variability in inhalation flow rate vs. time profiles; an observation that was believed to be important in reducing inter-subject inhalation variability that may translate into reduced variability in aerosol drug deposition in the lungs, especially for flow rate dependent DPIs such as Novolizer (Newman et al, 2000). The inhalation profiles showed that decreased air flow resistance produced increase in PIFR while V was unchanged. The results also showed that males inhaled faster and more deeply than females although no significant relationship was observed between lung function values of volunteers and their observed inhalation variables values, probably because of the small sample size studied in the clinic. In this study, we described a method of creating inhalation profiles that could be used for the *in vitro* deposition studies described in earlier Chapters, to reflect and the range of inhalation profiles used by adults during typical DPI use. We showed that the shape of the inhalation profiles can indeed be simulated using sine-waves and that a statistical analysis of the clinical results closely resembled the simulated profiles used in the earlier deposition studies in Chapters 3 and 4. While this study didn't account for the variation in mouthpiece design of marketed DPIs this was thought to have little effect on inhalation pattern; even so, it cannot be ruled out. Moreover, the scope of the study design was limited to healthy volunteers and the

observations made here probably do not reflect the situation for subjects with altered lung function.

CHAPTER 7

SUMMARY AND GENERAL CONCLUSIONS

This thesis describes the development and the literature validation of new *in vitro* methods to predict regional drug deposition from DPIs. Studies were designed in which deposition was quantified in three, differently sized airway models that were based on the anatomical literature that describes the respiratory tract of normal humans. Prior to model construction by rapid prototyping, efforts were made to ensure that the small, medium and large MT-TB model's geometry was comparable statistically with the mean – 2SD, mean and mean + 2SD volumetric dimensions of the upper human airways, respectively; furthermore that a mouthpiece adapter capable of sealing an inhaler realistically in the lip cavity of the model could be constructed for each inhaler to be tested *in vitro*. Although, there are many other physical airway models reported in the literature, we used the one developed by Xi and Longest, mainly due to the ready availability of information about this model as it was developed in-house. This gave us the flexibility to create different airway models by modifying the original airway geometry; for example different scaled models or models with different insertion angle. *In vivo*,

clinical deposition data, derived from gamma scintigraphic studies of DPIs in which the inhalation maneuver was also described, was selected from the literature. This *in vivo* data was employed for the purpose of challenging the predictivity of the new *in vitro* methods across a variety of marketed powder inhalers. In short, deposition was studied *in vitro* from marketed powder inhalers using the geometrically characterized models partnered with appropriate inspiratory profiles; the resultant *in vitro* data was compared to that reported from the clinical studies, to evaluate the predictability and robustness of the new methods.

In conclusion, and as described in detail in Chapter 3, the three MT-TB airway models, partnered with carefully selected inhalation flow rate vs. time profiles, were able to predict the ‘average’ as well as the observed variability seen *in vivo* for drug deposition in the lungs of trained healthy adults using commercially manufactured Budesonide inhalers from Meda Pharmaceuticals. The robustness of the new *in vitro* methods was confirmed by assessing the accuracy with which ‘average’ regional drug deposition could be predicted across a range of commercially available DPIs, irrespective of changing inhaler characteristics such as device design, dispersion mechanism(s), powder formulation and the magnitude of each inhaler’s resistance to air flow (Chapter 4). Average *in vitro* drug deposition from 5 different marketed DPIs showed excellent agreement with reported *in vivo* values, with absolute prediction errors of $\leq 2\%$ for all DPIs except Relenza where it seemed likely that the poor IVIVC in that case resulted from inaccurate assessments of its device retention during the *in vivo* scintigraphy studies in the literature. In Chapter 5 a study was performed to illustrate the ease with which the new *in vitro* methods can be adapted to study sources of aerosol drug deposition variability such as the effect of inhaler orientation. That study not only further underlined the usefulness of these *in vitro* techniques but showed how certain inhalers, in which aerosol momentum was minimized at the

mouthpiece, appeared to be much less likely than others to be affected by user variables such as the angle with which an inhaler is inserted between the lips. Such studies can provide useful information for designing new inhalers.

Chapters 3 and 4 employed simulated inhalation profiles to study *in vitro* drug deposition across inhalers with a broad variety of airflow resistances. The simulation techniques that were chosen to represent the inspiration of trained normal subjects, as described in the clinical literature used to validate these *in vitro* methods, were described in detail in Chapter 3 (section 3.2.2). To confirm the form of these flow rate vs. time profiles and to expand our knowledge on the effects of training, the average and range of flow rate versus time profiles used by inhaler-naïve adults inhaling in accord with both written and oral directions were collected by asking a group of human subjects to inhale through an instrumented drug-free inhalation flow cell and analyzing the resultant data (Chapter 6). The sine wave simulations used for *in vitro* testing earlier was found to be representative of the real profiles collected from normal human adults following training. Unfortunately, the maximum volume capacity of the breath simulator was limited to 4.0 L; in the clinical study, we observed several cases when volunteers inhaled more than this. Therefore, while it has been shown that effect of much larger volumes on Novolizer emptying may be minimal (Delvadia et al, 2010), the same may not be true for all other DPIs. Obviously, the breath simulator with larger volume capacity (like 7 L) would allow simulation of inhalation volume variability more accurately and this should be sought in future studies. However, different inhalation profiles (inhalation flow rate versus time curves with statistically different properties) resulted from different forms of patient training while male adults were seen to inhale faster and deeper than females. The inhalation profiles showed that as air flow resistance of an inhalation device increased, PIFR also decreases and that exposure to the written instructions that

usually accompany a DPI product generally produced suboptimal inspiratory maneuvers. In particular, critical inspiratory parameters such as PIFR and V, that can affect drug dispersion and drug dose to the lung from many powder systems on the market, were found to be statistically larger when subjects were subjected to personal training in device usage by a health professional (in addition to reading the device instructions alone).

Overall, through this project, new *in vitro* test methods were proposed that show great promise as *in vivo* predictors for the median and range of aerosol drug deposition seen in the respiratory tract of trained human subjects. It is to be hoped that these methods can be used in future as a means of comparing the efficiency of different inhalers without recourse to expensive clinical testing, as well as a foundation for the design of new inhalation platforms with improved efficiency and reproducibility.

REFERENCES

- Akapo, S. O., & Asif, M. (2003). Validation of a RP-HPLC method for the assay of formoterol and its related substances in formoterol fumarate dihydrate drug substance. *J Pharm Biomed Anal*, 33(5), 935-945.
- Anderson, M., Philipson, K., Svartengren, M., & Camner, P. (1995). Human deposition and clearance of 6-micron particles inhaled with an extremely low flow rate. *Exp Lung Res*, 21(1), 187-195.
- Anderson, M., Svartengren, M., & Camner, P. (1999). Human tracheobronchial deposition and effect of a cholinergic aerosol inhaled by extremely slow inhalations. *Exp Lung Res*, 25(4), 335-352.
- Atkins, P. J. (2005). Dry powder inhalers: an overview. *Respir Care*, 50(10), 1304.
- Borgstrom, L., Bondesson, E., Moren, F., Trofast, E., & Newman, S. (1994). Lung deposition of budesonide inhaled via Turbuhaler: a comparison with terbutaline sulphate in normal subjects. *Eur Respir J*, 7(1), 69-73.
- Borgstrom, L., Olsson, B., & Thorsson, L. (2006). Degree of throat deposition can explain the variability in lung deposition of inhaled drugs. *J Aerosol Med*, 19(4), 473-483.
- Brand, P., Meyer, T., Weuthen, T., Timmer, W., Berkel, E., Wallenstein, G., et al. (2007). Lung deposition of radiolabeled tiotropium in healthy subjects and patients with chronic obstructive pulmonary disease. *J Clin Pharmacol*, 47(10), 1335-1341.
- Brillet, P. Y., Fetita, C. I., Saragaglia, A., Brun, A. L., Beigelman-Aubry, C., Preteux, F., et al. (2008). Investigation of airways using MDCT for visual and quantitative assessment in COPD patients. *Int J Chron Obstruct Pulmon Dis*, 3(1), 97-107.

- Broeders, M. E. A. C., Sanchis, J., Levy, M. L., Crompton, G. K., Dekhuijzen, P. N. R., & on behalf of the, A. W. G. (2009). The ADMIT series - Issues in inhalation therapy. 2) improving technique and clinical effectiveness. *Prim Care Respir J*, 18(2), 76-82.
- Burnell, P. K., Asking, L., Borgstrom, L., Nichols, S. C., Olsson, B., Prime, D., et al. (2007). Studies of the human oropharyngeal airspaces using magnetic resonance imaging IV--the oropharyngeal retention effect for four inhalation delivery systems. *J Aerosol Med*, 20(3), 269-281.
- Byron, P. R., Delvadia, R. R., Longest, P. W., & Hindle, M. (2010a). *Stepping into the trachea with realistic physical models: Uncertainties in regional drug deposition from powder inhalers*. Paper presented at the Proceedings of Respiratory Drug Delivery 2010.
- Byron, P. R., Hindle, M., Lange, C. F., Longest, P. W., McRobbie, D., Oldham, M. J., et al. (2010b). *In vivo-in vitro* correlations: predicting pulmonary drug deposition from pharmaceutical aerosols. *J Aerosol Med Pulm Drug Deliv*, 23 Suppl 2, S59-69.
- Cass, L. M., Brown, J., Pickford, M., Fayinka, S., Newman, S. P., Johansson, C. J., et al. (1999). Pharmacoscintigraphic evaluation of lung deposition of inhaled zanamivir in healthy volunteers. *Clin Pharmacokinet*, 36 Suppl 1, 21-31.
- Cegla, U. H. (2004). Pressure and inspiratory flow characteristics of dry powder inhalers. *Respir Med*, 98 Suppl A, S22-28.
- Chapter 3 Physiological data for reference man. (1975). *Annals of the ICRP/ICRP Publication*, 23, 335-365.
- Cherng, C.-H., Wong, C.-S., Hsu, C.-H., & Ho, S.-T. (2002). Airway length in adults: estimation of the optimal endotracheal tube length for orotracheal intubation. *J Clin Anesth*, 14(4), 271-274.
- Chodosh, S., Flanders, J. S., Kesten, S., Serby, C. W., Hochrainer, D., & Witek, T. J. (2001). Effective delivery of particles with the HandiHaler® dry powder inhalation system over a range of chronic obstructive pulmonary disease severity. *J Aerosol Med*, 14(3), 309-315.
- Clark, A. R., & Egan, M. (1994). Modelling the deposition of inhaled powdered drug aerosols. *J Aerosol Sci*, 25(1), 175-186.

- Clark, A. R., & Hollingworth, A. M. (1993). The relationship between powder inhaler resistance and peak inspiratory conditions in healthy volunteers--implications for *in vitro* testing. *J Aerosol Med*, 6(2), 99-110.
- de Boer, A. H., Gjaltema, D., & Hagedoorn, P. (1996). Inhalation characteristics and their effects on *in vitro* drug delivery from dry powder inhalers Part 2: Effect of peak flow rate (PIFR) and inspiration time on the *in vitro* drug release from three different types of commercial dry powder inhalers. *Int J Pharm*, 138(1), 45-56.
- de Boer, A.H., Hagedoorn, P., & Gjaltema, D. (2006). Air classifier technology (ACT) in dry powder inhalation Part 4. Performance of air classifier technology in the Novolizer multi-dose dry powder inhaler. *Int J Pharm*, 310(1-2), 81-89.
- DeHaan, W. H., & Finlay, W. H. (2001). *In vitro* monodisperse aerosol deposition in a mouth and throat with six different inhalation devices. *J Aerosol Med*, 14(3), 361-367.
- Delvadia, R. R., Byron, P. R., Longest, P. W., & Hindle, M. (2010). *In vitro prediction of regional drug deposition from dry powder inhalers*. Paper presented at the Proceedings of Respiratory Drug Delivery 2010.
- Dolovich, M. B. (2004). Practical aspects of imaging techniques employed to study aerosol deposition and clearance. In A. J. Hickey (Ed.), *Pharmaceutical inhalation aerosol technology* (1 ed., Vol. 134, pp. 171-213). New York Basil: Marcel Dekker, Inc.
- Ehtezazi, T., Horsfield, M. A., Barry, P. W., Goodenough, P., & O'Callaghan, C. (2005). Effect of device inhalational resistance on the three-dimensional configuration of the upper airway. *J Pharma Sci*, 94(7), 1418-1426.
- Ehtezazi, T., Horsfield, M. A., Barry, P. W., & O'callaghan, C. (2004). Dynamic change of the upper airway during inhalation via aerosol delivery devices. *Journal of Aerosol Medicine*, 17(4), 325-334.
- Ehtezazi, T., Saleem, I., Shrubbs, I., Allanson, D., Jenkinson, I., & O'Callaghan, C. (2010). The interaction between the oropharyngeal geometry and aerosols via pressurised metered dose inhalers. *Pharm Res*, 27(1), 175-186.
- Fadl, A., Wang, J., Zhang, Z., & Sung Cheng, Y. (2007). Effects of MDI spray angle on aerosol penetration efficiency through an oral airway cast. *J Aerosol Sci*, 38(8), 853-864.

- Fenton, C., Keating, G. M., & Plosker, G. L. (2003). Novolizer: A multidose dry powder inhaler. *Drugs*, 63(22), 2437-2445.
- Finlay, W. H., Golshahi, L., Noga, M., & Flores-Mir, C. (2010). *Choosing 3-D mouth-Throat dimensions: A rational merging of medical imaging and aerodynamics*. Paper presented at the Proceedings of Respiratory Drug Delivery 2010.
- Finlay, W. H., & Martin, A. R. (2008). Recent advances in predictive understanding of respiratory tract deposition. *J Aerosol Med Pulm Drug Deliv*, 21(2), 189-206.
- Fouke, J. M., Pimmel, R. L., & Bromberg, P. A. (1981). Direct dynamic measurements of tracheal diameter. *J Appl Physiol*, 51(3), 767-771.
- Frijlink, H. W., & De Boer, A. H. (2004). Dry powder inhalers for pulmonary drug delivery. *Expert Opin Drug Deliv*, 1(1), 67-86.
- Gonda I (2004) Targeting by deposition. In: A.J. Hickey, (Ed.). *Pharmaceutical inhalation aerosol technology* Vol 134. 1 ed. Marcel Dekker, Inc.: New York Basil; pp. 65-88.
- Grgic, B., Finlay, W. H., Burnell, P. K. P., & Heenan, A. F. (2004). *In vitro* intersubject and intrasubject deposition measurements in realistic mouth-throat geometries. *J Aerosol Sci*, 35(8), 1025-1040.
- Hankinson, J. L., Odencrantz, J. R., & Fedan, K. B. (1999). Spirometric reference values from a sample of the general U.S. population. *Am J Respir Crit Care Med*, 159(1), 179-187.
- Horsfield, K., & Cumming, G. (1968). Morphology of the bronchial tree in man. *J Appl Physiol*, 24(3), 373-383.
- Housiadas, C., & Lazaridis, M. (2010). Inhalation Dosimetry Modelling. In M. Lazaridis & I. Colbeck (Eds.), *Human exposure to pollutants via dermal absorption and inhalation* (Vol. 17): Springer Netherlands., 185-236
- International Committee for Harmonization Q2B: Validation of analytical procedures: methodology. Retrieved 06/03/2010, from <http://www.fda.gov/cder/guidance/index.htm>
- Islam, N., & Gladki, E. (2008). Dry powder inhalers (DPIs)—A review of device reliability and innovation. *Int J Pharm*, 360(1-2), 1-11.

- Jaafar-Maalej, C., Andrieu, V., Elaissari, A., & Fessi, H. (2009). Assessment methods of inhaled aerosols: technical aspects and applications. *Expert Opin Drug Deliv*, 6(9), 941-959.
- Kamiya, A., Sakagami, M., & Byron, P. R. (2009). Cascade impactor practice for a high dose dry powder inhaler at 90 L/min: NGI versus modified 6-stage and 8-stage ACI. *J Pharm Sci*, 98(3), 1028-1039.
- Lavorini, F., Levy, M. L., Corrigan, C., & Crompton, G. (2010). The ADMIT series - issues in inhalation therapy. 6) Training tools for inhalation devices. *Prim Care Respir J*, 19(4), 335-341.
- Leader, J. K., Rogers, R. M., Fuhrman, C. R., Sciruba, F. C., Zheng, B., Thompson, P. F., et al. (2004). Size and morphology of the trachea before and after lung volume reduction surgery. *AJR Am J Roentgenol*, 183(2), 315-321.
- Longest, P. W. (2011). Upper Airway Models. Retrieved 17 August, 2011, from <http://www.rddonline.com/resources/tools/models.php>
- Longest, P. W., & Hindle, M. (2009). Evaluation of the Respimat Soft Mist inhaler using a concurrent CFD and *in vitro* approach. *J Aerosol Med Pulm Drug Deliv*, 22(2), 99-112.
- Longest, P. W., Hindle, M., & Das Choudhuri, S. (2009). Effects of generation time on spray aerosol transport and deposition in models of the mouth-throat geometry. *J aerosol Med Pulm Drug Del*, 22(2), 67-83.
- Marion, M. S. (2001). Spirometry reference values for American Indian adults. *Chest*, 120(2), 489.
- Marion, M. S., Leonardson, G. R., Rhoades, E. R., Welty, T. K., & Enright, P. L. (2001). Spirometry reference values for American Indian adults: results from the strong heart study. *Chest*, 120(2), 489-495.
- Martin, T., Bandi, N., Shulz, R., Roberts, C., & Kompella, U. (2002). Preparation of budesonide and budesonide-PLA microparticles using supercritical fluid precipitation technology. *AAPS PharmSciTech*, 3(3), 16-26.
- McRobbie, D. W. (2003). Studies of the human oropharyngeal airspaces using magnetic resonance imaging. I. Validation of a three-dimensional MRI method for producing ex

- vivo virtual and physical casts of the oropharyngeal airways during inspiration. *J Aerosol Med*, 16(4), 401.
- McRobbie, D. W. (2005). Studies of the human oropharyngeal airspaces using magnetic resonance imaging. III. The effects of device resistance with forced maneuver and tidal breathing on upper airway geometry. *J Aerosol Med*, 18(3), 325.
- Meyer, T., Brand, P., Ehlich, H., Kobrich, R., Meyer, G., Riedinger, F., et al. (2004). Deposition of Foradil P in human lungs: comparison of *in vitro* and *in vivo* data. *J Aerosol Med*, 17(1), 43-49.
- Miller, M. R., Hankinson, J., Brusasco, V., Burgos, F., Casaburi, R., Coates, A., et al. (2005). Standardisation of spirometry. *Eur Respir J*, 26(2), 319-338.
- Mitchell, J., Newman, S., & Chan, H. K. (2007). *In vitro* and *in vivo* aspects of cascade impactor tests and inhaler performance: a review. *AAPS PharmSciTech*, 8(4), E110.
- Montaudon, M., Desbarats, P., Berger, P., De Dietrich, G., Marthan, R., & Laurent, F. (2007). Assessment of bronchial wall thickness and lumen diameter in human adults using multi-detector computed tomography: comparison with theoretical models. *J Anat*, 211(5), 579-588.
- Newman, S & Peart, J. (2009a) Dry powder inhalers. In S. Newman, P. Anderson, P. Byron, R. Dalby, and J. Peart, (Ed.). *Respiratory Drug Delivery:Essential Theory and Practice*. Richmond USA: RDD Online/Virginia Commonwealth University, 257-307.
- Newman, S. (2009b). *In vivo* assessment of pulmonary drug delivery. In S. Newman, P. Anderson, P. Byron, R. Dalby, and J. Peart, (Ed.). *Respiratory Drug Delivery:Essential Theory and Practice*. Richmond USA: RDD Online/Virginia Commonwealth University, 97-133
- Newman, S. P., & Chan, H. K. (2008). *In vitro/in vivo* comparisons in pulmonary drug delivery. *J Aerosol Med Pulm Drug Deliv*, 21(1), 77-84.
- Newman, S. P., Pitcairn, G. R., Adkin, D. A., Vidgren, M. T., & Silvasti, M. (2001). Comparison of beclomethasone dipropionate delivery by Easyhaler® dry powder inhaler and pMDI plus large volume spacer. *J Aerosol Med*, 14(2), 217-225.

- Newman, S. P., Pitcairn, G. R., Hirst, P. H., Bacon, R. E., O'Keefe, E., Reiners, M., et al. (2000). Scintigraphic comparison of budesonide deposition from two dry powder inhalers. *Eur Respir J*, 16(1), 178-183.
- Newman, S. P., Wilding, I. R., & Hirst, P. H. (2000c). Human lung deposition data: the bridge between *in vitro* and clinical evaluations for inhaled drug products? *Int J Pharm*, 208(1-2), 49-60.
- Nikiforov, A. I., & Schlesinger, R. B. (1985). Morphometric variability of the human upper bronchial tree. *Respir Physio*, 59(3), 289-299.
- Olsson, B., Borgstrom, L., Svensson, M., & Lundbeck, H. (2008). *Modeling oropharyngeal cast deposition to predict lung delivery from powder inhalers*. Paper presented at the Proceedings of Respiratory Drug Delivery.
- Osmanliev, D., Bowley, N., Hunter, D. M., & Pride, N. B. (1982). Relation between tracheal size and forced expiratory volume in one second in young men. *Am Rev Respir Dis*, 126(1), 179-182.
- Pellegrino, R., Viegi, G., Brusasco, V., Crapo, R. O., Burgos, F., Casaburi, R., et al. (2005). Interpretative strategies for lung function tests. *Eur Respir J*, 26(5), 948-968.
- Pitcairn, G., Lunghetti, G., Ventura, P., & Newman, S. (1994). A comparison of the lung deposition of salbutamol inhaled from a new dry powder inhaler, at two inhaled flow rates. *Int J Pharm*, 102(1-3), 11-18.
- Pritchard, J. N. (2001). The influence of lung deposition on clinical response. *J Aerosol Med*, 14 Suppl 1, S19-26.
- Pritchard, S. E., & McRobbie, D. W. (2004). Studies of the human oropharyngeal airspaces using magnetic resonance imaging. II. The use of three-dimensional gated MRI to determine the influence of mouthpiece diameter and resistance of inhalation devices on the oropharyngeal airspace geometry. *J Aerosol Med*, 17(4), 310-324.
- Raabe, O. G., Yeh, H. C., Schum, G. M., & Phalen, R. F. (1976). Tracheobronchial Geometry: Human, Dog, Rat, Hamster. Retrieved 10/12/2010, from Lovelace Foundation for Medical Education and Research: <http://mae.ucdavis.edu/wexler/lungs/LF53-Raabe/>

- Rahmatalla, M. F., Zuberbuhler, P. C., Lange, C. F., & Finlay, W. H. (2002). *In vitro* effect of a holding chamber on the mouth-throat deposition of QVAR (hydrofluoroalkane-beclomethasone dipropionate). *J Aerosol Med*, 15(4), 379-385.
- Rootmensen, G. N., van Keimpema, A. R., Jansen, H. M., & de Haan, R. J. (2010). Predictors of incorrect inhalation technique in patients with asthma or COPD: a study using a validated videotaped scoring method. *J Aerosol Med Pulm Drug Deliv*, 23(5), 323-328.
- Scheuch, G., Bennett, W., Borgström, L., Clark, A., Dalby, R., Dolovich, M., et al. (2010). Deposition, imaging, and clearance: What remains to be done? *J Aerosol Med Pulm Drug Deliv*, 23(S2), S-39-S-57.
- Smutney, C. C., Friedman, E. M., Polidoro, J. M., & Amin, N. (2009). Inspiratory efforts achieved in use of the Technosphere® Insulin Inhalation System. *J Diabetes Sci Technol (Online)*, 3(5), 1175.
- Son, Y.-J., & McConville, J. T. (2008). Advancements in dry powder delivery to the lung. *Drug Dev Ind Pharm*, 34(9), 948-959.
- Stapleton, K., Guentsch, E., Hoskinson, M., & Finlay, W. (2000). On the suitability of k-turbulence modeling for aerosol deposition in the mouth and throat: a comparison with experiment. *J Aerosol Sci*, 31(6), 739-749.
- Telko, M. J., & Hickey, A. J. (2005). Dry powder inhaler formulation. *Respir Care*, 50(9), 1209.
- Tian, G., Longest, P., Su, G., Walenga, R. L., & Hindle, M. (2011a). Development of a stochastic individual path (SIP) model for predicting the tracheobronchial deposition of pharmaceutical aerosols: Effects of transient inhalation and sampling the airways. *J Aerosol Sci*, 42(11), 781-799.
- Tian, G., Longest, P. W., Su, G., & Hindle, M. (2011b). Characterization of respiratory drug delivery with enhanced condensational growth (ECG) using an individual path model of the entire tracheobronchial airways. *Ann Biomed Eng*, 39(3), 1136-1153.
- USP. General Chapter <601> Aerosols, Nasal Sprays, Metered Dose Inhalers, and Dry powder inhalers. (2009) *United States Pharmacopeia - National Formulary*: United States Convention: Washington, DC.

- van Beerendonk, I., Mesters, I., Mudde, A. N., & Tan, T. (1998). Assessment of the inhalation technique in outpatients with asthma or chronic obstructive pulmonary disease using a metered-dose inhaler or dry powder device. *J Asthma*, 35(3), 273-279.
- Vidgren, M., Arppe, J., Vidgren, P., Vainio, P., Silvasti, M., & Tukiainen, H. (1994). Pulmonary deposition of ^{99m}Tc-labelled salbutamol particles in healthy volunteers after inhalation from a metered-dose inhaler and from a novel multiple-dose powder inhaler. *S.T.P. pharma sciences*, 4(1), 29-32.
- Vock, P., Spiegel, T., Fram, E. K., & Effmann, E. L. (1984). CT Assessment of the adult intrathoracic cross section of the trachea. *J Comput Tomogr*, 8(6), 1076-1082.
- Weda, M., Zanen, P., Boer, A. H. d., Barends, D. M., & Frijlink, H. W. (2004). An investigation into the predictive value of cascade impactor results for side effects of inhaled salbutamol. *Int J Pharma*, 287(1-2), 79-87.
- Weibel, E. R. (1963). Principles and methods for the morphometric study of the lung and other organs. *Lab Invest*, 12, 131-155.
- Weibel, E. R. (Ed.). (1964). *Morphometrics of the lung*. American Physiological Society, Washington, D.C.
- Xi, J., & Longest, P. W. (2007). Transport and deposition of micro-aerosols in realistic and simplified models of the oral airway. *Ann Biomed Eng*, 35(4), 560-581.
- Xi, J., & Longest, P. W. (2008). Effects of oral airway geometry characteristics on the diffusional deposition of inhaled nanoparticles. *J Biomech Eng*, 130(1), 011008.
- Yang, W., Peters, J. I., & Williams, R. O. (2008). Inhaled nanoparticles—a current review. *Int J Pharm*, 356(1), 239-247.
- Yeh, H. C., Phalen, R. F., & Raabe, O. G. (1976). Factors influencing the deposition of inhaled particles. *Environ Health Perspect*, 15, 147-156.
- Yeh, H. C., & Schum, G. M. (1980). Models of human lung airways and their application to inhaled particle deposition. *Bull Math Biol*, 42(3), 461-480.

APPENDICES

APPENDIX A
ORIGINAL DATA SHEETS

Table A.1: *In vitro* results for budesonide deposition from **Budelin** Novolizers in **Medium MT-TB model** using inhalation profiles selected to represent the PIFR and V values in the first column (**Chapter 3**).

Study parameters	Budesonide recovery (µg)						% of total budesonide recovery				
	Device	MT	Trachea	Bronchi	Chamber + Filter	Total recovery	Device	MT	Trachea	Bronchi	Chamber + Filter
PIFR: 54 L/min V: 2.77 L Model: MT-TB _M	41.78	125.85	0.61	0.00	28.12	196.37	21.28	64.09	0.31	0.00	14.32
	75.58	123.92	0.51	0.52	31.71	232.24	32.54	53.36	0.22	0.22	13.66
	57.44	134.80	0.47	1.20	36.36	230.27	24.95	58.54	0.20	0.52	15.79
	35.55	119.00	0.00	0.98	34.35	189.88	18.72	62.67	0.00	0.51	18.09
	39.98	133.13	0.00	0.50	28.76	202.38	19.76	65.78	0.00	0.25	14.21
Average	50.07	127.34	0.32	0.64	31.86	210.23	23.45	60.89	0.15	0.30	15.21
SD	16.48	6.57	0.30	0.47	3.54	19.71	5.60	4.99	0.14	0.22	1.79
PIFR: 65 L/min V: 2.96 L Model: MT-TB _M	17.78	124.11	0.51	0.00	36.45	178.85	9.94	69.39	0.29	0.00	20.38
	37.17	122.07	0.00	0.94	48.82	209.00	17.79	58.40	0.00	0.45	23.36
	24.52	135.02	0.59	1.20	41.11	202.45	12.11	66.69	0.29	0.59	20.31
	39.72	130.02	0.00	0.98	45.15	215.88	18.40	60.23	0.00	0.46	20.92
	50.59	127.70	0.00	0.00	50.05	228.34	22.16	55.93	0.00	0.00	21.92
Average	33.96	127.78	0.22	0.63	44.32	206.90	16.08	62.13	0.12	0.30	21.38
SD	12.95	5.09	0.30	0.58	5.61	18.38	4.97	5.69	0.16	0.28	1.28
PIFR: 99 L/min V: 3.13 L Model: MT-TB _M	24.86	119.10	1.15	0.00	59.44	204.55	12.16	58.23	0.56	0.00	29.06
	35.38	120.14	0.75	1.18	61.95	219.40	16.13	54.76	0.34	0.54	28.24
	29.64	116.56	0.87	1.36	58.77	207.19	14.30	56.26	0.42	0.66	28.37
	33.09	98.71	1.71	0.00	62.09	195.61	16.92	50.46	0.88	0.00	31.74
	21.63	110.52	1.31	0.94	59.01	193.40	11.18	57.14	0.68	0.49	30.51
Average	28.92	113.01	1.16	0.70	60.25	204.03	14.14	55.37	0.58	0.34	29.58
SD	5.68	8.82	0.38	0.65	1.63	10.37	2.47	3.02	0.21	0.31	1.51

Table A.2: *In vitro* results for budesonide deposition from **Budelin Novolizers** in **Small MT-TB model** using inhalation profiles selected to represent the PIFR and V values in the first column (**Chapter 3**).

Study parameters	Budesonide recovery (µg)						% of total budesonide recovery				
	Device	MT	Trachea	Bronchi	Chamber + Filter	Total recovery	Device	MT	Trachea	Bronchi	Chamber + Filter
PIFR: 73 L/min V: 1.11 L Model: MT-TB _s	107.89	99.51	2.09	0.95	21.60	232.04	46.49	42.89	0.90	0.41	9.31
	88.67	101.21	1.44	0.84	20.05	212.21	41.78	47.69	0.68	0.40	9.45
	105.14	74.02	1.82	0.88	26.83	208.69	50.38	35.47	0.87	0.42	12.86
	110.13	68.76	1.98	0.65	28.77	210.29	52.37	32.70	0.94	0.31	13.68
	106.24	78.54	1.56	0.74	22.12	209.20	50.78	37.54	0.75	0.35	10.57
Average	103.61	84.41	1.78	0.81	23.88	214.49	48.36	39.26	0.83	0.38	11.17
SD	8.56	14.98	0.27	0.12	3.73	9.91	4.27	6.01	0.11	0.05	2.00
PIFR: 59 L/min V: 1.30 L Model: MT-TB _s	105.18	78.07	1.45	0.64	27.32	212.66	49.46	36.71	0.68	0.30	12.85
	109.90	85.20	1.21	0.71	23.95	220.97	49.73	38.56	0.55	0.32	10.84
	116.09	73.68	0.98	0.00	19.83	210.58	55.13	34.99	0.47	0.00	9.42
	94.99	109.80	1.40	0.00	18.01	224.19	42.37	48.98	0.63	0.00	8.03
	118.80	91.14	0.00	0.00	24.30	234.24	50.72	38.91	0.00	0.00	10.37
Average	108.99	87.58	1.01	0.27	22.68	220.53	49.48	39.63	0.46	0.12	10.30
SD	9.46	14.10	0.59	0.37	3.73	9.52	4.58	5.46	0.27	0.17	1.78
PIFR: 40 L/min V: 0.83 L Model: MT-TB _s	135.21	71.09	0.00	0.47	9.95	216.72	62.39	32.80	0.00	0.21	4.59
	82.72	130.94	0.00	0.81	9.45	223.92	36.94	58.48	0.00	0.36	4.22
	121.85	60.48	0.00	0.77	14.04	197.14	61.81	30.68	0.00	0.39	7.12
	131.83	62.37	0.00	0.00	11.64	205.83	64.05	30.30	0.00	0.00	5.65
	120.66	100.62	0.00	0.00	10.90	232.18	51.97	43.34	0.00	0.00	4.70
Average	118.45	85.10	0.00	0.41	11.19	215.16	55.43	39.12	0.00	0.19	5.26
SD	20.93	30.25	0.00	0.40	1.80	13.97	11.37	12.06	0.00	0.19	1.17

Table A.1: *In vitro* results for budesonide deposition from **Budelin Novolizers** in **Large MT-TB model** using inhalation profiles selected to represent the PIFR and V values in the first column (**Chapter 3**).

Study parameters	Budesonide recovery (µg)						% of total budesonide recovery				
	Device	MT	Trachea	Bronchi	Chamber + Filter	Total recovery	Device	MT	Trachea	Bronchi	Chamber + Filter
PIFR: 125 L/min V: 4.00 L Model: MT-TB _L	35.73	98.33	0.53	0.00	91.39	225.97	15.81	43.51	0.23	0.00	40.44
	30.05	107.65	0.00	0.00	77.24	214.94	13.98	50.08	0.00	0.00	35.94
	23.12	89.76	0.00	0.00	71.06	183.94	12.57	48.80	0.00	0.00	38.63
	25.76	111.53	0.00	0.00	81.07	218.35	11.80	51.08	0.00	0.00	37.13
	27.84	112.59	0.00	0.00	89.28	229.71	12.12	49.01	0.00	0.00	38.87
Average	28.50	103.97	0.11	0.00	82.01	214.58	13.26	48.50	0.05	0.00	38.20
SD	4.78	9.73	0.23	0.00	8.43	18.11	1.65	2.93	0.10	0.00	1.73
PIFR: 71 L/min V: 4.00 L Model: MT-TB _L	37.00	149.93	0.00	0.00	57.37	244.30	15.15	61.37	0.00	0.00	23.48
	38.36	132.96	0.00	0.00	62.87	234.19	16.38	56.77	0.00	0.00	26.85
	26.53	122.73	0.00	0.00	60.06	209.32	12.68	58.63	0.00	0.00	28.69
	26.01	128.73	0.00	0.00	58.13	212.86	12.22	60.48	0.00	0.00	27.31
	33.68	125.80	0.00	0.00	59.61	219.09	15.37	57.42	0.00	0.00	27.21
Average	32.32	132.03	0.00	0.00	59.61	223.95	14.36	58.93	0.00	0.00	26.71
SD	5.78	10.69	0.00	0.00	2.13	14.83	1.81	1.96	0.00	0.00	1.93
PIFR: 68 L/min V: 4.00 L Model: MT-TB _L	25.25	124.02	0.00	0.00	56.68	205.94	12.26	60.22	0.00	0.00	27.52
	28.50	129.31	0.00	0.00	48.24	206.05	13.83	62.76	0.00	0.00	23.41
	22.47	131.02	0.00	0.00	59.60	213.09	10.55	61.48	0.00	0.00	27.97
	33.77	156.68	0.00	0.00	56.46	246.92	13.68	63.46	0.00	0.00	22.86
	29.12	143.21	0.00	0.00	53.21	225.54	12.91	63.50	0.00	0.00	23.59
Average	27.82	136.85	0.00	0.00	54.84	219.51	12.65	62.28	0.00	0.00	25.07
SD	4.27	13.13	0.00	0.00	4.33	17.28	1.33	1.41	0.00	0.00	2.46

Table A.4: *In vitro* results for budesonide deposition from **Pulmicort Turbuhaler** in **Medium MT-TB model** using inhalation profiles selected to represent the PIFR and V values in the first column (**Chapter 4**).

Study parameters	Budesonide recovery (µg)						% of total budesonide recovery				
	Device	MT	Trachea	Bronchi	Chamber + Filter	Total recovery	Device	MT	Trachea	Bronchi	Chamber + Filter
PIFR: 58 L/min V: 2.90 L Model: MT-TB _M	50.24	67.45	2.64	1.59	42.58	164.50	30.54	41.00	1.60	0.97	25.88
	42.85	64.43	1.45	1.73	47.93	158.39	27.05	40.68	0.92	1.09	30.26
	37.76	68.67	2.32	2.09	39.82	150.66	25.06	45.58	1.54	1.39	26.43
	42.50	52.92	1.19	2.38	39.26	138.26	30.74	38.28	0.86	1.72	28.40
	58.07	64.03	1.78	1.53	36.83	162.25	35.79	39.47	1.10	0.94	22.70
Average	46.28	63.50	1.88	1.86	41.29	154.81	29.84	41.00	1.20	1.22	26.73
SD	7.96	6.23	0.60	0.36	4.24	10.64	4.10	2.78	0.35	0.33	2.84

Table A.5: *In vitro* results for albuterol sulfate (expressed as equivalent albuterol base) deposition from **Salbutamol Easyhaler** in **Medium MT-TB model** using inhalation profiles selected to represent the PIFR and V values in the first column (**Chapter 4**).

Study parameters	Albuterol recovery (µg)						% of total albuterol recovery				
	Device	MT	Trachea	Bronchi	Chamber + Filter	Total recovery	Device	MT	Trachea	Bronchi	Chamber + Filter
PIFR: 57.8 L/min V: 2.62 L Model: MT-TB _M	Not performed	144.36	3.12	2.31	61.04	210.82	N/A	68.47	1.48	1.10	28.95
		133.69	3.63	2.45	53.37	193.15		69.22	1.88	1.27	27.63
		114.90	2.92	1.86	48.68	168.37		68.24	1.74	1.11	28.91
		134.00	2.87	1.57	50.32	188.76		70.99	1.52	0.83	26.66
		123.00	1.78	2.05	47.70	174.53		70.47	1.02	1.17	27.33
		Average		129.99	2.86	2.05		52.22	187.13	69.48	1.53
SD		11.32	0.68	0.35	5.38	16.67	1.21	0.33	0.16	1.01	

Table A.6: *In vitro* results for zanamivir deposition from **Relenza Diskhaler** in **Medium MT-TB model** using inhalation profiles selected to represent the PIFR and V values in the first column (**Chapter 4**).

Study parameters	Zanamivir recovery (µg)						% of total zanamivir recovery				
	Device	MT	Trachea	Bronchi	Chamber + Filter	Total recovery	Device	MT	Trachea	Bronchi	Chamber + Filter
PIFR: 84 L/min V: 2.78 L Model: MT-TB _M	1031.38	2105.23	144.86	48.07	908.55	4388.10	23.50	47.98	3.30	1.10	20.70
	1306.01	2456.84	165.73	52.48	1175.03	5378.49	24.28	45.68	3.08	0.98	21.85
	1020.16	2829.32	120.70	77.01	1131.01	4980.50	20.48	56.81	2.42	1.55	22.71
	1248.84	2442.13	89.71	67.60	1040.64	4888.92	25.54	49.95	1.83	1.38	21.29
	1145.41	2347.06	130.50	45.76	942.19	4610.92	24.84	50.90	2.83	0.99	20.43
Average	1150.36	2436.12	130.30	58.18	1039.49	4849.38	23.73	50.26	2.69	1.20	21.40
SD	127.53	261.01	28.32	13.53	115.50	376.95	1.96	4.17	0.58	0.25	0.91

Table A.7: *In vitro* results for tiotropium bromide (expressed as equivalent tiotropium base) deposition from **Spiriva Handihaler** in **Medium MT-TB model** using inhalation profiles selected to represent the PIFR and V values in the first column (**Chapter 4**).

Study parameters	Tiotropium recovery (µg)						% of total tiotropium bromide recovery				
	Device	MT	Trachea	Bronchi	Chamber + Filter	Total recovery	Device	MT	Trachea	Bronchi	Chamber + Filter
PIFR: 30 L/min V: 2.62 L Model: MT-TB _M	19.34	9.83	0.00	0.00	5.81	34.98	55.28	28.10	0.00	0.00	16.62
	16.23	10.50	0.00	0.00	5.85	32.58	49.83	32.23	0.00	0.00	17.94
	19.81	8.97	0.00	0.00	5.40	34.18	57.96	26.24	0.00	0.00	15.80
	18.45	10.03	0.00	0.00	5.94	34.42	53.60	29.14	0.00	0.00	17.26
	15.90	10.30	0.00	0.00	6.12	32.32	49.20	31.87	0.00	0.00	18.94
Average	17.95	9.92	0.00	0.00	5.82	33.70	53.17	29.51	0.00	0.00	17.31
SD	1.79	0.59	0.00	0.00	0.27	1.18	3.69	2.54	0.00	0.00	1.20

Table A.8: *In vitro* results for formoterol fumarate deposition from **Foradil Aerolizer** in **Medium MT-TB model** using inhalation profiles selected to represent the PIFR and V values in the first column (**Chapter 4**).

Study parameters	Formoterol fumarate recovery (µg)						% of total tiotropium bromide recovery				
	Device	MT	Trachea	Bronchi	Chamber + Filter	Total recovery	Device	MT	Trachea	Bronchi	Chamber + Filter
PIFR: 84.5 L/min V: 2.78 L Model: MT-TB _M	4.31	4.44	0.00	0.00	2.60	11.35	37.96	39.13	0.00	0.00	22.91
	4.41	4.89	0.00	0.00	2.49	11.78	37.40	41.47	0.00	0.00	21.13
	4.11	4.93	0.00	0.00	2.35	11.39	36.11	43.25	0.00	0.00	20.64
	3.92	4.67	0.00	0.00	2.59	11.18	35.03	41.80	0.00	0.00	23.17
	4.36	4.71	0.00	0.00	2.39	11.46	38.05	41.10	0.00	0.00	20.85
Average	4.22	4.73	0.00	0.00	2.48	11.43	36.91	41.35	0.00	0.00	21.74
SD	0.20	0.19	0.00	0.00	0.11	0.22	1.31	1.49	0.00	0.00	1.20

Table A.9: *In vitro* results for albuterol sulfate (expressed as albuterol base) deposition from **Novolizer (drug only formulation)** in **different angled Medium MT models** using square wave inhalation profile; PIFR = 75 L/min, V = 4 L; **Chapter 5.**

Angle	Albuterol sulfate recovery (µg)				% of total albuterol recovery		
	Device	MT	Chamber + Filter	Emitted	Device	MT	Chamber + Filter
-20	275.00	419.00	508.00	1202.00	22.88	34.86	42.26
	287.00	391.50	469.50	1148.00	25.00	34.10	40.90
	220.50	337.00	371.00	928.50	23.75	36.30	39.96
	250.50	369.00	424.50	1044.00	23.99	35.34	40.66
	282.00	393.50	477.50	1153.00	24.46	34.13	41.41
Average	263.00	382.00	450.10	1095.10	24.02	34.95	41.04
SD	27.58	30.76	53.37	109.48	0.80	0.92	0.86
-10	255.00	320.00	436.50	1011.50	25.21	31.64	43.15
	252.50	369.50	509.00	1131.00	22.33	32.67	45.00
	243.50	300.50	391.00	935.00	26.04	32.14	41.82
	236.50	305.50	367.00	909.00	26.02	33.61	40.37
	276.00	354.50	448.50	1079.00	25.58	32.85	41.57
Average	252.70	330.00	430.40	1013.10	25.04	32.58	42.38
SD	14.96	30.54	55.03	93.78	1.55	0.75	1.77
0	255.50	288.00	482.00	1025.50	24.91	28.08	47.00
	235.00	245.00	408.00	888.00	26.46	27.59	45.95
	276.50	247.00	448.50	972.00	28.45	25.41	46.14
	250.50	297.00	487.50	1035.00	24.20	28.70	47.10
	247.00	289.00	488.50	1024.50	24.11	28.21	47.68
Average	252.90	273.20	462.90	989.00	25.63	27.60	46.77
SD	15.20	25.08	34.81	61.64	1.84	1.28	0.72
10	274.00	269.50	472.00	1015.50	26.98	26.54	46.48

	270.00	331.00	609.00	1210.00	22.31	27.36	50.33
	292.50	280.50	551.50	1124.50	26.01	24.94	49.04
	266.50	277.50	524.50	1068.50	24.94	25.97	49.09
	229.50	237.50	447.00	914.00	25.11	25.98	48.91
Average	266.50	279.20	520.80	1066.50	25.07	26.16	48.77
SD	22.99	33.62	64.35	111.60	1.74	0.88	1.40
20	284.50	336.00	556.00	1176.50	24.18	28.56	47.26
	313.50	315.50	603.50	1232.50	25.44	25.60	48.97
	242.00	271.00	481.00	994.00	24.35	27.26	48.39
	230.50	239.50	422.00	892.00	25.84	26.85	47.31
	266.00	274.00	472.00	1012.00	26.28	27.08	46.64
Average	267.30	287.20	506.90	1061.40	25.22	27.07	47.71
SD	33.27	38.39	72.18	139.82	0.92	1.06	0.94

Table A.10: *In vitro* results for albuterol sulfate (expressed as albuterol base) deposition from **Novolizer (Salbulin formulation)** in **different angled Medium MT models** using square wave inhalation profile; PIFR = 75 L/min, V = 4 L; **Chapter 5.**

Angle	Albuterol recovery (µg)					% of total albuterol recovery			
	Device	MT	TB	Chamber+Filter	Total recovery	Device	MT	TB	Chamber+Filter
-20	4.13	74.15	1.11	26.35	105.74	3.91	70.13	1.05	24.92
	4.50	72.07	0.75	28.97	106.28	4.23	67.81	0.70	27.25
	4.74	70.40	0.76	29.66	105.56	4.49	66.70	0.72	28.10
	4.41	69.22	0.67	26.44	100.74	4.37	68.71	0.67	26.25
	4.39	71.32	0.75	28.36	104.81	4.19	68.04	0.71	27.06
Average	4.43	71.43	0.81	27.96	104.63	4.24	68.28	0.77	26.72
SD	0.22	1.86	0.17	1.50	2.24	0.22	1.26	0.16	1.20
-10	3.87	69.40	0.75	32.06	106.07	3.65	65.43	0.71	30.22
	4.27	74.02	0.95	30.26	109.50	3.90	67.60	0.86	27.64
	3.33	71.78	0.72	37.29	113.11	2.94	63.45	0.64	32.96
	4.56	78.69	0.75	27.54	111.54	4.09	70.55	0.67	24.69
	4.17	70.28	0.85	30.15	105.45	3.95	66.65	0.80	28.60
Average	4.04	72.83	0.80	31.46	109.14	3.71	66.73	0.74	28.82
SD	0.47	3.71	0.09	3.63	3.34	0.46	2.63	0.09	3.07
0	2.91	64.86	0.76	38.05	106.59	2.73	60.86	0.71	35.70
	3.68	65.17	0.64	27.83	97.33	3.79	66.96	0.66	28.60
	4.55	68.01	1.04	33.10	106.70	4.27	63.74	0.97	31.02
	4.74	77.50	0.84	29.42	112.50	4.21	68.89	0.75	26.15
	4.78	65.83	1.07	32.62	104.31	4.58	63.11	1.03	31.28
Average	4.13	68.28	0.87	32.21	105.48	3.92	64.71	0.82	30.55
SD	0.82	5.30	0.18	3.94	5.47	0.72	3.20	0.17	3.55

10	3.79	65.76	0.94	35.64	106.13	3.57	61.96	0.89	33.58
	4.86	72.34	0.87	30.67	108.74	4.47	66.53	0.80	28.20
	3.60	66.49	0.65	34.60	105.34	3.42	63.12	0.61	32.85
	4.58	70.84	1.04	28.45	104.92	4.37	67.52	1.00	27.12
	4.51	68.89	0.62	30.98	104.99	4.29	65.61	0.59	29.50
Average	4.27	68.86	0.82	32.07	106.02	4.02	64.95	0.78	30.25
SD	0.54	2.80	0.19	2.97	1.59	0.49	2.33	0.17	2.85
20	4.02	69.96	0.96	31.36	106.31	3.78	65.81	0.91	29.50
	3.89	64.92	0.83	31.25	100.89	3.85	64.35	0.82	30.98
	4.32	69.29	0.93	36.48	111.01	3.89	62.42	0.83	32.86
	4.30	67.53	0.65	35.33	107.81	3.99	62.64	0.60	32.77
	5.51	69.84	0.95	30.70	107.00	5.15	65.27	0.89	28.69
Average	4.41	68.31	0.86	33.03	106.60	4.13	64.10	0.81	30.96
SD	0.64	2.13	0.13	2.67	3.67	0.57	1.53	0.12	1.88

Table A.11: *In vitro* results for albuterol sulfate deposition from **Proventil HFA** in **different angled Medium MT-TB models** using square wave inhalation profile; PIFR = 30 L/min, inhalation time - ~10s; TB deposition was below LOQ (also below 1% of nominal dose) in all cases; **Chapter 5.**

	Albuterol sulfate recovery (µg)				% of total albuterol recovery		
	Device	MT	Chamber + Filter	Total recovery	Device	MT	Chamber + Filter
-20	24.42	51.58	40.42	116.42	20.98	44.31	34.72
	16.39	58.86	40.61	115.86	14.15	50.80	35.05
	17.24	54.72	46.10	118.06	14.60	46.35	39.05
	20.69	58.60	47.04	126.33	16.38	46.39	37.24
	17.21	52.45	40.25	109.91	15.66	47.72	36.62
Average	19.19	55.24	42.88	117.32	16.35	47.11	36.53
SD	3.36	3.39	3.38	5.91	2.73	2.40	1.75
-10	20.81	51.40	51.32	123.53	16.85	41.61	41.54
	15.60	45.92	40.66	102.18	15.27	44.94	39.79
	17.06	44.04	44.16	105.26	16.21	41.84	41.95
	18.29	49.32	48.66	116.27	15.73	42.42	41.85
	16.74	45.24	44.20	106.18	15.77	42.61	41.63
Average	17.70	47.18	45.80	110.68	15.96	42.68	41.35
SD	1.99	3.07	4.19	8.92	0.60	1.33	0.89
0	18.87	41.46	56.40	116.73	16.17	35.52	48.32
	16.48	45.92	49.78	112.18	14.69	40.93	44.38
	16.72	40.92	55.00	112.64	14.84	36.33	48.83
	19.38	48.09	55.25	122.72	15.79	39.19	45.02
	17.22	43.45	52.90	113.57	15.16	38.26	46.58
Average	17.73	43.97	53.87	115.57	15.33	38.05	46.62
SD	1.31	3.03	2.61	4.37	0.63	2.18	1.96

10	17.07	40.00	53.16	110.23	15.49	36.29	48.23
	20.53	40.24	60.36	121.13	16.95	33.22	49.83
	19.75	45.24	57.94	122.93	16.07	36.80	47.13
	16.74	43.60	59.50	119.84	13.97	36.38	49.65
	16.75	40.89	55.44	113.08	14.81	36.16	49.03
Average	18.17	41.99	57.28	117.44	15.46	35.77	48.77
SD	1.83	2.31	2.97	5.49	1.14	1.45	1.11
20	19.04	48.06	52.50	119.60	15.92	40.18	43.90
	20.34	43.28	48.18	111.80	18.19	38.71	43.09
	24.72	39.38	49.96	114.06	21.67	34.53	43.80
	16.21	40.42	45.47	102.10	15.88	39.59	44.53
	18.56	45.44	53.89	117.89	15.74	38.54	45.71
Average	19.77	43.32	50.00	113.09	17.48	38.31	44.21
SD	3.14	3.57	3.36	6.87	2.55	2.22	0.98

Table A.12: *In vitro* results for albuterol sulfate (expressed as equivalent albuterol base) deposition from **Respimat SMI** in **different angled Medium MT-TB models** using square wave inhalation profile; PIFR = 30 L/min, inhalation time - ~10s; **Chapter 5.**

	Albuterol recovery (µg)					% of total albuterol recovery			
	Device	MT	TB	Chamber+Filter	Total recovery	Device	MT	TB	Chamber+Filter
-20	16.28	5.32	1.80	43.16	66.56	24.46	7.99	2.70	64.84
	9.00	8.33	1.00	36.12	54.45	16.53	15.30	1.84	66.34
	7.32	6.61	1.27	49.08	64.28	11.39	10.28	1.98	76.35
	9.66	7.62	1.51	44.32	63.11	15.31	12.07	2.39	70.23
	9.91	7.89	1.41	44.08	63.29	15.66	12.47	2.23	69.64
Average	10.43	7.15	1.40	43.35	62.34	16.67	11.62	2.23	69.48
SD	3.42	1.20	0.30	4.65	4.62	4.78	2.71	0.34	4.45
-10	21.36	5.68	1.36	49.08	77.48	27.57	7.33	1.76	63.35
	11.94	4.34	0.83	46.24	63.35	18.85	6.85	1.31	72.99
	3.80	8.71	1.97	48.64	63.12	6.02	13.80	3.12	77.06
	10.66	5.73	1.76	50.80	68.95	15.46	8.31	2.55	73.68
	13.50	7.21	1.57	49.36	71.64	18.84	10.06	2.19	68.90
Average	12.25	6.33	1.50	48.82	68.91	17.35	9.27	2.19	71.19
SD	6.30	1.67	0.44	1.66	6.03	7.76	2.81	0.70	5.26
0	17.42	5.10	1.78	49.08	73.38	23.74	6.95	2.43	66.88
	14.78	4.51	0.84	36.48	56.61	26.11	7.97	1.48	64.44
	9.14	8.61	2.41	55.68	75.84	12.05	11.35	3.18	73.42
	5.14	12.39	2.23	49.36	69.12	7.44	17.93	3.23	71.41
	9.96	6.83	1.24	44.80	62.83	15.85	10.87	1.97	71.30
Average	11.29	7.49	1.70	47.08	67.56	17.04	11.01	2.46	69.49
SD	4.85	3.17	0.66	7.08	7.86	7.84	4.29	0.76	3.70
10	17.04	4.16	1.21	44.12	66.53	25.61	6.25	1.82	66.32

	5.18	6.38	1.44	50.28	63.28	8.19	10.08	2.28	79.46
	10.30	6.93	1.95	54.68	73.86	13.95	9.38	2.64	74.03
	9.66	18.48	1.77	48.00	77.91	12.40	23.72	2.27	61.61
	11.08	5.79	1.18	44.56	62.61	17.70	9.25	1.88	71.17
Average	10.65	8.35	1.51	48.33	68.84	15.57	11.74	2.18	70.52
SD	4.24	5.76	0.34	4.36	6.76	6.57	6.86	0.33	6.89
20	6.72	5.26	1.04	40.60	53.62	12.53	9.81	1.94	75.72
	10.36	5.00	0.80	39.84	56.00	18.50	8.93	1.43	71.14
	8.38	9.46	3.04	62.40	83.28	10.06	11.36	3.65	74.93
	9.00	7.80	3.41	53.16	73.37	12.27	10.63	4.65	72.45
	8.36	7.13	1.44	46.24	63.17	13.23	11.29	2.28	73.20
Average	8.56	6.93	1.95	48.45	65.89	13.32	10.40	2.79	73.49
SD	1.31	1.85	1.20	9.45	12.39	3.13	1.03	1.33	1.85

Table A.13: Aerodynamic particle size distribution of **Salbulin Novolizer Formulation; Chapter 5.**

Flowrate – 75 L/min (Volumetric Flowrate) for 3.2 sec; 4L air (TSI vacuum pump)

Impactor – Next Generation Impactor – Inhaler was attached directly to pre-separator (induction port was not used)

Inhaler – Salbulin Novolizer (120 µg albuterol sulfate/dose eq to 100 µg albuterol base)

No of shots – 2 shots

		% of total albuterol (as base) recovery						
		#1	#2	#3	#4	MEAN	SD	CV
	Device	10.7	7.5	9.3	6.4	8.5	1.9	22.6
	Adaptor	37.8	41.8	42.9	44.4	41.7	2.9	6.9
< 11.75 µm	Presep	22.5	24.7	23.9	25.7	24.2	1.4	5.6
7.15 - 11.75 µm	inlet	0.4	0.4	0.3	0.6	0.4	0.1	19.1
3.97 - 7.15 µm	S1	2.2	1.6	1.6	1.8	1.8	0.3	16.0
2.52 - 3.97 µm	S2	6.0	4.8	4.6	5.7	5.3	0.7	12.5
1.49 - 2.52 µm	S3	11.5	11.2	9.5	12.9	11.3	1.4	12.4
0.84 - 1.49 µm	S4	7.0	6.4	6.7	7.8	6.9	0.6	8.6
0.48 - 0.84 µm	S5	2.0	1.5	1.2	1.1	1.4	0.4	26.8
0.29 - 0.48 µm	S6	0.0	0.0	0.0	0.0	0.0	0.0	-
< 0.29 µm	Filter	0.0	0.0	0.0	0.0	0.0	0.0	-
	MMAD	1.99	1.95	1.93	1.97	1.96	0.03	1.32
	GSD	1.75	1.71	1.75	1.71	1.73	0.02	1.33
	Emitted (ug)	208.2	203.8	195.8	217.7	206.3	9.1	4.4
	Metered (ug)	233.1	220.3	215.9	232.5	225.4	8.7	3.8
	Impactor (ug)	120.2	111.7	103.1	121.0	114.0	8.4	7.4

Table A.13: Aerodynamic particle size distribution of Novolizer drug only formulation; Chapter 5.

Flow – 75 L/min for 3.2 sec; 4L air

Impactor – Next Generation Impactor – Inhaler was attached directly to pre-separator (induction port was not attached)

Inhaler – Novolizer loaded with approx. 1.2 mg albuterol sulfate eq. to 1000 mg albuterol base

No of shots – Single shots

		All as % of albuterol (as base) emitted dose (except Device retention as % of metered)						
		#1	#2	#3	#4	MEAN	SD	CV
	Device	25.2	33.6	30.6	31.2	30.2	3.5	11.7
	Adaptor	35.9	38.0	36.4	36.4	36.7	0.9	2.5
< 11.75 um	Presep	5.6	5.3	5.6	5.8	5.6	0.2	3.6
7.15 - 11.75 um	inlet	1.2	1.2	1.2	1.2	1.2	0.0	2.6
3.97 - 7.15 um	S1	6.5	6.6	7.3	7.1	6.9	0.4	5.7
2.52 - 3.97 um	S2	19.3	18.6	18.8	19.2	19.0	0.3	1.7
1.49 - 2.52 um	S3	22.4	21.7	21.3	21.1	21.6	0.6	2.7
0.84 - 1.49 um	S4	8.0	7.5	8.4	8.2	8.0	0.4	4.6
0.48 - 0.84 um	S5	0.9	0.9	0.9	0.8	0.9	0.0	5.2
0.29 - 0.48 um	S6	0.1	0.1	0.1	0.1	0.1	0.0	17.3
< 0.29 um	Filter	0.1	0.1	0.1	0.1	0.1	0.0	19.1
	MMAD	2.42	2.43	2.44	2.45	2.44	0.01	0.53
	GSD	1.59	1.60	1.61	1.59	1.60	0.01	0.60
	Emitted (ug)	934.6	658.8	771.0	872.2	809.2	120.8	14.9
	Metered (ug)	1250.2	992.4	1110.9	1268.2	1155.4	129.4	11.2
	Impactor (ug)	599.5	408.4	490.6	554.6	513.3	83.0	16.2

Table A.14 – Aerodynamic particle size distribution of micronized albuterol sulfate delivered through Novolizer containing drug only formulation that escaped from -20° MT model; Chapter 5.

Flow – 75 L/min for 3.2 sec; 4L air

Impactor – Next Generation Impactor – Inhaler was attached directly to pre-separator via -20° MT model in-between instead of USP induction port. (MT Model coated with silicone spray)

Inhaler – Novolizer loaded with approx. 1.2 mg albuterol sulfate eq. to 1000 mg albuterol base

No of shots – Single shot

		All as % of emitted albuterol (as base) dose (except Device retention as % of metered)						
Angle = -20		#1	#2	#3	#4	MEAN	SD	CV
	Device	35.9	37.2	29.7	31.2	33.5	3.6	10.7
	MT	46.9	46.7	47.8	48.5	47.5	0.9	1.8
< 11.75 um	Presep	2.3	3.4	3.2	3.5	3.1	0.6	18.4
7.15 - 11.75 um	inlet	0.8	0.9	0.7	0.9	0.8	0.1	11.0
3.97 - 7.15 um	S1	3.9	4.0	3.9	3.8	3.9	0.1	2.5
2.52 - 3.97 um	S2	14.8	13.8	14.3	14.0	14.2	0.4	3.1
1.49 - 2.52 um	S3	21.6	21.9	20.7	20.3	21.1	0.7	3.5
0.84 - 1.49 um	S4	7.5	7.6	7.8	7.4	7.6	0.2	2.4
0.48 - 0.84 um	S5	1.3	1.2	1.3	1.2	1.2	0.1	4.3
0.29 - 0.48 um	S6	0.2	0.2	0.1	0.2	0.2	0.0	20.0
< 0.29 um	Filter	0.8	0.4	0.2	0.3	0.4	0.3	70.0
	MMAD	2.24	2.22	2.24	2.25	2.24	0.01	0.56
	GSD	1.63	1.64	1.63	1.63	1.63	0.01	0.31
	Emitted (ug)	599.0	511.0	804.8	460.7	593.9	151.8	25.6
	Metered (ug)	934.0	813.5	1145.3	669.7	890.6	201.2	22.6
	Impactor (ug)	318.0	272.5	419.8	237.2	311.9	79.2	25.4

Table A.15 – Aerodynamic particle size distribution of albuterol sulfate delivered through Novolizer containing drug only formulation that escaped from +10° MT model; **Chapter 5.**

Flow – 75 L/min for 3.2 sec; 4L air

Impactor – Next Generation Impactor – Inhaler was attached directly to pre-separator via +10° MT model in-between instead of USP induction port. (MT Model coated with silicone spray)

Inhaler – Novolizer loaded with approx. 1.2 mg albuterol sulfate eq. to 1000 mg albuterol

Number of shots – Single shot

		All as % of emitted albuterol (as base) dose (except Device retention as % of metered)						
Angle = +10		#1	#2	#3	#4	MEAN	SD	CV
	Device	35.0	39.2	35.3	33.1	35.6	2.6	7.2
	MT	36.0	36.5	35.6	36.3	36.1	0.4	1.0
< 11.75 um	Presep	2.8	3.3	3.3	3.1	3.1	0.2	7.5
7.15 - 11.75 um	inlet	0.9	1.1	1.1	1.1	1.0	0.1	7.3
3.97 - 7.15 um	S1	5.6	5.7	5.8	6.0	5.8	0.2	3.2
2.52 - 3.97 um	S2	18.3	17.9	17.8	17.3	17.8	0.4	2.4
1.49 - 2.52 um	S3	25.4	24.5	25.8	25.3	25.3	0.6	2.3
0.84 - 1.49 um	S4	8.5	8.8	8.4	9.0	8.7	0.3	3.2
0.48 - 0.84 um	S5	1.3	1.4	1.4	1.3	1.3	0.1	5.1
0.29 - 0.48 um	S6	0.2	0.2	0.2	0.2	0.2	0.0	2.9
< 0.29 um	Filter	1.0	0.8	0.6	0.4	0.7	0.3	36.3
	MMAD	2.28	2.29	2.29	2.28	2.29	0.01	0.25
	GSD	1.63	1.64	1.64	1.65	1.64	0.01	0.50
	Emitted (ug)	587.7	392.1	745.3	679.9	601.3	153.7	25.6
	Metered (ug)	903.7	645.1	1152.3	1015.9	929.3	215.0	23.1
	Impactor (ug)	376.2	249.1	479.8	432.9	384.5	99.7	25.9

APPENDIX B

REPRESENTATIVE CHROMATOGRAMS, CALIBRATION CURVES AND METHOD VALIDATION RESULTS FOR HPLC METHODS USED IN CHAPTERS 3, 4 AND 5.

(Refer section 4.2.3 and Table 4.3 for method details)

B.1 TIOTROPIM BROMIDE

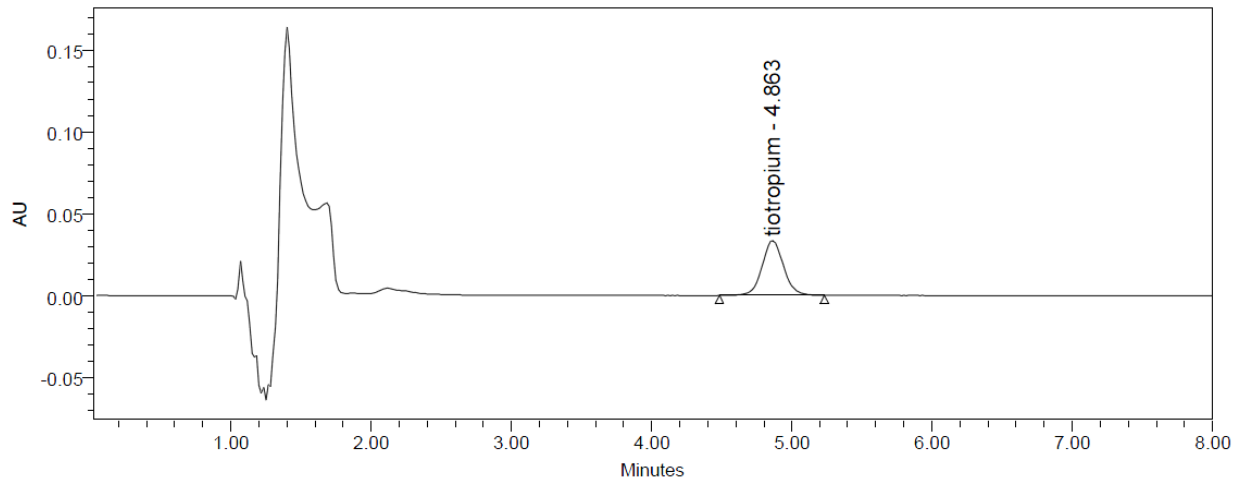


Figure B.1: Representative chromatogram for tiotropium bromide (as tiotropium base)(2.2 $\mu\text{g/mL}$).

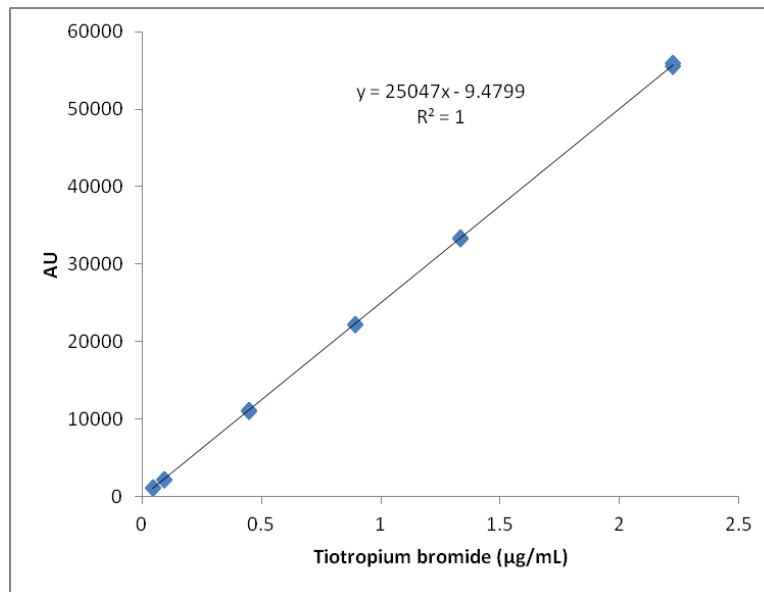


Figure B.2: Calibration curve for tiotropium bromide (as tiotropium base). Linear regression performed on the response across concentrations.

Table B.1: Chromatographic area for tiotropium bromide (expressed as equivalent tiotropium base) working standards.

Working Standard	Con. (µg/mL)	Area 1 (AU)	Area 2 (AU)
S1	0.0445	1120	1134
S2	0.0889	2234	2216
S3	0.445	11156	11070
S4	0.889	22239	22275
S5	1.334	33464	33295
S6	2.224	55886	55543

Table B.2: Chromatographic area for tiotropium bromide (expressed as equivalent tiotropium base) quality control standards, with imprecision (%RSD) and inaccuracy (%DFN) assessments.

	Nominal (µg/mL)	Area (AU)	Calculated (µg/mL)	% DFN (% inaccuracy)	% average DFN	%RSD (% imprecision)
LQC 1	0.0667	1641	0.066	-1.21		
LQC 2	0.0667	1664	0.067	0.17	-0.89	0.88
LQC 3	0.0667	1637	0.066	-1.45		
MQC 1	0.667	17128	0.684	2.58		
MQC 2	0.667	17110	0.683	2.47	2.40	0.22
MQC 3	0.667	17056	0.681	2.15		
HQC 1	1.779	44437	1.774	-0.25		
HQC 2	1.779	44365	1.772	-0.41	-0.27	0.14
HQC 3	1.779	44489	1.777	-0.14		

B.2 BUDESONIDE

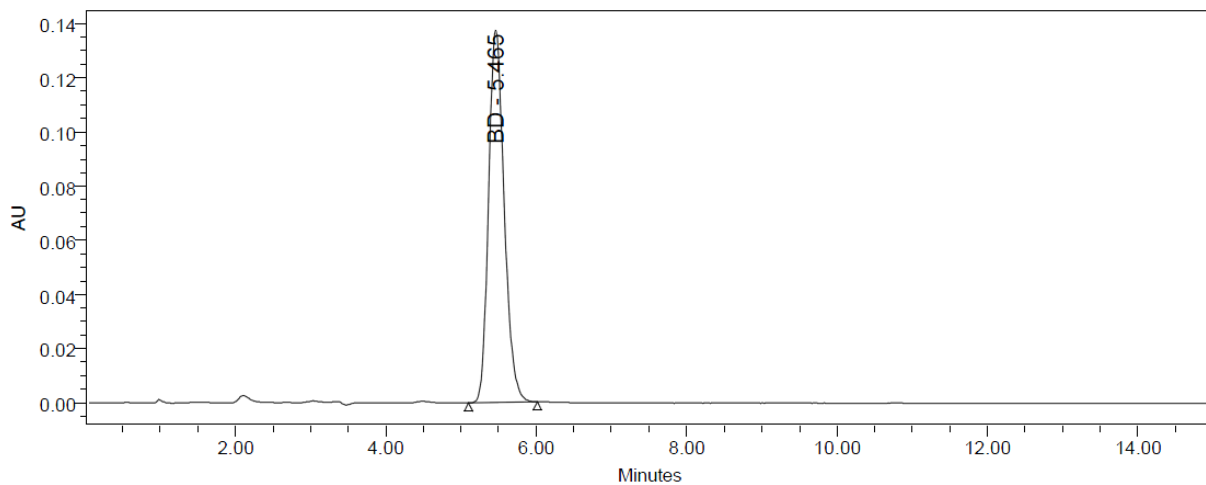


Figure B.3: Representative chromatogram for budesonide (9.93 $\mu\text{g/mL}$).

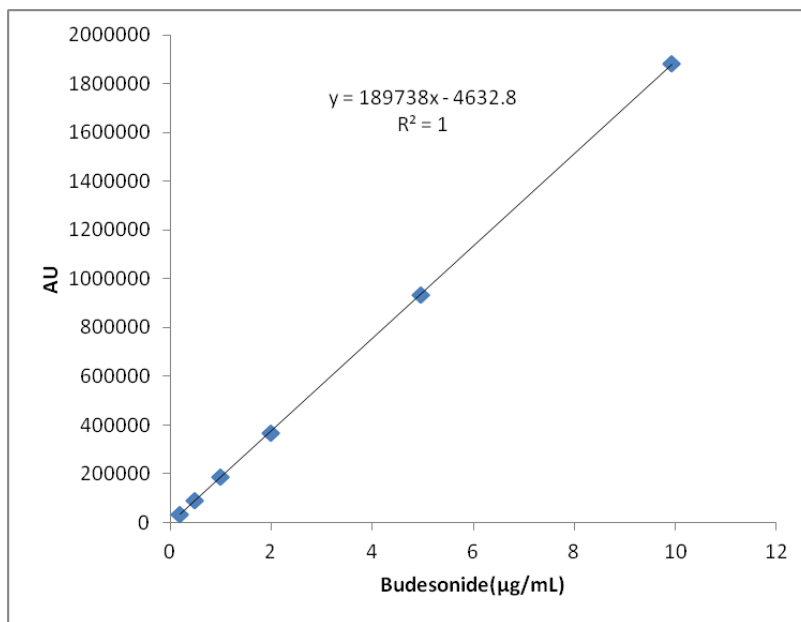


Figure B.4: Calibration curve for budesonide. Linear regression performed on the response across concentrations.

Table B.3: Chromatographic area for budesonide working standards.

Day 1	Con. ($\mu\text{g/mL}$)	Area 1 (AU)	Area 2 (AU)
S1	0.199	34518	34157
S2	0.496	90053	90083
S3	0.993	187069	188361
S4	1.986	368390	368204
S5	4.964	932717	932590
S6	9.928	1881535	1881836

Table B.4: Chromatographic area for budesonide quality control standards, with imprecision (%RSD) and inaccuracy (%DFN) assessments.

	Nominal ($\mu\text{g/mL}$)	Area (AU)	Calculated ($\mu\text{g/mL}$)	% DFN (% inaccuracy)	% average DFN	%RSD (% imprecision)
LQC 1	0.19856	34305	0.205	3.35		
LQC 2	0.19856	34171	0.205	3.00	2.86	0.56
LQC 3	0.19856	33881	0.203	2.23		
MQC 1	1.9856	373919	1.995	0.48		
MQC 2	1.9856	373801	1.995	0.45	0.46	0.02
MQC 3	1.9856	373829	1.995	0.46		
HQC 1	9.928	1896700	10.021	0.94		
HQC 2	9.928	1880991	9.938	0.10	0.39	0.47
HQC 3	9.928	1881408	9.940	0.12		

B3 ZANAMIVIR

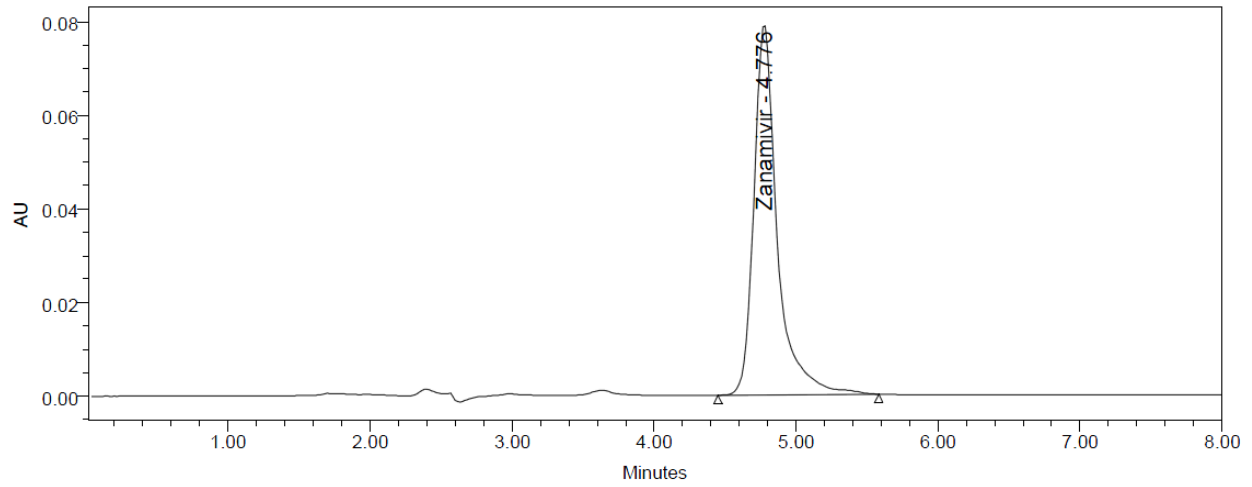


Figure B.5: Representative chromatogram for zanamivir (104.54 $\mu\text{g/mL}$).

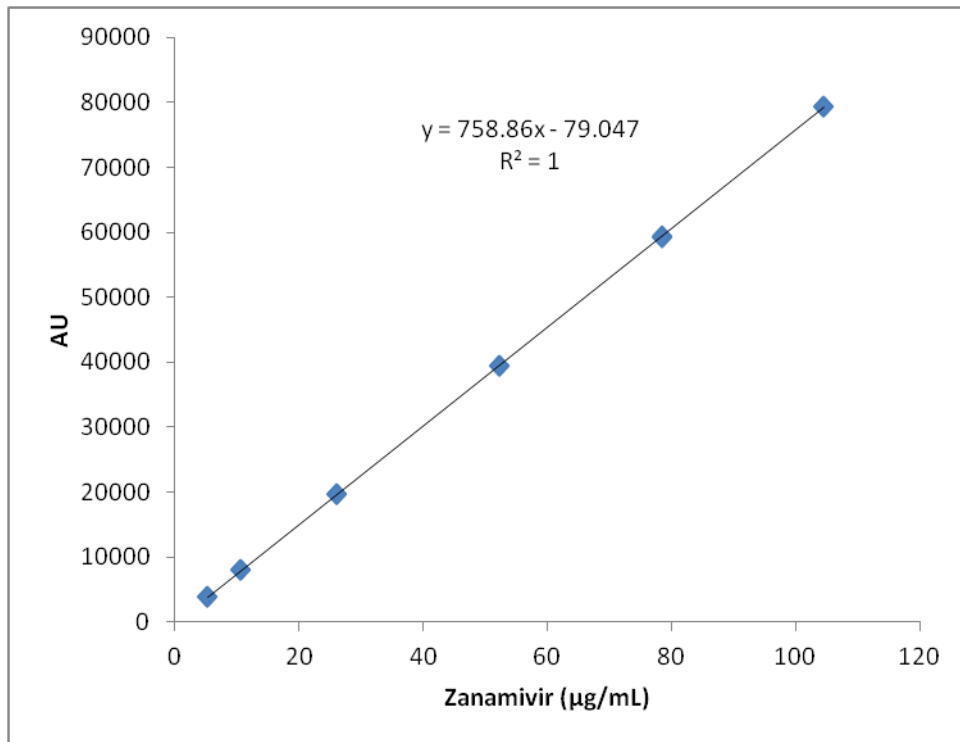


Figure B.6: Calibration curve for zanamivir. Linear regression performed on the response across concentrations.

Table B.5: Chromatographic area for zanamivir working standards.

Working Standard	Con. (µg/mL)	Area 1 (AU)	Area 2 (AU)
S1	5.227	3857	3872
S2	10.454	7954	7948
S3	26.135	19774	19747
S4	52.270	39482	39535
S5	78.405	59379	59211
S6	104.54	79296	79454

Table B.6: Chromatographic area for zanamivir quality control standards, with imprecision (%RSD) and inaccuracy (%DFN) assessments.

	Nominal (µg/mL)	Area (AU)	Calculated (µg/mL)	% DFN (% inaccuracy)	% average DFN	%RSD (% imprecision)
LQC 1	7.841	5813	7.764	-0.98		
LQC 2	7.841	5799	7.746	-1.21	-1.06	0.13
LQC 3	7.841	5812	7.763	-0.99		
MQC 1	39.203	29526	39.013	-0.49		
MQC 2	39.203	29511	38.993	-0.54	-0.60	0.15
MQC 3	39.203	29441	38.901	-0.77		
HQC 1	91.473	69797	92.080	0.66		
HQC 2	91.473	69209	91.305	-0.18	0.10	0.49
HQC 3	91.473	69215	91.313	-0.17		

B.4 FORMOTEROL FUMARATE

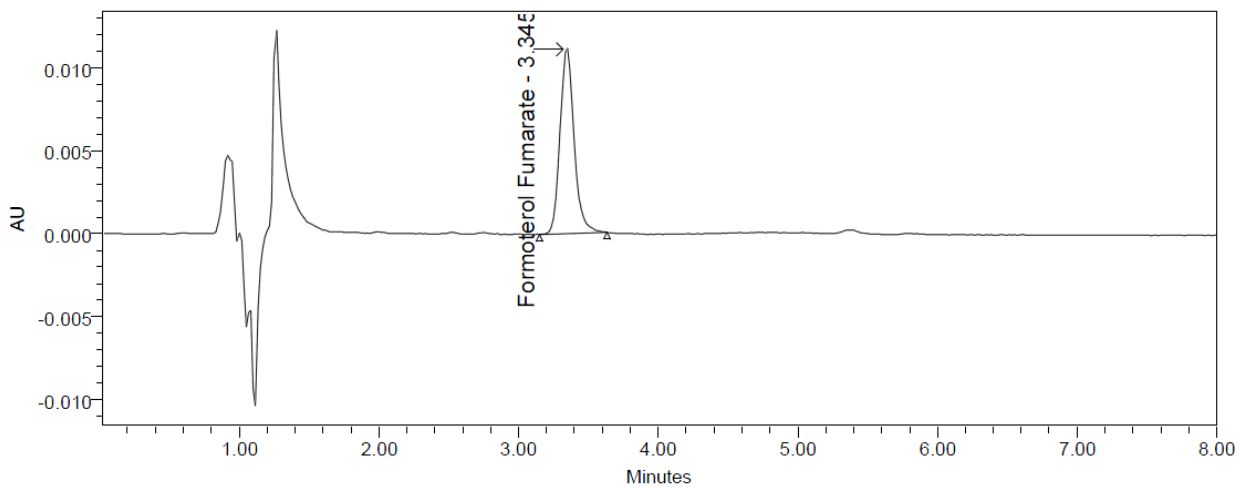


Figure B.7: Representative chromatogram for formoterol fumarate (0.96 µg/mL).

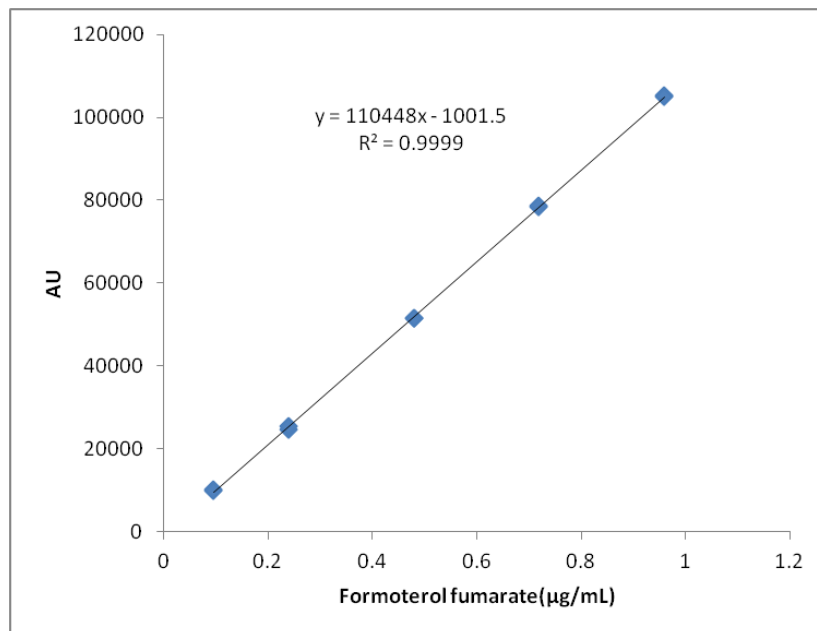


Figure B.8: Calibration curve for formoterol fumarate. Linear regression performed on the response across concentrations.

Table B.7: Chromatographic area for formoterol fumarate working standards.

Working Standard	Con. (µg/mL)	Area 1 (AU)	Area 2 (AU)
S1	0.096	10161	9981
S2	0.240	24697	25517
S3	0.480	51668	51524
S4	0.719	78517	78579
S5	0.959	105156	104969

Table B.8: Chromatographic area for formoterol fumarate quality control standards, with imprecision (%RSD) and inaccuracy (%DFN) assessments

	Nominal (µg/mL)	Area (AU)	Calculated (µg/mL)	% DFN (% inaccuracy)	% average DFN	%RSD (% imprecision)
LQC 1	0.1918	20216	0.192	0.16		
LQC 2	0.1918	20159	0.192	-0.11	-0.51	0.94
LQC 3	0.1918	19848	0.189	-1.58		
HQC 1	0.8631	92828	0.850	-1.57		
HQC 2	0.8631	93205	0.853	-1.18	-1.44	0.24
HQC 3	0.8631	92818	0.849	-1.58		

B.5 ALBUTEROL SULFATE

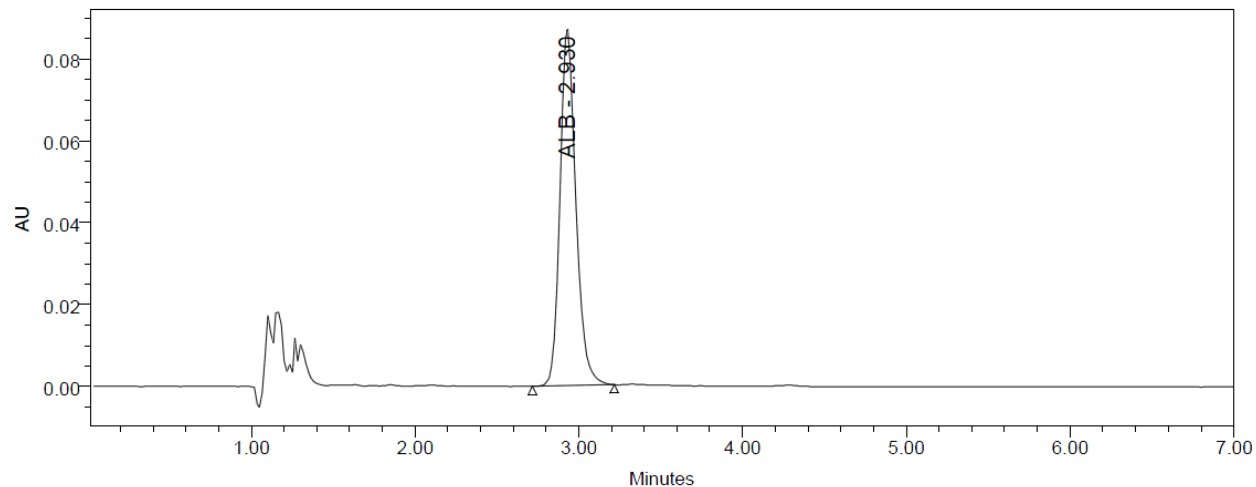


Figure B.9: Representative chromatogram for albuterol sulfate (expressed as equivalent albuterol base) (10.13 $\mu\text{g/mL}$).

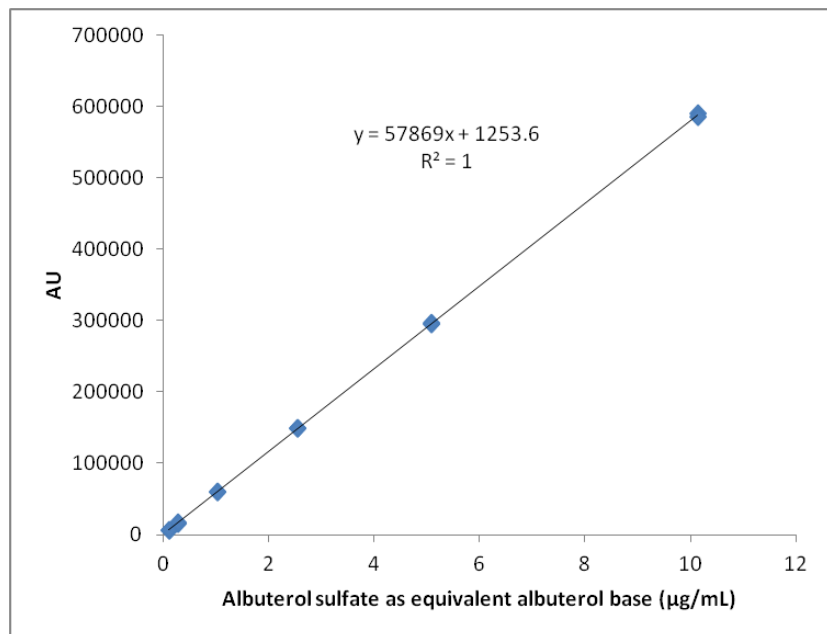


Figure B.10: Calibration curve for albuterol sulfate (expressed as equivalent albuterol base). Linear regression performed on the response across concentrations.

Table B.9: Chromatographic area for albuterol sulfate (expressed as equivalent albuterol base) working standards (concentrations as eq albuterol base).

Working Standard	Con. (µg/mL)	Area 1 (AU)	Area 2 (AU)
S6	0.101	6140	6298
S5	0.253	15557	16693
S4	1.013	58924	59886
S3	2.533	148578	149223
S2	5.067	295934	294104
S1	10.133	589632	584680

Table B.10: Chromatographic area for albuterol sulfate (expressed as equivalent albuterol base) quality control standards, with imprecision (%RSD) and inaccuracy (%DFN) assessments (concentrations as eq albuterol base).

	Nominal (µg/mL)	Area (AU)	Calculated (µg/mL)	% DFN (% inaccuracy)	% average DFN	%RSD (% imprecision)
LQC 1	0.608	36140	0.603	-0.85		
LQC 2	0.608	35829	0.597	-1.73	-0.84	0.91
LQC 3	0.608	36462	0.608	0.07		
MQC 1	3.8	230887	3.968	4.43		
MQC 2	3.8	226063	3.885	2.23	2.49	1.77
MQC 3	3.8	222952	3.831	0.82		
HQC 1	7.6	445272	7.673	0.96		
HQC 2	7.6	444304	7.656	0.74	0.79	0.15
HQC 3	7.6	443995	7.651	0.67		

APPENDIX C

INHALATION CELL – DESIGN, CONSTRUCTION AND CALIBRATION OF AIRFLOW RESISTANCE TUBES USED IN CLINICAL STUDY

C.1 Standard resistance tubes:

39 mm long resistance tubes with different internal diameter circular channels were custom manufactured (Custom Design and Fabrication South, LLC, Petersburg, VA) from solid polycarbonate (Table C.2). Air flow resistances of the inhalation flow cell (described in Chapter 6, section 6.2) containing each of these tubes were measured as follows: The inhalation flow cell (see Figure 6.1) was attached to the breath simulator (ASL 5000, IngMar, Pittsburgh, PA) and air was drawn at known but steady volumetric flow rates (Q_e) from the mouthpiece of the flow cell; the corresponding pressure drop (ΔP) (in cmH_2O from atmospheric pressure) across the inhalation flow cell was simultaneously measured by the breath simulator and recorded. The procedure was repeated for different flow rates as shown in Table C.1. Air flow resistances ($\text{kPa}^{0.5} \cdot \text{L}^{-1} \cdot \text{min}$) of the inhalation flow cell containing different diameter tubes were then calculated from the slope of linear regression of ' $\Delta P^{0.5}$ ' versus ' Q_e ' profiles for individual tubes; Figure C.1 shows an example for the 3.5 mm tube (Tube A, Table C.2). The calculated airflow resistances of inhalation flow cell with different diameter tubes are shown in Table C.2. Because air flow resistance is often reported in $\text{kPa} \cdot \text{L}^{-1} \cdot \text{min}$, pressure drop values were converted to kPa from cmH_2O ($1 \text{ cmH}_2\text{O} = 0.098 \text{ kPa}$) before plotting the graph.

Table C.1: Pressure drop across the inhalation flow cell containing different internal diameter resistance tubes (each tube was 39 mm long) at different volumetric flow rates (Q exiting the mouthpiece of the inhalation flow cell); notably, the ASM 5000 is a calibration instrument in which the volume of air withdrawn by the simulator is defined precisely by the displacement of its piston. Internal diameters of the tubes are shown in parentheses for Tubes A through H.

Flow rate* (L/min)	Pressure drop (cm H ₂ O)								
	Tube A (0.35 mm)	Tube B (0.40 mm)	Tube C (0.45 mm)	Tube D (0.50 mm)	Tube E (0.55 mm)	Tube F (0.60 mm)	Tube G (0.65 mm)	Tube G (0.70 mm)	Tube H (0.75 mm)
5	1.2	0.7	0.5						
10	3.8	2.3	1.7	1.3	1.0	0.9	0.8	0.8	0.7
15	7.8	4.6							
20	13.1	7.8	5.5	4.0	3.2	2.7	2.3	2.2	2.0
25	19.9	11.7							
30	27.7	16.3	11.3	8.0	6.4	5.1	4.5	4.1	3.7
35	36.9								
40	46.9	27.7	19.0	13.4	10.7	8.4	7.4	6.7	6.1
45	58.1								
50	67.7	41.5	28.3	20.1	15.9	12.4	10.4	9.8	8.8
60		57.8	39.4	28.0	22.1	17.2	15.0	13.4	12.1
65		66.6							
70			52	36.8	29.1	22.5	19.7	17.5	15.7
80			66	46.7	37.0	28.5	25.0	22.2	19.9
90				57.6	45.7	35.1	30.9	27.2	24.9
100				69.4	55.1	42.2	37.1	32.8	29.3
110					65.1	50.0	44.0	38.7	34.7
120						58.1	51.3	45.1	40.7
130						67.0	59.0	52.0	46.6
140							67.1	59.0	52.9
150								66.5	59.6
160									66.6

* Flow rate set on breath simulator is the volumetric flow rate of air leaving the mouthpiece of inhalation flow cell at a pressure of 1atmosphere minus the pressure drop shown in the table.

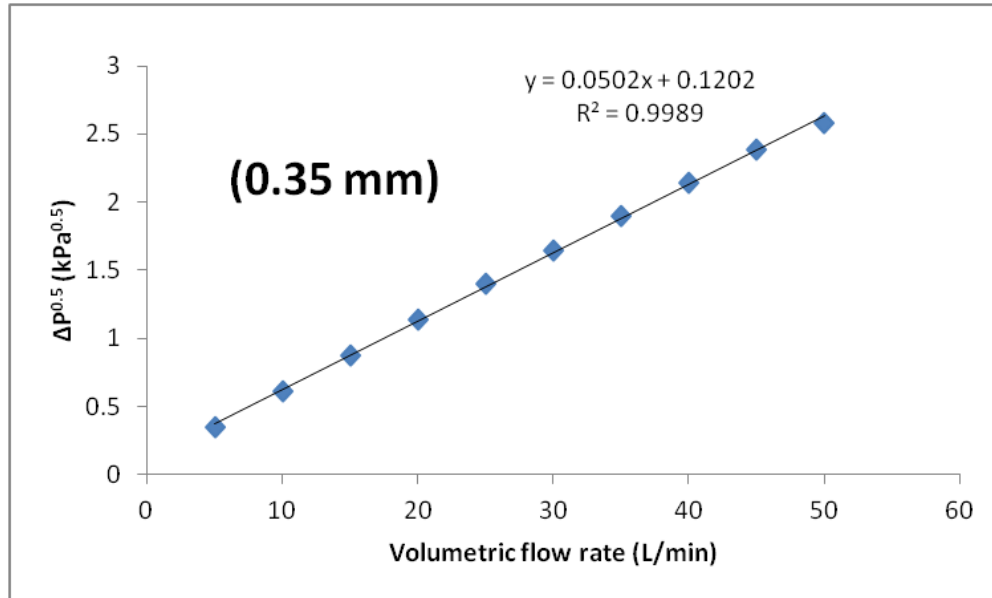


Figure C.1: Linear regression plot for $\Delta P^{0.5}$ versus volumetric flow rate for inhalation flow cell with 0.35 mm tube (Tube A)

Table C.2 Airflow resistance of inhalation flow cell with different internal diameters resistance tubes (39 mm long)

Standard resistance tube	Internal channel diameter (mm)	Air flow resistance of inhalation flow cell (kPa ^{0.5} .L ⁻¹ .min)
Tube A	3.5	0.0502
Tube B	4.0	0.0381
Tube C	4.5	0.0309
Tube D	5.0	0.0250
Tube E	5.5	0.0221
Tube F	6.0	0.0188
Tube G	6.5	0.0176
Tube H	7.0	0.0162
Tube I	7.5	0.0153

C.2 Resistance tubes that mimic airflow resistance of marketed DPIs

The relationship between the air flow resistance of the inhalation flow cell and the diameter of the resistance tube was (Table C.2) was used to calculate the internal diameters of tubes to produce airflow resistances comparable to those of marketed powder inhalers shown in Table C.4.

The following steps were performed to calculate the tube diameters for use in the clinic:

Step 1: Four tubes, from Table C.2, were selected that produced air flow resistance values that bracketed each target resistance (Shown in table C.4). For example, the target resistance of $0.0467 \text{ kPa}^{0.5} \cdot \text{L}^{-1} \cdot \text{min}$, used the data from tubes A, B, C, and D in Table C.2 as shown in Table C.3.

Table C.3: Tubes selected to calculate the desired diameter to produce an air flow resistance of $0.0467 \text{ kPa}^{0.5} \cdot \text{L}^{-1} \cdot \text{min}$

Tube	Internal diameter of resistance tubes (mm)	Inhalation flow cell air flow resistance ($\text{kPa}^{0.5} \cdot \text{L}^{-1} \cdot \text{min}$)
A	3.5	0.0502
Desired	x	0.0467
B	4	0.0381
C	4.5	0.0309
D	5	0.025

Step 2: Inhalation flow cell resistance versus tube diameter for the four selected tubes was plotted as shown in Figure C.2. The polynomial equation shown within the graph was used to produce the curve fit to the data shown on the top-right side of Figure C.2.

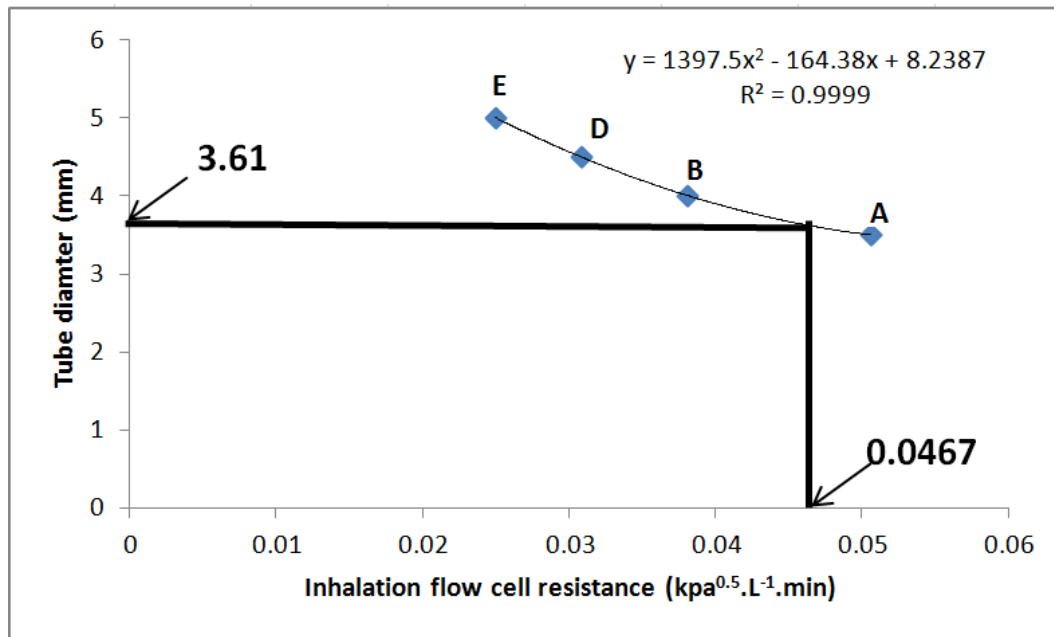


Figure C.2: Polynomial plot for tube diameter versus inhalation flow cell resistance.

Step 3: The desired internal diameter of the tube was calculated by interpolation – e.g. the polynomial equation was solved for the target tube resistance (x input). In this case, the desired tube diameter was 3.61 mm.

Table C.4 shows each of the polynomial equations used to calculate the diameters used in the clinic to mimick the powder inhalers tested *in vitro* (Chapter 6).

Table C.4 Summary of the method used to design the resistance tubes used in the inhalation cell for the clinical study.

Desired air flow resistance of inhalation flow cell (kPa ^{0.5} .L ⁻¹ .min)**	Polynomial equations used to calculate the desired internal tube diameter*	Calculated internal tube diameter (mm)
0.0467 (Handihaler)		3.61
0.0435 (Easyhaler)	$y = 1397.5x^2 - 164.38x + 8.2387$; (A-D)	3.73
0.0352 (Turbuhaler)		4.18
0.0239 (Novolizer)	$y = 5324x^2 - 390.63x + 11.48$; (C-F)	5.19
0.0198 (Relenza)	$y = 10758x^2 - 648.13x + 14.502$; (D-G)	5.89
0.0176 (Aerolizer)	ALREADY BUILT (G)	6.50

*‘y’ is diameter in mm, ‘x’ is air flow resistance in kPa^{0.5}.L⁻¹.min; parentheses shows the standard tubes (from Table C.2) used to derive the polynomial equation.

** desired air flow resistances are the resistances of marketed DPIs shown in parentheses.

Tubes 1 through 6 were constructed at machine shop with the requisite internal diameters. Table C.5 shows the diameter of the tubes constructed along with their air flow resistance determined according to the method described above. As expected, the actual resistances were quite comparable to the desired values shown in Table C.4.

Table C.5: Diameter of the constructed resistance tubes and corresponding inhalation flow cell air flow resistance following testing similar to that described in Table C.1; tube numbers are shown along with the names of those DPIs (in parentheses) whose air flow resistance they were designed to mimic.

Tube name	Actual tube Diameter (mm)	Actual resistance of inhalation flow cell
Tube 1 (Handihaler)	3.6	0.0462
Tube 2 (Easyhaler)	3.8	0.0432
Tube 3 (Turbuhaler)	4.2	0.0344
Tube 4 (Novolizer)	5.2	0.0241
Tube 5 (Relenza)	5.8	0.0200
Tube 6 (Aerolizer)	6.5	0.0179

APPENDIX D

**CALCULATION OF AIR FLOW RATE LEAVING THE MOUTHPIECE OF
INHALATION FLOW CELL BASED ON FLOW RATE MEASUREMENTS MADE AT
ITS AIR INLET**

D.1 Calculation of the volumetric flow rate leaving the mouthpiece

The output of the mass flowmeter used to instrument the inhalation flow cell (described in Chapter 6, section 6.2; Figure 6.1) was factory calibrated to measure and record volumetric flow rate passing through the cell in “normal liters”, L_n , per minute (in short, the device converts mass flow rate, measured by miniaturized thermal sensor, to volumetric flow rate, Q_n , assuming a “normal temperature”, T_n , of 273.15 °K and a “normal pressure” $P_n = 1013$ mbar, every 5 msec during inspiration. However, inhalation profiles defined in terms of the volumetric air flow rate leaving the mouthpiece of the inhalation flow cell, as seen by the patient were desired; these values were larger than the volumetric flow rates entering the cell because of the pressure drop over the cell or inhaler and resultant expansion of air leaving the cell. The pressure of air exiting the mouthpiece, P_e , is affected by the air flow resistance of the entire cell and the inspiratory effort exerted by the patient. The flow-meter measured value of L_n at any given time is thus related to the flow rate exiting the mouthpiece and the corresponding pressure drop over the cell according to the gas laws. The volumetric flow rate of the air leaving the mouthpiece of inhalation flow cell at any time t at room temperature, T_r , in °K, and pressure, P_e , in mbar, was calculated using the combined gas equation expressed per unit time.

$$\frac{P_n \times Q_n}{T_n} = \frac{P_e \times Q_e}{T_r} \dots \dots \dots (Eq D.1)$$

Where volume was replaced by the volumetric flow rate, Q and the subscript e represents air at room temperature exiting the mouthpiece of the inhalation cell. At any point in an inspiration, equation D.1 contains two unknowns. Therefore, values for Q_e were generated using the known relationships between P_e and Q_n following prediction of P_e from Q_n at specific resistance values (See section D.2). This resulted in flow rate corrections that could be applied to the breath

simulator, in order to generate a chosen inspiratory profile. Section D.2 below describes an example of a typical flow rate correction.

D.2 Prediction of P_e

The inhalation flow cell was attached to the breath simulator and air withdrawn at precisely known but different steady volumetric flow rates from the mouthpiece. Values for Q_n (from mass flow meter of the inhalation flow cell) at steady state were measured corresponding to P_e values recorded using the pressure-tap present in the BS chamber with a known resistance tube in place. Linear regression plots of $\Delta P^{0.5}$ vs. Q_n were constructed for the different diameter resistance tubes (in Table C.4) in the inhalation flow cell to enable the values of P_e to be paired with Q_n assuming that $\Delta P = P_o - P_e$, where P_o was assumed constant and equal to standard atmospheric pressure (1013 mbar). Table D.2 describes the regression equations for the different diameter tubes with the pressure drop unit in $\text{cmH}_2\text{O}^{0.5}$; values were multiplied by appropriate conversion factors to convert to mbar (for flow rate conversion; $1 \text{ cmH}_2\text{O} = 0.980665 \text{ mbar}$). The example for Tube 1 follows:

Table D.1: Results for flow rate and corresponding pressure drop for Tube 1

Flow rate set on Breath simulator (L/min)	Q_n (Ln/min) (recorded on the mass flow meter of inhalation cell)	ΔP (cm H ₂ O)	$\Delta P^{0.5}$ (mbar ^{0.5})
10	9.07	2.4	1.53
20	18.17	10.5	3.21
30	25.93	20.8	4.52
40	33.94	37.1	6.03
50	40.9	55.3	7.36

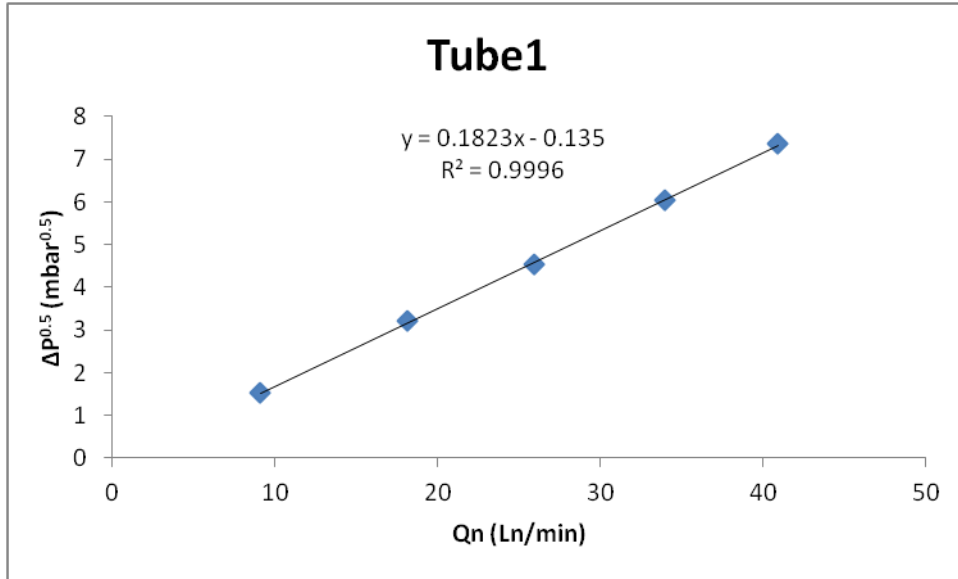


Figure D.1: Pressure drop (mbar^{0.5}) vs. Flow rate (Ln/min) for Tube 1 in Table 6.2

Assume for example that the flow rate recorded on the inhalation flow cell $Q_n = 40$ Ln/min for Tube 1. Using the regression equation from Table D.2 for tube 1, the flow rate leaving the mouthpiece can be calculated as follows:

- Flow rate recorded by inhalation flow cell = $Q_n = 40.0$ Ln/min
- Normal pressure = $P_n = 1013$ mbar (assumed constant)
- Normal temperature = $T_n = 0^\circ\text{C} = 273.15$ °K
- Room temperature = $T_r = 25^\circ\text{C} = 298.15$ °K
- Calculated pressure drop (based on the linear regression equation shown in Figure D.1)
 $= \Delta P = [(0.1823 \times 40) - 0.135]^2 = 51.22$ mbar (Equation in Table D.2)

Thus, flow rate leaving the mouthpiece of inhalation flow cell from equation D.1 is

$$= \frac{1013 \times 40 \times 298.15}{273.15 \times (1013 - \Delta P)} = 46.0 \text{ L/min}$$

Other flow rate corrections , to convert Qn (measured through the cell in the clinic) for different tubes to Qe (required for programming the breath simulator) were made using a spreadsheet in an identical fashion throughout.

Table D.2: $\Delta P^{0.5}$ (mbar^{0.5}) vs. Qn (Ln/min) linear regression equations for different resistance tubes shown in Table C.4.

Tube	$\Delta P^{0.5}$ (mbar^{0.5}) vs. Qn (Ln/min) equation
Tube1	$\Delta P^{0.5} = 0.1823 * Qn - 0.1350$
Tube2	$\Delta P^{0.5} = 0.1730 * Qn - 0.2588$
Tube3	$\Delta P^{0.5} = 0.1364 * Qn - 0.0903$
Tube4	$\Delta P^{0.5} = 0.0889 * Qn - 0.3906$
Tube5	$\Delta P^{0.5} = 0.0747 * Qn + 0.4322$
Tube6	$\Delta P^{0.5} = 0.0659 * Qn + 0.4349$

APPENDIX E

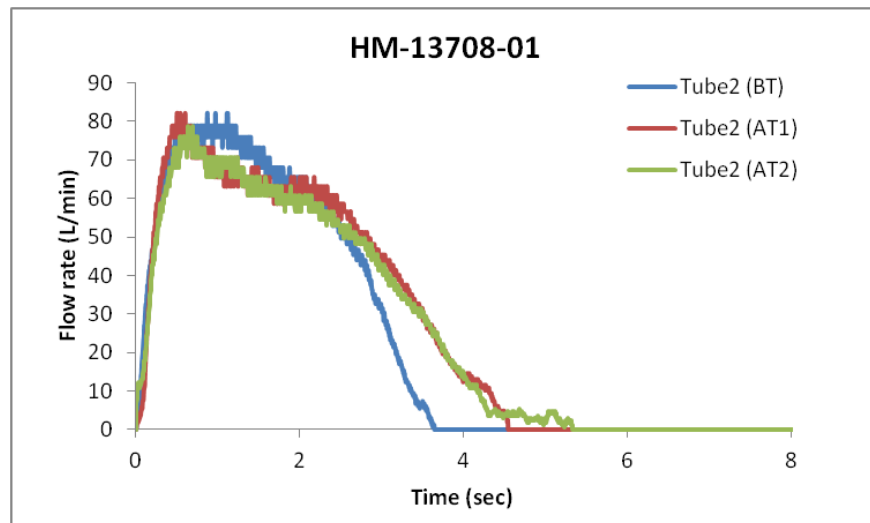
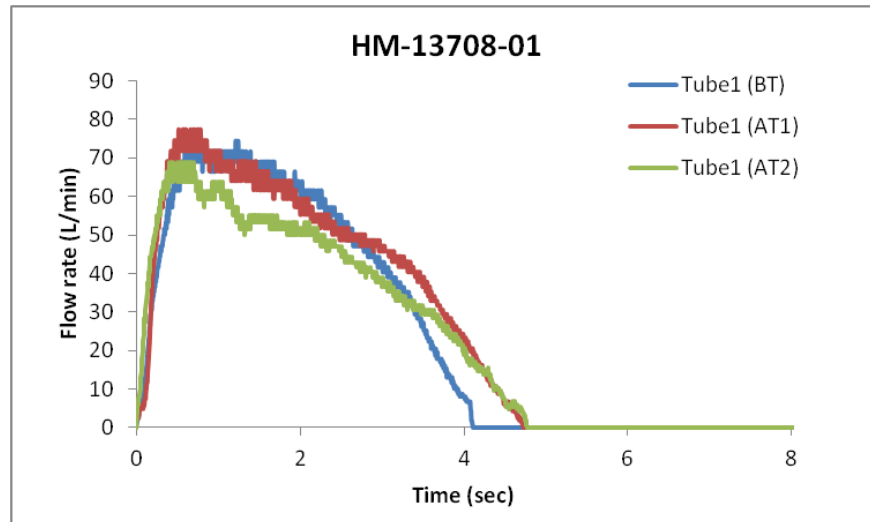
DATA FOR FLOW RATE VS TIME FOR INDIVIDUAL VOLUNTEERS INHALING THROUGH THE FLOW CELL

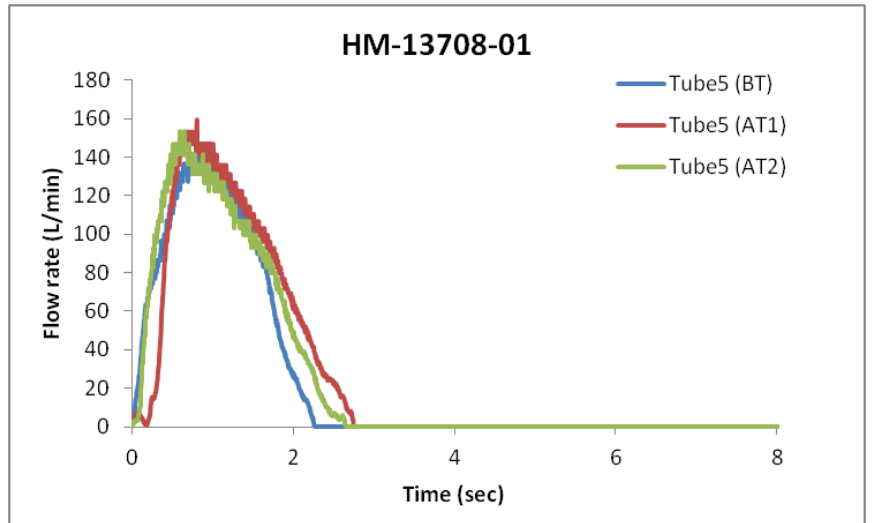
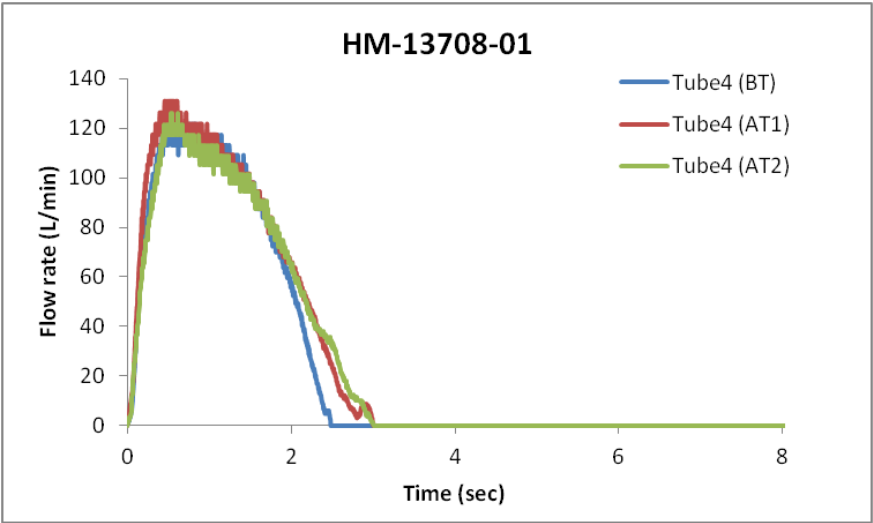
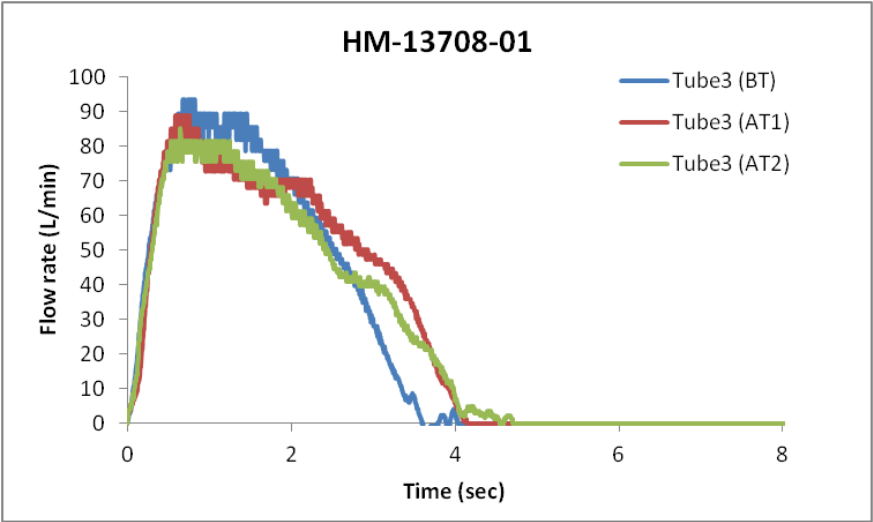
- Inhalation flow cell is defined in Chapter 6, Section 6.2, and Appendices C & D.
- Methods used to document inhalation profiles are described in Chapter 6, Section 6.3
- Flow rate is reported as volumetric flow rate leaving the inhalation flow cell mouth piece.
BT, AT1 and AT2 refer to ‘Before training’, ‘After training 1’ and ‘After training 2’ respectively.
- ‘Order’ columns in the tables describe random sequences of the resistance tubes used to document the inhalation profiles, seperately for each training status.

HM-13708-01

Description: Gender: Male, Ethnicity: Indian, Height: 177 cm, Weight: 66 kg, Age: 23 yrs

Figure E1: Inhalation profiles of Volunteer HM-13708-01.





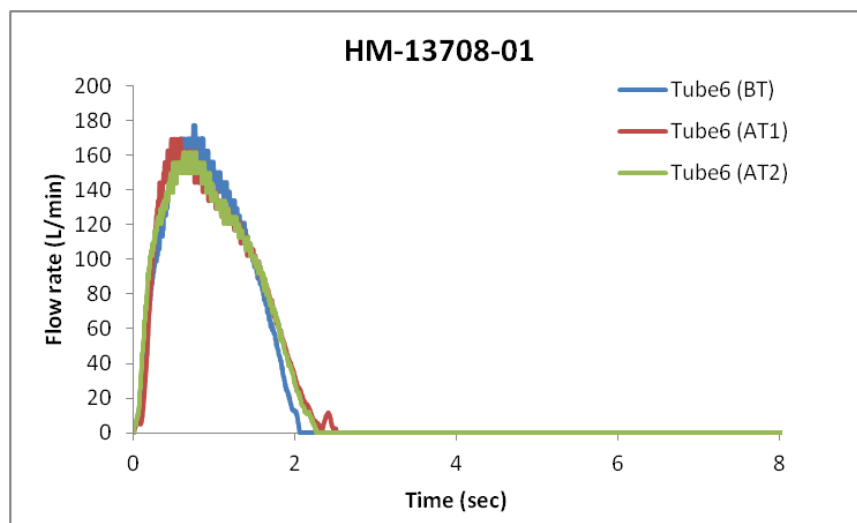


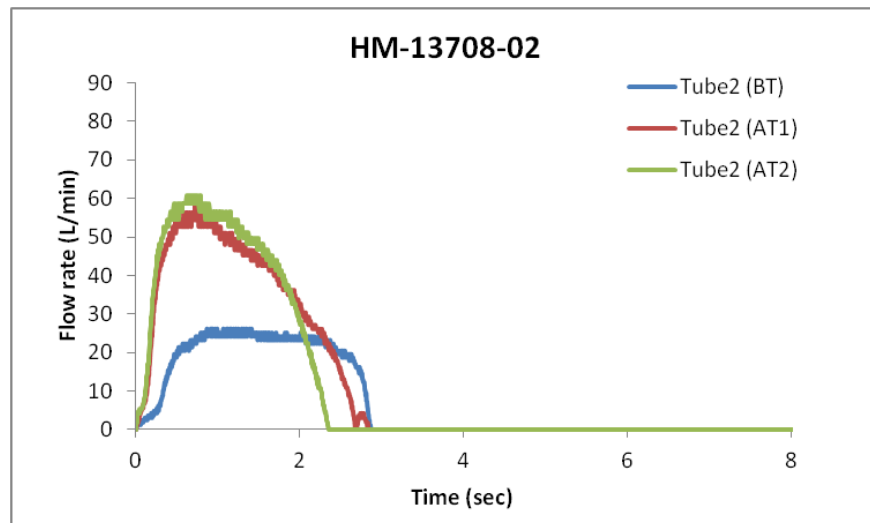
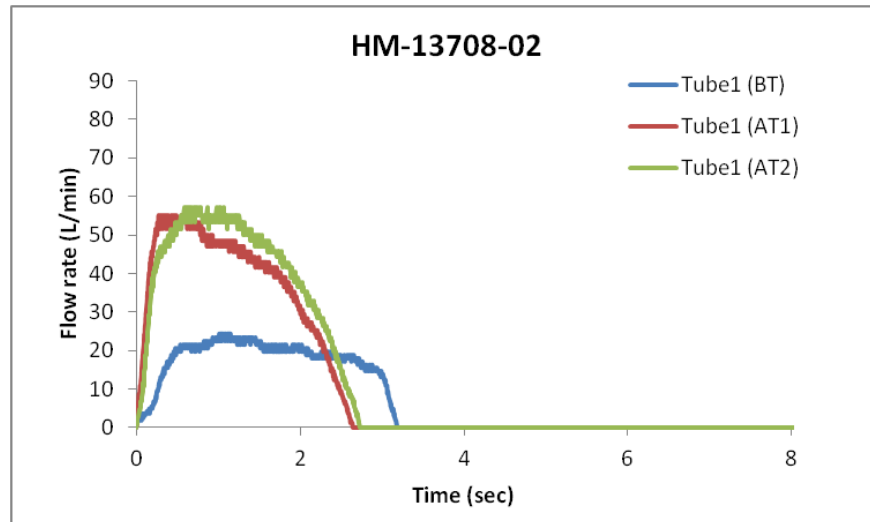
Table E1: Summary of inhalation parameters of volunteer: HM-13708-01

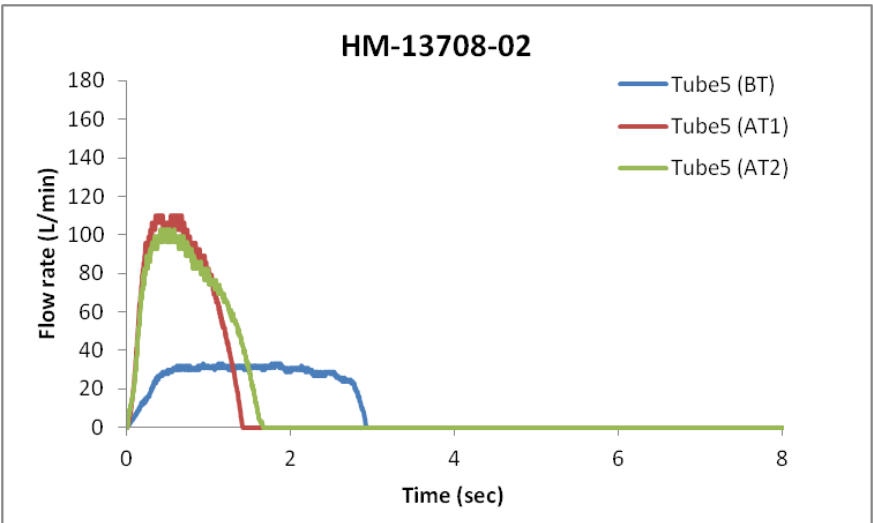
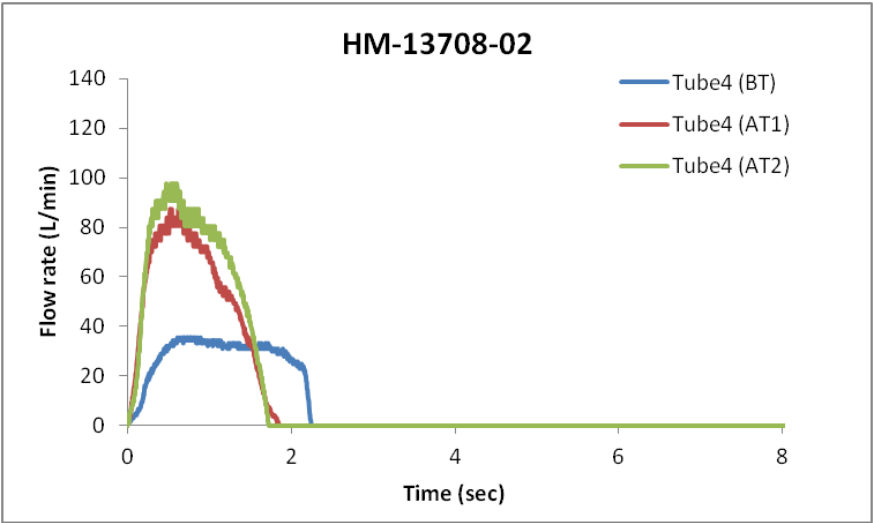
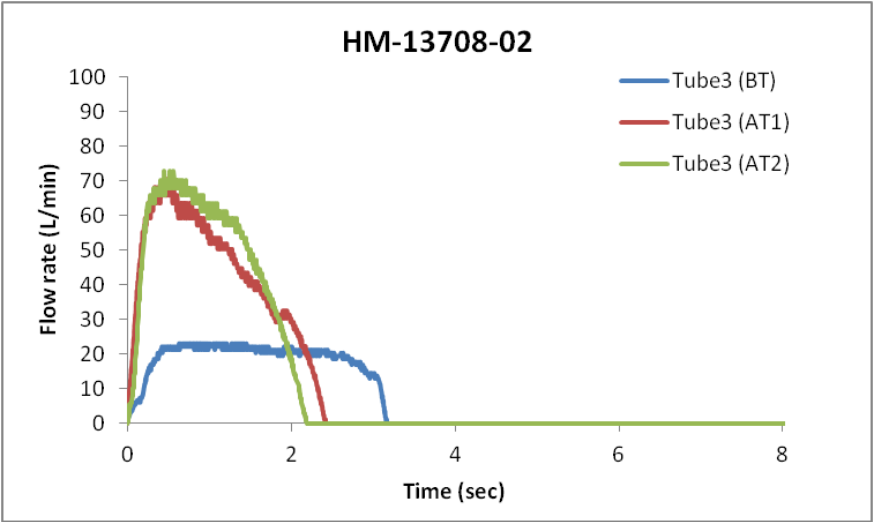
Training	Tube	Order	PIFR (L/min)	V (L)	tmax (sec)	ttotal (sec)
Before training	Tube1	4	74.6	3.326	0.655	4.110
After training 1	Tube1	1	77.3	3.617	0.520	4.725
After training 2	Tube1	5	69.0	3.222	0.410	4.770
Before training	Tube2	6	82.3	3.220	0.870	3.645
After training 1	Tube2	5	82.2	3.582	0.500	4.545
After training 2	Tube2	4	78.9	3.483	0.640	5.340
Before training	Tube3	2	93.5	3.418	0.680	3.635
After training 1	Tube3	6	89.1	3.692	0.590	4.145
After training 2	Tube3	6	85.2	3.494	0.650	4.555
Before training	Tube4	5	121.9	3.370	0.460	2.485
After training 1	Tube4	2	130.9	3.733	0.460	3.005
After training 2	Tube4	2	126.1	3.596	0.535	3.010
Before training	Tube5	1	142.0	3.236	0.715	2.270
After training 1	Tube5	4	159.6	3.643	0.810	2.755
After training 2	Tube5	3	153.1	3.573	0.600	2.655
Before training	Tube6	3	177.4	3.548	0.740	2.055
After training 1	Tube6	3	169.2	3.662	0.465	2.515
After training 2	Tube6	1	162.1	3.643	0.615	2.260

HM-13708-02

Description: Gender:Female, Ethnicity: Caucasian, Height: 164 cm, Weight: 64 kg, Age: 25 yrs

Figure E2: Inhalation profiles of Volunteer HM-13708-02





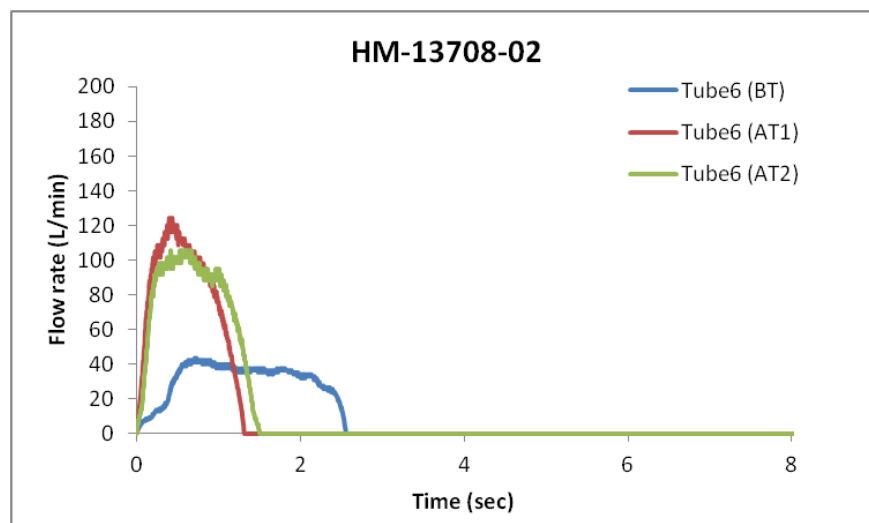


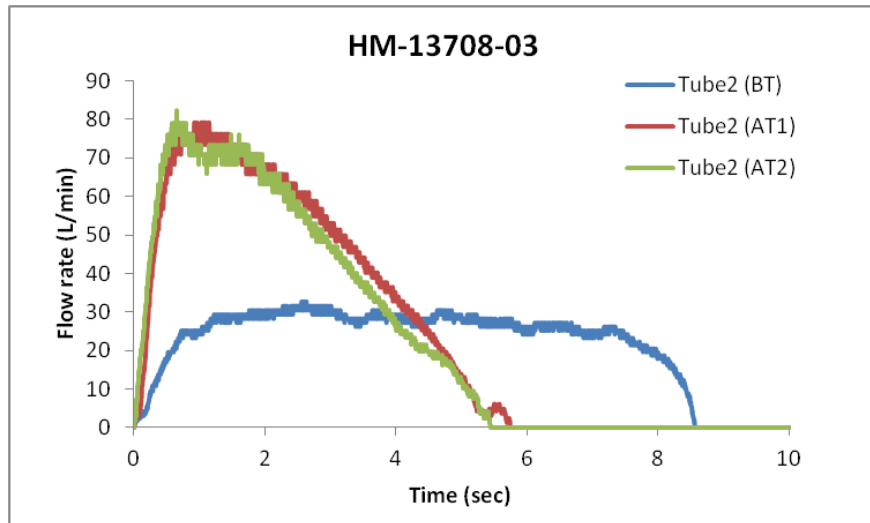
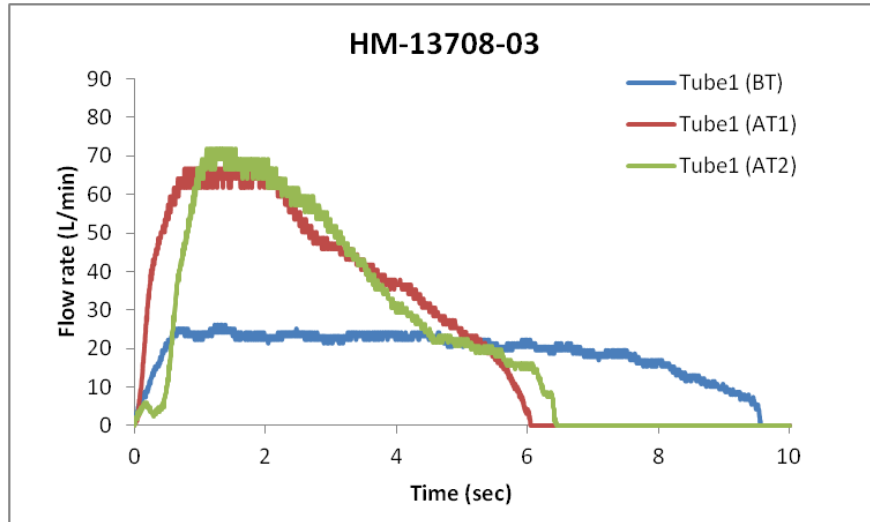
Table E2: Summary of inhalation parameters of volunteer: HM-13708-02

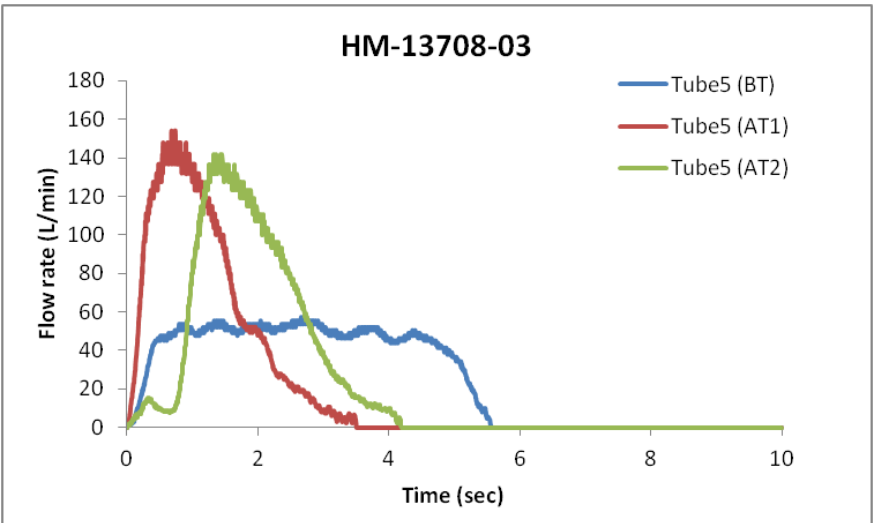
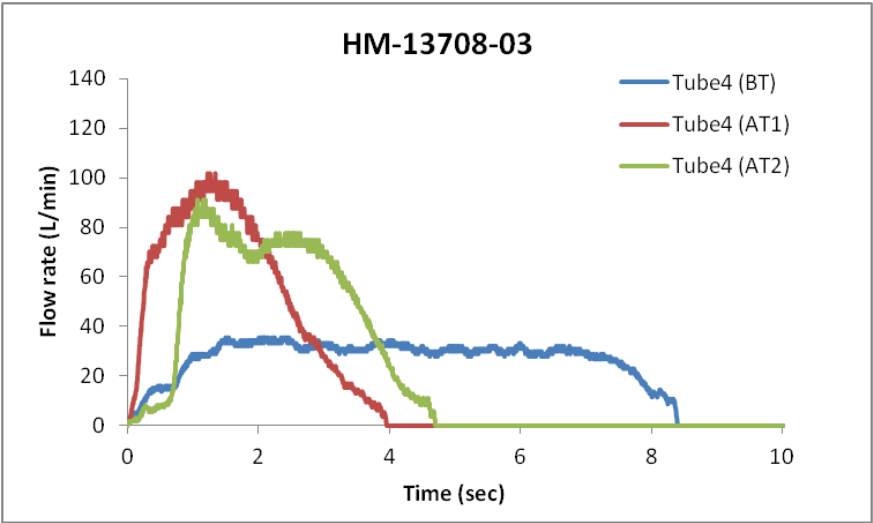
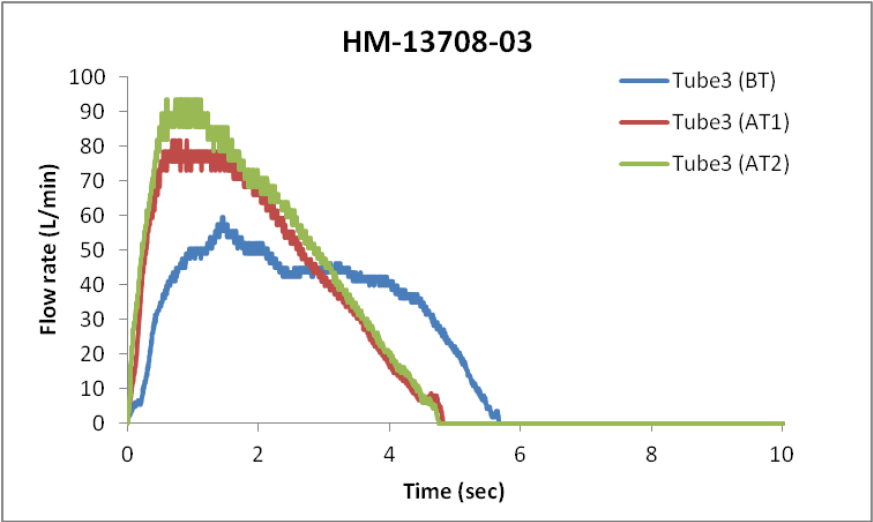
Training	Tube	Order	PIFR (L/min)	V (L)	tmax (sec)	ttotal (sec)
Before training	Tube1	3	24.3	0.935	1.015	3.185
After training 1	Tube1	5	55.1	1.661	0.275	2.645
After training 2	Tube1	3	57.1	1.810	0.585	2.725
Before training	Tube2	6	26.2	0.948	0.865	2.870
After training 1	Tube2	1	58.5	1.670	0.720	2.685
After training 2	Tube2	4	60.8	1.629	0.620	2.355
Before training	Tube3	2	23.2	1.002	0.635	3.170
After training 1	Tube3	2	70.3	1.743	0.455	2.425
After training 2	Tube3	2	72.8	1.761	0.450	2.190
Before training	Tube4	5	35.7	1.037	0.615	2.250
After training 1	Tube4	3	87.2	1.590	0.525	1.860
After training 2	Tube4	5	97.8	1.830	0.480	1.725
Before training	Tube5	1	33.3	1.311	0.930	2.930
After training 1	Tube5	4	110.2	1.758	0.350	1.415
After training 2	Tube5	6	102.9	1.853	0.410	1.670
Before training	Tube6	4	43.8	1.320	0.715	2.565
After training 1	Tube6	6	124.6	1.780	0.405	1.320
After training 2	Tube6	1	105.4	1.852	0.425	1.510

HM-13708-03

Description: Gender: Male, Ethnicity: Caucasian, Height: 169 cm, Weight: 67 kg, Age: 19 yrs

Figure E3: Inhalation profiles of Volunteer HM-13708-03





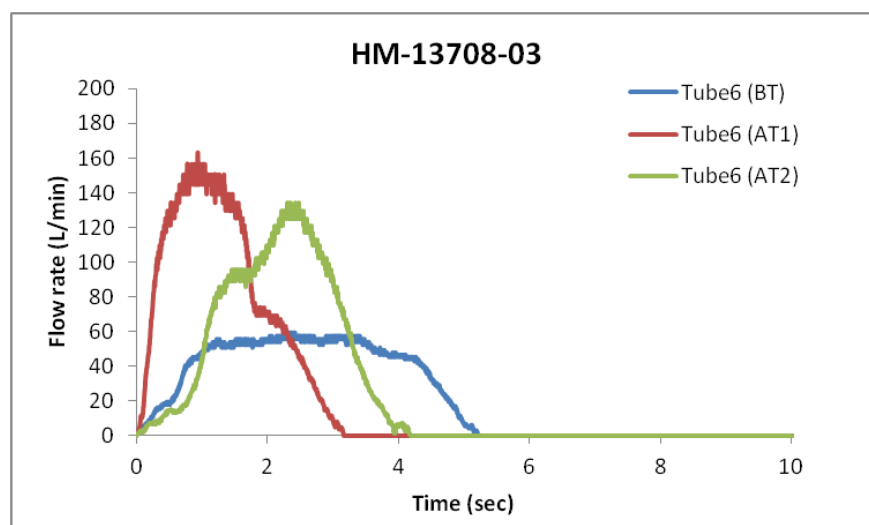


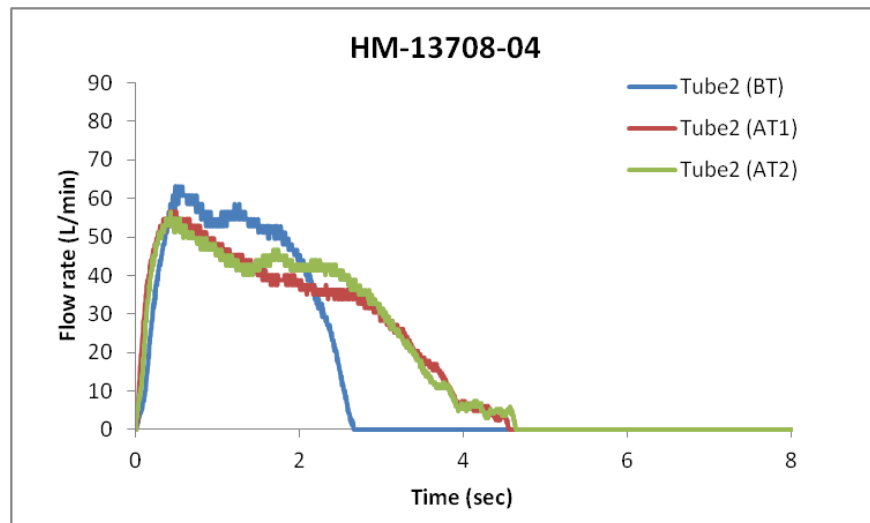
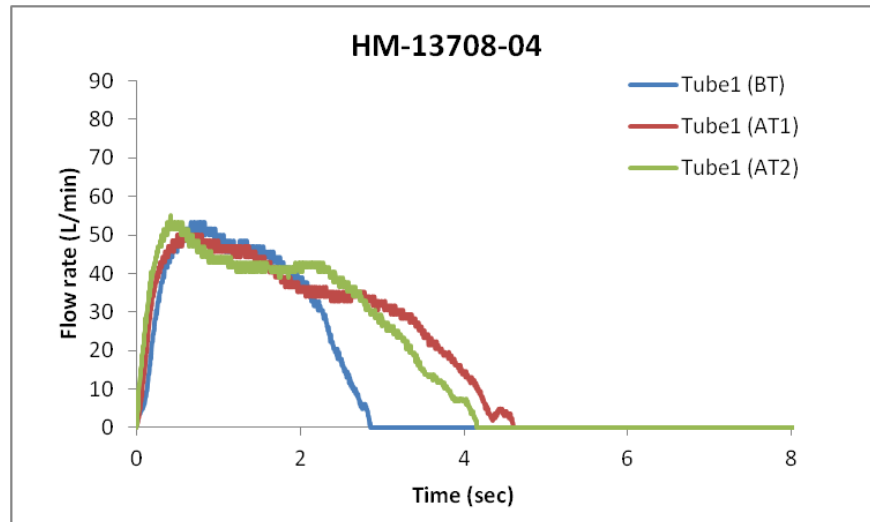
Table E3: Summary of inhalation parameters of volunteer: HM-13708-03

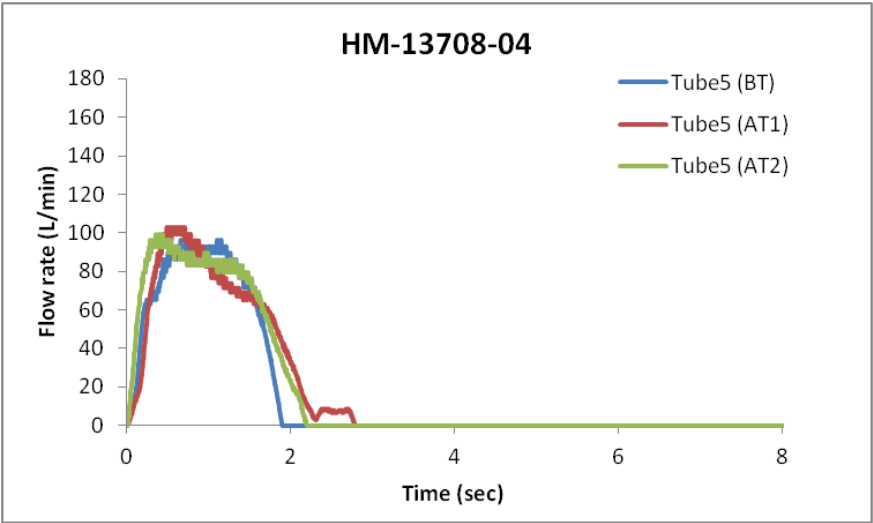
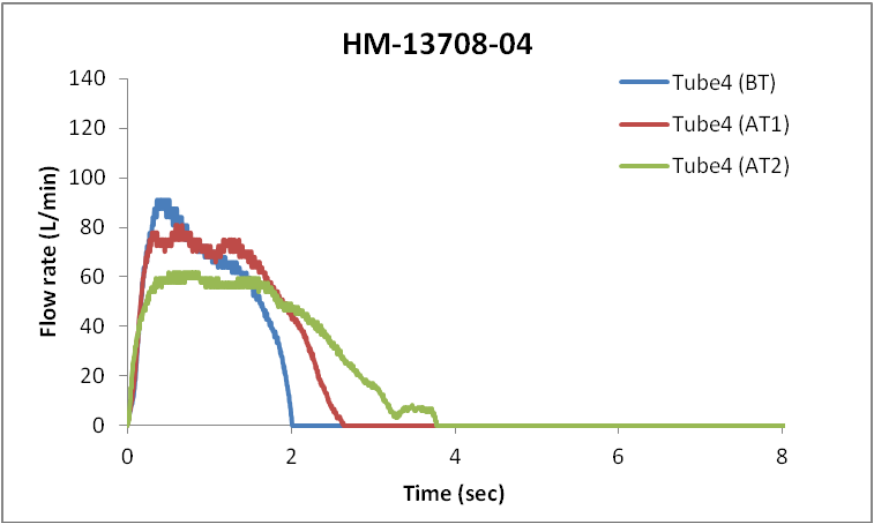
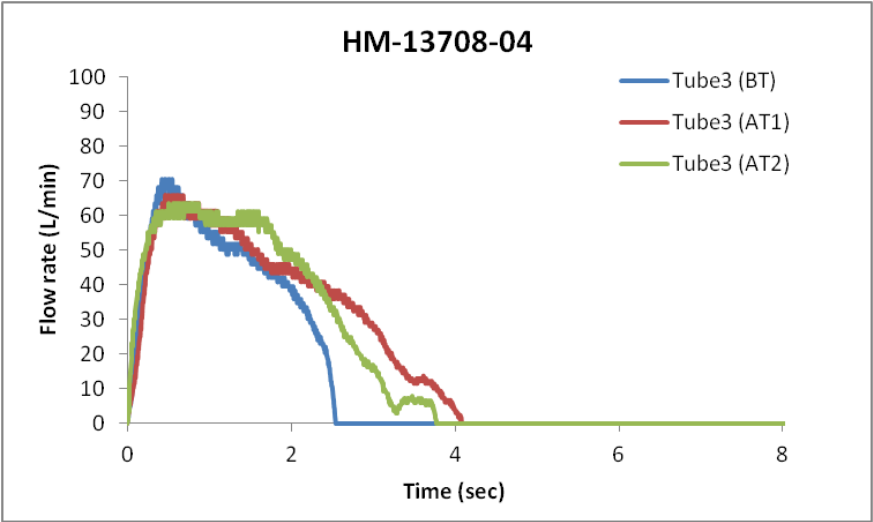
Training	Tube	Order	PIFR (L/min)	V (L)	tmax (sec)	ttotal (sec)
Before training	Tube1	6	26.3	3.117	1.230	9.555
After training 1	Tube1	2	66.7	4.258	0.770	6.045
After training 2	Tube1	3	71.9	4.014	1.100	6.440
Before training	Tube2	4	32.8	3.579	2.560	8.565
After training 1	Tube2	4	79.2	4.282	0.920	5.750
After training 2	Tube2	1	82.4	4.096	0.660	5.445
Before training	Tube3	1	59.5	3.475	1.450	5.670
After training 1	Tube3	1	81.9	3.768	0.690	4.820
After training 2	Tube3	2	93.5	4.171	0.600	4.750
Before training	Tube4	3	35.7	3.858	1.500	8.395
After training 1	Tube4	5	101.9	3.645	1.230	3.960
After training 2	Tube4	4	91.2	3.841	1.075	4.705
Before training	Tube5	2	57.5	4.107	2.660	5.560
After training 1	Tube5	6	153.8	3.733	0.680	3.505
After training 2	Tube5	6	141.9	3.913	1.330	4.195
Before training	Tube6	5	59.2	3.593	2.265	5.215
After training 1	Tube6	3	162.8	4.468	0.940	3.165
After training 2	Tube6	5	134.1	4.260	2.310	4.180

HM-13708-04

Description: Gender:Female, Ethnicity: Asian, Height: 147 cm, Weight: 50 kg, Age: 23 yrs

Figure E4: Inhalation profiles of Volunteer HM-13708-04





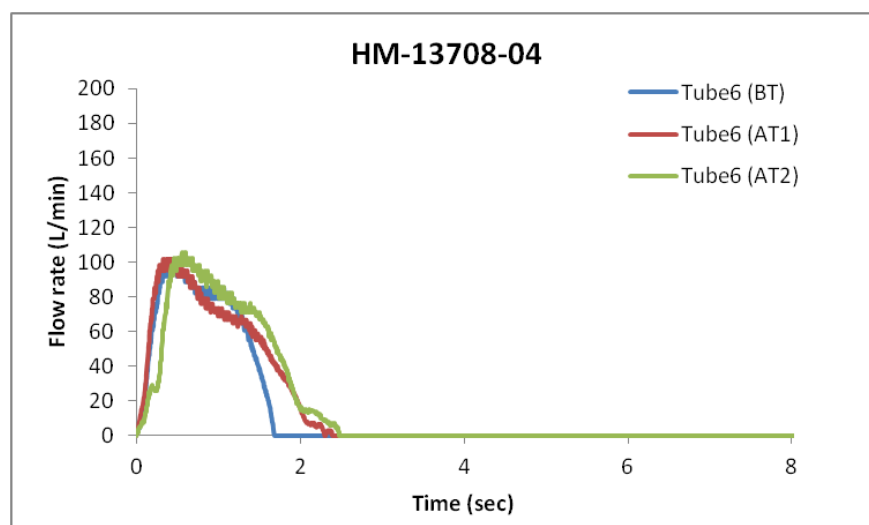


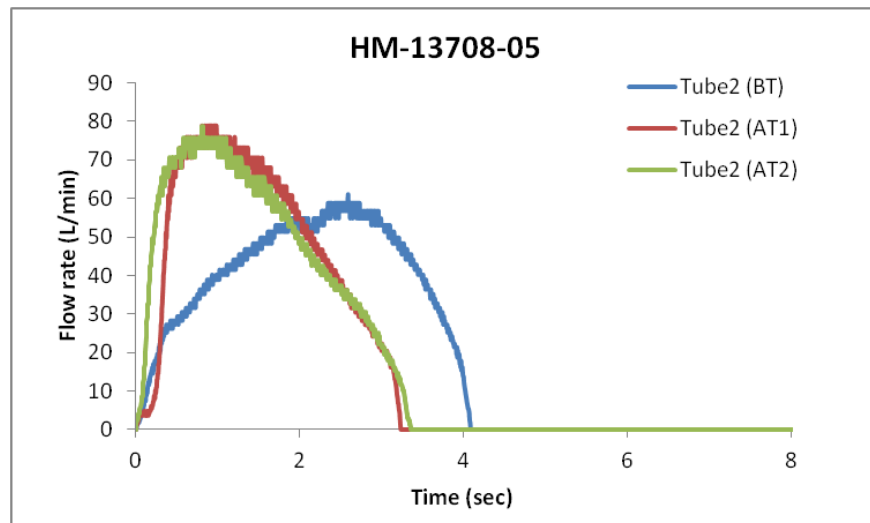
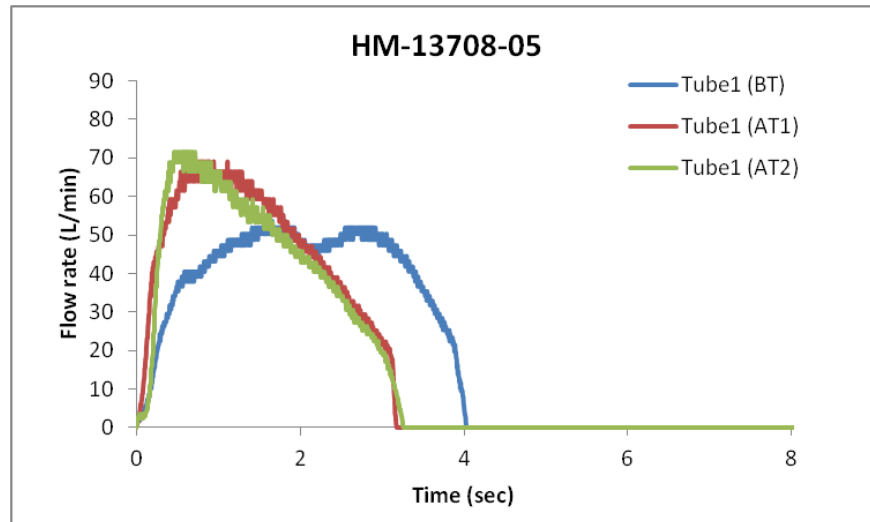
Table E4: Summary of inhalation parameters of volunteer: HM-13708-04

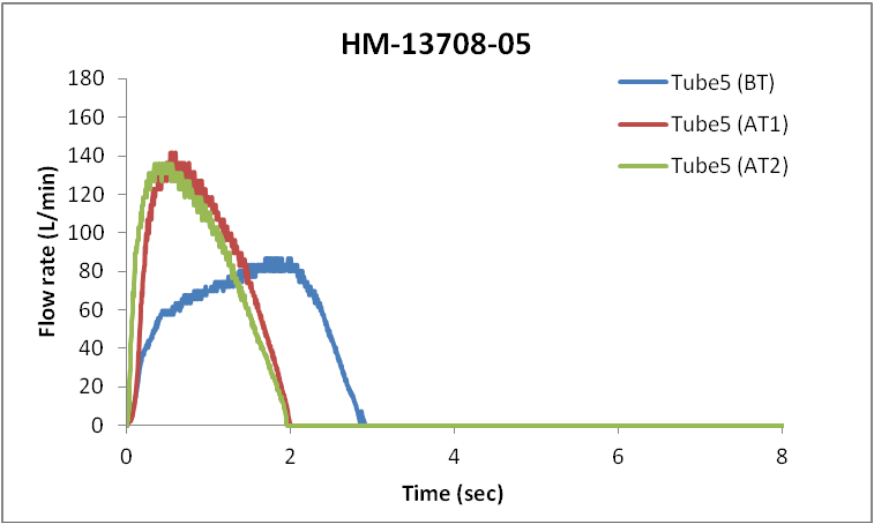
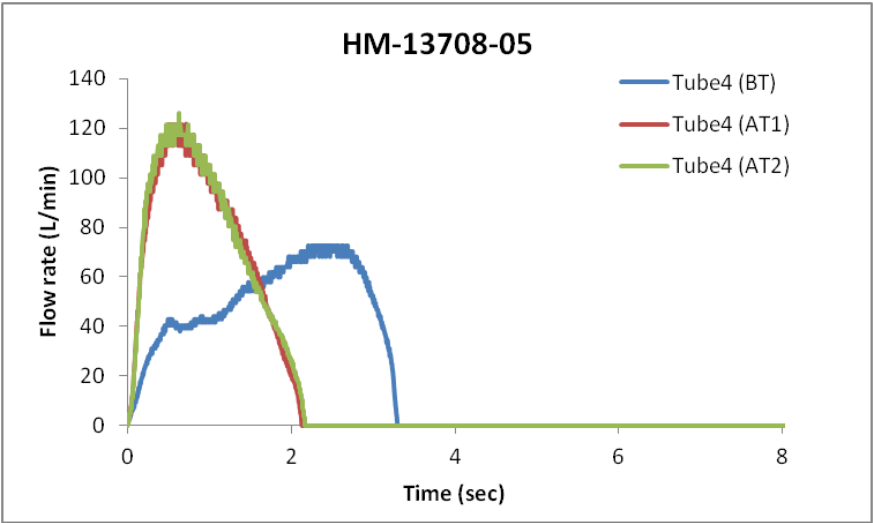
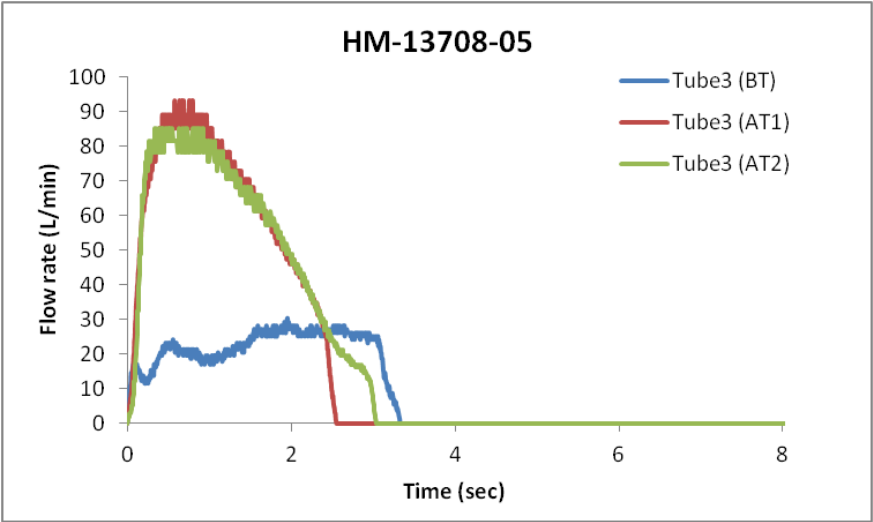
Training	Tube	Order	PIFR (L/min)	V (L)	tmax (sec)	ttotal (sec)
Before training	Tube1	2	53.4	1.696	0.670	2.860
After training 1	Tube1	4	50.1	2.428	0.505	4.605
After training 2	Tube1	4	55.2	2.321	0.415	4.160
Before training	Tube2	6	63.2	1.916	0.480	2.660
After training 1	Tube2	6	56.6	2.399	0.415	4.555
After training 2	Tube2	3	56.6	2.457	0.425	4.640
Before training	Tube3	3	70.6	1.920	0.425	2.545
After training 1	Tube3	5	65.9	2.564	0.465	4.085
After training 2	Tube3	6	63.6	2.484	0.505	3.775
Before training	Tube4	4	91.0	1.989	0.365	2.015
After training 1	Tube4	1	80.7	2.370	0.595	2.640
After training 2	Tube4	2	61.6	2.432	0.510	3.780
Before training	Tube5	1	96.4	2.175	0.655	1.895
After training 1	Tube5	3	103.2	2.438	0.485	2.780
After training 2	Tube5	5	99.6	2.467	0.365	2.200
Before training	Tube6	5	102.1	1.881	0.390	1.690
After training 1	Tube6	2	102.0	2.174	0.330	2.300
After training 2	Tube6	1	105.6	2.251	0.555	2.480

HM-13708-05

Description: Gender:Female, Ethnicity: Caucasian, Height: 158 cm, Weight: 60 kg, Age: 48 yrs

Figure E5: Inhalation profiles of Volunteer HM-13708-05





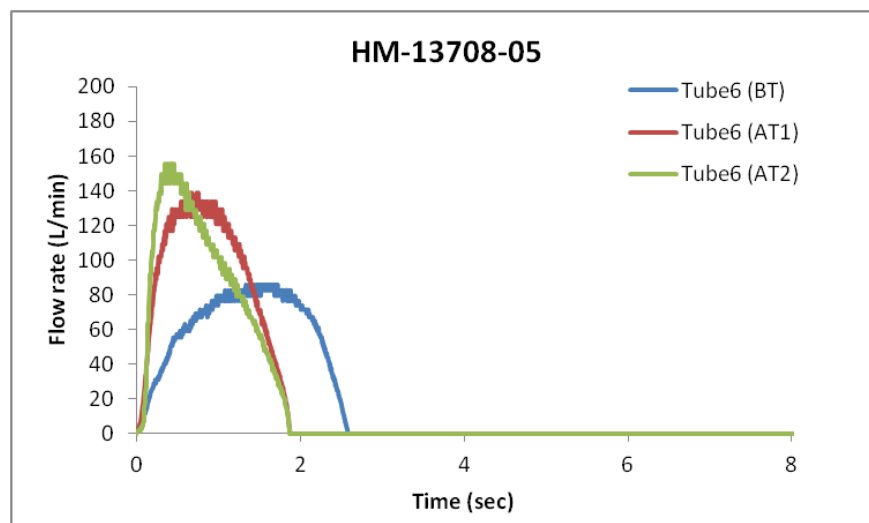


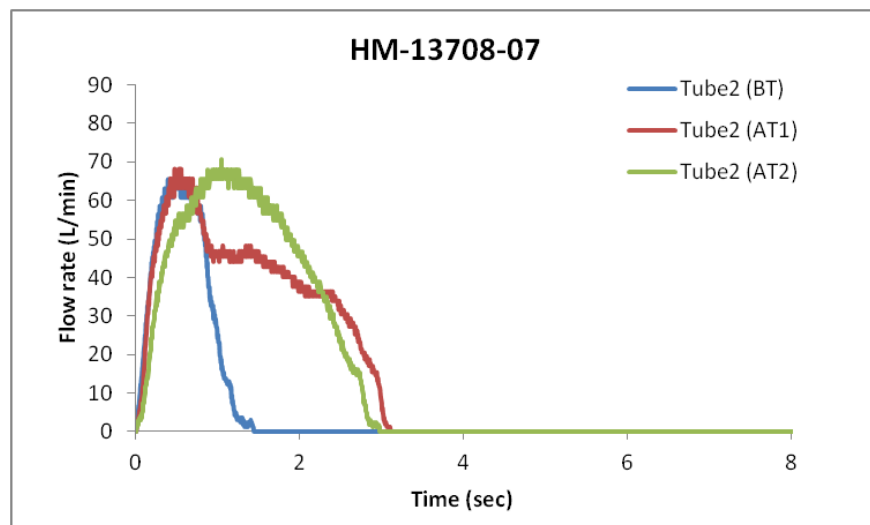
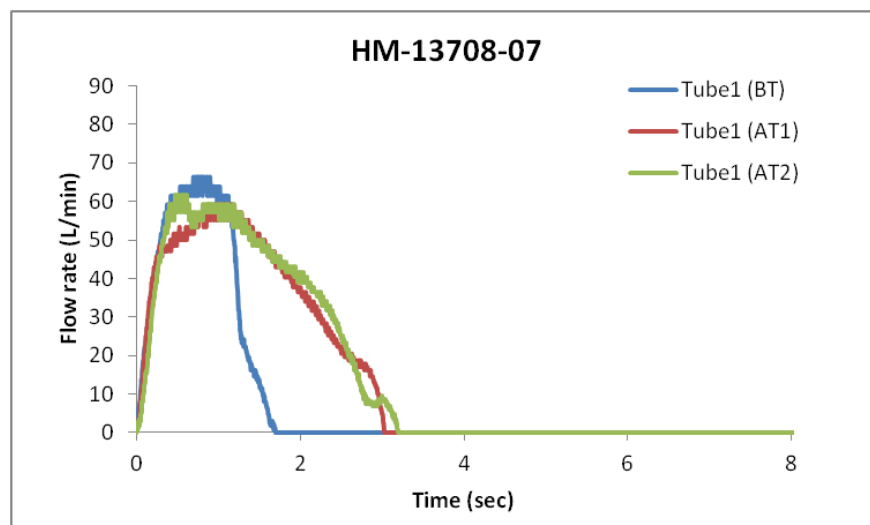
Table E5: Summary of inhalation parameters of volunteer: HM-13708-05

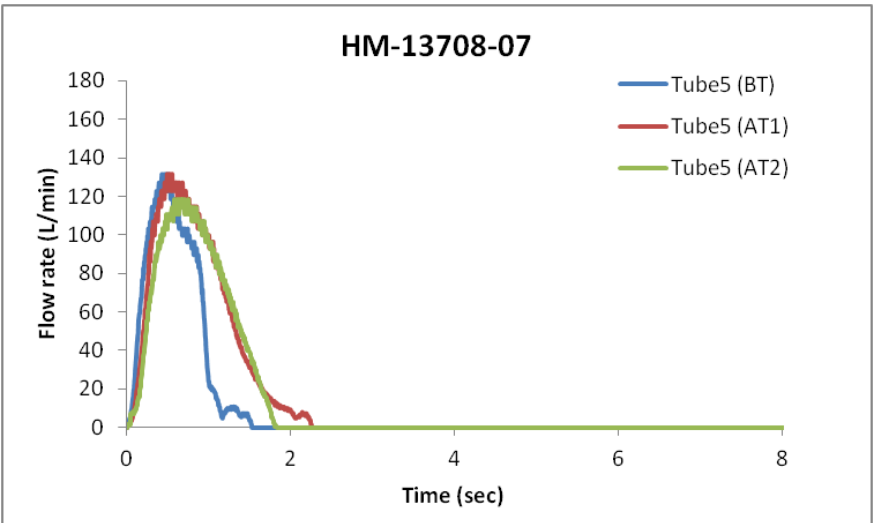
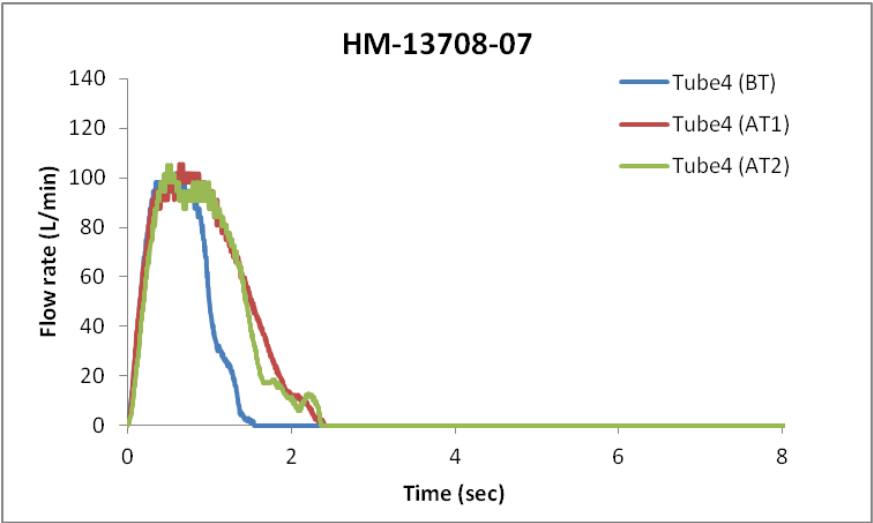
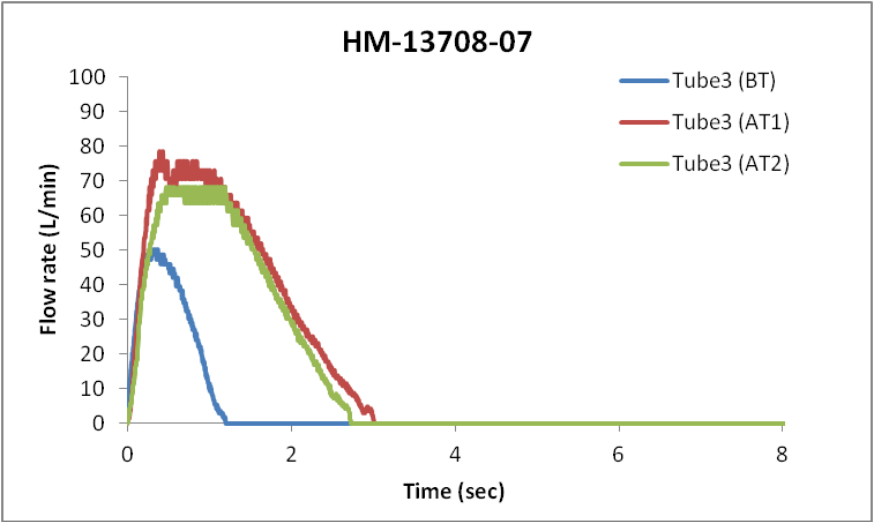
Training	Tube	Order	PIFR (L/min)	V (L)	tmax (sec)	ttotal (sec)
Before training	Tube1	6	53.5	2.701	1.570	4.030
After training 1	Tube1	2	69.0	2.489	0.705	3.180
After training 2	Tube1	5	71.7	2.378	0.460	3.260
Before training	Tube2	4	61.0	2.790	2.590	4.090
After training 1	Tube2	5	78.9	2.644	0.805	3.235
After training 2	Tube2	1	78.9	2.728	0.810	3.360
Before training	Tube3	1	30.3	1.203	1.955	3.330
After training 1	Tube3	4	93.2	2.606	0.580	2.555
After training 2	Tube3	3	85.2	2.701	0.335	3.035
Before training	Tube4	3	72.7	2.743	2.210	3.300
After training 1	Tube4	6	121.7	2.655	0.500	2.135
After training 2	Tube4	4	126.1	2.691	0.630	2.170
Before training	Tube5	5	86.5	2.868	1.690	2.905
After training 1	Tube5	3	141.5	2.873	0.530	1.995
After training 2	Tube5	2	136.1	2.837	0.340	1.960
Before training	Tube6	2	85.9	2.600	1.340	2.585
After training 1	Tube6	1	138.7	2.852	0.630	1.880
After training 2	Tube6	6	155.8	2.741	0.350	1.870

HM-13708-07

Description: Gender:Female, Ethnicity: African, Height: 163 cm, Weight: 63 kg, Age: 30 yrs

Figure E6: Inhalation profiles of Volunteer HM-13708-07





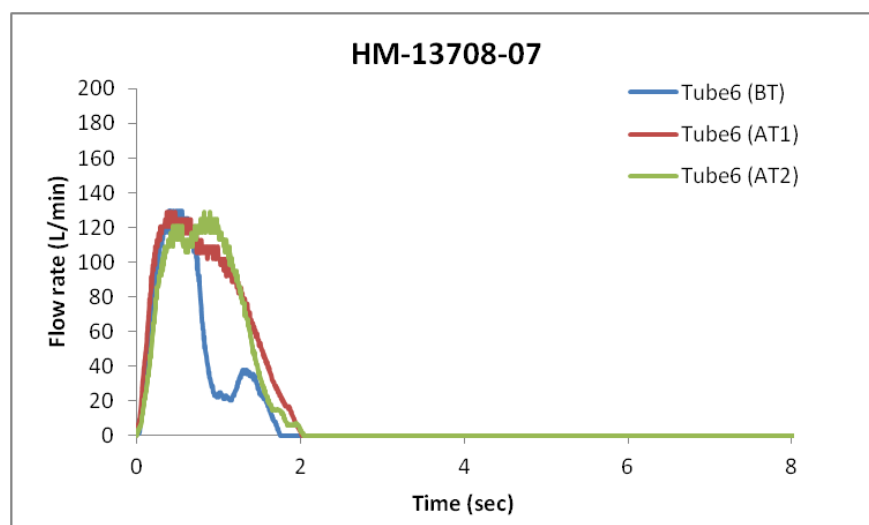


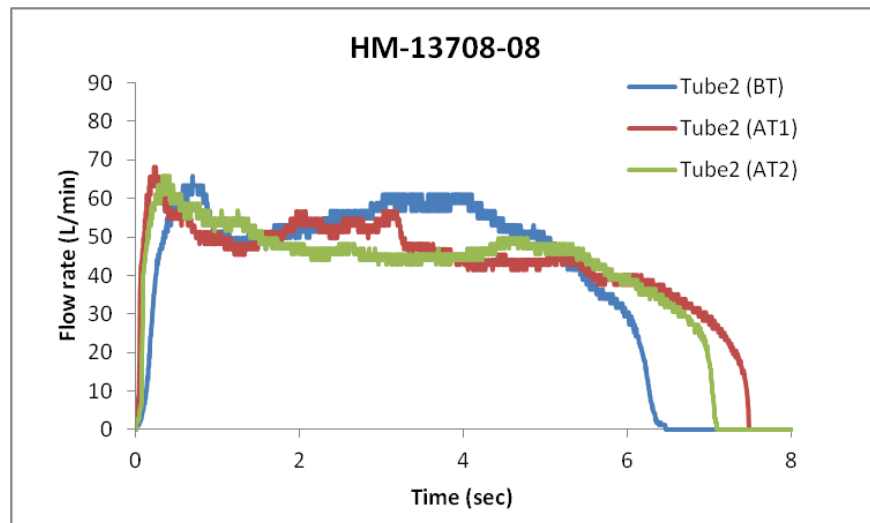
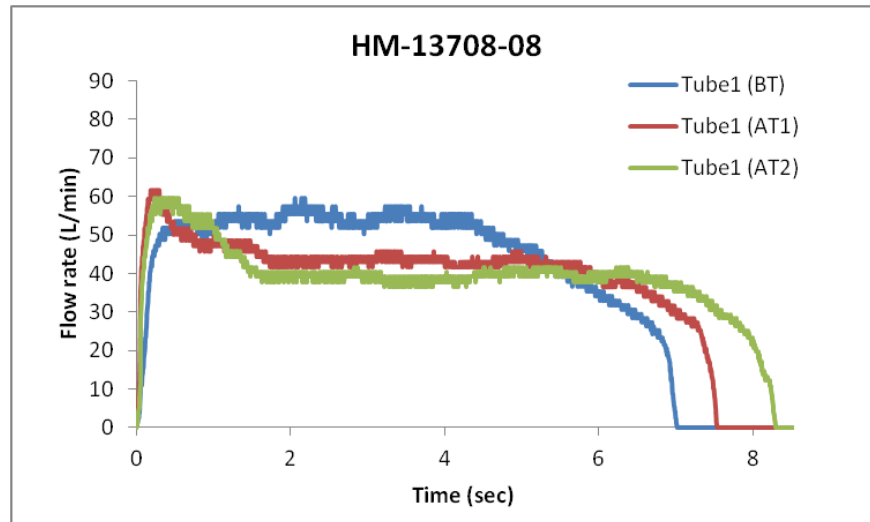
Table E6: Summary of inhalation parameters of volunteer: HM-13708-07

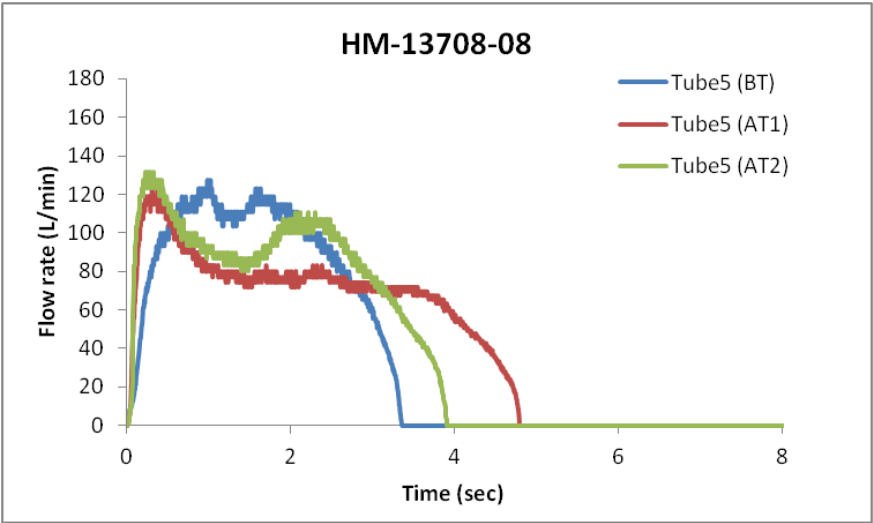
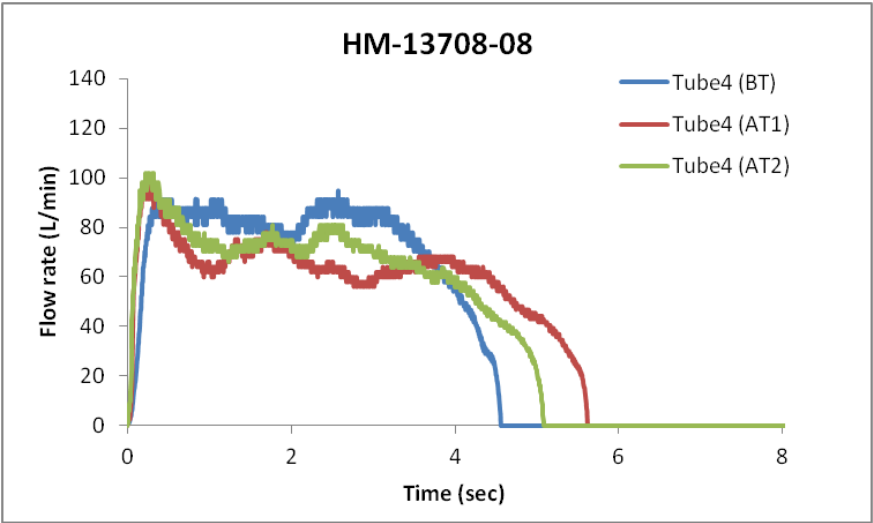
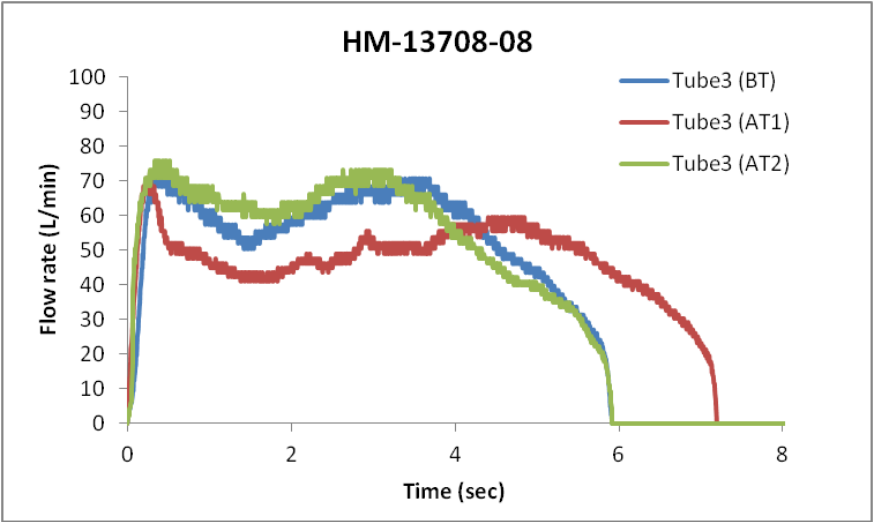
Training	Tube	Order	PIFR (L/min)	V (L)	tmax (sec)	ttotal (sec)
Before training	Tube1	5	66.5	1.193	0.700	1.700
After training 1	Tube1	6	59.3	1.960	0.880	3.030
After training 2	Tube1	1	61.6	2.019	0.480	3.195
Before training	Tube2	2	65.7	0.861	0.390	1.440
After training 1	Tube2	1	68.1	2.036	0.470	3.110
After training 2	Tube2	5	70.6	2.142	1.050	2.980
Before training	Tube3	3	50.4	0.604	0.285	1.205
After training 1	Tube3	4	78.4	2.206	0.395	3.015
After training 2	Tube3	3	68.2	1.931	0.470	2.730
Before training	Tube4	4	101.7	1.466	0.520	1.550
After training 1	Tube4	5	105.3	2.249	0.640	2.405
After training 2	Tube4	4	105.3	2.102	0.490	2.370
Before training	Tube5	6	131.6	1.544	0.425	1.525
After training 1	Tube5	2	131.4	2.209	0.490	2.260
After training 2	Tube5	6	118.5	2.029	0.580	1.835
Before training	Tube6	1	129.3	1.653	0.400	1.760
After training 1	Tube6	3	129.2	2.586	0.375	2.020
After training 2	Tube6	2	129.2	2.364	0.820	2.045

HM-13708-08

Description: Gender: Male, Ethnicity: Caucasian, Height: 186 cm, Weight: 98 kg, Age: 52 yrs

Figure E7: Inhalation profiles of Volunteer HM-13708-08





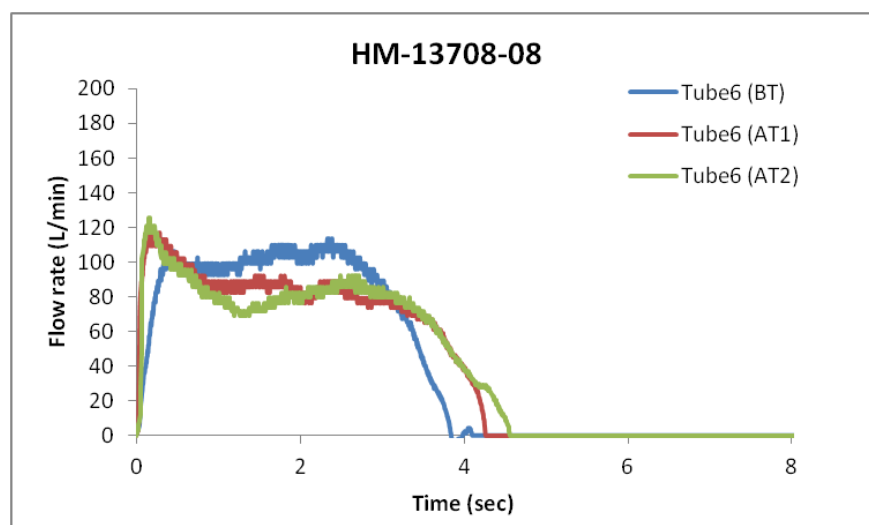


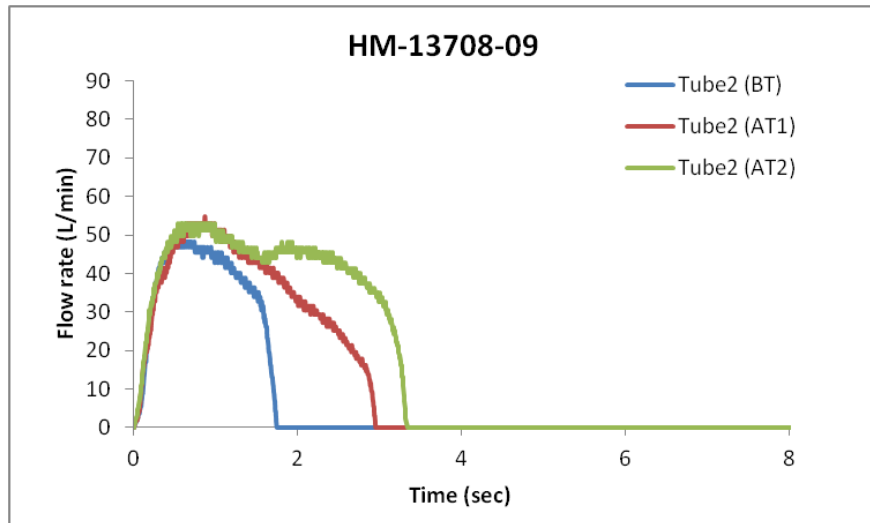
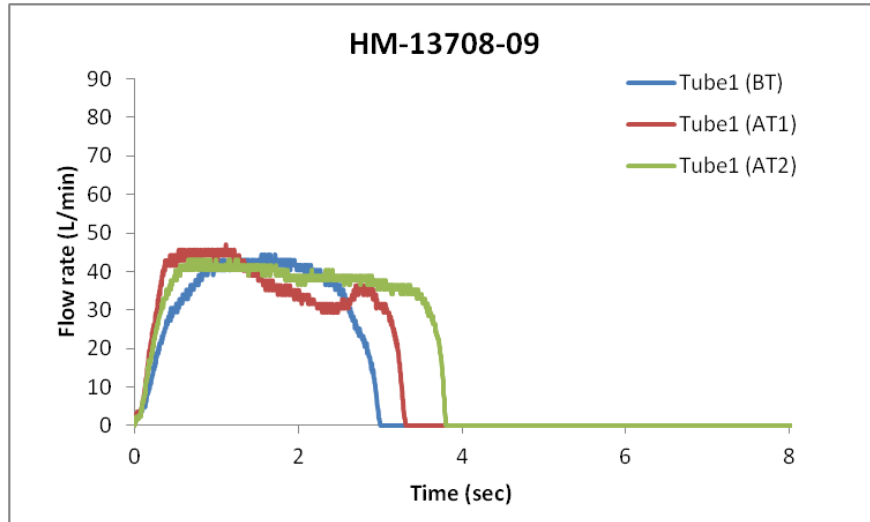
Table E7: Summary of inhalation parameters of volunteer: HM-13708-08

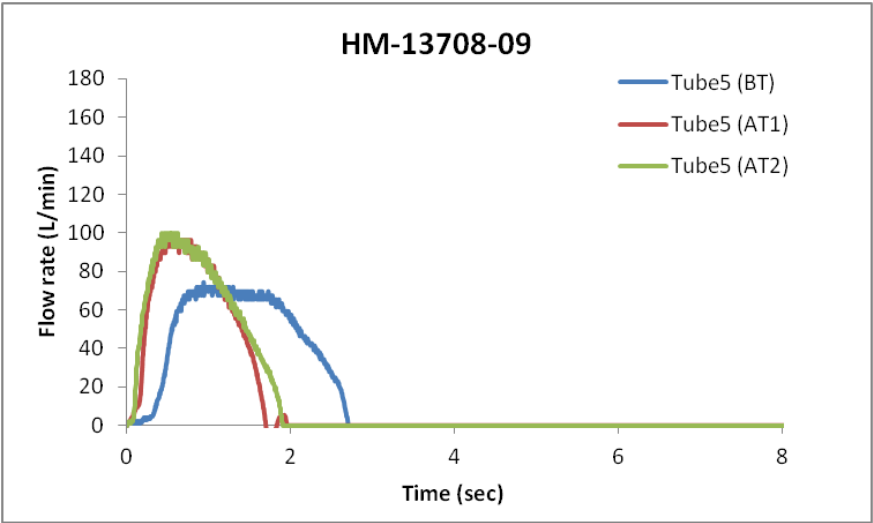
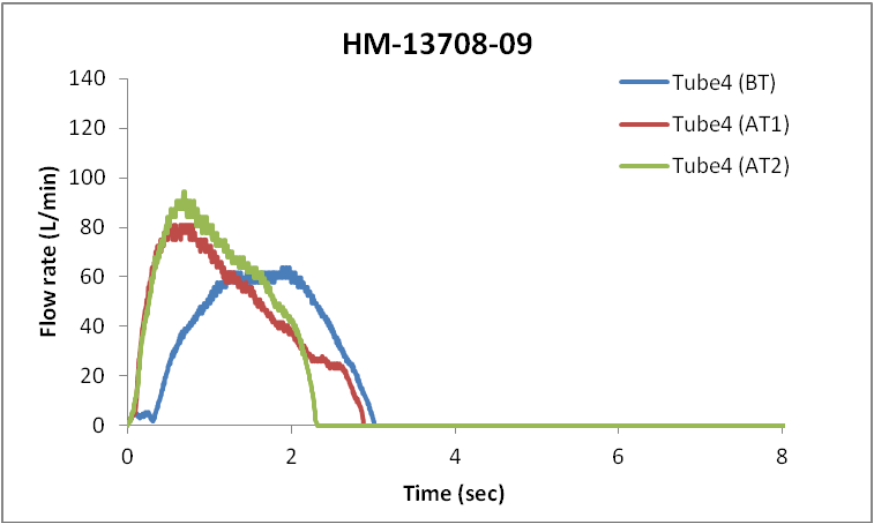
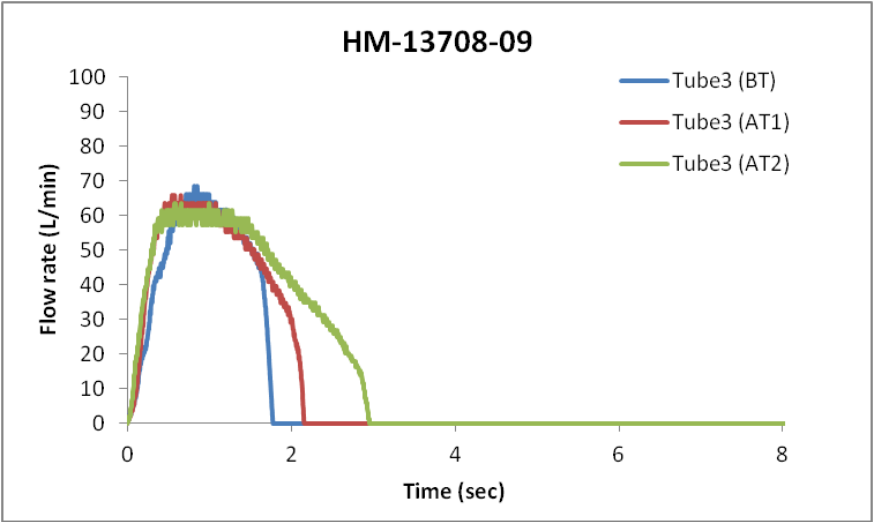
Training	Tube	Order	PIFR (L/min)	V (L)	tmax (sec)	ttotal (sec)
Before training	Tube1	4	59.5	5.455	2.060	7.015
After training 1	Tube1	4	61.8	5.264	0.190	7.535
After training 2	Tube1	6	59.5	5.429	0.240	8.290
Before training	Tube2	3	65.8	5.167	0.690	6.470
After training 1	Tube2	5	68.3	5.571	0.220	7.490
After training 2	Tube2	4	65.8	5.300	0.330	7.100
Before training	Tube3	6	73.2	5.393	0.365	5.920
After training 1	Tube3	1	70.8	5.649	0.240	7.195
After training 2	Tube3	3	75.8	5.522	0.335	5.920
Before training	Tube4	5	94.8	5.564	2.575	4.560
After training 1	Tube4	3	98.4	5.743	0.230	5.620
After training 2	Tube4	5	101.9	5.596	0.220	5.085
Before training	Tube5	2	127.6	5.020	0.980	3.360
After training 1	Tube5	2	123.2	5.743	0.305	4.795
After training 2	Tube5	2	131.9	5.557	0.225	3.910
Before training	Tube6	1	113.5	5.493	2.335	3.865
After training 1	Tube6	6	117.2	5.600	0.165	4.265
After training 2	Tube6	1	125.3	5.522	0.150	4.560

HM-13708-09

Description: Gender:Female, Ethnicity: Hispanic, Height: 158 cm, Weight: 57 kg, Age: 34 yrs

Figure E8: Inhalation profiles of Volunteer HM-13708-09





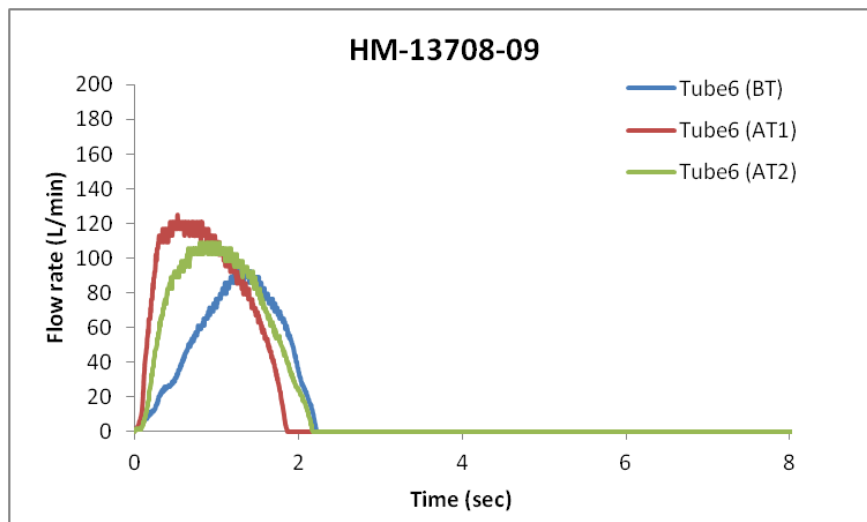


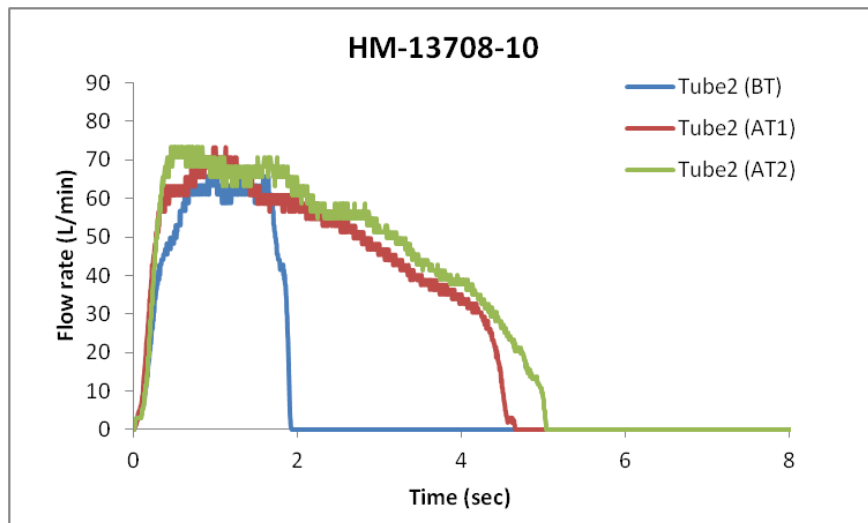
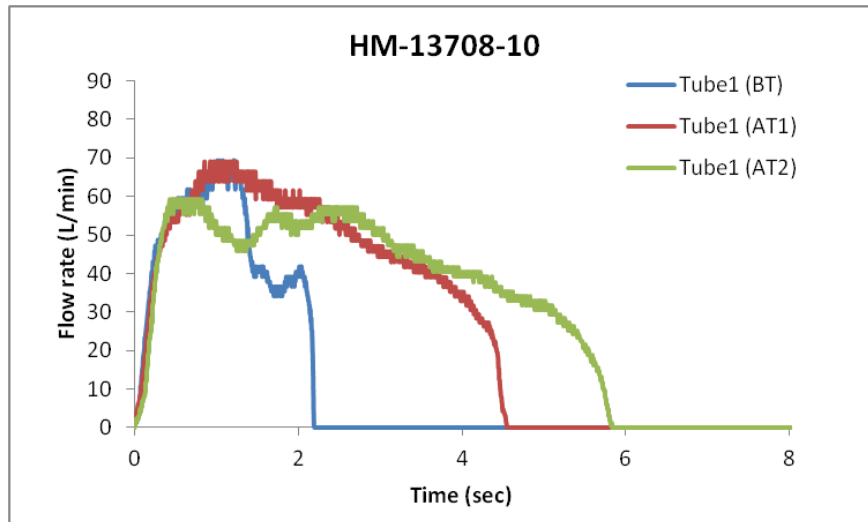
Table E8: Summary of inhalation parameters of volunteer: HM-13708-09

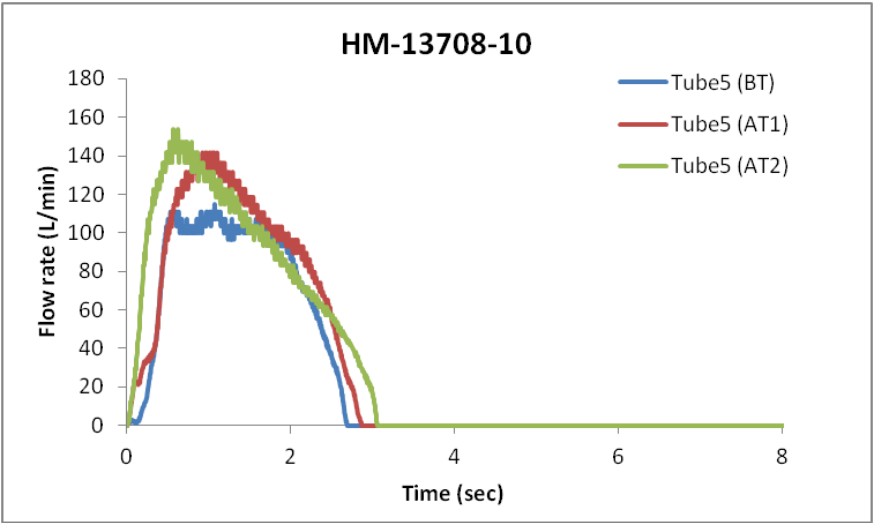
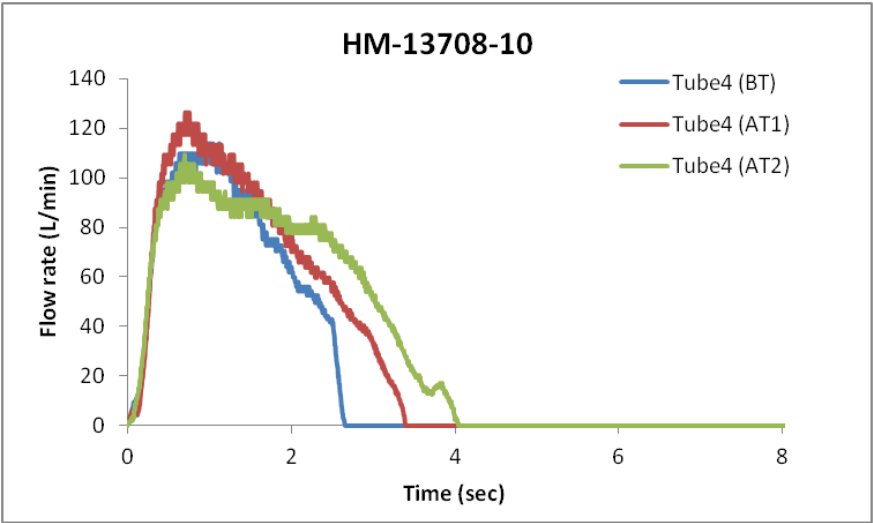
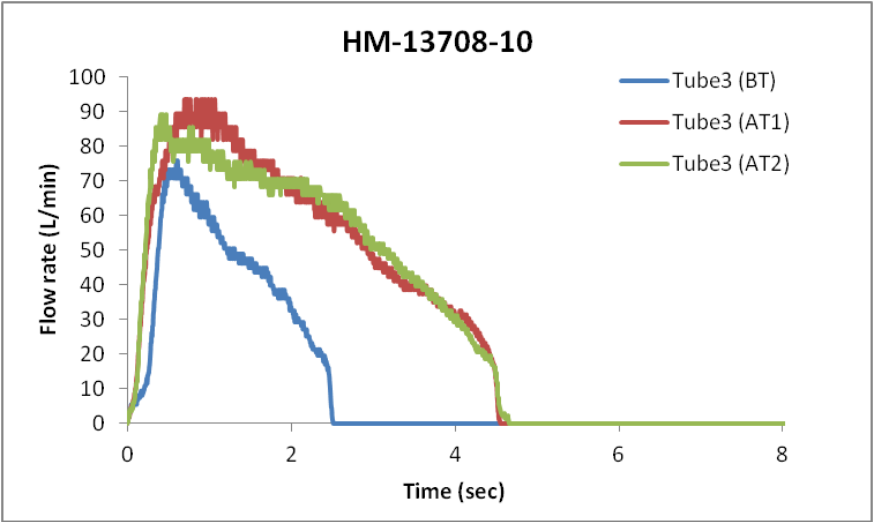
Training	Tube	Order	PIFR (L/min)	V (L)	tmax (sec)	ttotal (sec)
Before training	Tube1	2	44.4	1.652	1.555	3.005
After training 1	Tube1	4	47.1	1.897	1.120	3.315
After training 2	Tube1	1	43.0	2.249	0.665	3.805
Before training	Tube2	6	49.7	1.057	0.500	1.745
After training 1	Tube2	2	54.7	1.748	0.865	2.950
After training 2	Tube2	4	52.9	2.288	0.545	3.340
Before training	Tube3	5	68.3	1.391	0.820	1.780
After training 1	Tube3	1	65.9	1.683	0.550	2.160
After training 2	Tube3	6	63.6	2.132	0.570	2.955
Before training	Tube4	1	63.9	1.978	1.890	3.015
After training 1	Tube4	5	80.8	2.245	0.500	2.885
After training 2	Tube4	2	94.5	2.247	0.680	2.315
Before training	Tube5	3	74.3	2.122	0.935	2.705
After training 1	Tube5	3	96.4	1.785	0.460	1.745
After training 2	Tube5	3	99.7	2.005	0.430	1.910
Before training	Tube6	4	92.3	1.929	1.220	2.225
After training 1	Tube6	6	125.0	2.575	0.530	1.870
After training 2	Tube6	5	109.2	2.500	0.800	2.175

HM-13708-10

Description: Gender: Male, Ethnicity: Caucasian, Height: 179 cm, Weight: 91 kg, Age: 31 yrs

Figure E9: Inhalation profiles of Volunteer HM-13708-10





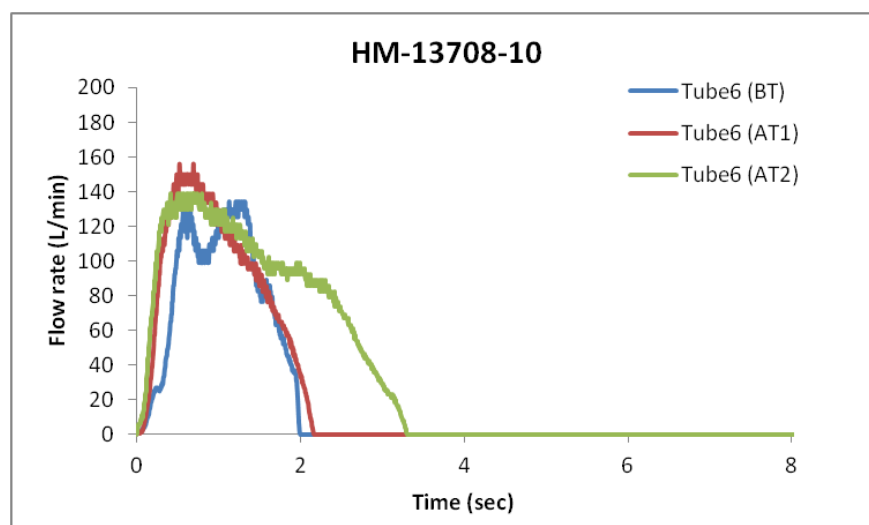


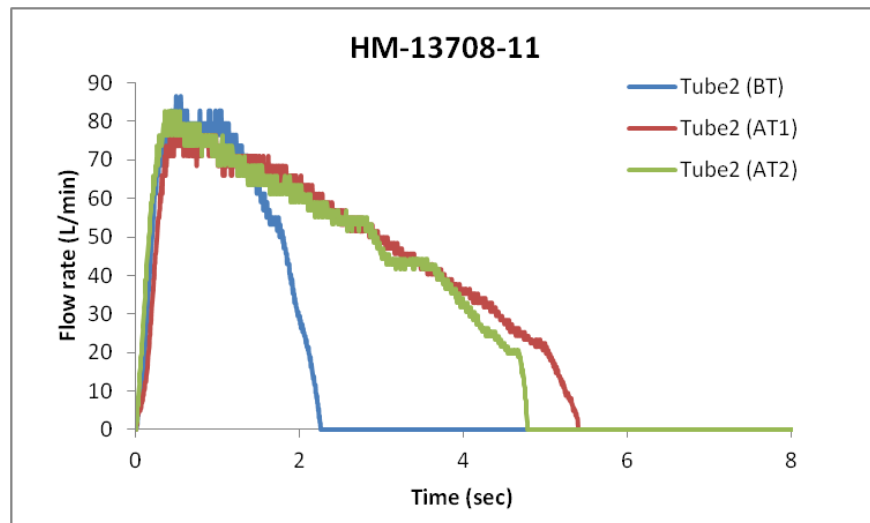
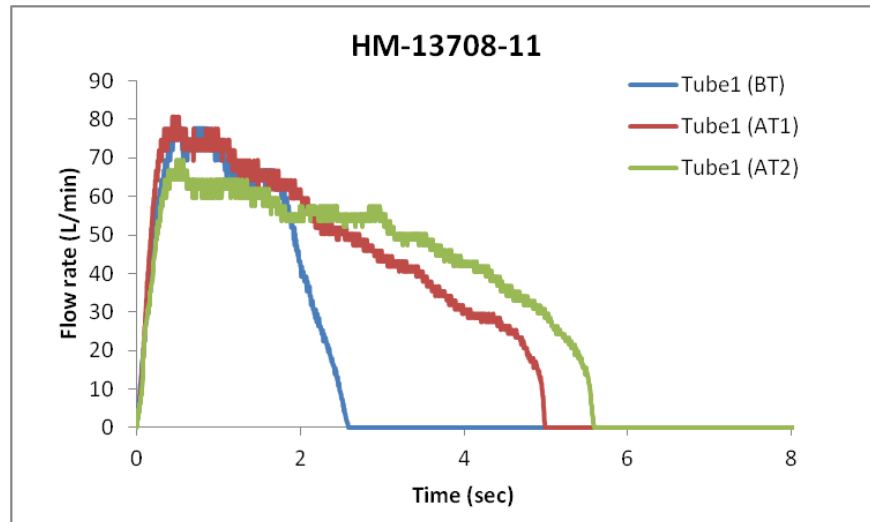
Table E9: Summary of inhalation parameters of volunteer: HM-13708-10

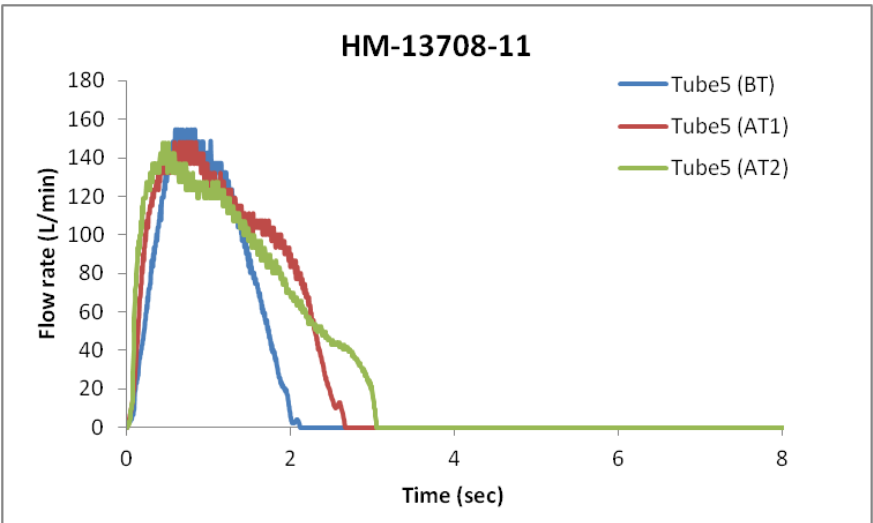
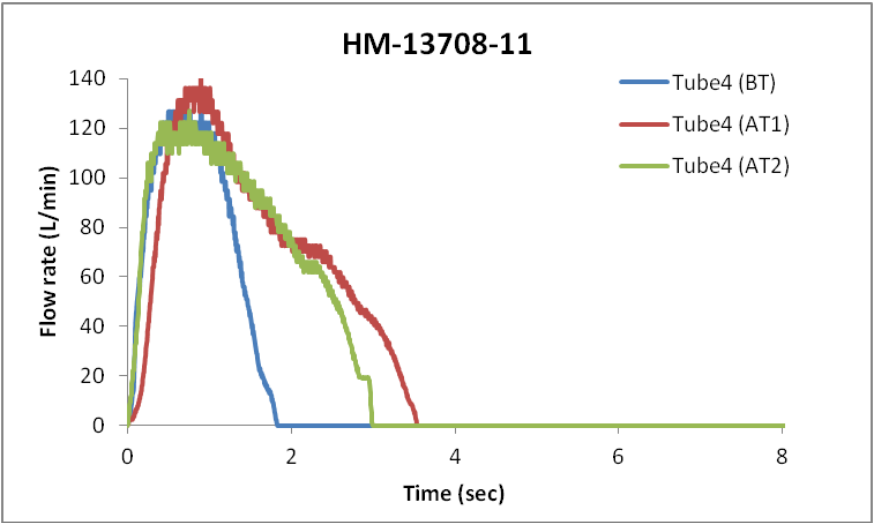
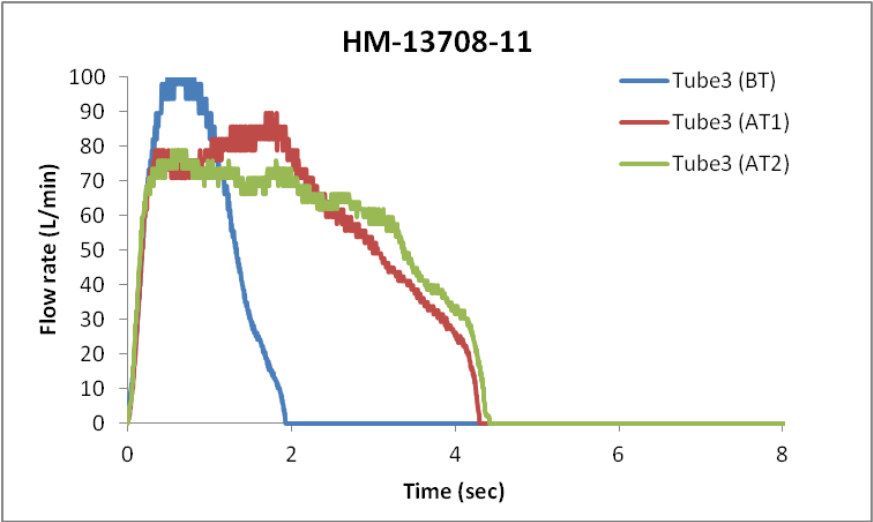
Training	Tube	Order	PIFR (L/min)	V (L)	tmax (sec)	ttotal (sec)
Before training	Tube1	3	69.3	1.720	1.015	2.200
After training 1	Tube1	4	69.2	3.626	0.860	4.550
After training 2	Tube1	6	59.4	4.134	0.430	5.835
Before training	Tube2	2	65.8	1.602	0.720	1.925
After training 1	Tube2	1	73.4	3.720	0.970	4.655
After training 2	Tube2	5	73.4	4.144	0.460	5.040
Before training	Tube3	5	75.8	1.739	0.600	2.515
After training 1	Tube3	5	93.4	4.261	0.700	4.555
After training 2	Tube3	1	89.3	4.248	0.400	4.655
Before training	Tube4	1	113.7	3.242	0.910	2.660
After training 1	Tube4	6	126.4	4.003	0.710	3.395
After training 2	Tube4	4	109.4	4.318	0.695	4.040
Before training	Tube5	6	114.8	3.416	1.070	2.690
After training 1	Tube5	2	141.7	4.155	0.920	2.865
After training 2	Tube5	3	153.6	4.505	0.570	3.060
Before training	Tube6	4	134.0	2.690	0.660	2.005
After training 1	Tube6	3	156.1	3.259	0.530	2.170
After training 2	Tube6	2	138.9	4.761	0.415	3.305

HM-13708-11

Description: Gender: Male, Ethnicity: Caucasian, Height: 177 cm, Weight: 90 kg, Age: 40 yrs

Figure E10: Inhalation profiles of Volunteer HM-13708-11





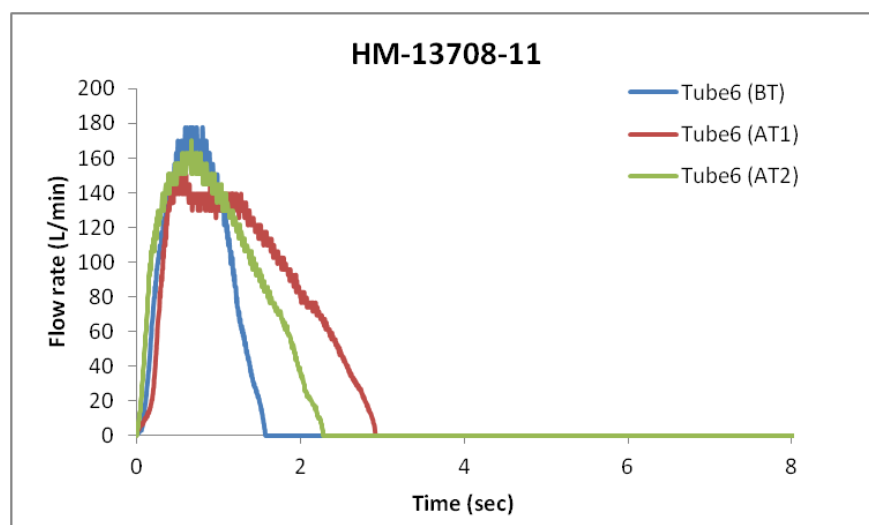


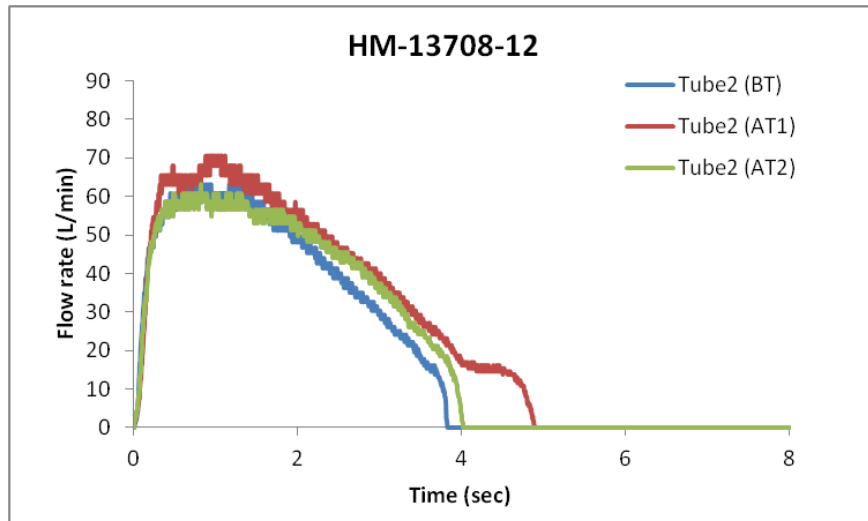
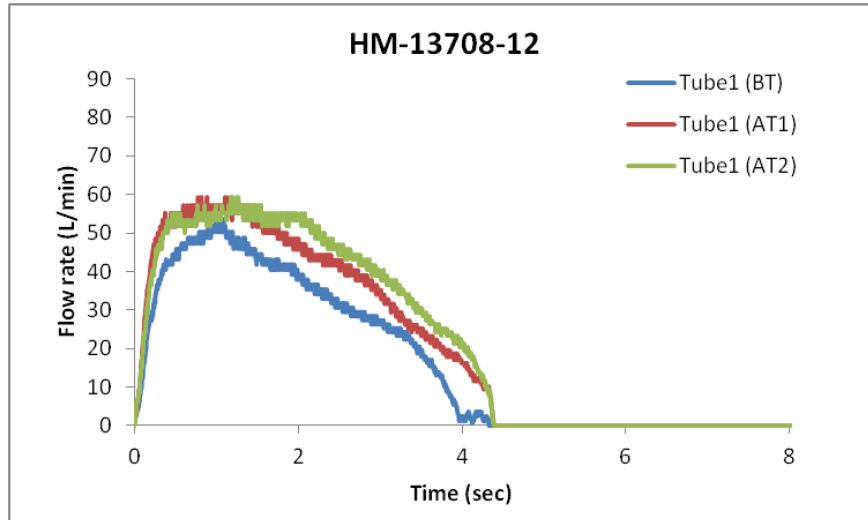
Table E10: Summary of inhalation parameters of volunteer: HM-13708-11

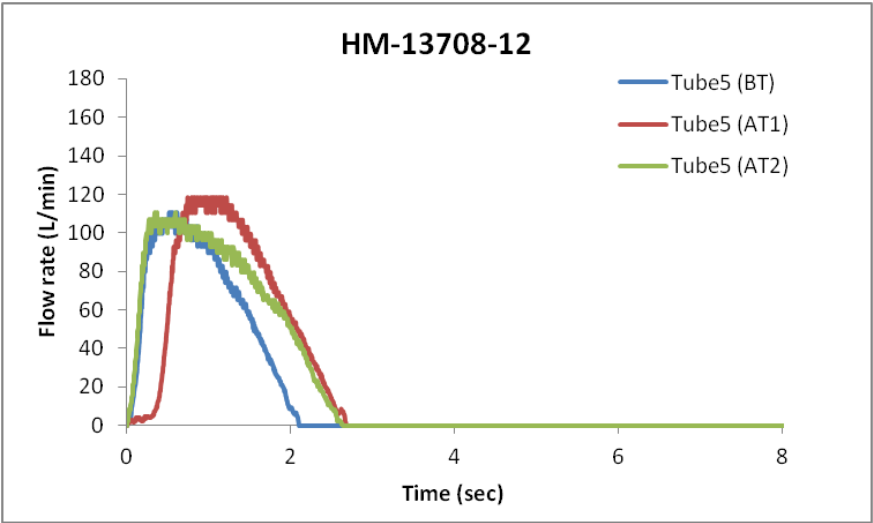
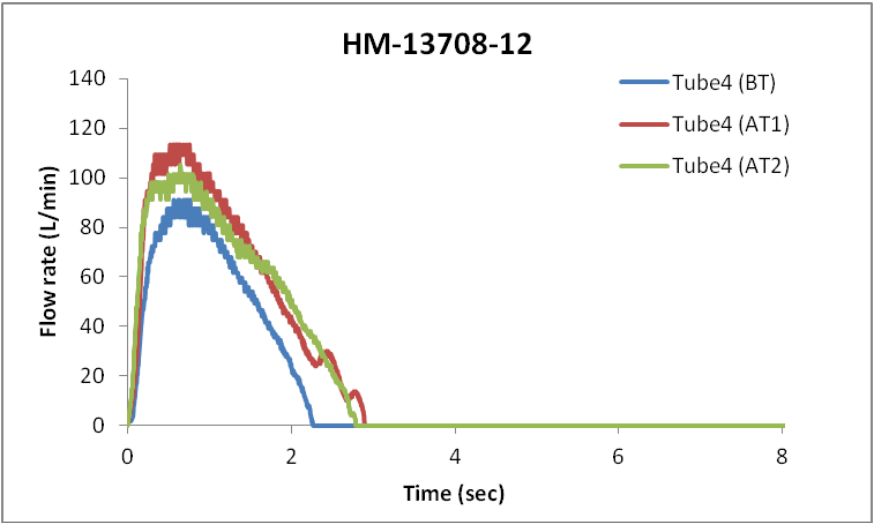
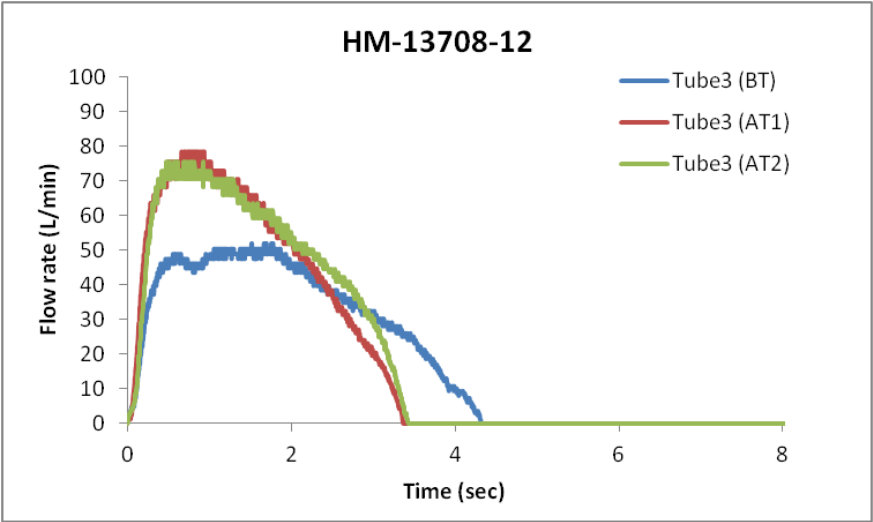
Training	Tube	Order	PIFR (L/min)	V (L)	tmax (sec)	ttotal (sec)
Before training	Tube1	2	77.8	2.298	0.440	2.590
After training 1	Tube1	3	80.8	4.057	0.445	4.990
After training 2	Tube1	1	69.5	4.414	0.490	5.585
Before training	Tube2	3	86.5	2.171	0.490	2.255
After training 1	Tube2	5	79.4	4.310	0.565	5.405
After training 2	Tube2	3	82.7	4.128	0.365	4.785
Before training	Tube3	6	106.9	1.927	0.615	1.935
After training 1	Tube3	1	89.6	4.204	1.695	4.300
After training 2	Tube3	2	78.9	4.264	0.550	4.425
Before training	Tube4	4	127.0	2.489	0.505	1.835
After training 1	Tube4	4	141.7	4.324	0.900	3.535
After training 2	Tube4	5	126.9	4.032	0.750	2.995
Before training	Tube5	1	154.5	3.134	0.590	2.115
After training 1	Tube5	2	148.2	4.216	0.580	2.665
After training 2	Tube5	6	147.9	4.369	0.450	3.055
Before training	Tube6	5	177.9	2.701	0.600	1.580
After training 1	Tube6	6	150.8	4.375	0.450	2.92
After training 2	Tube6	4	170.1	3.764	0.670	2.285

HM-13708-12

Description: Gender: Male, Ethnicity: Asian, Height: 172 cm, Weight: 64 kg, Age: 30 yrs

Figure E11: Inhalation profiles of Volunteer HM-13708-12





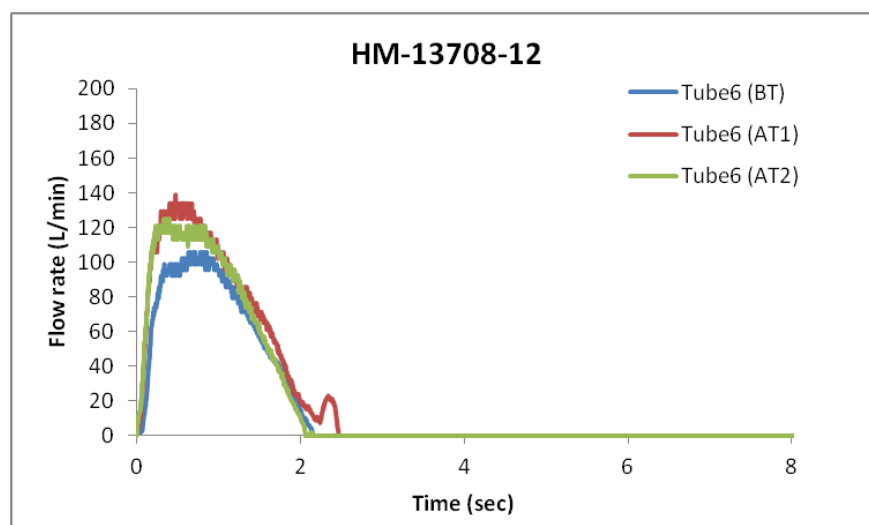


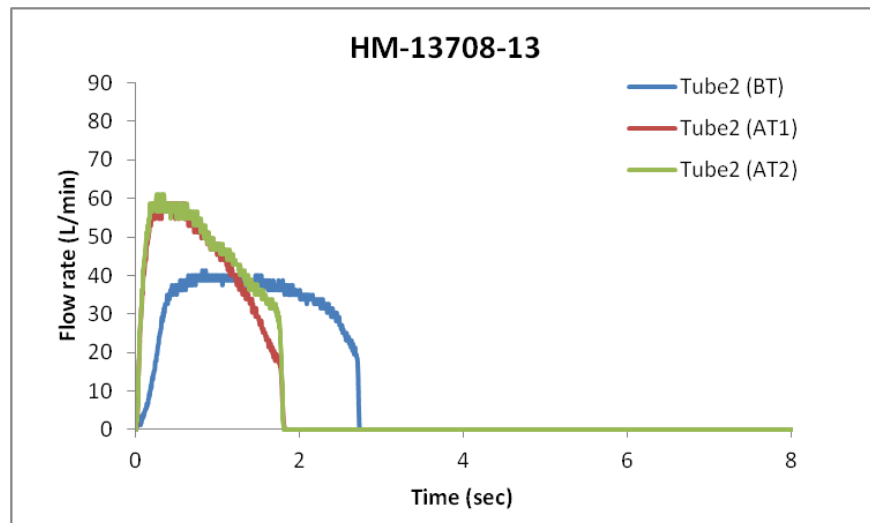
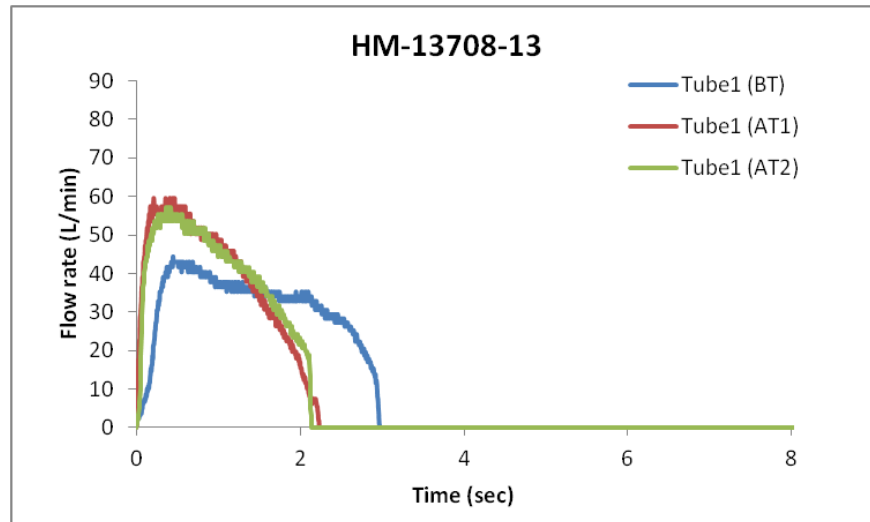
Table E11: Summary of inhalation parameters of volunteer: HM-13708-12

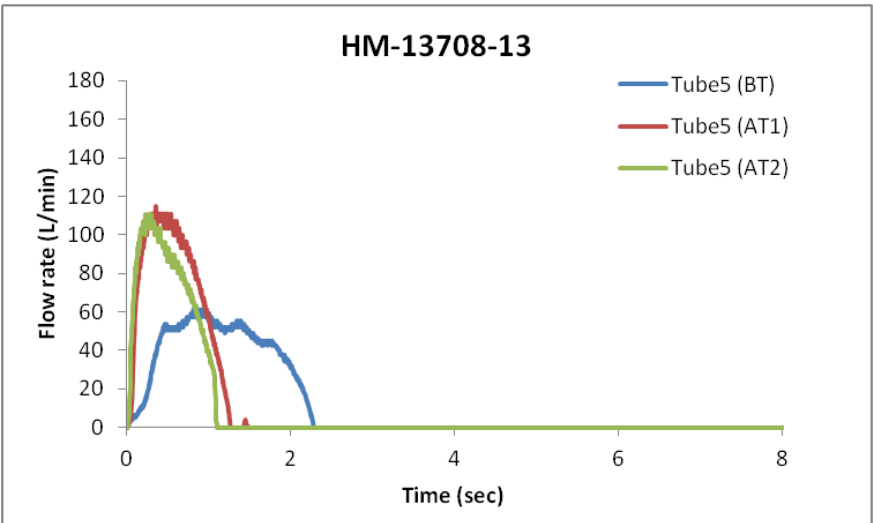
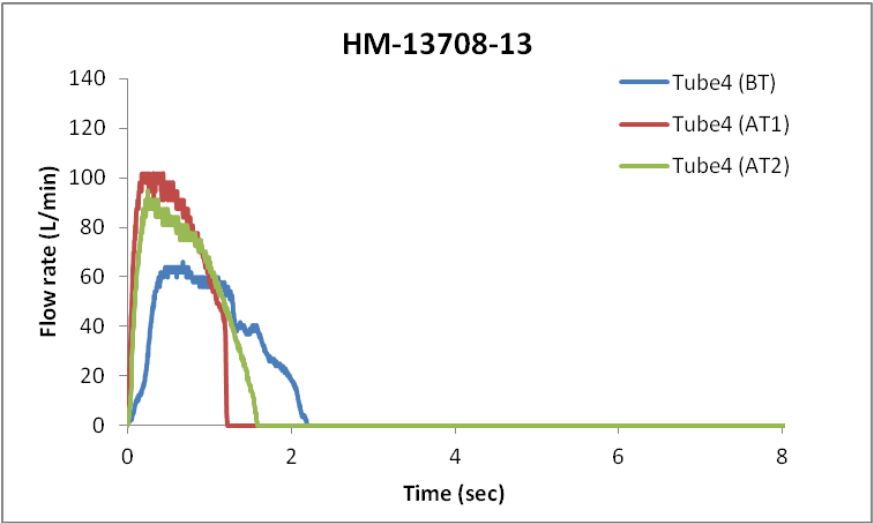
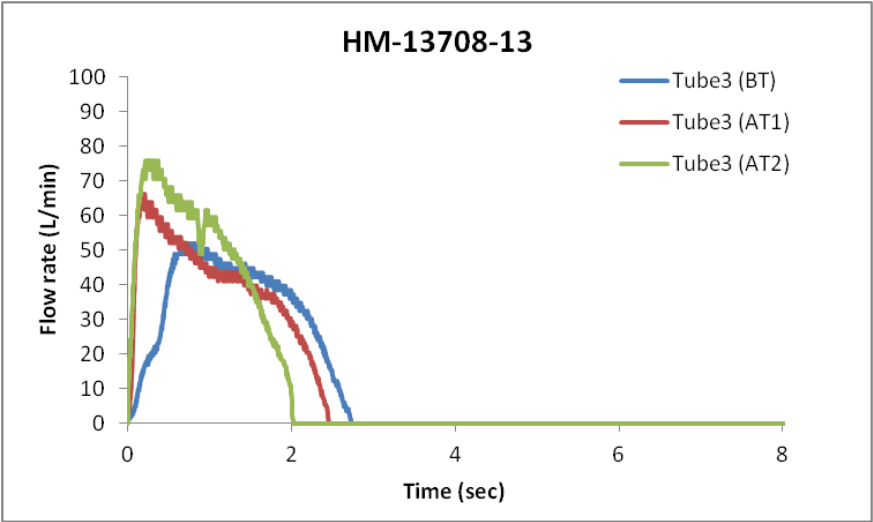
Training	Tube	Order	PIFR (L/min)	V (L)	tmax (sec)	ttotal (sec)
Before training	Tube1	2	53.5	2.218	1.000	4.330
After training 1	Tube1	6	59.3	2.835	0.780	4.390
After training 2	Tube1	6	59.3	3.027	1.175	4.390
Before training	Tube2	4	63.3	2.741	0.560	3.830
After training 1	Tube2	1	70.7	3.414	0.875	4.895
After training 2	Tube2	4	63.2	2.926	0.820	4.030
Before training	Tube3	1	52.0	2.481	1.520	4.320
After training 1	Tube3	5	78.5	2.751	0.665	3.370
After training 2	Tube3	5	75.6	2.848	0.480	3.430
Before training	Tube4	6	91.1	2.079	0.570	2.270
After training 1	Tube4	3	113.3	3.022	0.525	2.905
After training 2	Tube4	2	105.4	2.921	0.650	2.79
Before training	Tube5	5	110.9	2.340	0.515	2.100
After training 1	Tube5	4	118.6	2.836	0.740	2.680
After training 2	Tube5	3	110.7	3.021	0.340	2.645
Before training	Tube6	3	105.8	2.340	0.640	2.155
After training 1	Tube6	2	138.8	3.032	0.480	2.475
After training 2	Tube6	1	125.0	2.733	0.330	2.085

HM-13708-13

Description: Gender:Female, Ethnicity: African, Height: 163 cm, Weight: 62 kg, Age: 27 yrs

Figure E12: Inhalation profiles of Volunteer HM-13708-13





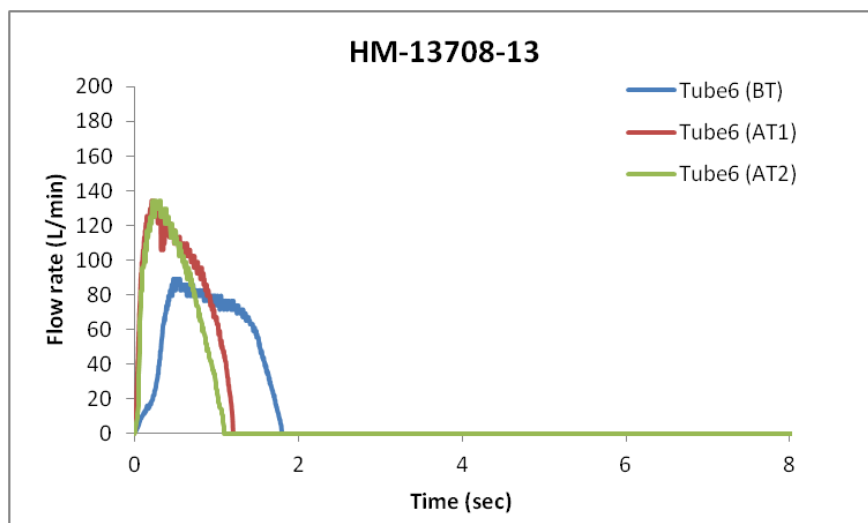


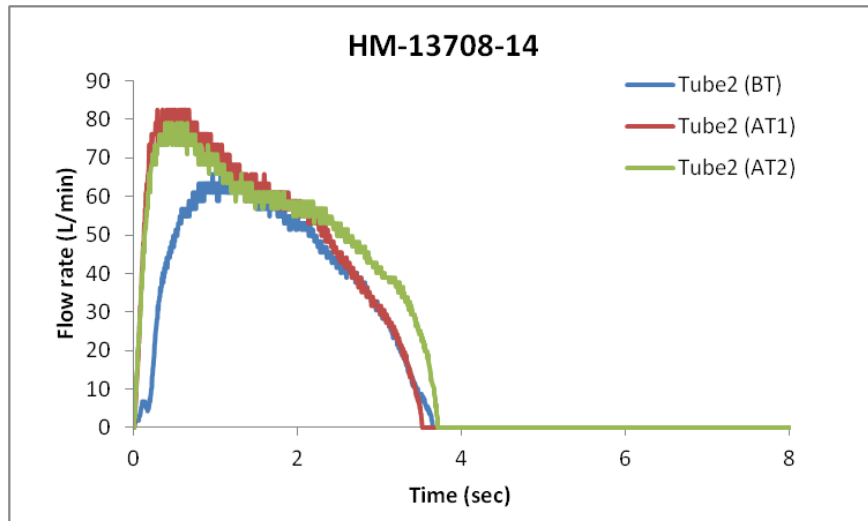
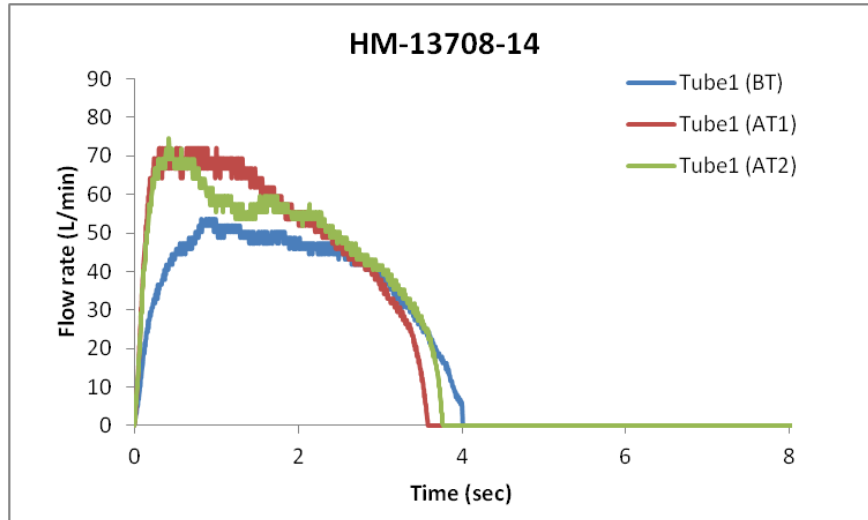
Table E12: Summary of inhalation parameters of volunteer: HM-13708-13

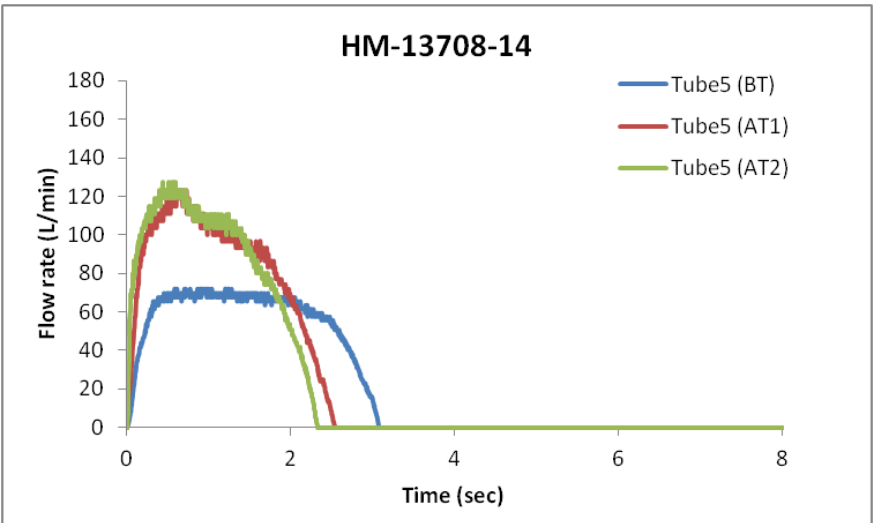
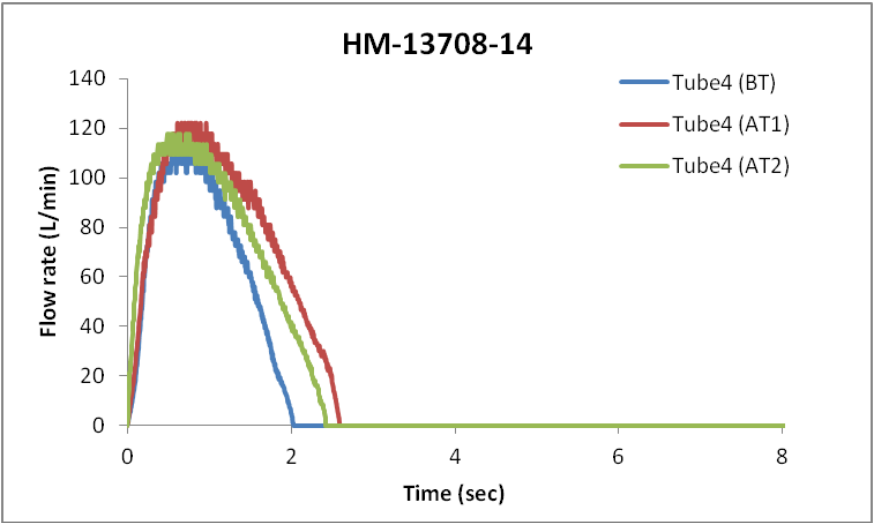
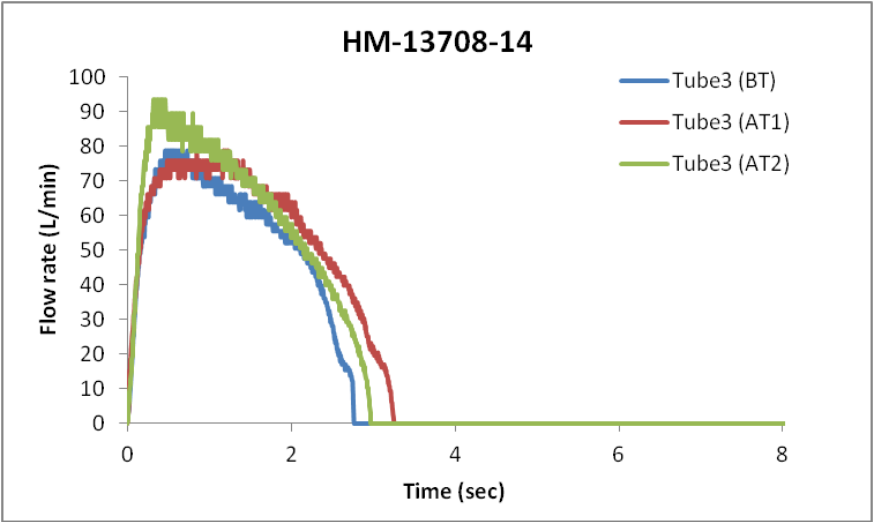
Training	Tube	Order	PIFR (L/min)	V (L)	tmax (sec)	ttotal (sec)
Before training	Tube1	5	44.4	1.552	0.450	2.975
After training 1	Tube1	5	59.4	1.444	0.215	2.235
After training 2	Tube1	1	57.3	1.442	0.365	2.145
Before training	Tube2	2	41.5	1.473	0.810	2.730
After training 1	Tube2	4	58.8	1.274	0.195	1.820
After training 2	Tube2	4	61.0	1.361	0.255	1.810
Before training	Tube3	1	52.0	1.533	0.690	2.735
After training 1	Tube3	1	66.1	1.622	0.175	2.460
After training 2	Tube3	6	75.7	1.659	0.215	2.025
Before training	Tube4	3	66.0	1.454	0.680	2.195
After training 1	Tube4	3	101.9	1.571	0.180	1.225
After training 2	Tube4	5	94.7	1.593	0.250	1.590
Before training	Tube5	6	61.4	1.549	0.810	2.285
After training 1	Tube5	6	114.7	1.553	0.350	1.280
After training 2	Tube5	2	110.8	1.345	0.230	1.105
Before training	Tube6	4	89.2	1.728	0.480	1.805
After training 1	Tube6	2	134.1	1.812	0.215	1.210
After training 2	Tube6	3	134.0	1.514	0.215	1.100

HM-13708-14

Description: Gender: Male, Ethnicity: African, Height: 182 cm, Weight: 91 kg, Age: 41 yrs

Figure E13: Inhalation profiles of Volunteer HM-13708-14





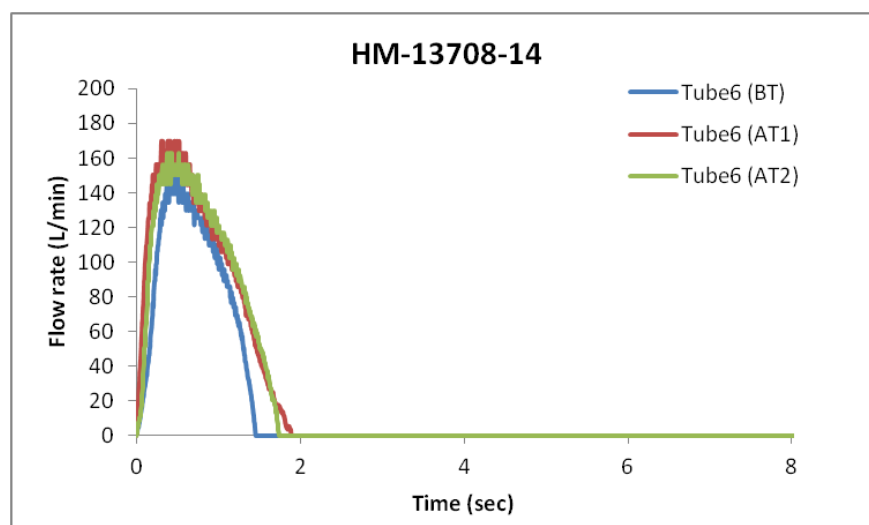


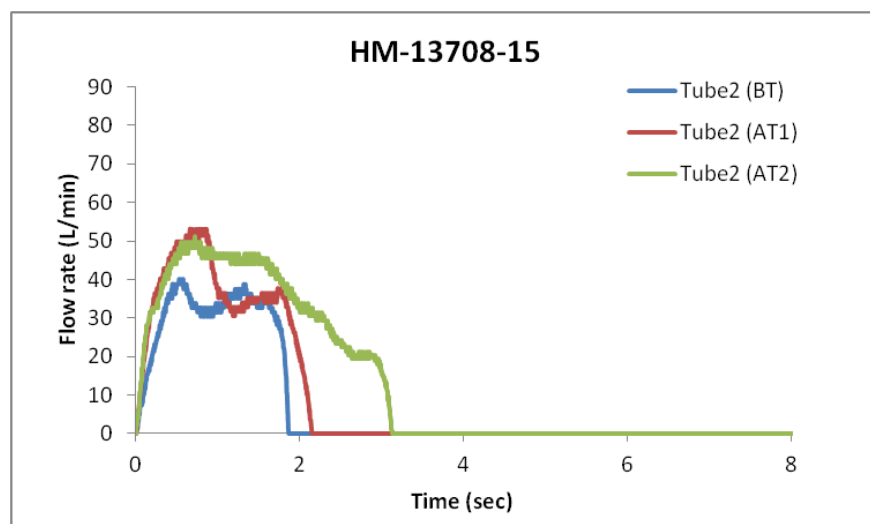
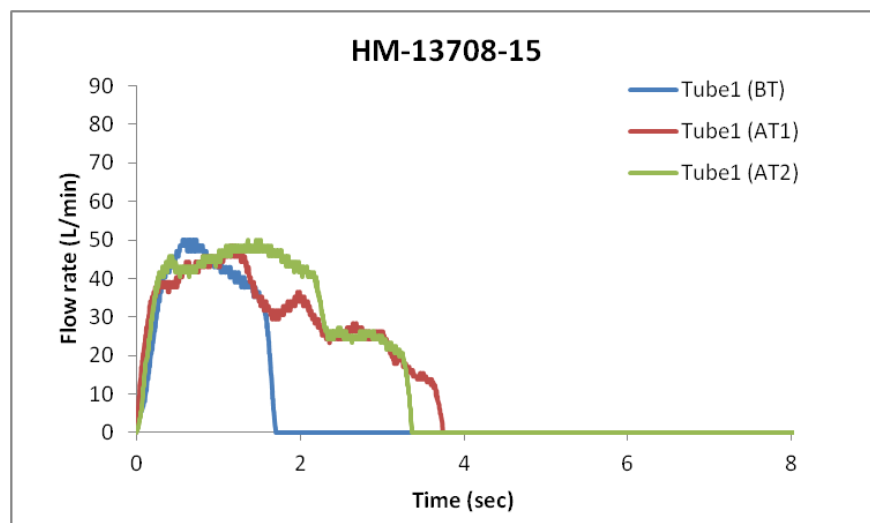
Table E13: Summary of inhalation parameters of volunteer: HM-13708-14

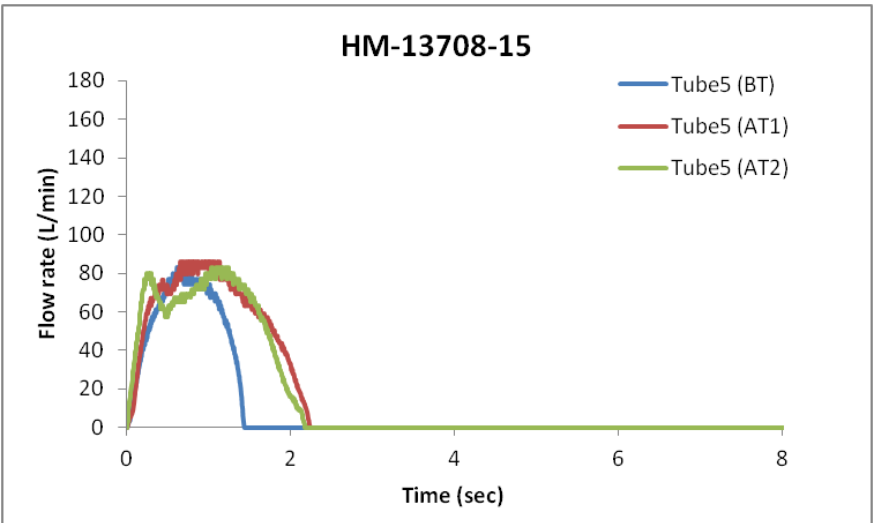
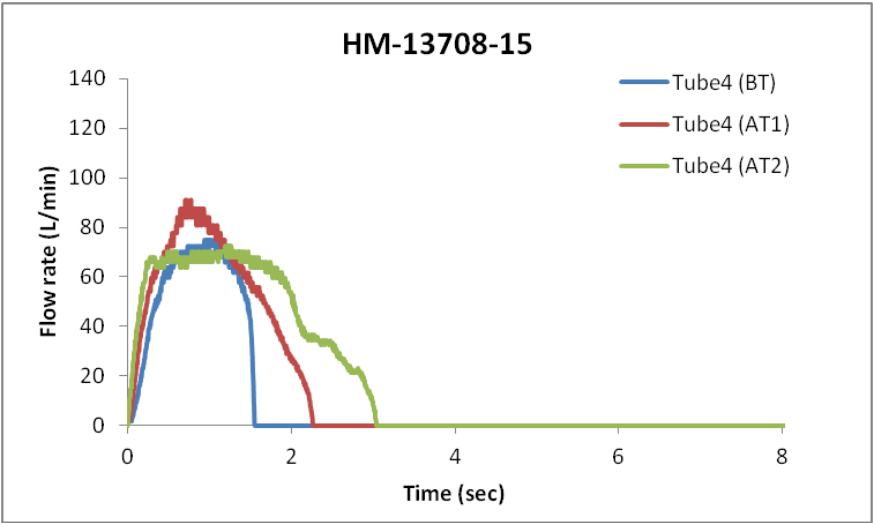
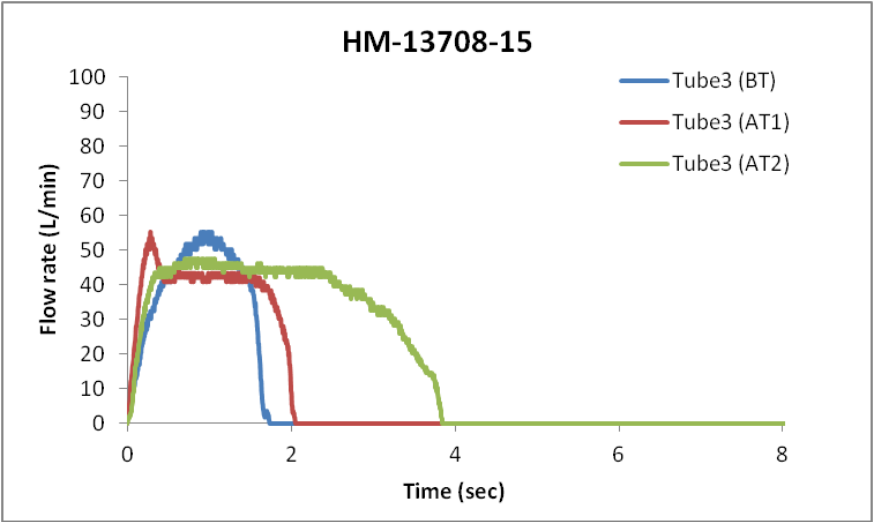
Training	Tube	Order	PIFR (L/min)	V (L)	tmax (sec)	ttotal (sec)
Before training	Tube1	5	53.6	2.623	0.820	4.010
After training 1	Tube1	6	72.0	3.096	0.305	3.585
After training 2	Tube1	5	74.7	3.112	0.425	3.770
Before training	Tube2	3	65.8	2.557	0.960	3.650
After training 1	Tube2	3	82.5	3.134	0.285	3.520
After training 2	Tube2	4	79.2	3.308	0.385	3.720
Before training	Tube3	4	78.8	2.548	0.465	2.770
After training 1	Tube3	2	78.7	3.038	0.850	3.260
After training 2	Tube3	2	93.5	2.991	0.315	2.975
Before training	Tube4	2	109.7	2.356	0.550	2.030
After training 1	Tube4	4	122.2	3.340	0.615	2.595
After training 2	Tube4	3	117.8	3.083	0.485	2.425
Before training	Tube5	6	72.0	2.916	0.580	3.075
After training 1	Tube5	1	123.2	3.519	0.575	2.540
After training 2	Tube5	6	127.4	3.435	0.440	2.330
Before training	Tube6	1	150.6	2.248	0.455	1.460
After training 1	Tube6	5	169.9	3.062	0.310	1.900
After training 2	Tube6	1	162.8	2.961	0.370	1.745

HM-13708-15

Description: Gender:Female, Ethnicity: Caucasian, Height: 168 cm, Weight: 62 kg, Age: 45 yrs

Figure E14: Inhalation profiles of Volunteer HM-13708-15





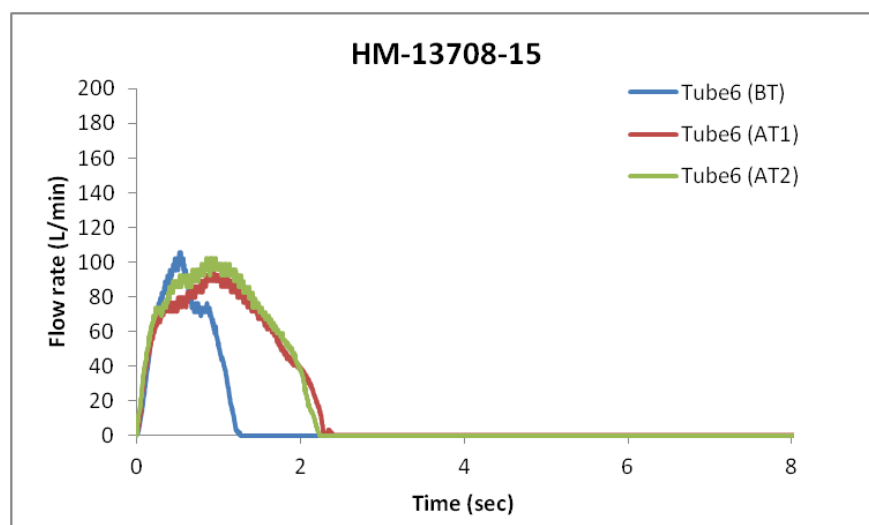


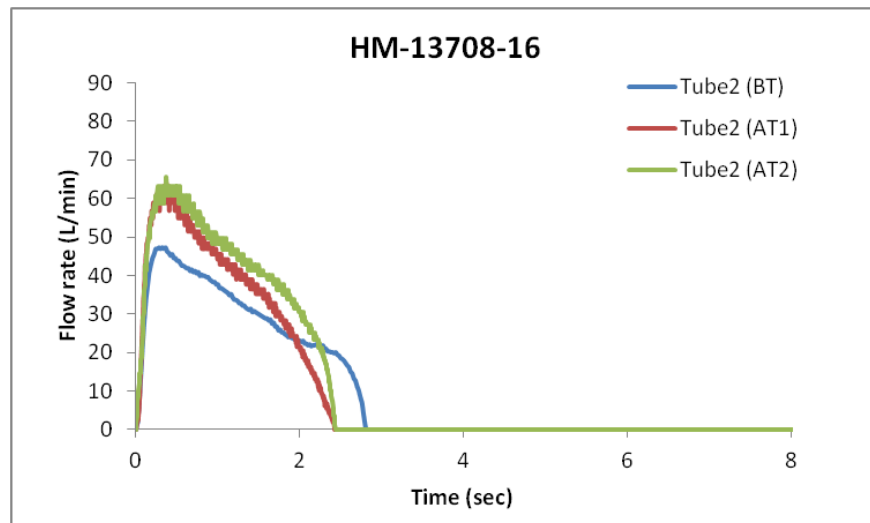
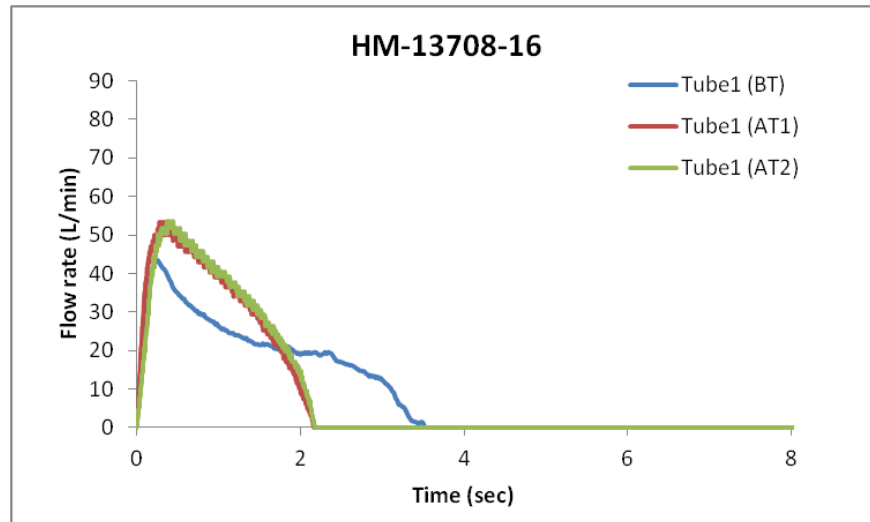
Table E14: Summary of inhalation parameters of volunteer: HM-13708-15

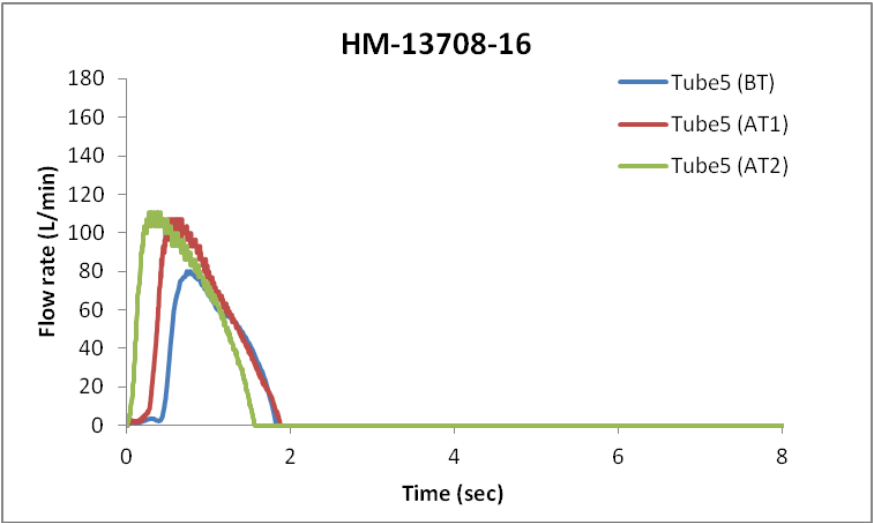
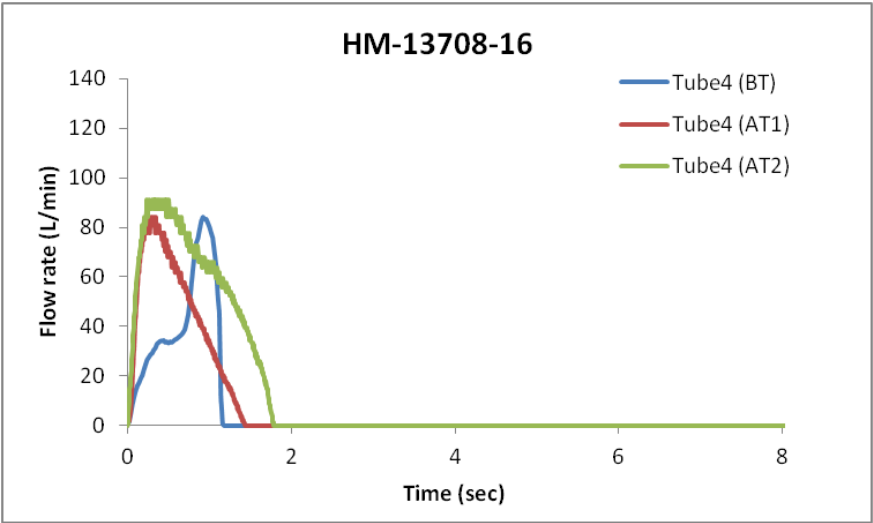
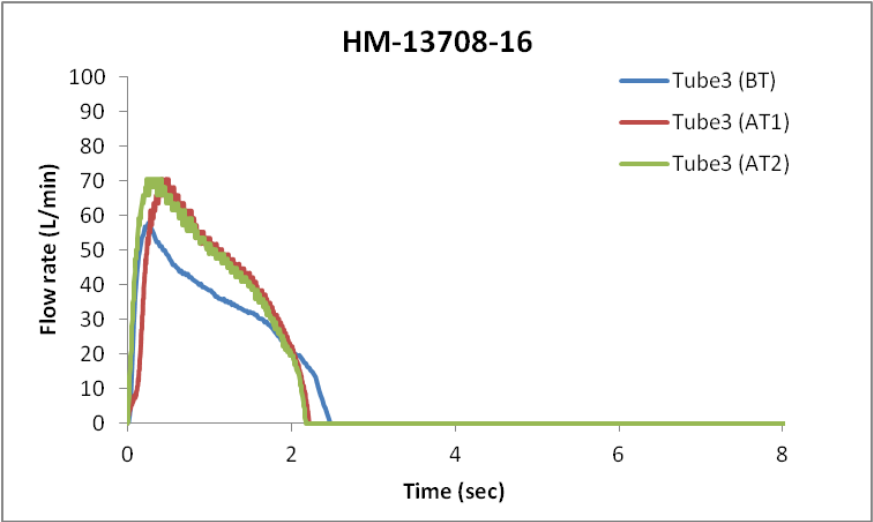
Training	Tube	Order	PIFR (L/min)	V (L)	tmax (sec)	ttotal (sec)
Before training	Tube1	4	50.1	1.030	0.570	1.705
After training 1	Tube1	4	48.6	1.906	1.155	3.745
After training 2	Tube1	6	50.1	1.999	1.360	3.365
Before training	Tube2	3	40.1	0.944	0.525	1.865
After training 1	Tube2	5	53.0	1.260	0.660	2.150
After training 2	Tube2	4	51.3	1.810	0.720	3.135
Before training	Tube3	6	55.4	1.110	0.900	1.740
After training 1	Tube3	1	55.4	1.315	0.285	2.055
After training 2	Tube3	3	47.5	2.378	0.705	3.850
Before training	Tube4	5	75.0	1.411	0.945	1.560
After training 1	Tube4	3	91.1	2.088	0.710	2.270
After training 2	Tube4	5	72.5	2.592	1.195	3.040
Before training	Tube5	2	83.1	1.349	0.610	1.435
After training 1	Tube5	2	86.3	2.208	0.650	2.235
After training 2	Tube5	2	83.0	2.099	1.030	2.175
Before training	Tube6	1	105.7	1.271	0.530	1.275
After training 1	Tube6	6	95.5	2.398	0.945	2.300
After training 2	Tube6	1	102.2	2.571	0.855	2.240

HM-13708-16

Description: Gender:Female, Ethnicity: African, Height: 166 cm, Weight: 76 kg, Age: 42 yrs

Figure E15: Inhalation profiles of Volunteer HM-13708-16





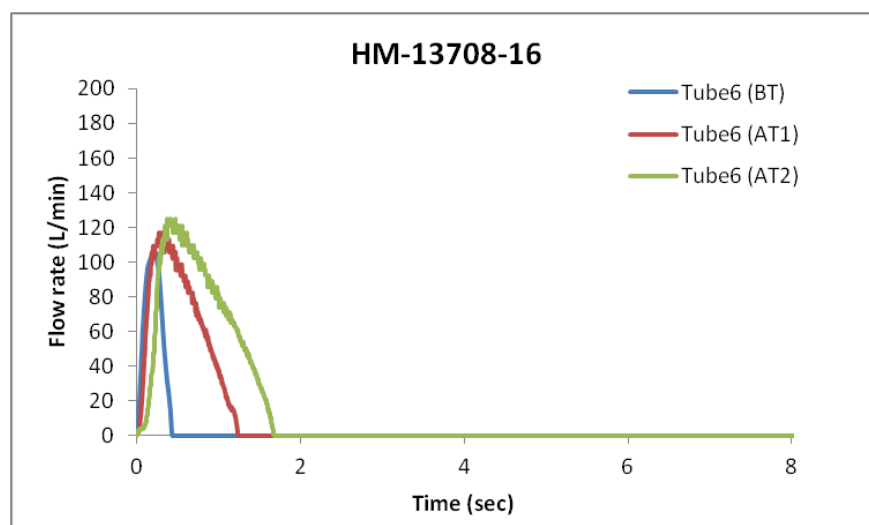


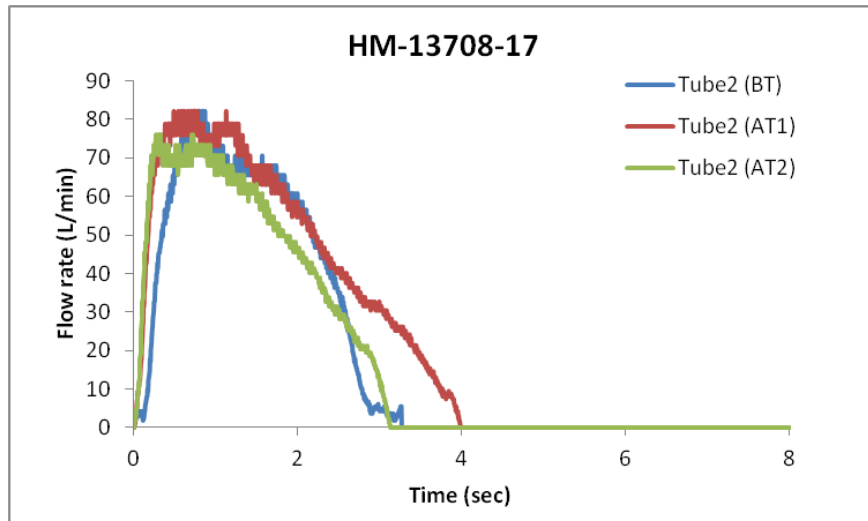
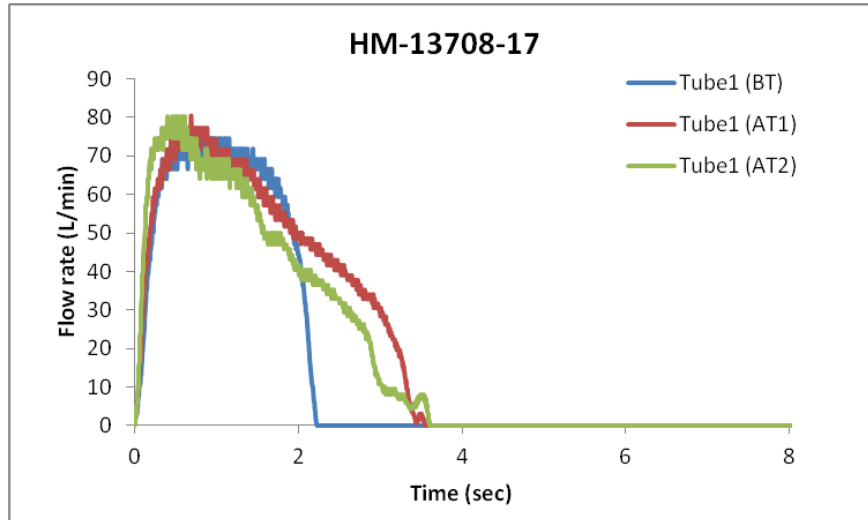
Table E15: Summary of inhalation parameters of volunteer: HM-13708-16

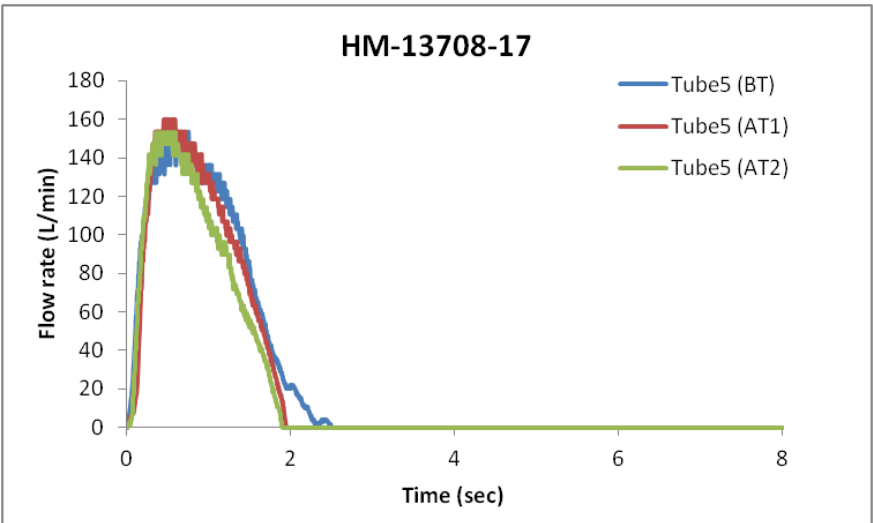
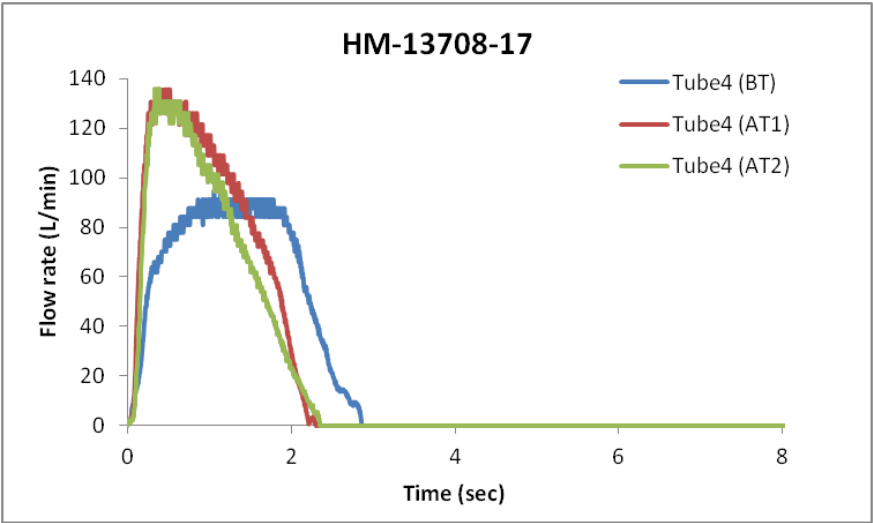
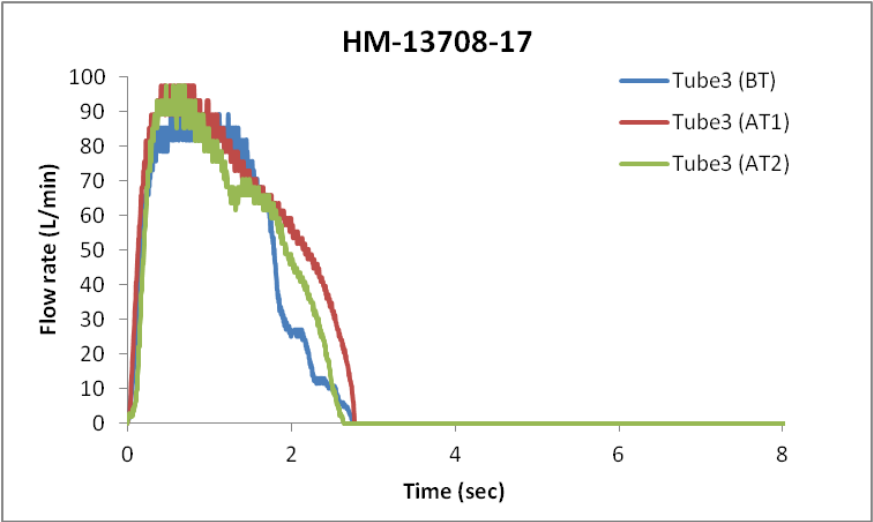
Training	Tube	Order	PIFR (L/min)	V (L)	tmax (sec)	ttotal (sec)
Before training	Tube1	1	43.4	1.239	0.265	3.525
After training 1	Tube1	5	53.5	1.197	0.285	2.170
After training 2	Tube1	6	53.5	1.204	0.370	2.175
Before training	Tube2	5	47.2	1.388	0.320	2.810
After training 1	Tube2	2	63.3	1.494	0.350	2.425
After training 2	Tube2	2	65.7	1.709	0.375	2.440
Before training	Tube3	4	58.0	1.355	0.260	2.480
After training 1	Tube3	6	70.6	1.559	0.425	2.220
After training 2	Tube3	1	70.6	1.628	0.240	2.180
Before training	Tube4	2	84.3	0.806	0.925	1.185
After training 1	Tube4	3	84.2	1.079	0.260	1.440
After training 2	Tube4	4	91.1	1.757	0.240	1.785
Before training	Tube5	6	80.0	1.207	0.770	1.825
After training 1	Tube5	4	107.1	1.655	0.510	1.875
After training 2	Tube5	5	110.8	1.783	0.280	1.565
Before training	Tube6	3	106.0	0.466	0.200	0.440
After training 1	Tube6	1	117.1	1.373	0.280	1.245
After training 2	Tube6	3	125.1	1.927	0.380	1.680

HM-13708-17

Description: Gender: Male, Ethnicity: Caucasian, Height: 169 cm, Weight: 68 kg, Age: 22 yrs

Figure E16: Inhalation profiles of Volunteer HM-13708-17





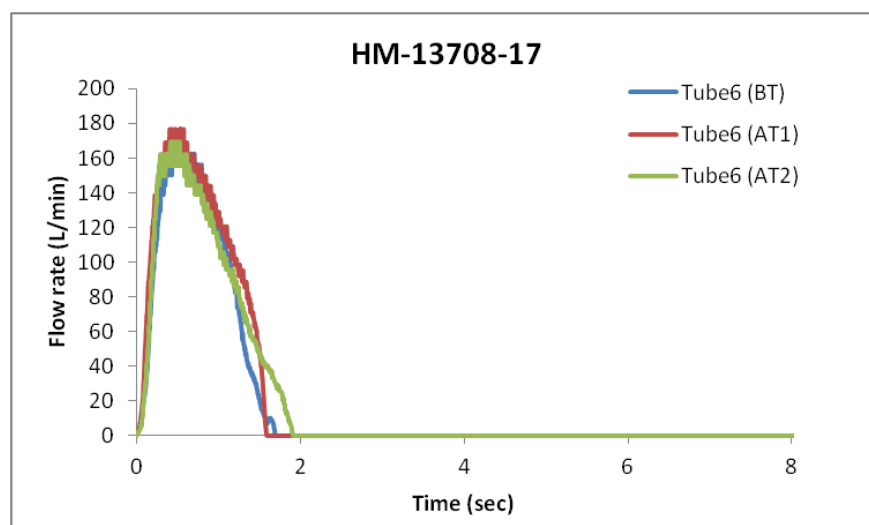


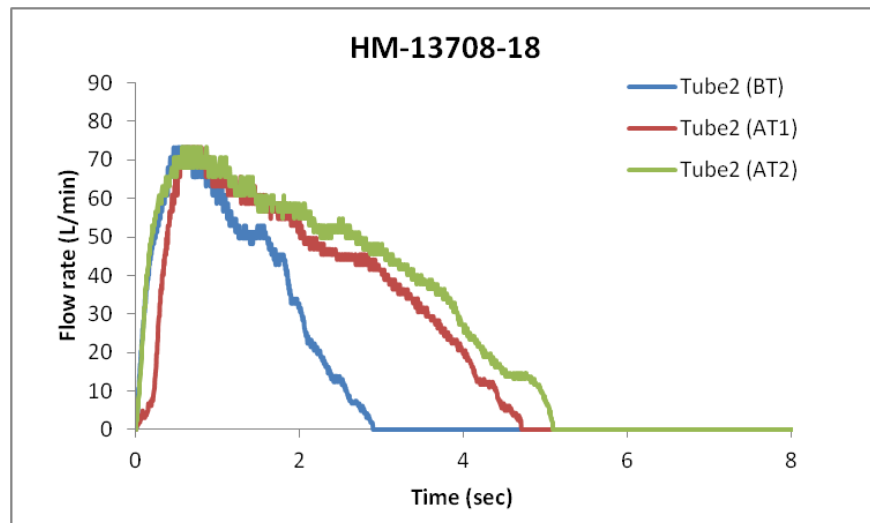
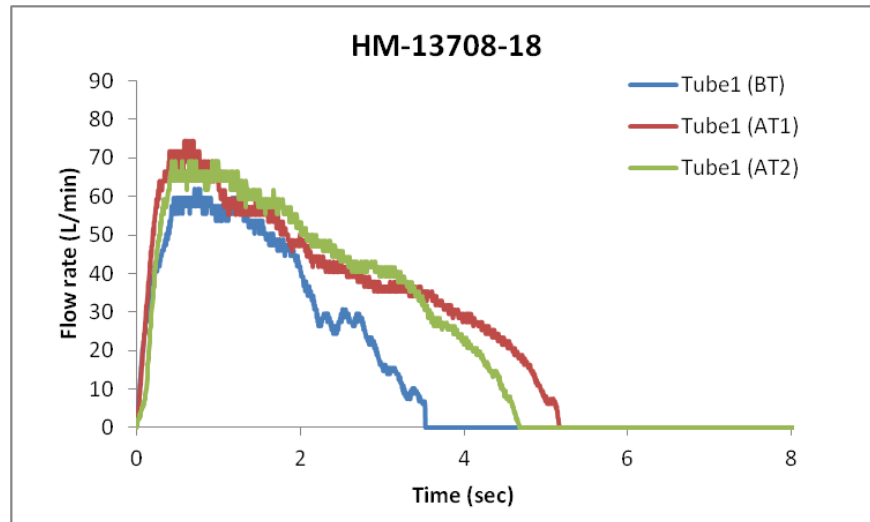
Table E16: Summary of inhalation parameters of volunteer: HM-13708-17

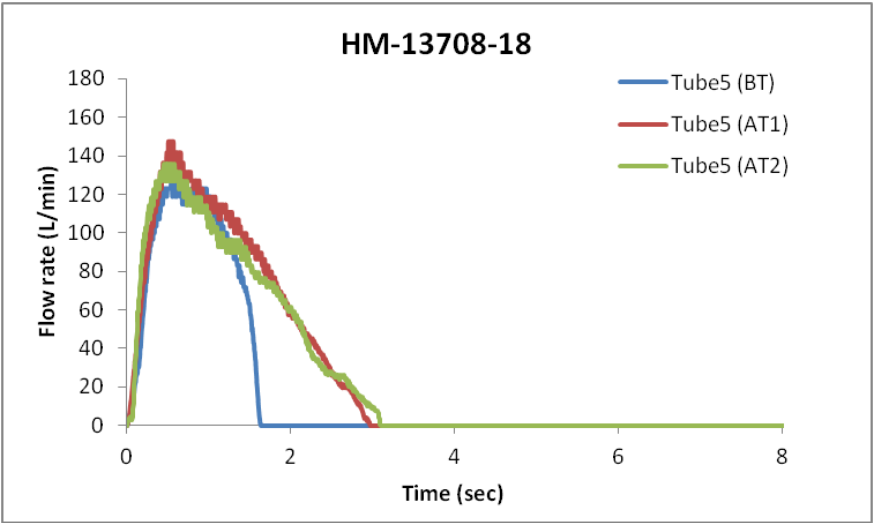
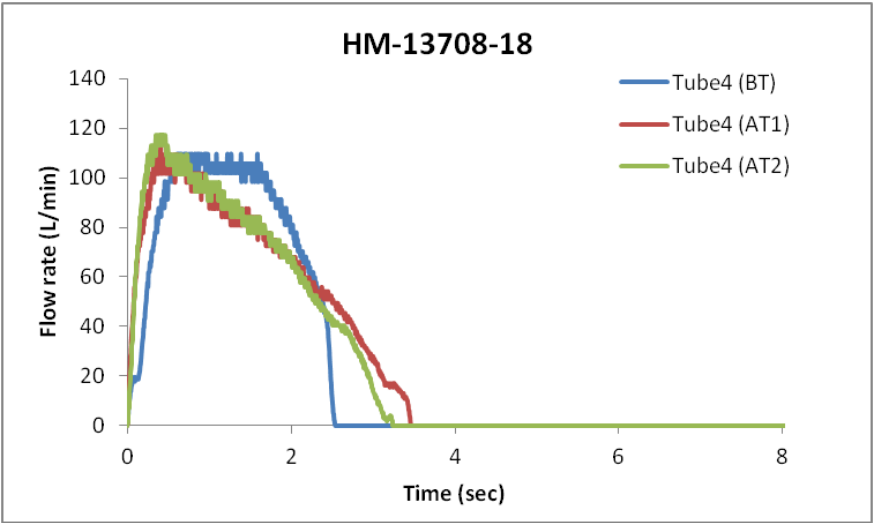
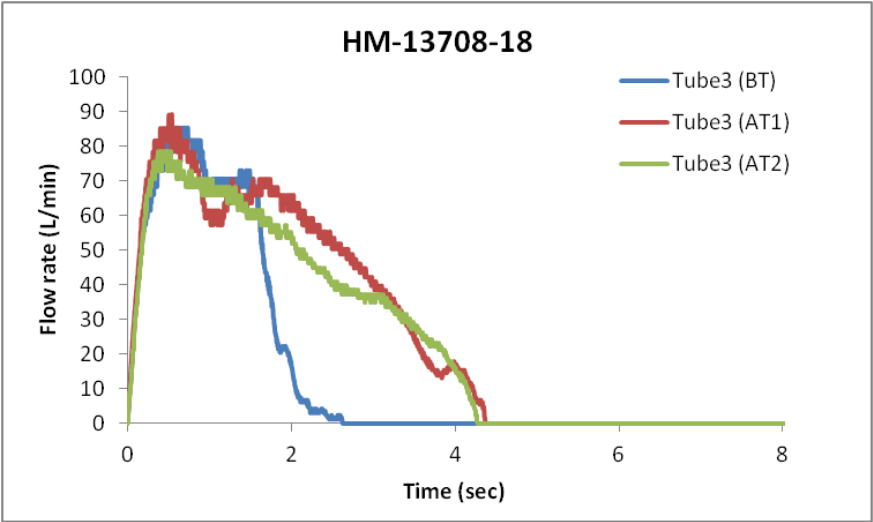
Training	Tube	Order	PIFR (L/min)	V (L)	tmax (sec)	ttotal (sec)
Before training	Tube1	2	74.6	2.152	0.545	2.230
After training 1	Tube1	1	80.4	2.867	0.695	3.545
After training 2	Tube1	2	80.4	2.598	0.400	3.610
Before training	Tube2	5	82.3	2.536	0.735	3.270
After training 1	Tube2	3	82.2	3.226	0.485	3.990
After training 2	Tube2	4	76.0	2.536	0.270	3.135
Before training	Tube3	4	89.2	2.466	0.535	2.755
After training 1	Tube3	5	97.5	2.991	0.415	2.775
After training 2	Tube3	6	97.5	2.583	0.470	2.640
Before training	Tube4	1	94.7	2.991	1.060	2.865
After training 1	Tube4	6	135.8	3.169	0.360	2.305
After training 2	Tube4	1	135.8	2.833	0.340	2.355
Before training	Tube5	3	153.8	3.380	0.605	2.495
After training 1	Tube5	4	159.8	3.117	0.450	1.945
After training 2	Tube5	5	153.4	2.833	0.360	1.905
Before training	Tube6	6	169.4	2.666	0.545	1.695
After training 1	Tube6	2	176.9	3.032	0.410	1.595
After training 2	Tube6	3	169.3	2.893	0.415	1.915

HM-13708-18

Description: Gender: Male, Ethnicity: Indian, Height: 174 cm, Weight: 70 kg, Age: 28 yrs

Figure E17: Inhalation profiles of Volunteer HM-13708-18





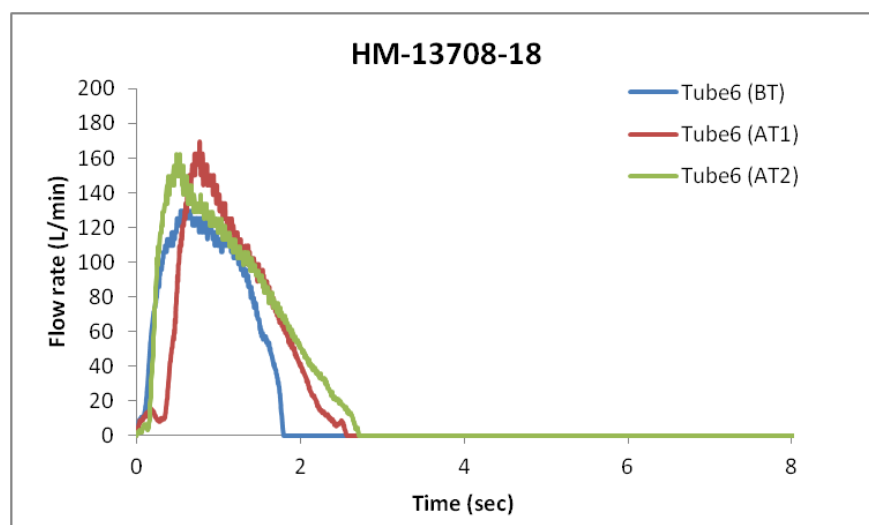


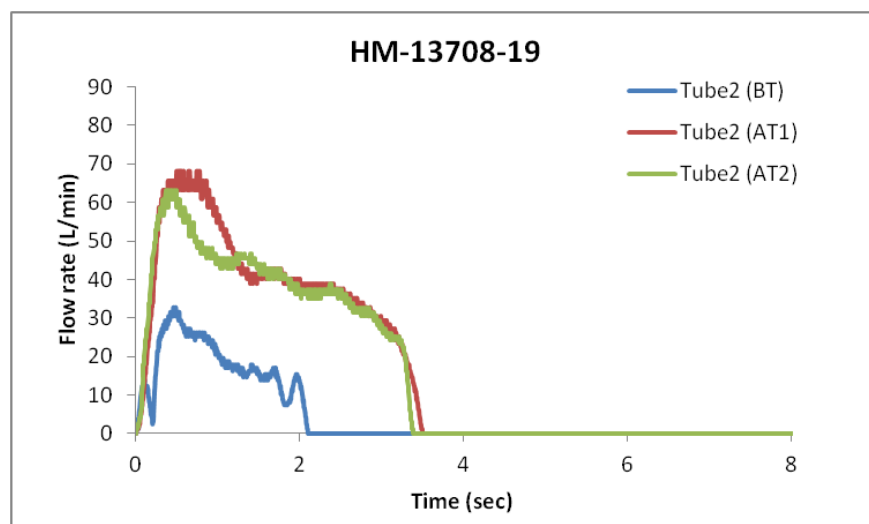
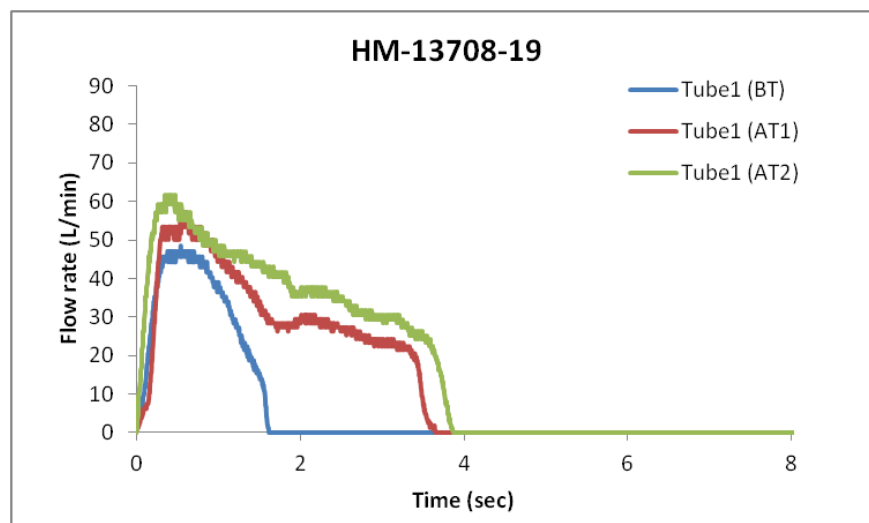
Table E17: Summary of inhalation parameters of volunteer: HM-13708-18

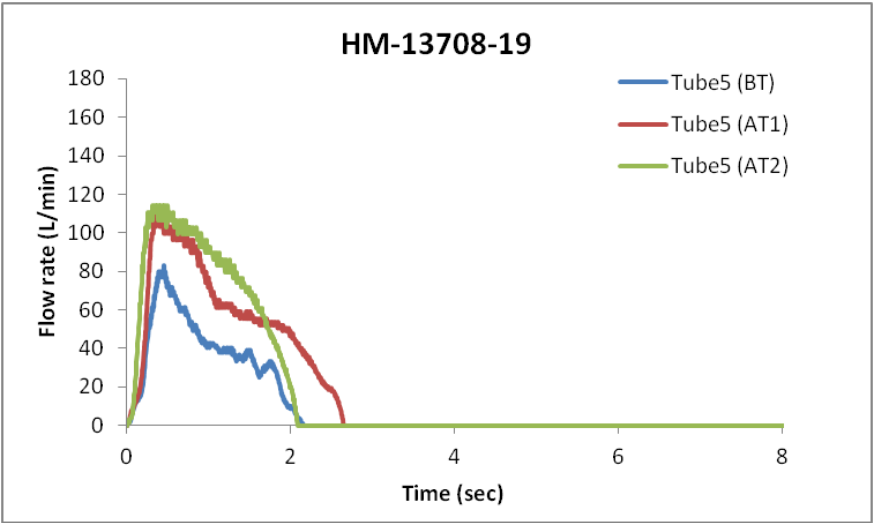
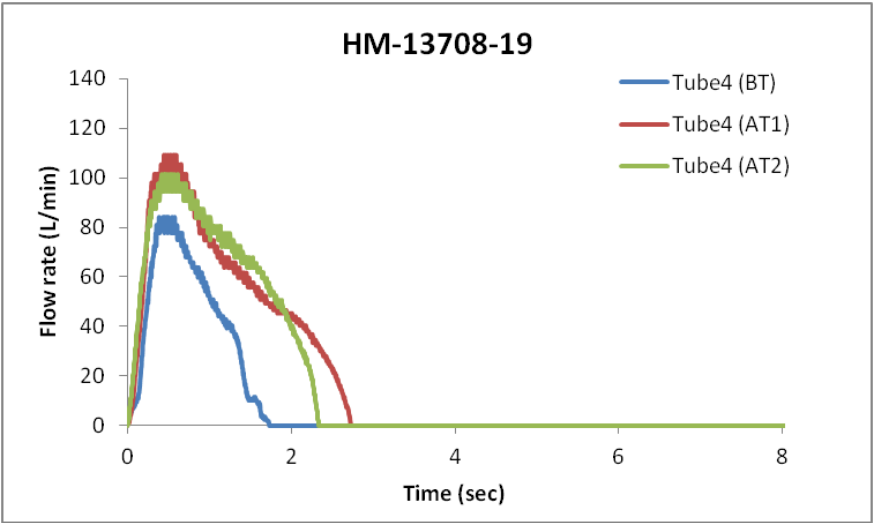
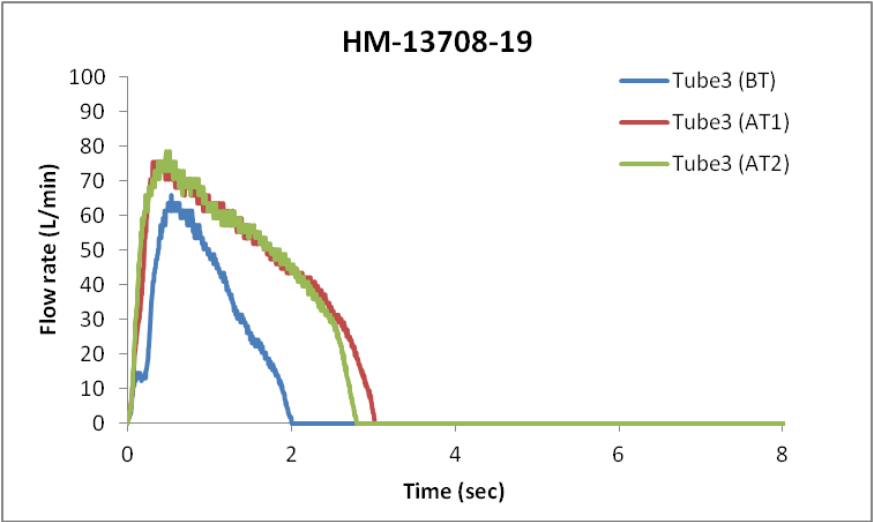
Training	Tube	Order	PIFR (L/min)	V (L)	tmax (sec)	ttotal (sec)
Before training	Tube1	3	61.8	2.216	0.715	3.530
After training 1	Tube1	2	74.5	3.510	0.590	5.165
After training 2	Tube1	4	69.1	3.307	0.430	4.675
Before training	Tube2	6	73.4	1.982	0.460	2.895
After training 1	Tube2	5	73.3	3.183	0.570	4.710
After training 2	Tube2	5	73.2	3.785	0.570	5.100
Before training	Tube3	5	85.4	2.076	0.530	2.630
After training 1	Tube3	1	89.2	3.582	0.510	4.370
After training 2	Tube3	3	78.4	3.285	0.370	4.275
Before training	Tube4	1	109.6	3.463	0.610	2.540
After training 1	Tube4	6	113.2	3.795	0.410	3.465
After training 2	Tube4	2	117.3	3.699	0.345	3.240
Before training	Tube5	4	127.5	2.437	0.540	1.635
After training 1	Tube5	4	147.3	3.778	0.505	2.970
After training 2	Tube5	6	136.1	3.629	0.455	3.105
Before training	Tube6	2	129.7	2.624	0.545	1.80
After training 1	Tube6	3	169.2	3.019	0.775	2.570
After training 2	Tube6	1	162.2	3.583	0.495	2.715

HM-13708-19

Description: Gender:Female, Ethnicity: Indian, Height: 161 cm, Weight: 62 kg, Age: 28 yrs

Figure E18: Inhalation profiles of Volunteer HM-13708-19





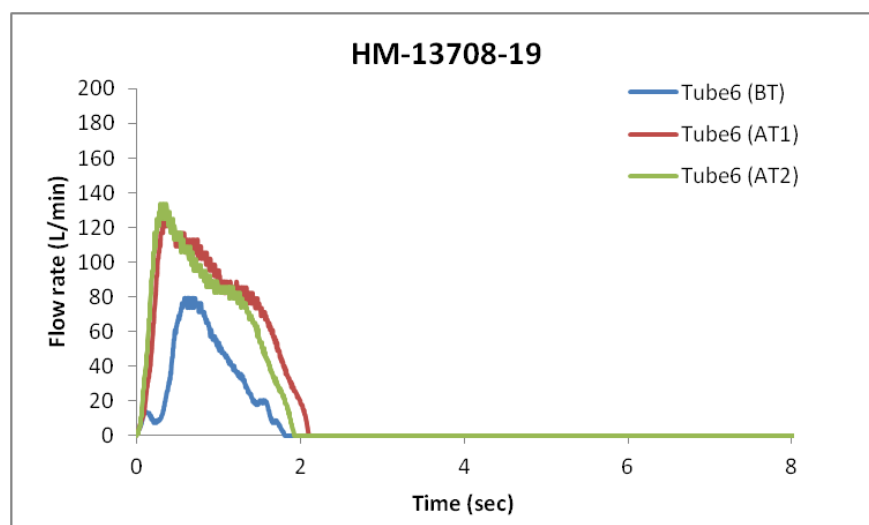


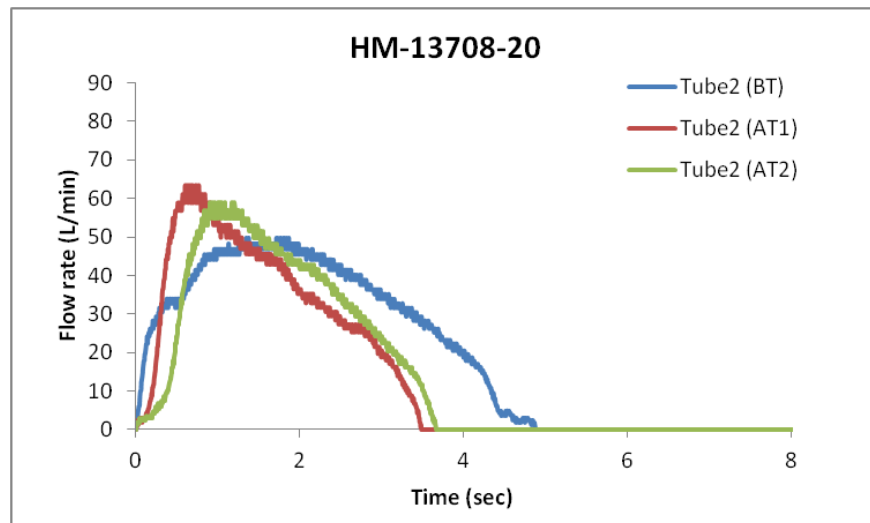
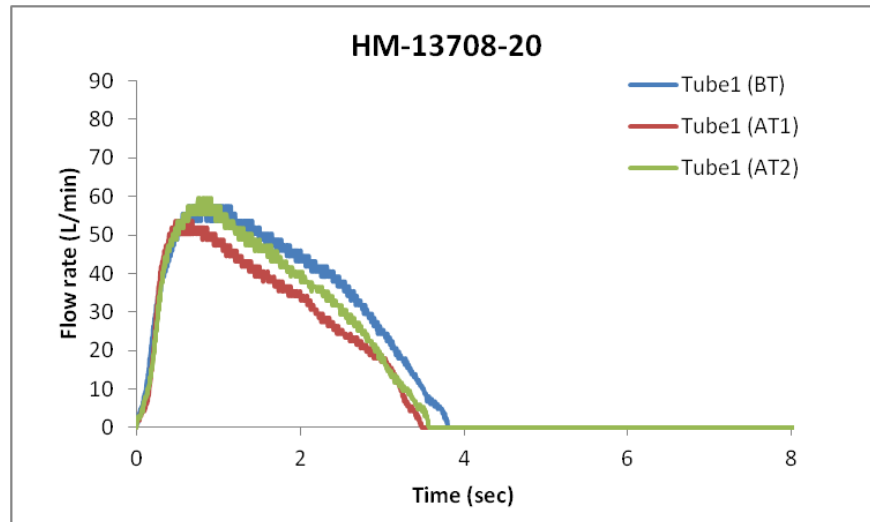
Table E18: Summary of inhalation parameters of volunteer: HM-13708-19

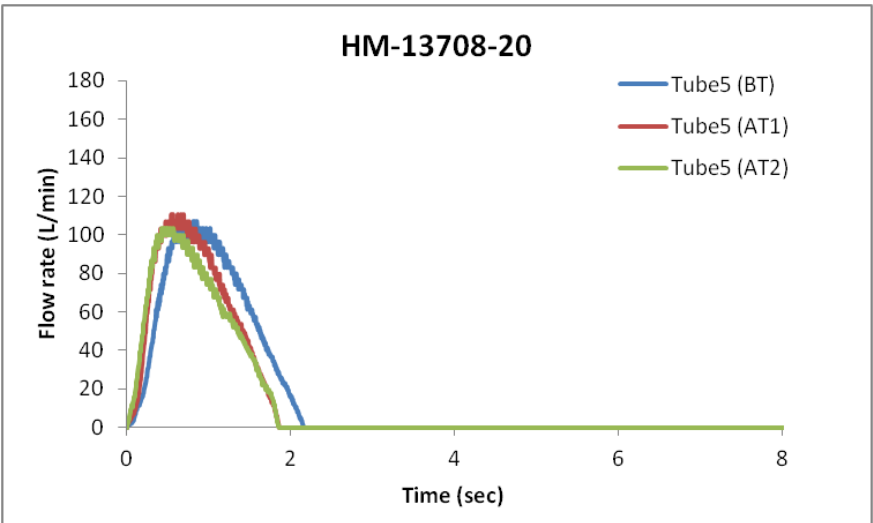
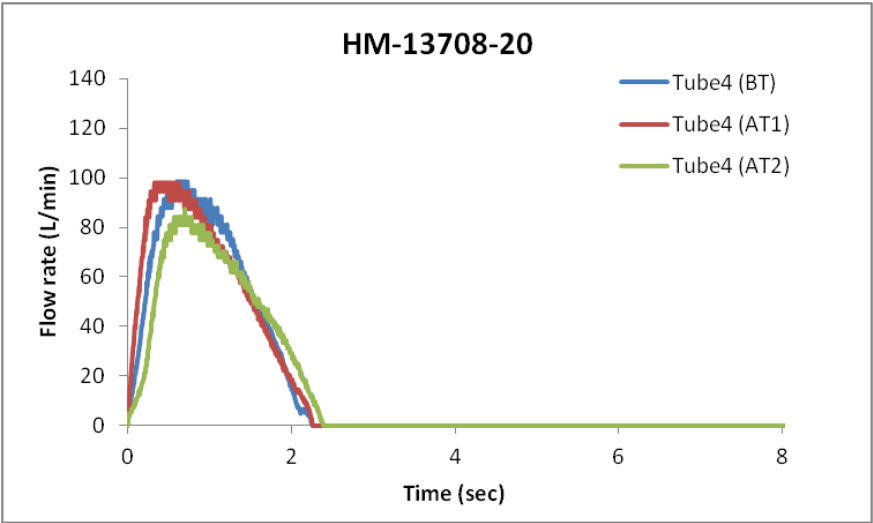
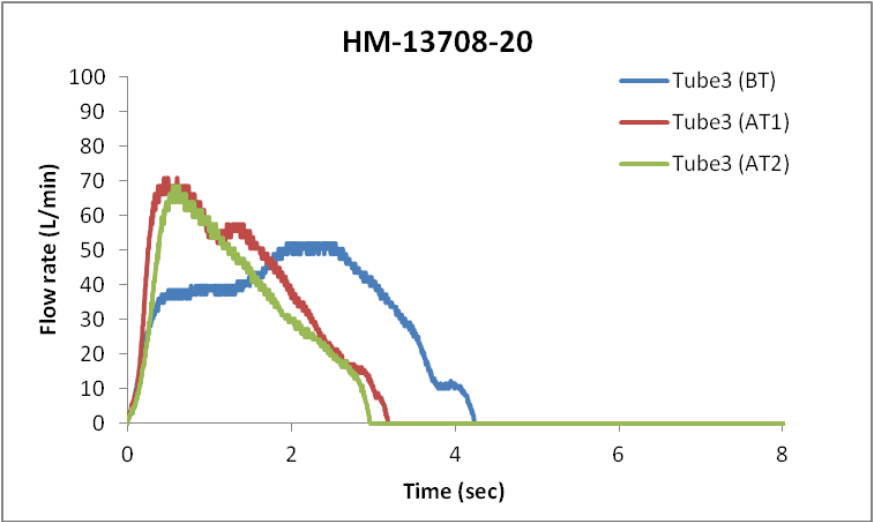
Training	Tube	Order	PIFR (L/min)	V (L)	tmax (sec)	ttotal (sec)
Before training	Tube1	6	48.6	0.863	0.545	1.620
After training 1	Tube1	6	57.2	1.890	0.590	3.655
After training 2	Tube1	3	61.6	2.436	0.355	3.865
Before training	Tube2	1	32.7	0.631	0.455	2.100
After training 1	Tube2	1	68.1	2.337	0.495	3.500
After training 2	Tube2	1	63.1	2.196	0.370	3.390
Before training	Tube3	3	65.9	1.171	0.540	2.010
After training 1	Tube3	3	75.5	2.398	0.315	3.020
After training 2	Tube3	2	78.4	2.336	0.470	2.795
Before training	Tube4	5	84.0	1.281	0.390	1.735
After training 1	Tube4	5	109.1	2.622	0.450	2.735
After training 2	Tube4	4	101.5	2.525	0.415	2.335
Before training	Tube5	2	82.9	1.359	0.450	2.155
After training 1	Tube5	4	110.5	2.519	0.355	2.650
After training 2	Tube5	6	114.4	2.566	0.315	2.095
Before training	Tube6	4	79.1	1.087	0.590	1.815
After training 1	Tube6	2	124.8	2.607	0.330	2.110
After training 2	Tube6	5	133.6	2.399	0.295	1.925

HM-13708-20

Description: Gender:Female, Ethnicity: Asian, Height: 170 cm, Weight: 51 kg, Age: 38 yrs

FigureE19: Inhalation profiles of Volunteer HM-13708-20





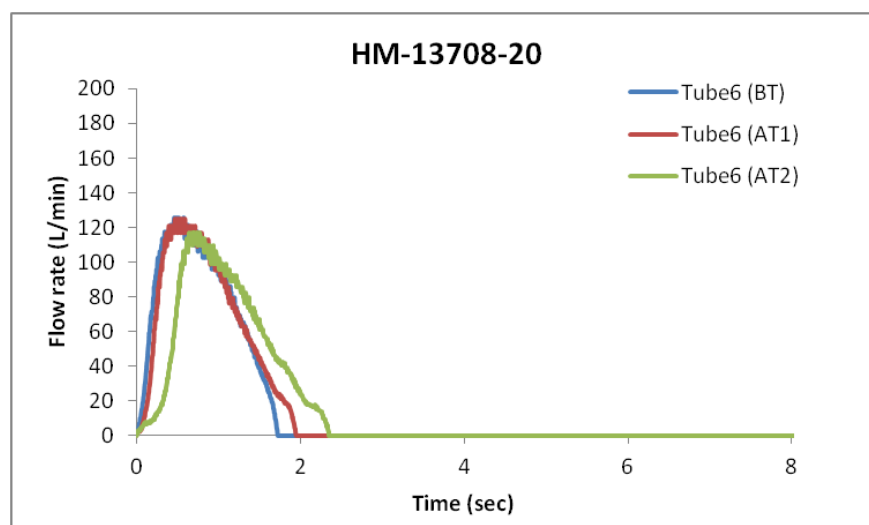


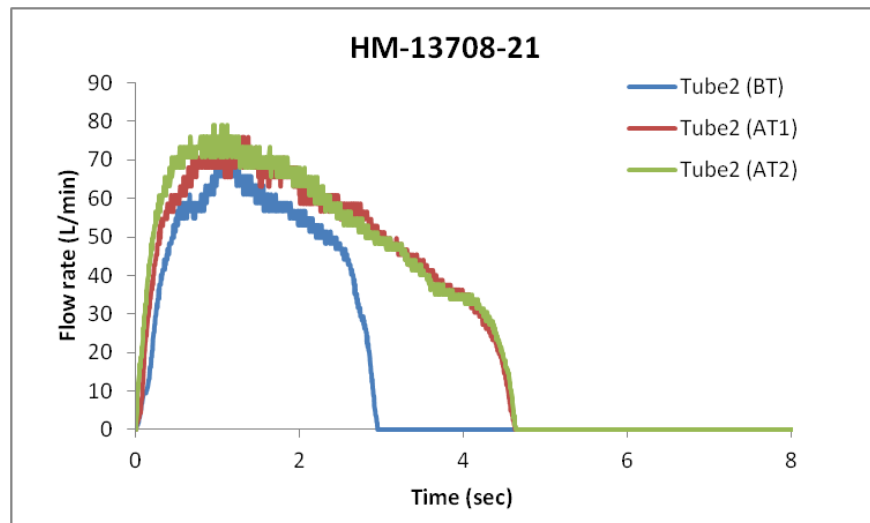
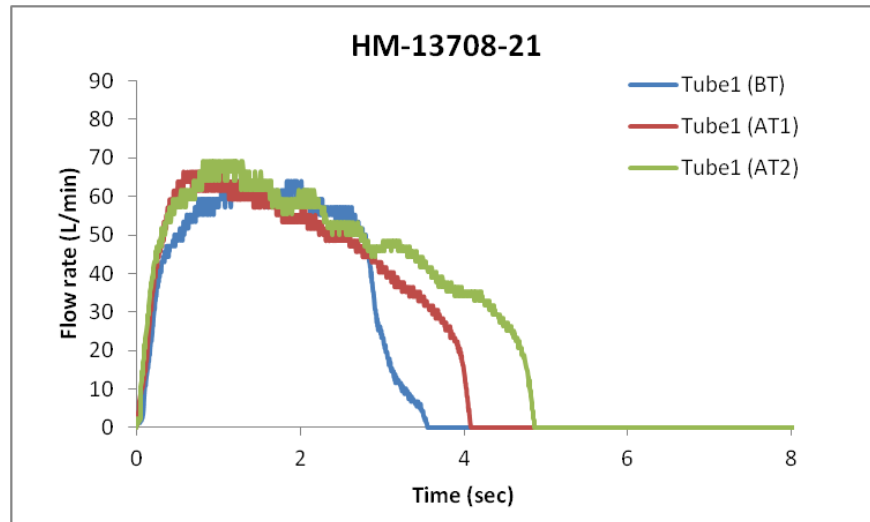
Table E19: Summary of inhalation parameters of volunteer: HM-13708-20

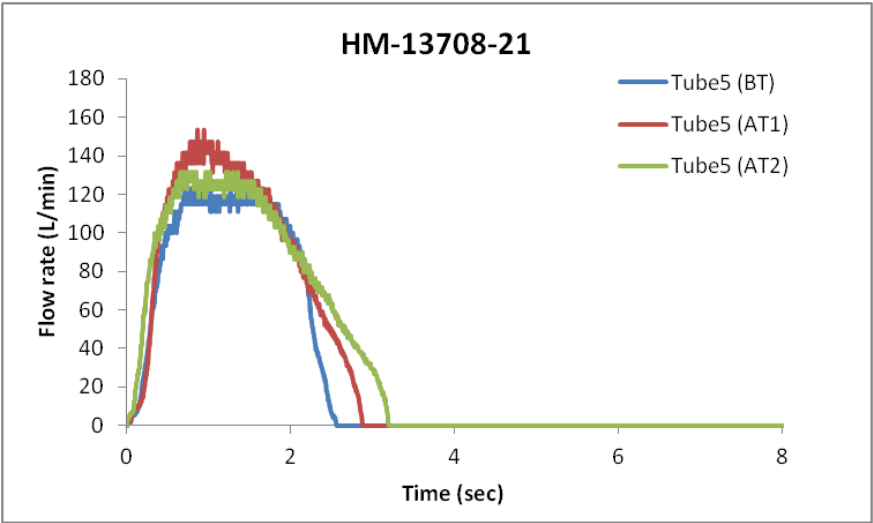
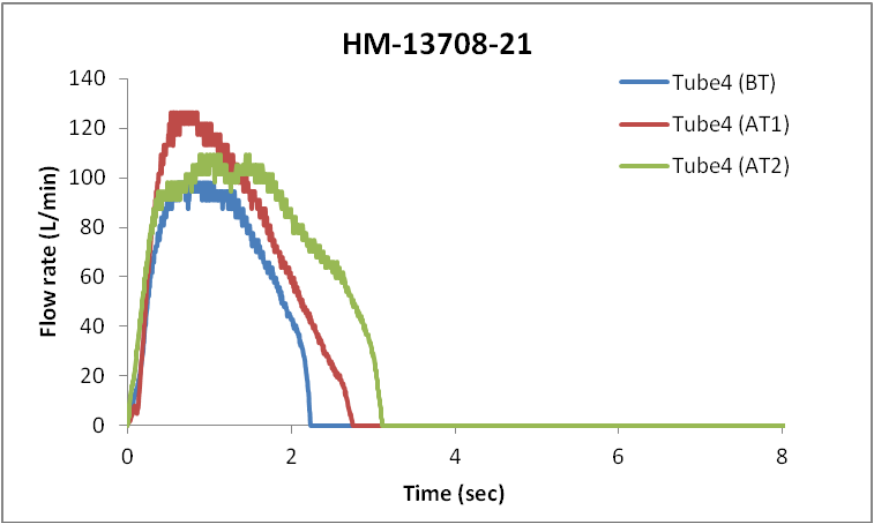
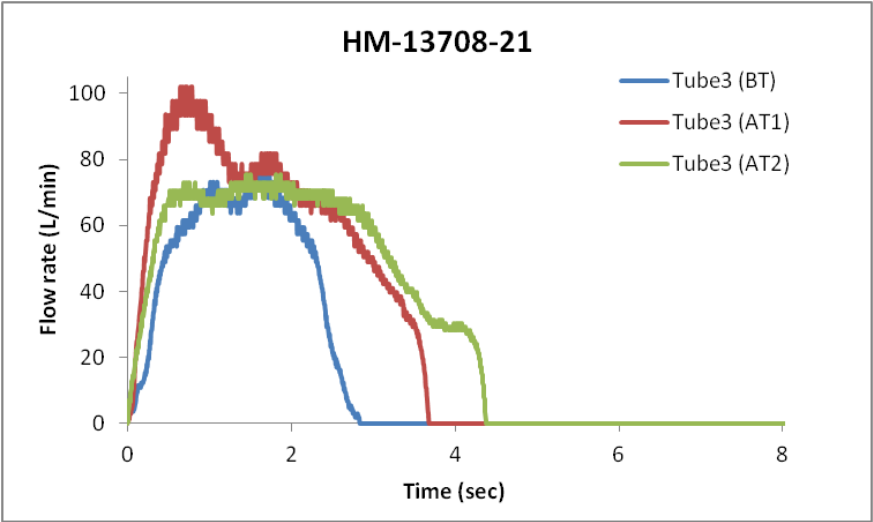
Training	Tube	Order	PIFR (L/min)	V (L)	tmax (sec)	ttotal (sec)
Before training	Tube1	1	57.4	2.307	0.645	3.805
After training 1	Tube1	5	53.5	1.825	0.480	3.485
After training 2	Tube1	6	59.5	2.069	0.750	3.570
Before training	Tube2	5	49.8	2.617	1.345	4.880
After training 1	Tube2	2	63.3	2.025	0.600	3.485
After training 2	Tube2	2	58.9	2.031	0.910	3.665
Before training	Tube3	4	52.1	2.463	1.950	4.240
After training 1	Tube3	6	70.7	2.117	0.450	3.185
After training 2	Tube3	1	68.5	1.801	0.555	2.965
Before training	Tube4	2	98.4	2.158	0.610	2.260
After training 1	Tube4	3	98.2	2.223	0.335	2.270
After training 2	Tube4	4	87.7	1.958	0.700	2.390
Before training	Tube5	6	107.2	2.165	0.675	2.160
After training 1	Tube5	4	110.8	1.985	0.540	1.860
After training 2	Tube5	5	103.6	1.880	0.435	1.860
Before training	Tube6	3	125.5	2.239	0.465	1.730
After training 1	Tube6	1	125.2	2.265	0.475	1.955
After training 2	Tube6	3	117.3	2.225	0.650	2.355

HM-13708-21

Description: Gender: Male, Ethnicity: Caucasian, Height: 181 cm, Weight: 112 kg, Age: 25 yrs

Figure E20: Inhalation profiles of Volunteer HM-13708-21





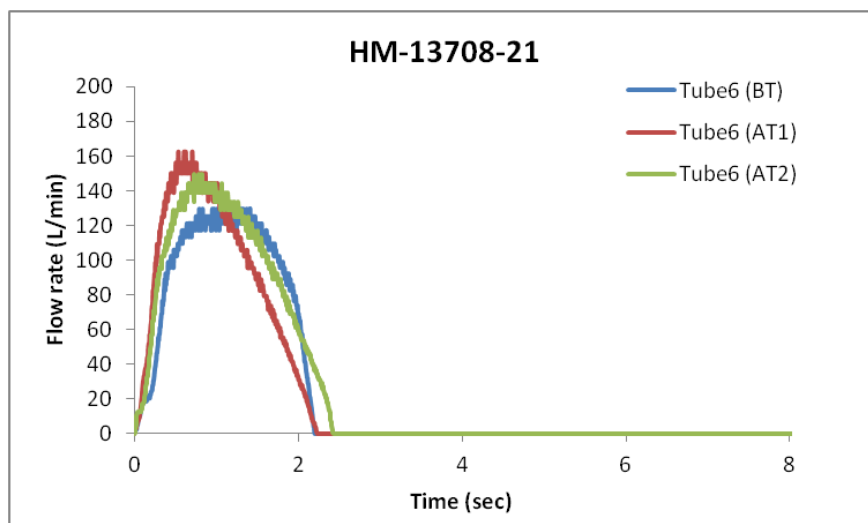


Table E20: Summary of inhalation parameters of volunteer: HM-13708-21

Training	Tube	Order	PIFR (L/min)	V (L)	tmax (sec)	ttotal (sec)
Before training	Tube1	2	64.1	2.677	1.050	3.555
After training 1	Tube1	5	66.5	3.187	0.580	4.085
After training 2	Tube1	4	69.1	3.859	0.810	4.865
Before training	Tube2	3	70.8	2.407	1.045	2.950
After training 1	Tube2	6	76.0	3.937	1.250	4.630
After training 2	Tube2	5	78.9	4.080	0.950	4.645
Before training	Tube3	5	75.7	2.332	1.550	2.840
After training 1	Tube3	2	101.9	3.945	0.650	3.685
After training 2	Tube3	3	75.6	4.010	1.450	4.380
Before training	Tube4	6	98.1	2.554	0.630	2.240
After training 1	Tube4	1	126.4	3.423	0.535	2.755
After training 2	Tube4	6	109.3	4.044	0.885	3.110
Before training	Tube5	1	122.9	3.714	0.700	2.560
After training 1	Tube5	3	153.6	4.390	0.860	2.880
After training 2	Tube5	2	131.4	4.595	0.660	3.205
Before training	Tube6	4	129.3	3.368	0.795	2.205
After training 1	Tube6	4	162.5	3.448	0.540	2.235
After training 2	Tube6	1	149.9	3.752	0.730	2.430

APPENDIX F

PLOTS OF INHALATION VARIABLE(S) OVER TRAINING STATUS FOR ALL VOLUNTEERS, FOR EACH RESISTANCE TUBE EMPLOYED

- Inhalation flow cell is defined in Chapter 6, Section 6.2, and Appendices C & D.
- Methods used to document inhalation profiles are described in Chapter 6, Section 6.3

Table F.1: Diameter of the resistance tubes used in the study and corresponding inhalation flow cell air flow resistance.

Tube name	Actual tube Diameter (mm)	Actual resistance of inhalation flow cell $\text{kPa}^{0.5} \cdot \text{L}^{-1} \cdot \text{min}$
Tube 1	3.6	0.0462
Tube 2	3.8	0.0432
Tube 3	4.2	0.0344
Tube 4	5.2	0.0241
Tube 5	5.8	0.0200
Tube 6	6.5	0.0179

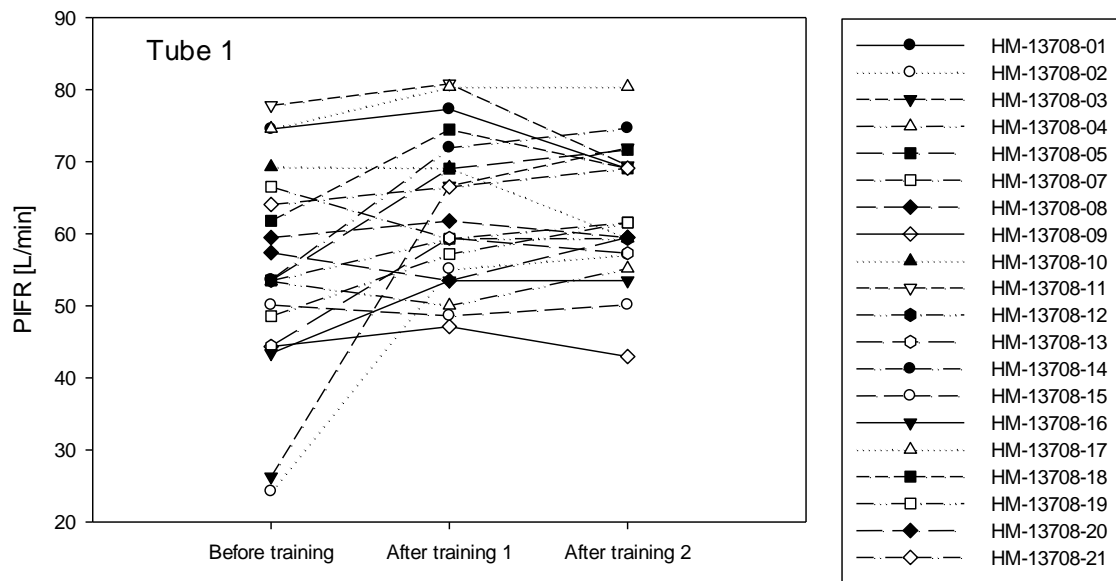


Figure F1: PIFR using Tube 1 over training status for all the volunteers

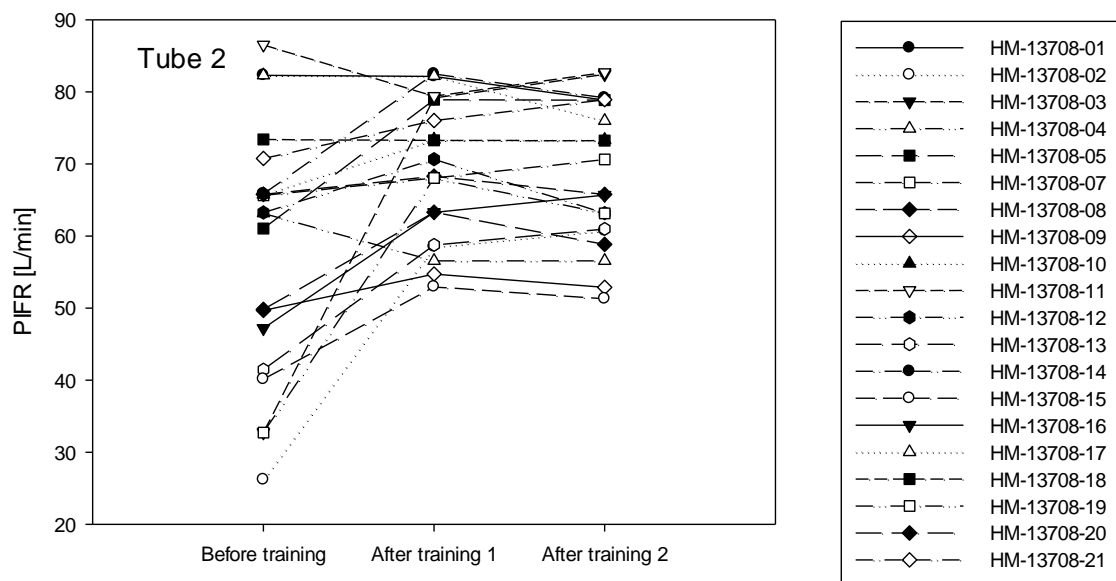


Figure F2: PIFR using Tube 2 over training status for all the volunteers

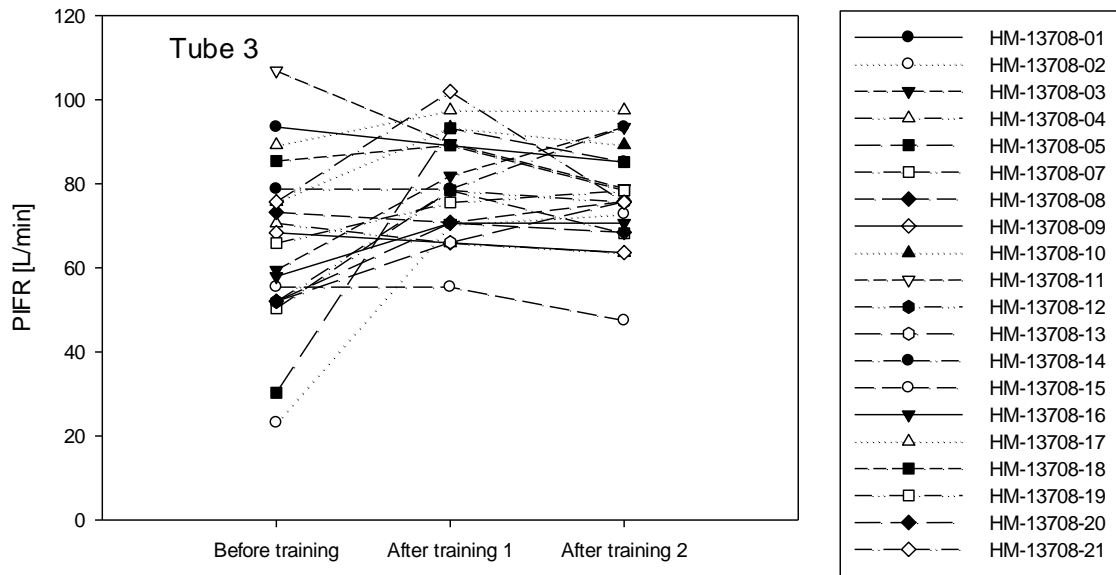


Figure F3: PIFR using Tube 3 over training status for all the volunteers

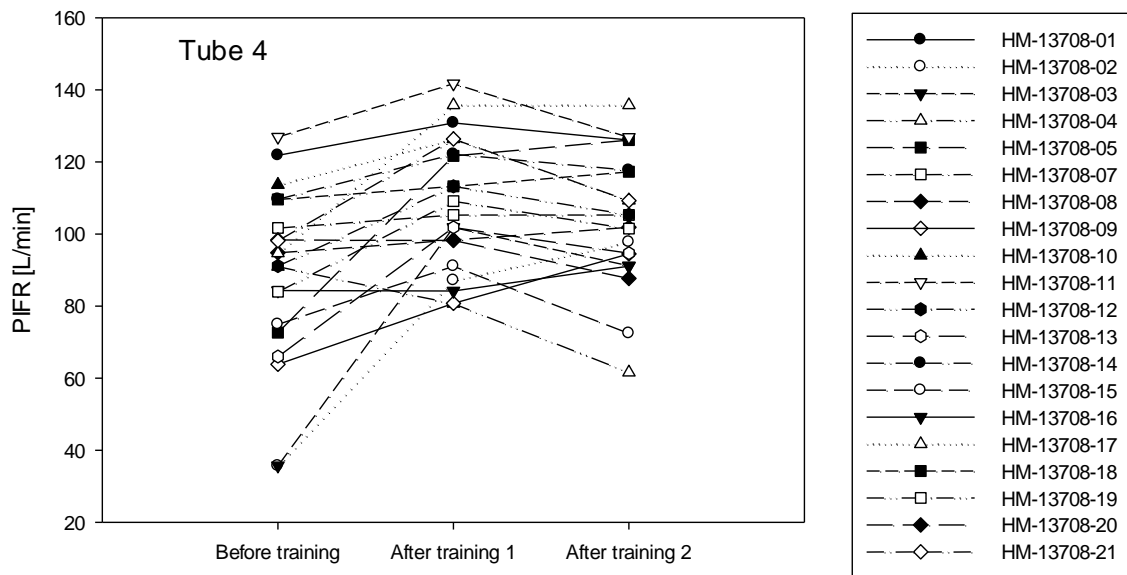


Figure F4: PIFR using Tube 4 over training status for all the volunteers

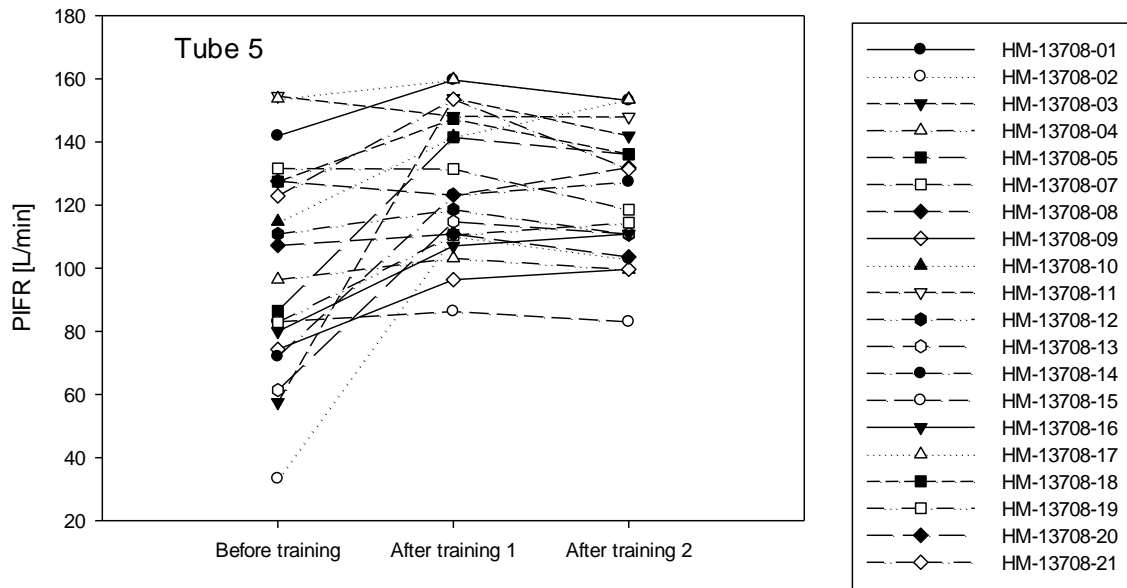


Figure F5: PIFR using Tube 5 over training status for all the volunteers

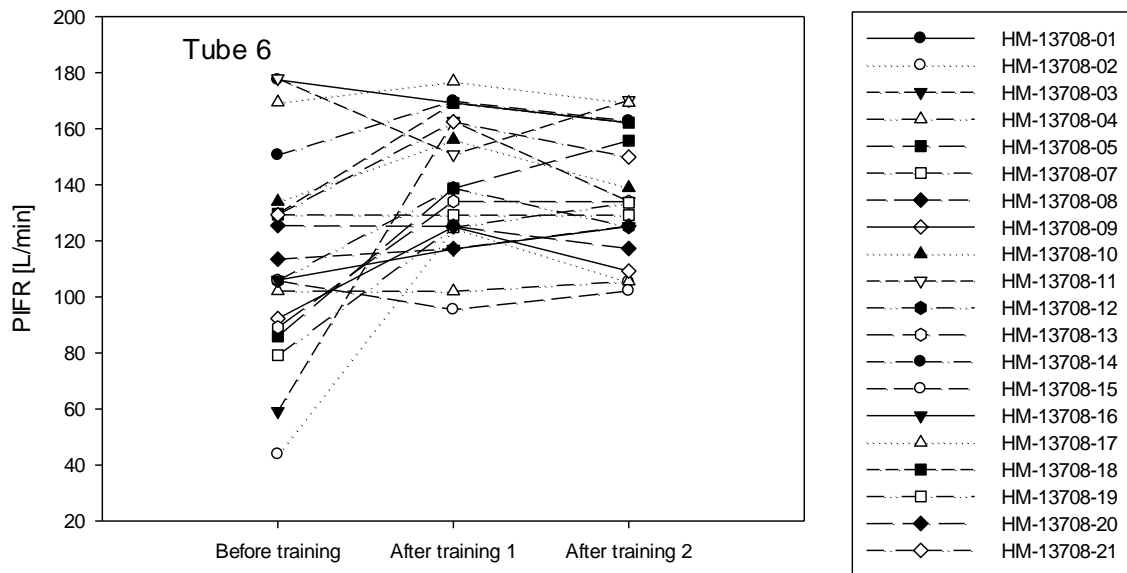


Figure F6: PIFR using Tube 6 over training status for all the volunteers

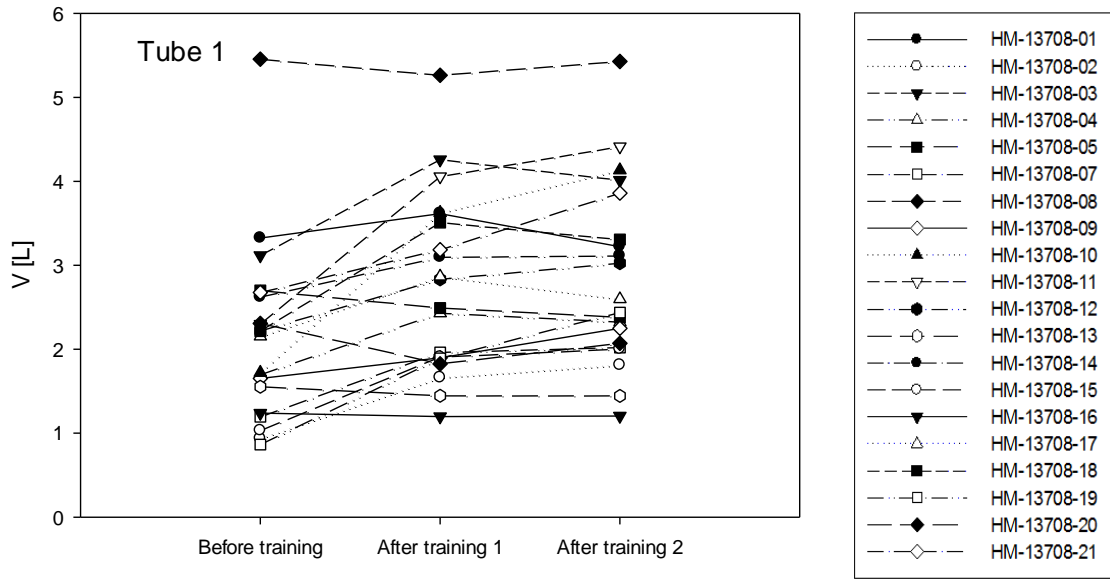


Figure F7: V using Tube 1 over training status for all the volunteers

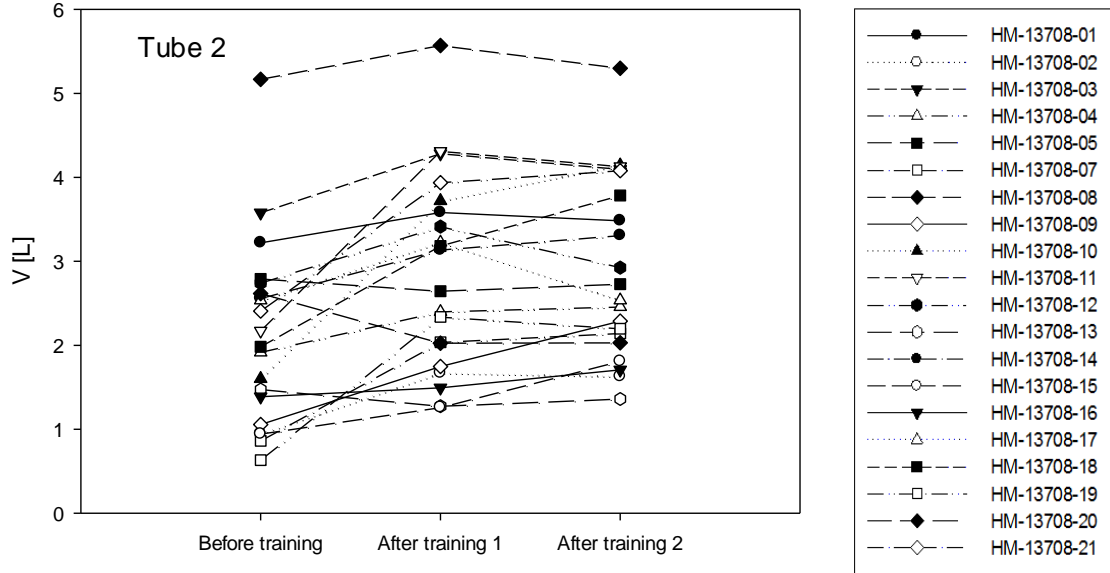


Figure F8: V using Tube 2 over training status for all the volunteers

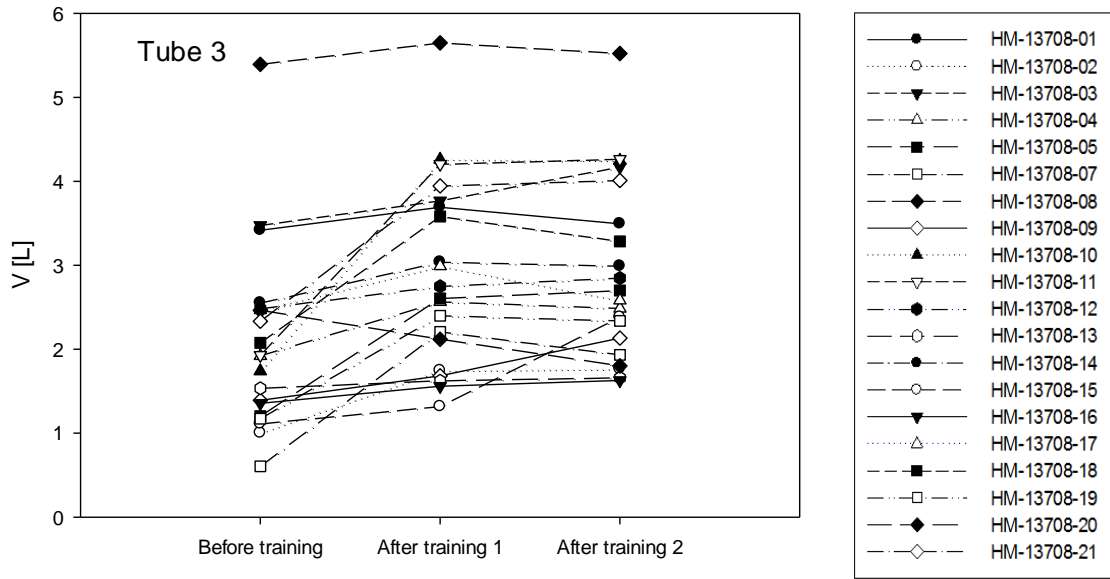


Figure F9: V using Tube 3 over training status for all the volunteers

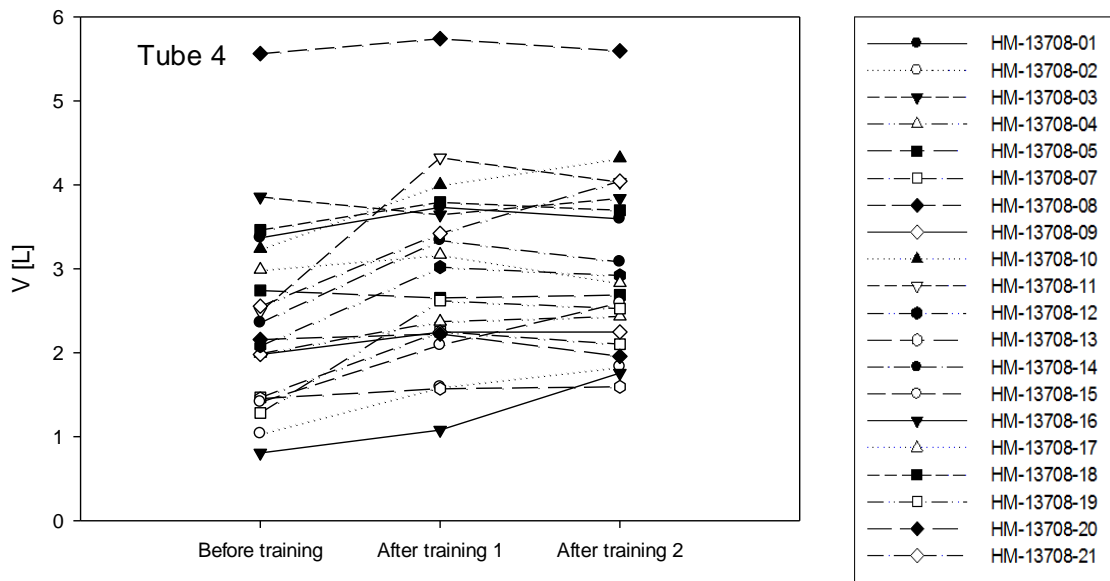


Figure F10: V using Tube 4 over training status for all the volunteers

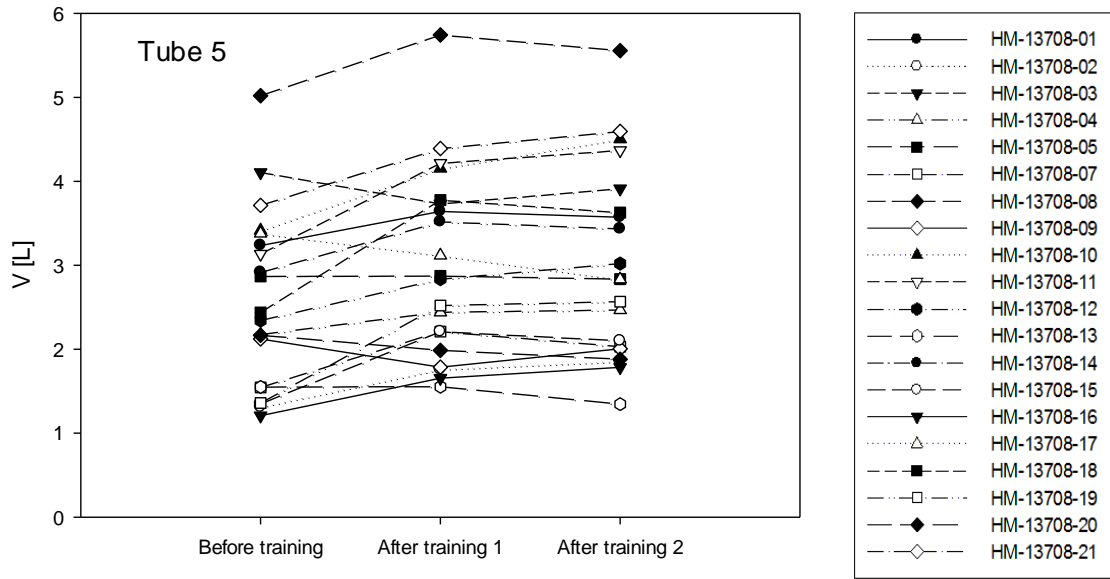


Figure F11: V using Tube 5 over training status for all the volunteers

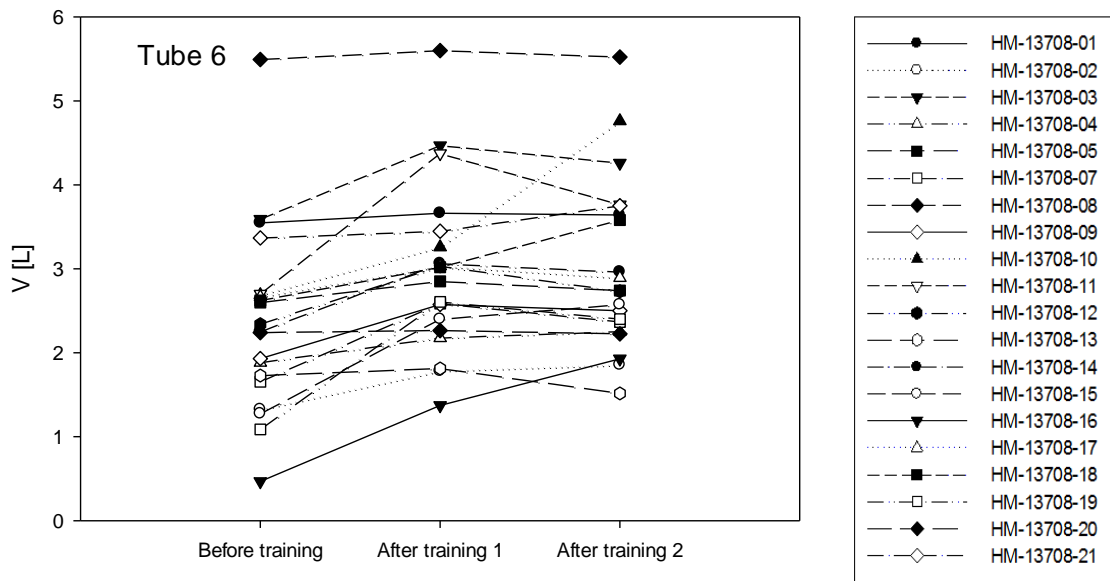


Figure F12: V using Tube 6 over training status for all the volunteers

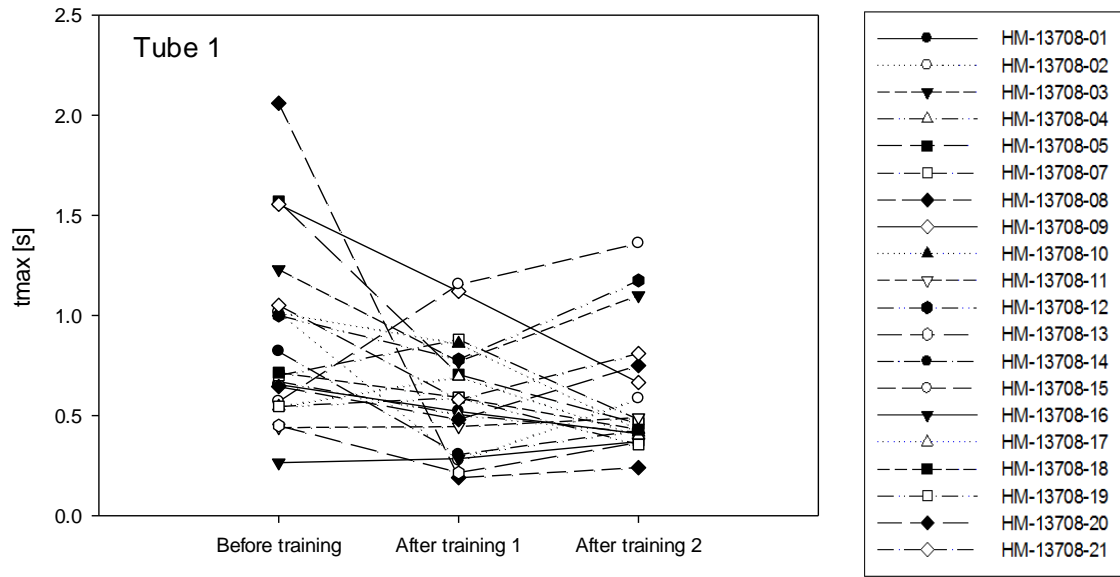


Figure F13: t_{max} using Tube 1 over training status for all the volunteers

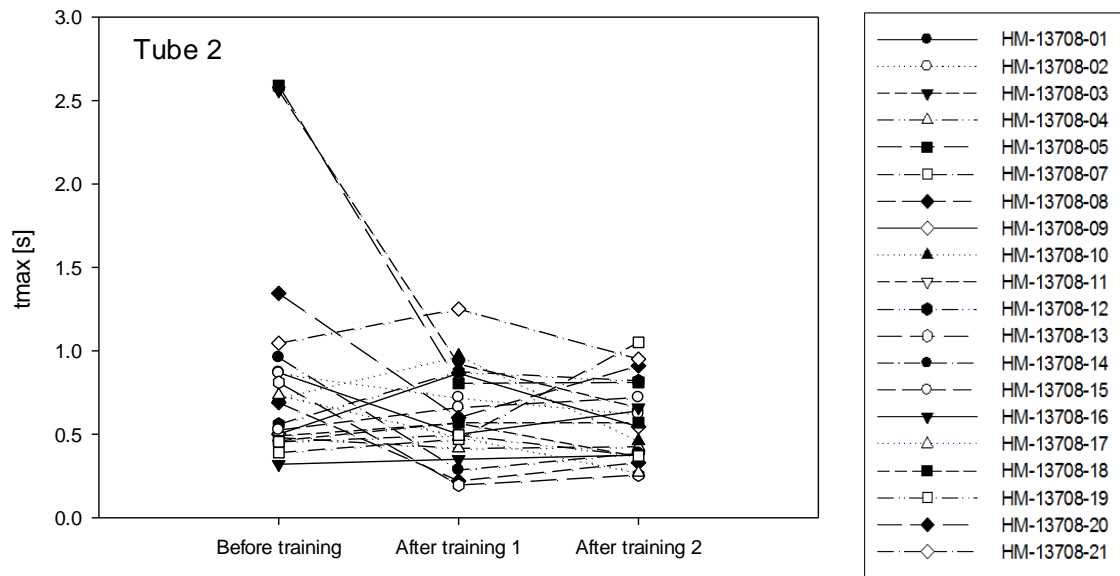


Figure F14: t_{max} using Tube 2 over training status for all the volunteers

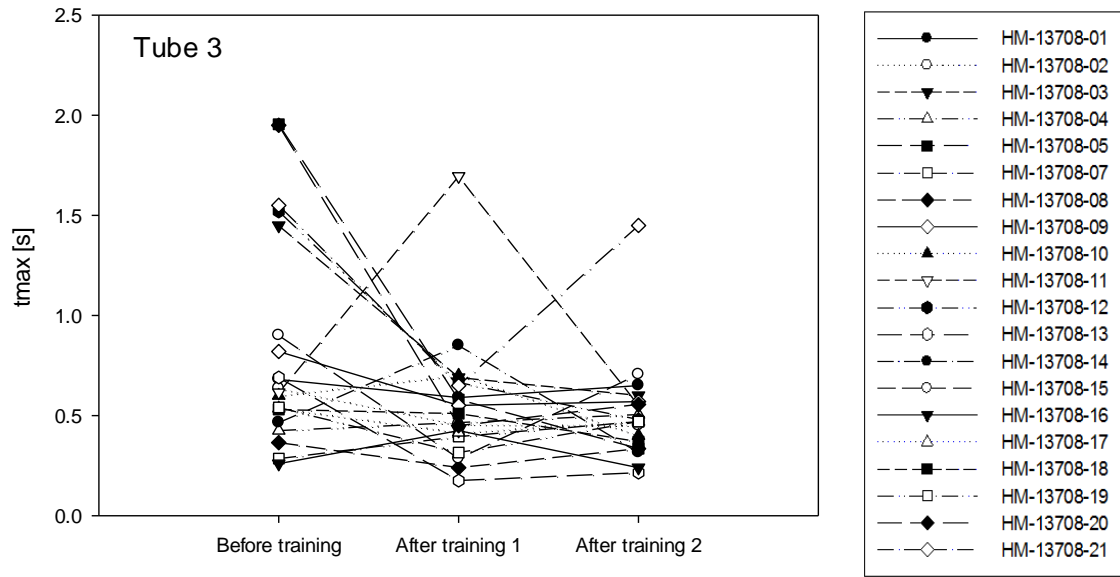


Figure F15: t_{max} using Tube 3 over training status for all the volunteers

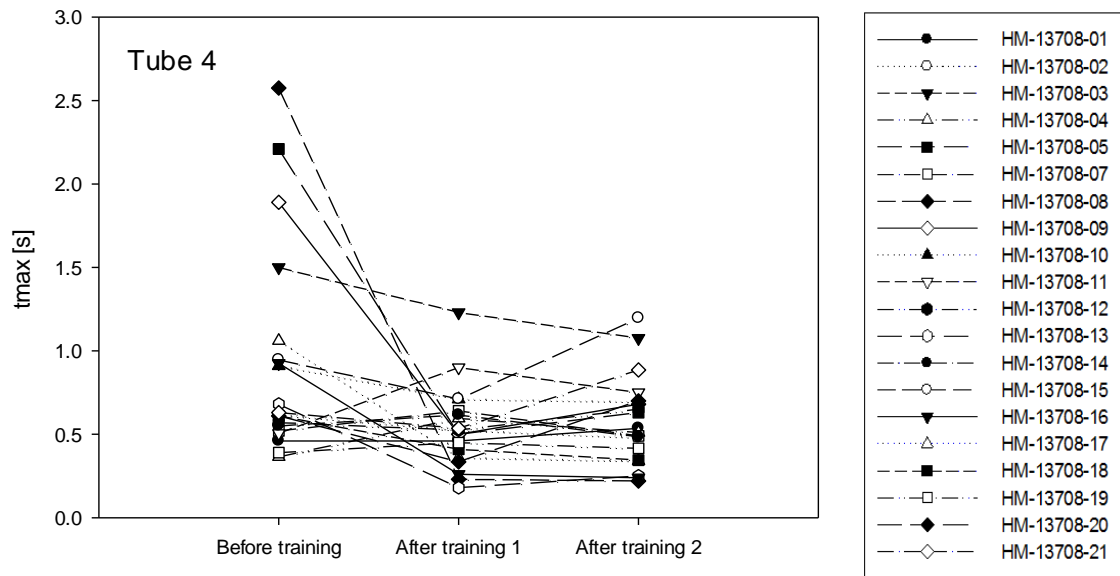


Figure F16: t_{max} using Tube 4 over training status for all the volunteers

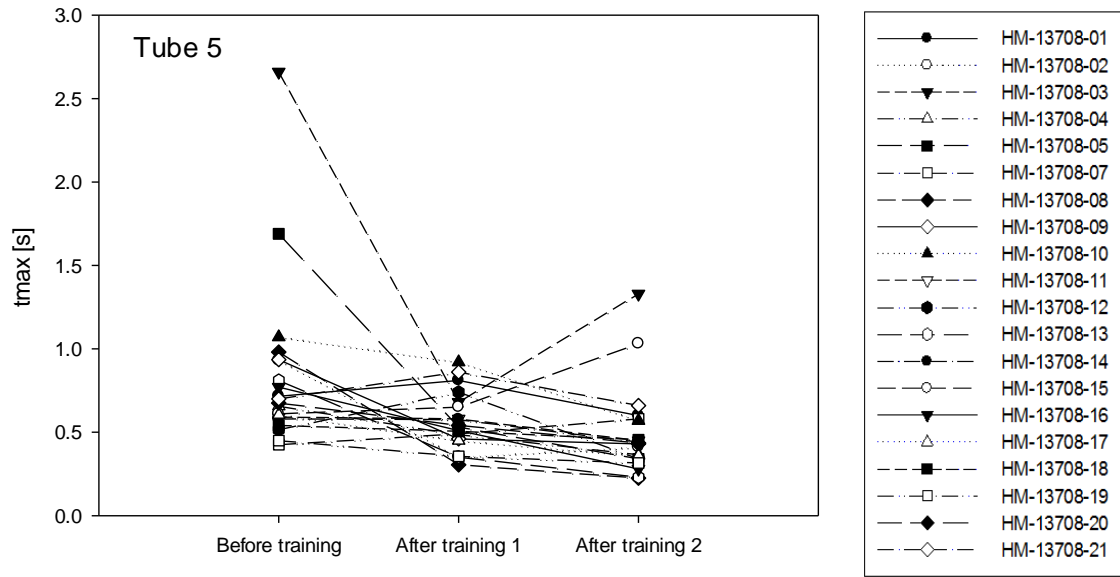


Figure F17: t_{\max} using Tube 5 over training status for all the volunteers

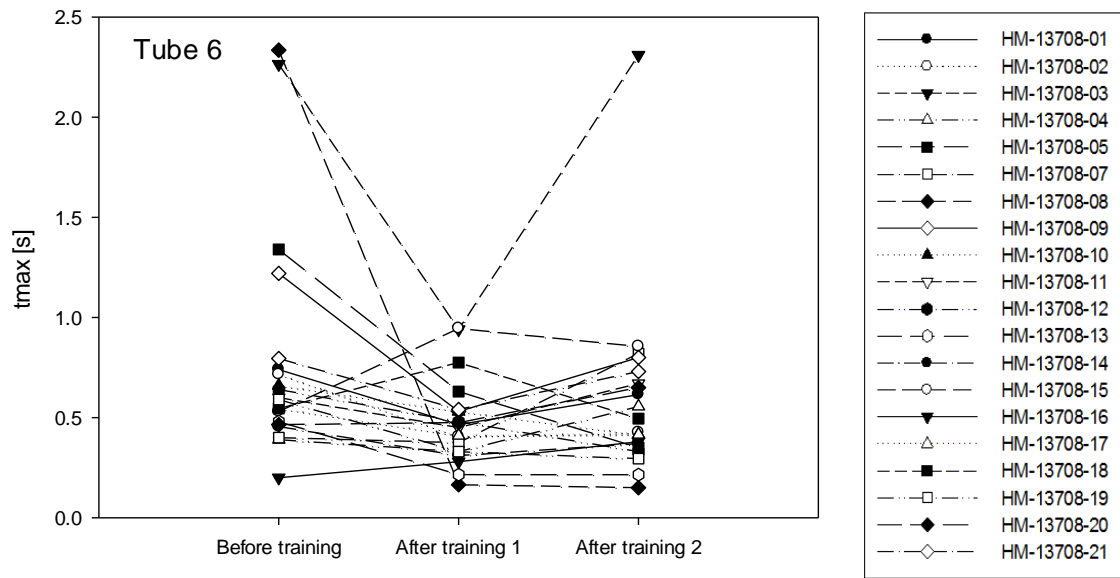


Figure F18: t_{\max} using Tube 6 over training status for all the volunteers

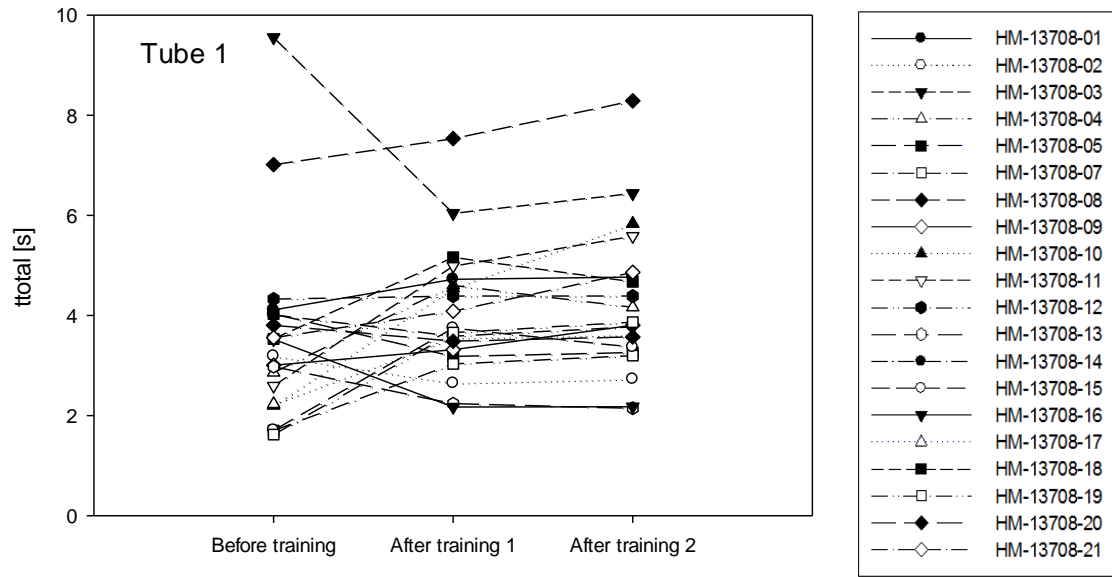


Figure F19: t_{total} using Tube 1 over training status for all the volunteers

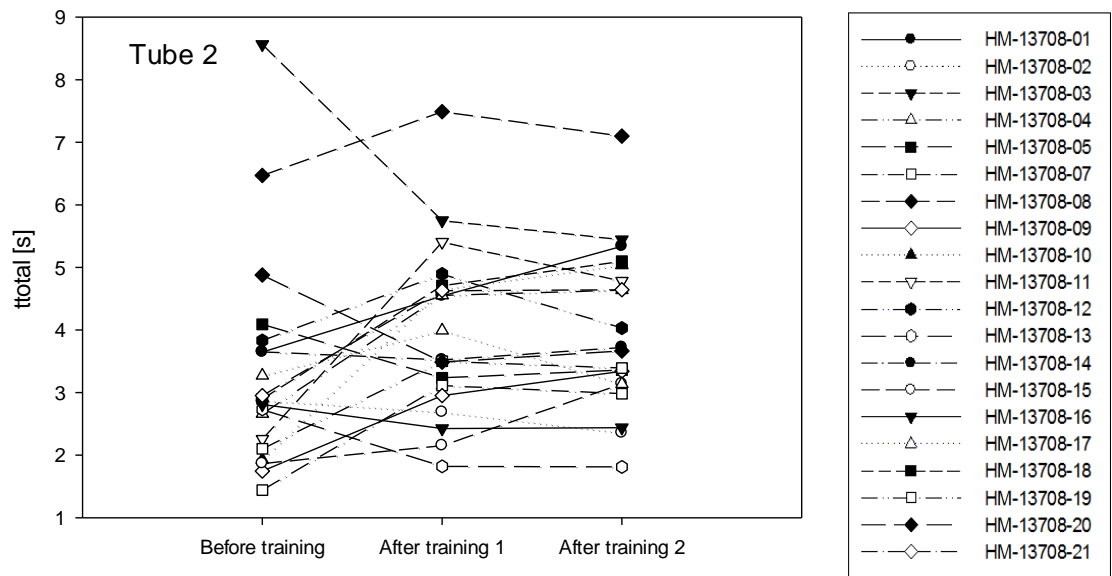


Figure F20: t_{total} using Tube 2 over training status for all the volunteers

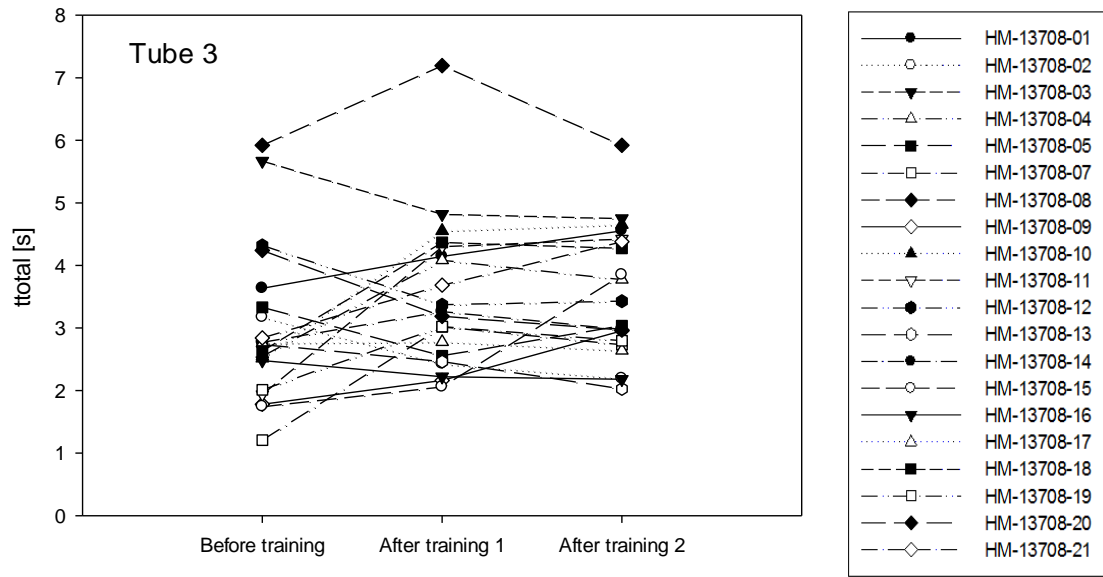


Figure F21: t_{total} using Tube 3 over training status for all the volunteers

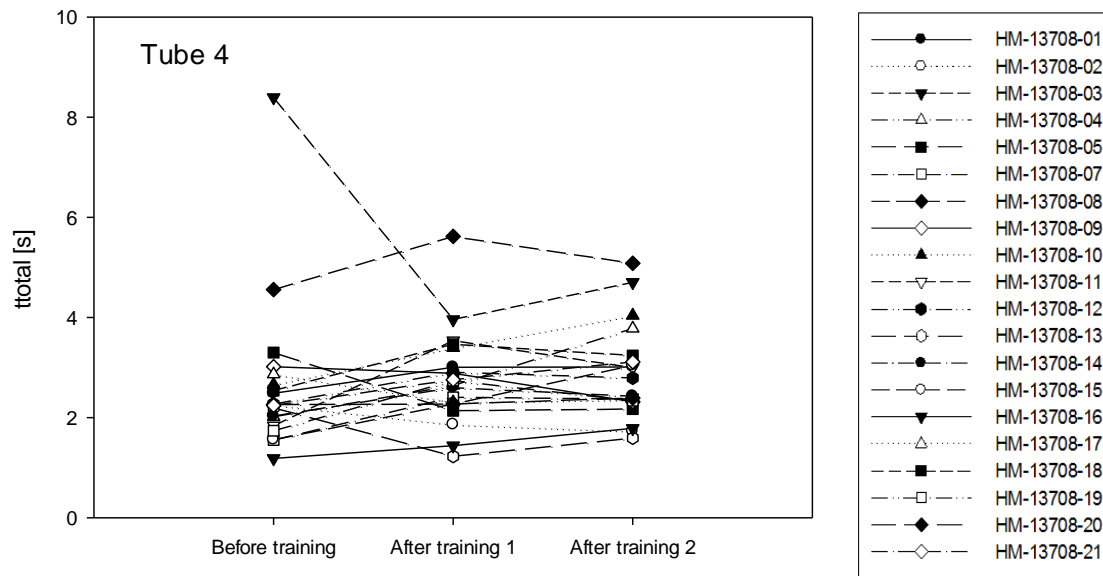


Figure F22: t_{total} using Tube 4 over training status for all the volunteers

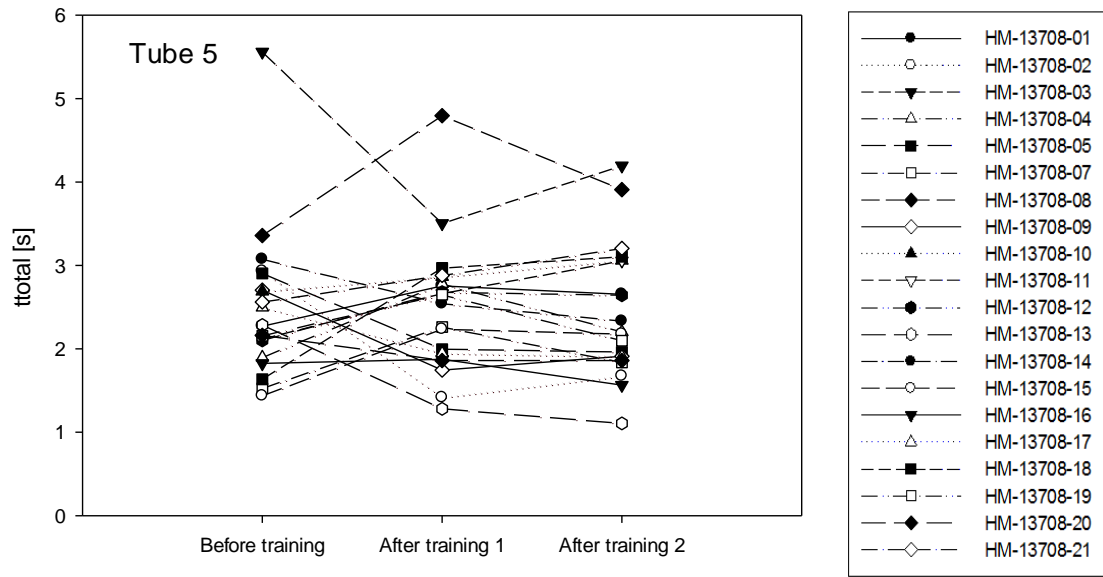


Figure F23: t_{total} using Tube 5 over training status for all the volunteers

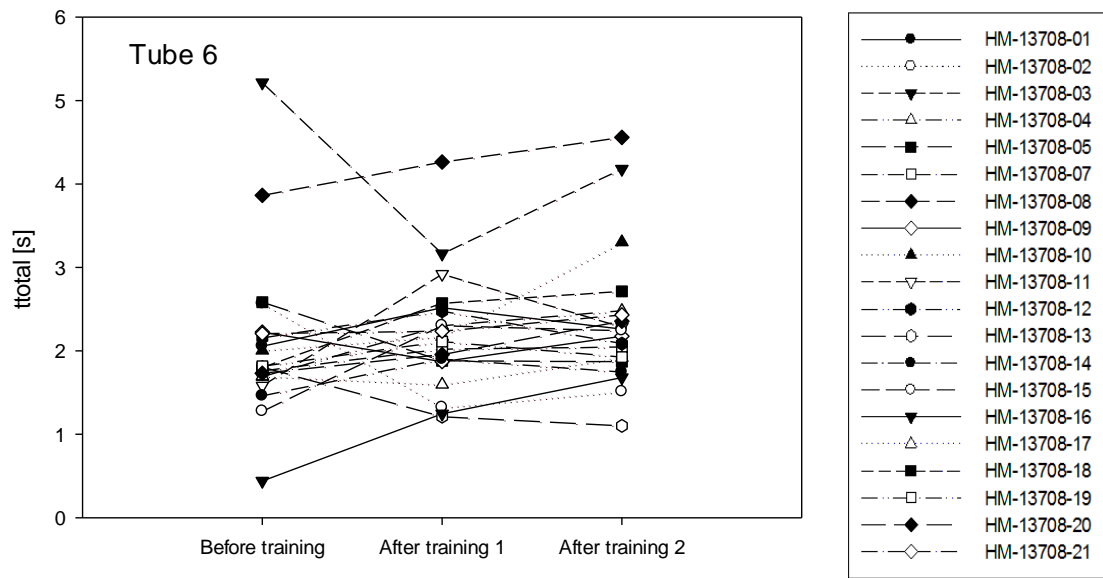


Figure F24: t_{total} using Tube 6 over training status for all the volunteers

APPENDIX G

**INDIVIDUAL RESULTS FOR 'COEFFICIENT OF DETERMINATION' (R SQUARED)
OF THE LINEAR REGRESSION PLOTS OF INHALATION VARIABLE(S) VALUES
VERSUS DIFFERENTLY TRANSFORMED VALUES FOR AIR FLOW RESISTANCE.**

Table G.1: Individual results for coefficient of determination (r squared) of the linear regression plots of PIFR versus differently transformed values of air flow resistance; values in **bold** indicates the transformation that gave best fit among four.

Training Status	Volunteer (HM-13708-)	R	1/R	LogR	R ^{0.5}
Before training	1	0.881	0.969	0.933	0.909
	2	0.727	0.829	0.786	0.758
	3	0.491 (NS)	0.447 (NS)	0.467 (NS)	0.479 (NS)
	4	0.986	0.961	0.985	0.988
	5	0.483 (NS)	0.616 (NS)	0.559 (NS)	0.523 (NS)
	7	0.757	0.869	0.826	0.794
	8	0.892	0.912	0.914	0.906
	9	0.805	0.826	0.818	0.812
	10	0.920	0.960	0.952	0.938
	11	0.930	0.983	0.964	0.949
	12	0.827	0.891	0.872	0.852
	13	0.770	0.839	0.810	0.791
	14	0.559 (NS)	0.590 (NS)	0.577 (NS)	0.568 (NS)
	15	0.859	0.944	0.911	0.882
	16	0.906	0.9311	0.928	0.919
	17	0.742	0.875	0.813	0.778
	18	0.982	0.975	0.990	0.989
	19	0.930	0.719	0.786	0.811
	20	0.857	0.944	0.913	0.888
	21	0.915	0.986	0.961	0.940
	After training 1	1	0.926	0.989	0.970
2		0.914	0.987	0.959	0.939
3		0.826	0.933	0.888	0.858
4		0.945	0.971	0.969	0.959
5		0.982	0.962	0.984	0.986
7		0.957	0.974	0.977	0.970
8		0.912	0.950	0.944	0.931
9		0.867	0.950	0.914	0.892
10		0.908	0.993	0.998	0.992
11		0.938	0.935	0.951	0.949
12		0.953	0.975	0.975	0.966
13		0.912	0.985	0.960	0.939
14		0.800	0.900	0.857	0.830
15		0.913	0.904	0.922	0.921
16		0.912	0.976	0.952	0.934
17		0.945	0.999	0.983	0.967
18		0.884	0.978	0.940	0.913
19		0.964	0.959	0.973	0.972

	20	0.956	0.992	0.984	0.972
	21	0.980	0.982	0.991	0.988
After training 2	1	0.940	0.990	0.976	0.960
	2	0.989	0.952	0.983	0.990
	3	0.760	0.830	0.801	0.782
	4	0.695	0.829	0.766	0.731
	5	0.939	0.985	0.976	0.959
	7	0.910	0.971	0.953	0.934
	8	0.936	0.960	0.961	0.951
	9	0.984	0.966	0.987	0.989
	10	0.915	0.919	0.928	0.924
	11	0.892	0.973	0.943	0.919
	12	0.972	0.982	0.989	0.983
	13	0.917	0.981	0.957	0.939
	14	0.884	0.955	0.927	0.907
	15	0.794	0.927	0.869	0.833
	16	0.919	0.982	0.960	0.941
	17	0.958	0.992	0.987	0.975
	18	0.895	0.983	0.949	0.924
	19	0.945	0.992	0.979	0.964
	20	0.915	0.992	0.963	0.941
	21	0.868	0.968	0.927	0.899

NS – Not significant ($\alpha = 0.05$)

Table G.2: Individual results for coefficient of determination (r squared) of the linear regression plots of V versus differently transformed values of air flow resistance; values in **bold** indicates transformation that gave best fit among four.

Training Status	Volunteer (HM-13708-)	R	1/R	LogR	R ^{0.5}
Before training	1	NS	NS	NS	NS
	2	0.782	0.891	0.843	0.818
	3	NS	NS	NS	NS
	4	NS	NS	NS	NS
	5	NS	NS	NS	NS
	7	NS	NS	NS	NS
	8	NS	NS	NS	NS
	9	NS	NS	NS	NS
	10	0.756	0.796	0.742	0.753
	11	NS	NS	NS	NS
	12	NS	NS	NS	NS
	13	NS	NS	NS	NS
	14	NS	NS	NS	NS
	15	0.800	0.685	0.755	0.779
	16	NS	NS	NS	NS
	17	NS	NS	NS	NS
	18	NS	NS	NS	NS
	19	NS	NS	NS	NS
	20	NS	NS	NS	NS
	21	NS	NS	NS	NS
	After training 1	1	NS	NS	NS
2		NS	NS	NS	NS
3		NS	NS	NS	NS
4		NS	NS	NS	NS
5		0.753	0.817	0.791	0.773
7		0.778	0.752	0.737	0.778
8		NS	NS	NS	NS
9		NS	NS	NS	NS
10		NS	NS	NS	NS
11		NS	NS	NS	NS
12		NS	NS	NS	NS
13		NS	NS	NS	NS
14		NS	NS	NS	NS
15		NS	NS	NS	NS
16		NS	NS	NS	NS
17		NS	NS	NS	NS
18		NS	NS	NS	NS
19		0.732	NS	0.670	NS

	20	NS	NS	NS	NS
	21	NS	NS	NS	NS
After training 2	1	0.734	NS	0.692	0.716
	2	NS	NS	NS	NS
	3	NS	NS	NS	NS
	4	NS	NS	NS	NS
	5	NS	NS	NS	NS
	7	NS	NS	NS	NS
	8	NS	NS	NS	NS
	9	NS	NS	NS	NS
	10	0.789	0.907	0.852	0.821
	11	NS	NS	NS	NS
	12	NS	NS	NS	NS
	13	NS	NS	NS	NS
	14	NS	NS	NS	NS
	15	NS	NS	NS	NS
	16	NS	NS	NS	NS
	17	0.874	0.909	0.906	0.893
	18	NS	NS	NS	NS
	19	NS	NS	NS	NS
	20	NS	NS	NS	NS
	21	NS	NS	NS	NS

NS – Not significant ($\alpha = 0.05$)

Table G.3: Individual results for coefficient of determination (r squared) of the linear regression plots of t_{\max} versus differently transformed values of air flow resistance (only significant relationships are shown); values in **bold** indicates the transformation that gave best fit among four.

Training Status	Volunteer (HM-13708-)	R	1/R	LogR	$R^{0.5}$
After training 1	09	0.785	NS	0.700	0.744
After training 2	02	0.791	0.698	0.750	0.772
After training 2	12	0.752	0.668	0.716	0.732

NS – Not significant ($\alpha = 0.05$)

Table G.4: Individual results for coefficient of determination (r squared) of the linear regression plots of t_{total} versus differently transformed values of air flow resistance; values in **bold** indicates transformation that gave best fit among four.

Training Status	Volunteer (HM-13708-)	R	1/R	LogR	R ^{0.5}
Before training	1	0.947	0.950	0.961	0.957
	2	0.373 (NS)	0.330 (NS)	0.358 (NS)	0.367 (NS)
	3	0.529 (NS)	0.504 (NS)	0.515 (NS)	0.522 (NS)
	4	0.969	0.976	0.984	0.978
	5	0.91	0.904	0.914	0.914
	7	0.051 (NS)	0.153 (NS)	0.098 (NS)	0.073 (NS)
	8	0.655	0.934	0.957	0.959
	9	0.031 (NS)	0.038 (NS)	0.038 (NS)	0.035 (NS)
	10	0.167 (NS)	0.066 (NS)	0.115 (NS)	0.141 (NS)
	11	0.657 (NS)	0.576 (NS)	0.617 (NS)	0.338 (NS)
	12	0.832	0.849	0.855	0.847
	13	0.862	0.900	0.890	0.878
	14	0.692	0.635 (NS)	0.667	0.681
	15	0.789	0.908	0.856	0.824
	16	0.849	0.831	0.847	0.83
	17	0.185 (NS)	0.316 (NS)	0.247 (NS)	0.215 (NS)
	18	0.855	0.849	0.858	0.858
	19	0.025 (NS)	0.011 (NS)	0.016 (NS)	0.02 (NS)
	20	0.807	0.857	0.846	0.83
	21	0.817	0.718	0.774	0.798
	After training 1	1	0.982	0.973	0.990
2		0.944	0.990	0.979	0.964
3		0.997	0.961	0.989	0.996
4		0.953	0.934	0.957	0.958
5		0.979	0.911	0.956	0.970
7		0.898	0.968	0.945	0.925
8		0.925	0.991	0.970	0.950
9		0.611 (NS)	0.598 (NS)	0.605 (NS)	0.609 (NS)
10		0.86	0.966	0.923	0.894
11		0.938	0.920	0.942	0.943
12		0.91	0.838	0.884	0.900
13		0.631 (NS)	0.681 (NS)	0.668 (NS)	0.652 (NS)
14		0.912	0.962	0.946	0.931
15		0.277 (NS)	0.173 (NS)	0.221 (NS)	0.248 (NS)
16		0.699	0.729	0.724	0.713
17		0.932	0.910	0.931	0.934
18		0.971	0.986	0.989	0.983
19		0.927	0.926	0.934	0.933

	20	0.955	0.955	0.969	0.966
	21	0.894	0.889	0.903	0.901
After training 2	1	0.923	0.950	0.950	0.939
	2	0.964	0.910	0.947	0.958
	3	0.848	0.744	0.800	0.825
	4	0.758	0.829	0.802	0.781
	5	0.958	0.960	0.972	0.967
	7	0.942	0.922	0.944	0.946
	8	0.933	0.838	0.895	0.916
	9	0.957	0.875	0.927	0.945
	10	0.936	0.907	0.931	0.936
	11	0.955	0.928	0.952	0.956
	12	0.974	0.948	0.970	0.975
	13	0.802	0.890	0.855	0.830
	14	0.964	0.944	0.963	0.966
	15	0.535 (NS)	0.695 (NS)	0.621 (NS)	0.578 (NS)
	16	0.846	0.859	0.867	0.860
	17	0.958	0.892	0.934	0.948
	18	0.941	0.940	0.953	0.950
	19	0.976	0.900	0.947	0.964
	20	0.913	0.835	0.887	0.903
	21	0.932	0.951	0.952	0.945

NS – Not significant ($\alpha = 0.05$)

APPENDIX H

IRB DOCUMENTS

(STUDY – HM-13708)

H.1 VCU IRB HM-13708 APPROVAL LETTER



MCV CAMPUS



DATE: July 12, 2011

TO: Peter R. Bryon, PhD
Department of Pharmaceutics
Box 980533

FROM: John D. Roberts, MD
Chairperson, VCU IRB Panel A
Box 980568

RE: **VCU IRB #: HM13708**
Title: Assessment of Inspiratory Profiles through Airflow Resistances Designed to Mimic Inhalers

BTT for VDR
7/12/11

Office of Research
Office of Research Subjects' Protection
Biotech Research Park, Bldg. 1
800 East Leigh Street, Ste. 114
P.O. Box 980568
Richmond, VA 23298-0568
(804) 828-0868 - Phone
(804) 828-1448 - Fax
(804) 828-1120 - TDD

On June 27, 2011, the following research study was approved by expedited review according to 45 CFR 46.110 Category 4. This determination reflects the revisions received in the Office of Research Subjects Protection on June 27, 2011. This approval includes the following items reviewed by this Panel:

RESEARCH APPLICATION/PROPOSAL: None

PROTOCOL: Assessment of Inspiratory Profiles through Airflow Resistances Designed to Mimic Inhalers
(VCU Research Plan, dated 5/12/11)

CONSENT/ASSENT:

- Research Subject Information and Consent Form (dated 6/01/11; 5 pages)

ADDITIONAL DOCUMENTS:

- Advertisement for Richmond Times Dispatch (received 6/01/11; 1 pages)
- Recruitment Flyer (received 6/27/11)

HIPAA PROCESS:

The following pathways for accessing and/or using PHI have been approved:

- Signed Authorization Form (independent form)

This approval expires on May 31, 2012. Federal Regulations/VCU Policy and Procedures require continuing review prior to continuation of approval past that date. Continuing Review report forms will be mailed to you prior to the scheduled review.

The Primary Reviewer assigned to your research study is Benjamin Van Tassell, PharmD. If you have any questions, please contact Dr. Van Tassell at bvtassell@vcu.edu or 828-4583; or you may contact Stephan Hicks, IRB Coordinator, VCU Office of Research Subjects Protection, at irbpanela@vcu.edu or 828-9876.

Attachment – Conditions of Approval

Conditions of Approval:

In order to comply with federal regulations, industry standards, and the terms of this approval, the investigator must (as applicable):

1. Conduct the research as described in and required by the Protocol.
2. Obtain informed consent from all subjects without coercion or undue influence, and provide the potential subject sufficient opportunity to consider whether or not to participate (unless Waiver of Consent is specifically approved or research is exempt).
3. Document informed consent using only the most recently dated consent form bearing the VCU IRB "APPROVED" stamp (unless Waiver of Consent is specifically approved).
4. Provide non-English speaking patients with a translation of the approved Consent Form in the research participant's first language. The Panel must approve the translated version.
5. Obtain prior approval from VCU IRB before implementing any changes whatsoever in the approved protocol or consent form, unless such changes are necessary to protect the safety of human research participants (e.g., permanent/temporary change of PI, addition of performance/collaborative sites, request to include newly incarcerated participants or participants that are wards of the state, addition/deletion of participant groups, etc.). Any departure from these approved documents must be reported to the VCU IRB immediately as an Unanticipated Problem (see #7).
6. Monitor all problems (anticipated and unanticipated) associated with risk to research participants or others.
7. Report Unanticipated Problems (UPs), including protocol deviations, following the VCU IRB requirements and timelines detailed in VCU IRB WPP VIII-7):
8. Obtain prior approval from the VCU IRB before use of any advertisement or other material for recruitment of research participants.
9. Promptly report and/or respond to all inquiries by the VCU IRB concerning the conduct of the approved research when so requested.
10. All protocols that administer acute medical treatment to human research participants must have an emergency preparedness plan. Please refer to VCU guidance on <http://www.research.vcu.edu/irb/guidance.htm>.
11. The VCU IRBs operate under the regulatory authorities as described within:
 - a) U.S. Department of Health and Human Services Title 45 CFR 46, Subparts A, B, C, and D (for all research, regardless of source of funding) and related guidance documents.
 - b) U.S. Food and Drug Administration Chapter I of Title 21 CFR 50 and 56 (for FDA regulated research only) and related guidance documents.
 - c) Commonwealth of Virginia Code of Virginia 32.1 Chapter 5.1 Human Research (for all research).

010507

H.2 SUBJECT INFORMATION AND CONSENT FORM (APPROVED BY VCU-IRB)

Page 1 of 5

RESEARCH SUBJECT INFORMATION AND CONSENT FORM

TITLE: Assessment of Inspiratory Profiles through Airflow Resistances Designed to Mimic Inhalers

VCU IRB PROTOCOL NUMBER: HM13708

INVESTIGATOR: Peter R. Byron, PhD

CO-INVESTIGATORS: Renish R. Delvadia, M.Pharm, PhD candidate

MEDICAL MONITOR: John N. Clore, MD



This consent form may contain words that you do not understand. Please ask the study doctor or the study staff to explain any words or information that you do not clearly understand. You may take home an unsigned copy of this consent form to think about or discuss with family or friends before making your decision.

PURPOSE OF THE STUDY

The purpose of this research is to study the breathing of healthy adults when using inhalers. No drugs will be used in this study, but the results will be used to design better inhalers. We are studying the way that breathing techniques affect the way that drugs deposit in the lungs and how breathing changes with inhaler design. We also studying the effect of instruction on breathing technique. You are being asked to participate in this study because you may meet the study entry requirements.

DESCRIPTION OF THE STUDY

Twenty healthy adults that are between the ages of 18-80 years will be enrolled in the study. After a brief phone interview, the study includes two visits over the course of 1-2 weeks. On your first visit, you will be asked to provide information about your age, gender and medical history. You will also undergo lung function testing. This test will check that your lungs are working normally. At the later, second visit, we will record the way you inhale through differently sized tubes, and how this may change, depending on the instructions you are given. Your participation in this study will last approximately 2 hours for visit 1 and 4 hours for visit 2.

PROCEDURES

If you decide to be in this research study, you will be asked to sign this consent form after you have had all your questions answered.

At your first study visit (Visit 1), age, gender and pertinent health information such as medical and smoking history, medication history and present medications will be

BVT / SH / 6/27/11
APPROVED

Assessment of Inspiratory Profiles through Airflow Resistances Designed to Mimic Inhalers 06/01/2011

reviewed. Your pulse rate, blood pressure, height and weight will be measured. Lung function tests will be performed where your breathing profiles will be recorded after specific instructions are given to you. These tests will help us to determine whether or not you are eligible for the second phase of the study.

Visit 2 will take place approximately one week after Visit 1. Your pulse rate and blood pressure will be measured. Once again, your breathing profiles will be documented but this time you will be asked to use a different device containing a tube through which you will inhale on about 20 occasions. The results will be studied to understand how they vary in response to different sized tubes and different instructions.

RISKS AND DISCOMFORTS

Forceful inhalation or exhalation on several occasions may cause headache, fatigue, dizziness and discomfort in some people. Furthermore, we will collect private information from you that will be kept confidential and stored for several years. Because circumstances exist, under which the investigators may be legally required to disclose this data to authorities such as the US Food and Drug Administration (FDA), there is a very small risk that your information may be shared with others.

BENEFITS TO YOU AND OTHERS

This is not a treatment study, and you will not receive any direct medical benefits from your participation. The information from this research study may lead in the future to the creation of better inhalers and better treatments for people

COSTS

There are no charges to you for any laboratory test, for the study visits or other tests related to the conduct of this study.

PAYMENT FOR PARTICIPATION

You will be paid \$200 if you complete both scheduled study visits. If you do not qualify for the second study visit, you will be paid \$25 for travel and \$ 25 per hour spent performing lung function tests in the first study visit. If you withdraw from visit 2 before trial completion, your payment for visit 2 will be \$25 for travel and \$25 per hour completed.

ALTERNATIVE

Your alternative is not to participate in this study.

CONFIDENTIALITY

Potentially identifiable information about you will consist of medical and smoking histories, and personal research data. Data is being collected only for research purposes.

BVT / SH / 6/27/11
APPROVED

Your data will be identified by ID numbers and birthdates, not names, and stored separately from medical records in a locked research area. All personal identifying information will be kept in password-protected files and these files will be stored for at least 5 years from study end. Other records, such as medical and smoking histories, spirometry test results, and inhalation profiles will be kept in a locked file cabinet for at least 5 years after the study ends. Access to all data will be limited to study personnel who are bound to maintain your confidentiality.

You should know that research data or medical information about you may be reviewed or copied by Virginia Commonwealth University, if applicable. Personal information about you might be shared with or copied by authorized officials of the Federal Food and Drug Administration, or the Department of Health and Human Services.

Although results of this research may be presented at meetings or in publications, identifiable personal information pertaining to participants will not be disclosed.

COMPENSATION FOR INJURY

Virginia Commonwealth University and the VCU Health System (formerly known as Medical College of Virginia Hospitals) have no plan for providing long-term care or compensation in the event that you suffer injury as a result of your participation in this research study.

If you are injured or if you become ill as a result of your participation in this study, contact your study doctor immediately. Your study doctor will arrange for short-term emergency care or referral if it is needed.

Fees for such treatment may be billed to you or to appropriate third party insurance. Your health insurance company may or may not pay for treatment of injuries as a result of your participation in this study.

VOLUNTARY PARTICIPATION AND WITHDRAWAL

Your participation in this study is voluntary. You may decide to not participate in this study. Your decision not to take part will involve no penalty or loss of benefits to which you are otherwise entitled. If you do participate, you may freely withdraw from the study at any time. Your decision to withdraw will involve no penalty or loss of benefits to which you are otherwise entitled.

Your participation in this study may be stopped at any time by the study doctor or the sponsor without your consent. The reasons might include:

- the study doctor thinks it necessary for your health or safety;
- you have not followed study instructions;
- the investigator has stopped the study; or
- administrative reasons require your withdrawal.

APPROVED
BUT / SAH / 6/27/11

H.3 ADVERTISEMENT (FOR FLYERS)

VCU Clinical Trials
Virginia Commonwealth University
Every Day, A New Discovery.



Do you breathe normally?

The VCU Department of Pharmaceutics, School of Pharmacy is conducting a research study for 18 to 65 year old healthy volunteers. **No blood or any other biological samples will be collected and you will not be exposed to drugs.**

You may be able to participate in this study if you **DO NOT** suffer from asthma or any other lung disease. Investigators will review additional criteria with you.

If you qualify for the study, you will be asked to come to the VCU School of Pharmacy twice over the course of one or two weeks. Each study subject will be reimbursed for their time and travel costs.

For your participation or any further information, please contact
Renish Delvadia
VCU Dept. of Pharmaceutics
(804)-615-7332 or (804)-828-6102
delvadia@vcu.edu

BUT / SH / 6/27/11
APPROVED

H.4 ADVERTISEMENT (FOR RICHMOND TIMES DISPATCH)

Advertisement for Richmond Times-Dispatch



Do you breathe normally?

The VCU Department of Pharmaceutics, School of Pharmacy is conducting a research study for 18 to 65 year old healthy volunteers. **No blood or any other biological samples will be collected and you will not be exposed to drugs.**

You may be able to participate in this study if you **DO NOT** suffer from asthma or any other lung disease. Investigators will review additional criteria with you.

If you qualify for the study, you will be asked to come to the VCU School of Pharmacy twice over the course of one or two weeks. Each study subject will be reimbursed for their time and travel costs.

For your participation or any further information, please contact
Renish Delvadia
VCU Dept. of Pharmaceutics
(804)-615-7332 or (804)-828-6102
delvadiar@vcu.edu

06/01/2011

BVT / SH / 6/27/11
APPROVED

Page 1 of 1

H.5 HIPPA CONSENT FORM

VCU Medical Center
Authorization For Use And Disclosure Of
Patient Health Information In Research

IRB Protocol #: _____ Study Name: **ASSESSMENT OF INSPIRATORY PROFILES THROUGH AIRFLOW RESISTANCES THAT MIMIC INHALERS**

Principal Investigator: **Byron Peter R.**

Research Subject/Participant Information

Printed Name: _____ Date of Birth: _____

Telephone #: _____

You have been given a consent form that tells you about this Research Study, and any activities or procedures that are part of the study. This form tells you what information about you may be used and given out in the study and who may give and receive the information. **By signing this form, you agree that the health information that identifies you may be used and disclosed as needed for this research.** The Health Insurance Portability and Accountability Act of 1996 (HIPAA) provides for the protection of your health information from unauthorized use or disclosure.

Authority to Request Protected Health Information

The following people and/or groups may request the subject's (as named above) Protected Health Information:
1) Principal Investigator and Research Staff 2) Study Sponsor 3) Research Collaborators 4) Institutional Review Boards 5) Data Safety Monitoring Boards 6) Government/Health Agencies 7) Others as Required by Law

Authority to Release Protected Health Information

The VCU Medical Center (VCUMC) may release the information identified in this authorization from the medical records of the research participant named above and provide this information to: 1) Health Care Providers at the VCUMC 2) Principal Investigator and Research Staff 3) Study Sponsor 4) Research Collaborators 5) Data Coordinators 6) Institutional Review Boards 7) Data Safety Monitoring Boards 8) Government/Health Agencies 9) Others as Required by Law

Please check type of information to be released (This section to be filled-out by the Primary Investigator)

<input type="checkbox"/> Complete health record	<input type="checkbox"/> Diagnosis & treatment codes	<input type="checkbox"/> Discharge summary
<input type="checkbox"/> History and physical exam	<input type="checkbox"/> Consultation reports	<input type="checkbox"/> Progress notes
<input type="checkbox"/> Laboratory test results	<input type="checkbox"/> X-ray reports	<input type="checkbox"/> X-ray films / images
<input type="checkbox"/> Photographs, videotapes	<input type="checkbox"/> Complete billing record	<input type="checkbox"/> Itemized bill

Other, (specify) – De-identified Spirometric data

Uses of Your Protected Health Information (This section to be filled out by the Principal Investigator)

Your health information as shown above will be used: (Check all that apply)

- To determine if you meet the requirements to be a subject
 To meet the Research Requirements For Safety Monitoring For Regulatory Issues

Other _____

Expiration of This Authorization (This section to be filled out by the Principal Investigator)

This authorization will expire when the Research Study is closed, or there is no need to review, analyze and consider the data generated by the research project, whichever is later.

This Research Study involves the use of a Data or Tissue Repository (bank) and will never expire.

Other _____

Right to Revoke Authorization and Re-disclosure

You may change your mind and revoke (take back) this Authorization at any time. Even if you revoke this Authorization the researchers at the VCUMC may still use or disclose health information they have already obtained about the Research

Participant/Subject as necessary to maintain the integrity or reliability of the current research. If you revoke this Authorization you may no longer be allowed to participate in the Research Study. To revoke this Authorization, you must write to the Principal Investigator named above or in the Informed Consent document.

I understand the information disclosed by this authorization may be subject to redisclosure by the recipient and no longer be protected by the Health Insurance Portability and Accountability Act of 1996.

Signature of Research Subject or Personal Representative

I understand that I do not have to sign this authorization, but if I do not, the above named research subject/participant may not be able to be in the research study. The VCUMC may not condition (withhold or refuse) treating the above named research subject/participant if you choose not to sign this Authorization. I can inspect, and in some cases copy, the Protected Health Information to be used or disclosed.

Signature: _____ Date: _____

A COPY OF THIS AUTHORIZATION IS TO BE GIVEN TO THE PERSON SIGNING

2
(This Form May Be Printed On Both Sides)

H.6 RESEARCH PLAN

VCU RESEARCH PLAN TEMPLATE

Use of this template is required to provide your VCU Research Plan to the IRB. Your responses should be written in terms for the non-scientist to understand. If a detailed research protocol (e.g., sponsor's protocol) exists, you may reference that protocol. **NOTE: If that protocol does not address all of the issues outlined in each Section Heading, you must address the remaining issues in this Plan. It is NOT acceptable to reference a research funding proposal.**

ALL Sections of the Human Subjects Instructions must be completed with the exception of the Section entitled "Special Consent Provisions." Complete that Section if applicable. When other Sections are not applicable, list the Section Heading and indicate "N/A."

NOTE: The Research Plan is required with ALL Expedited and Full review submissions and MUST follow the template, and include version number or date, and page numbers.

DO NOT DELETE SECTION HEADINGS OR THE INSTRUCTIONS.

I. TITLE

ASSESSMENT OF INSPIRATORY PROFILES THROUGH AIRFLOW RESISTANCES THAT MIMIC INHALERS

II. RESEARCH PERSONNEL

A. In the table below (add additional rows as needed), indicate: (1) all project personnel**

including the principal investigator and individuals from other institutions, (2) their qualifications, and (3) a brief description of their role or responsibilities on the study.

**** Personnel list should include anyone engaged in the research (VCU & non-VCU personnel) including independent investigators. Engaged means interacting or intervening with research participants and/or having access to identifiable private information about participants. See OHRP's guidance on "Engagement of Institutions in Research" at <http://www.hhs.gov/ohrp/humansubjects/guidance/engage08.html>.**

NAME OF INDIVIDUAL	INSTITUTION	QUALIFICATIONS	RESPONSIBILITIES
Peter Byron	VCU, Pharmaceuticals	PhD; Professor	Principal Investigator: Study supervisor, study coordination, data analysis, study reporting
Renishkumar	VCU,	M.Pharm; PhD candidate	Graduate Student

Delvadia	Pharmaceutics		Investigator: Consent process, recruitment, data collection and analysis
John Clore	VCU	MD; Professor	Medical Investigator: Medical monitor, patient safety

NOTE: If an independent investigator is “engaged,” and the research involves a DIRECT FEDERAL award made to VCU (or application for such), the independent investigator must sign a formal written agreement with VCU certifying terms for the protection of human subjects. For an agreement to be approved: (1) the PI must directly supervise all of the research activities, (2) agreement must follow the ORSP template, (3) IRB must agree to the involvement of the independent investigator, AND (4) agreement must be in effect prior to final IRB approval.

B. Describe the process that you will use to ensure that all persons assisting with the research are adequately informed about the protocol and their research-related duties and functions.

PETER BYRON, THE PI WILL PERSONALLY SUPERVISE RENISHKUMAR DELVADIA, THE GRADUATE STUDENT INVESTIGATOR. WE WILL ESTABLISH THE PATIENT REGISTRY TOGETHER AND ENSURE ITS SECURE STORAGE. ONLY THE PI AND GRADUATE STUDENT INVESTIGATOR WILL BE ALLOWED ACCESS TO IDENTIFIABLE INFORMATION.

III. CONFLICT OF INTEREST

Describe how the principal investigator and sub/co-investigators might benefit from the subject’s participation in this project or completion of the project in general. Do not describe (1) academic recognition such as publications or (2) grant or contract based support of VCU salary commensurate with the professional effort required for the conduct of the project

No conflicts of interest for the investigators have been identified related to this study.

IV. RESOURCES

Briefly describe the resources committed to this project including: (1) time available to conduct and complete the research, (2) facilities where you will conduct the research, (3) availability of medical or psychological resources that participants might require as a consequence of the research (if applicable), and (4) financial support.

- 1. THE STUDENT INVESTIGATOR WILL WORK FULL TIME ON THIS RESEARCH STUDY. THE PRINCIPAL INVESTIGATOR WILL SUPERVISE ALL RESEARCH ACTIVITIES. THE MEDICAL MONITOR WILL SUPERVISE PATIENT SAFETY RELATED TO THIS RESEARCH STUDY.**
- 2. THIS RESEARCH WILL BE CONDUCTED AT THE VCU AEROSOL RESEARCH LABORATORY AT THE VCU SCHOOL OF PHARMACY.**
- 3. THIS RESEARCH IS FUNDED IN PART BY UNRESTRICTED GIFTS HELD IN THE MEDICAL COLLEGE OF VIRGINIA FOUNDATION TO SUPPORT THE RESEARCH OF THE PRINCIPAL INVESTIGATOR.**

V. HYPOTHESIS

Briefly state the problem, background, importance of the research, and goals of the proposed project.

Literature suggests that pulmonary deposition from dry powder inhalers (DPIs) greatly depends upon the way patients inhale through them, primarily because DPIs use the patient's inhalation as an energy source to produce the aerosol cloud. Because of this, it is essential that we characterize the way that patients inhale through these devices.

It is hypothesized that different inhalation profiles (inhalation flow rate versus time curves) result from different forms of patient training. Furthermore, significant inter-subject variability in these profiles should exist that can, under some circumstances, depend on the design of different inhalation devices; this is because DPIs have different airflow resistances. We also hypothesize that the spread of flow rate versus time profiles for inhalation can be collected using a drug-free inhalation flow cell (section VIII). Finally, these profiles can be analyzed from a group of human subjects and used to define a mean and statistical range of inhalation flow rate versus time curves.

VI. SPECIFIC AIMS

THE GOAL OF THIS STUDY IS TO COLLECT PERTINENT INFORMATION (SAMPLE MEAN AND 95% CI) TO DOCUMENT THE RANGE OF INHALATION FLOW RATE VERSUS TIME PROFILES SEEN IN NORMAL SUBJECTS. SPECIFICALLY, WE WILL COLLECT PILOT DATA FROM 20 VOLUNTEERS WITHOUT LUNG DISEASE AND USE THE DATA TO:

- 5. DOCUMENT THE INHALATION FLOW RATE VERSUS TIME CURVES FOR ADULTS INHALING THROUGH DIFFERENT AIRFLOW RESISTANCES (USING THE INHALATION FLOW CELL SHOWN IN FIGURE 1).**

6. COMPARE THE PROFILES IN THE SAME SUBJECTS BEFORE AND AFTER HAVING RECEIVED BOTH WRITTEN AND PRACTICAL TRAINING IN THE INHALATION TECHNIQUES MOST COMMONLY ADVISED WITH DPIS.
7. DOCUMENT THE INTRA- AND INTER- SUBJECT VARIATIONS IN FLOW RATE VS. TIME WHEN SPECIFIC AIRFLOW RESISTANCES ARE EMPLOYED AND ATTEMPT TO RELATE THESE TO SUBJECT DEMOGRAPHICS (E.G. AGE, BODY WEIGHT, HEIGHT AND GENDER)
8. PROPOSE REPRESENTATIVE INHALATION PROFILES FOR FUTURE USE IN *IN VITRO* INHALER TEST METHODS THAT ARE PRESENTLY IN DEVELOPMENT

VII. BACKGROUND AND SIGNIFICANCE

Include information regarding pre-clinical and early human studies. Attach appropriate citations.

Following the launch of the pressurized metered dose inhaler (pMDI) in the 1950s, research and aerosol drug delivery via the lung has expanded. With chlorofluorocarbon (CFC) propellant replacement, DPIS have now become mainstay treatments for pulmonary disease [1] and it is well known that their performance depends on the way that patients use them. While this can be influenced by instruction leaflets, training and lung function, the design of DPIS is still in the rudimentary phase. In large part, this is because of poor *in vitro* performance testing that fails to concern itself with the way that patients actually inhale through each device. Reports that “> 94% of patients fail to use DPIS correctly” are common, indeed, failure to exhale before inhalation, failure to inhale rapidly and deeply and incorrect mouthpiece positioning [2] may all have a significant influence on regional drug deposition and clinical outcome. At this stage it is imperative that we document and characterize the inhalation profiles commonly used by healthy volunteers before and after training them in the use of DPIS. This study will enable us to assess likely inter-subject variability in the inhalation profiles of adults while using DPIS. It will also enable us to understand if a formal training helps in improving inhalation technique. Moreover, by linking the recorded profiles to an *in vitro* method under development (Section VIII.3), it should be possible to predict the *in vivo* regional aerosol drug deposition from DPIS [3]. Once validated, such an *in vitro* method can be extended to study the drug deposition from different inhalers in different patient subsets.

VIII. PRELIMINARY PROGRESS/DATA REPORT

If available.

1. Measurement of airflow resistances of different marketed DPIs

Airflow resistances of different marketed DPIs were measured. Each DPI was attached to a breath simulator (ASL 5000, IngMar, Pittsburgh, PA), and air withdrawn at different steady volumetric flowrates (Q) from the mouthpiece. Corresponding pressure drop across the inhaler (ΔP) was measured using a pressure-tapping in the breath simulator. A linear regression plot of $\Delta P^{0.5}$ vs. Q was constructed, and airflow resistance was estimated as the slope of the regression line. Table 1 depicts measured airflow resistances of DPIs. As can be seen, commercial DPIs show a wide range of airflow resistances. Because of this, it is likely that the to-be-measured flow profiles will be a function of airflow resistance.

Table 1 Measured airflow resistance marketed DPIs

Device	Measured airflow resistance (Pa ^{0.5} .L ⁻¹ . min)
Foradil [®] Aerolizer [®]	0.56
Relenza [®] Diskhaler [®]	0.63
Budelin [®] Novolizer [®]	0.76
Pulmocort [®] Turbuhaler [®]	1.11
Easyhaler [®]	1.38
Spiriva [®] Handihaler [®]	1.48
Pulvinal [®]	1.54

2. Inhalation flow cell

A drug-free inhalation flow cell with variable airflow resistance was constructed as shown in Figure 1. The purpose of this cell is to record the air flow rate vs. time profiles of volunteers inhaling through the mouthpiece at various airflow resistances. The resistances correspond to those of typical powder inhalers (Table 1). Upon inhalation through the mouthpiece, air moves through the mass flowmeter (Mass Flow Meter EM1, Sensirion Inc., CA, USA) and a resistance tube (a circular channel with different diameters), a low resistance microbial air-filter and a disposable mouthpiece. The flow rate vs. time profile can be recorded for each inhalation digitally (SensiViewer, Sensirion Inc., CA, USA) on a computer.

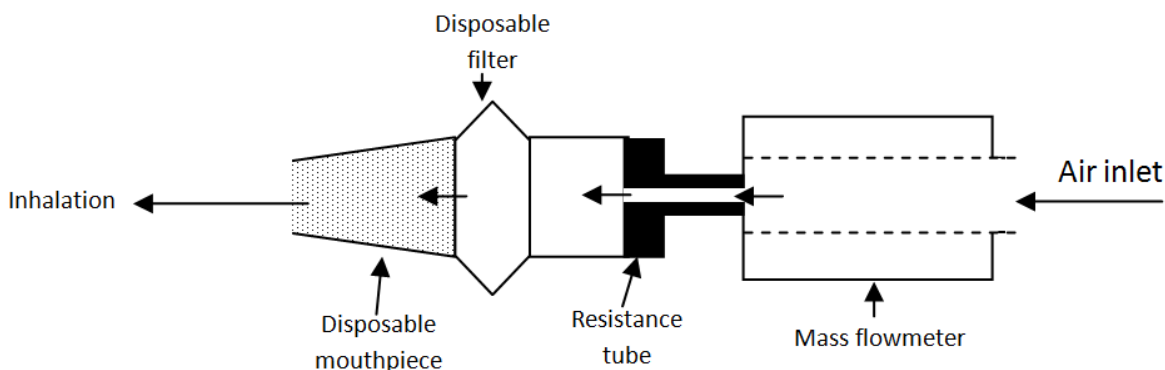


Figure 1 – Inhalation flow cell

The resistance tubes are fabricated with different diameters for insertion in the inhalation flow cell to generate different airflow resistances across the cell in such a way that they produce total airflow resistances comparable to those observed for different marketed DPIs listed in Table 1.

3. *In vitro* method to predict regional drug deposition from DPIs

Realistic inhalation maneuvers collected in the proposed study will be used to predict regional drug deposition from DPIs in a newly developed *in vitro* test methods. This is described briefly below:

A geometrically realistic physical lung model of the mouth throat (MT) and upper 3 generations of conducting airways (TB) has been constructed and installed in an airtight housing (Figure 2). During each inhalation cycle, air is withdrawn by a breath simulator at varying rate and volume through the inhaler connected to the MT and airway model via the low resistance filter. By coating the internal surfaces of the MT and TB regions with a glycerol-methanol (1:2) mixture, powder aerosol can be collected following collision with the walls during each simulated inhalation maneuvers. After each inhalation, drug deposited in the inhaler mouthpiece, MT and TB regions of the MT-TB model, and the Plexiglas® housing and filter can be recovered and analyzed.

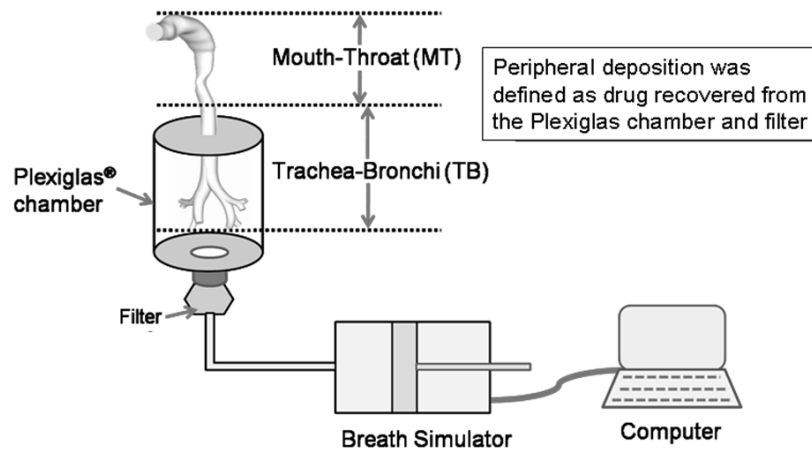


Figure 2 – *In vitro* experimental set up

In preliminary studies using computer generated inhalation profiles, we have demonstrated the functional capability of the *in vitro* model by showing the expected change in regional deposition pattern as a function of variations in inhalation maneuver [3]. The collection of realistic patient inhalation maneuvers with DPIs is the next logical step if *in vitro-in vivo* correlations (IVIVCs) are ultimately to be realized using this new *in vitro* method.

IX. RESEARCH METHOD AND DESIGN

Include a brief description of the project design including the setting in which the research will be conducted and procedures. If applicable, include a description of procedures being performed already for diagnostic or treatment purposes.

This protocol is designed to document the inhalation profiles commonly used by healthy volunteers who are 1) trained in DPI use solely by reading a typical package insert, and 2) formally trained in DPI use by a health professional such as a pharmacist. The objective is to collect a range of typical flow rate versus time profiles for subjects inhaling through different airflow resistances designed to mimic those seen in DPIs. To collect the needed information, however, subjects will not be exposed to any drug; rather we will collect data to show the likely inter-subject variability in the inhalation profiles of adults inhaling through different airflow resistances representative of the DPIs in Table 1. The ultimate goal of using these profiles is to simulate DPI performance *in vitro* that is predictive of their *in vivo* lung delivery

1. Study Design:

Twenty study subjects will be recruited from the general Richmond population through advertisements. Subjects must be able to come to Aerosol Research Laboratory (ARL) to participate in the study although an initial telephone interview will be conducted to determine eligibility to participate (See Appendix A) If the subject appears to qualify for the study, they will be invited to the ARL for a screening visit to be followed up by a second visit for inhalation profile collection.

On the first visit, potentially eligible subjects will be informed about the study. If they are willing to participate, formal consent will be obtained after all questions have been asked and answered. Each volunteer will be asked to provide demographic data, age, gender and health information such as medical and smoking history, medication history and present medications. Vital health measurements (blood pressure, pulse rate), height and weight measurements will be taken. An initial spirometric screen will be used to ensure normal pulmonary function (FEV1 >predicted Lower Limit of Normal (LLN); [4]).

If deemed eligible by the Medical Monitor, the subjects will be invited to participate in the second phase of the study. On the second visit, inhalation profiles will be collected from healthy male (n=10) and female (n=10) adults. Approximately 20 inhalation profiles will be collected from each eligible subject.

2. Study Population

Twenty eligible subjects will be enrolled in this pilot study (between 18 and 65 years old). Subjects will be eligible for inclusion in the study if they conform to the following criteria:

- a. Must be healthy as determined by a health questionnaire (Appendix A)
- b. Must not be currently pregnant (self reported)
- c. Must not have symptoms of an obstructive or restrictive lung disease or be suffering from allergies or congestion at the time of testing
- d. Must have FEV1 >LLN predicted
- e. Must be medically stable with no evidence of acute medical or psychiatric illness,
- f. Must have never used or been trained to use a DPI,

- g. Must not be currently using any inhaler, nasal spray or drug known to affect lung function, Bronchodilators and decongestants in any form are excluded
- h. Must be at least 4 feet 10 inch tall,
- i. Must weigh at least 110 pounds (50 kg) and be no more than 264 pounds (120kg)
- j. Must not currently, or in the past year, have used tobacco products

3. Collection of inhalation profiles

Inhalation flowrate vs. time profiles of each eligible volunteer inhaling through an inhalation flow cell will be recorded after the following instructions are provided in sequence.

Instruction A - Written instructions that represent typical patient leaflet directions for how to inhale when using the DPIs in Table 1 (Appendix B). Volunteers will be given a set of written instructions to read like those supplied with DPIs. After reading them they will be asked to inhale accordingly through the inhalation flow cell (as if they are using a powder inhaler and believing they are conforming to the instructions). Profiles will be recorded for each of six different resistance tubes placed in the inhalation flow cell in random order. The results from these experiments will provide information on the type and range of inspiratory maneuvers to be expected when subjects are not formally trained in the use of DPIs.

Instruction B – Verbal instructions and a practical demonstration of how to use a powder inhaler correctly in accord with literature guidelines [5]. Following training, volunteers will be asked to inhale through the inhalation flow cell in accord with the training provided earlier. Profiles will be recorded for each of six different resistance tubes placed in the inhalation flow cell in random order. Each experiment will be repeated once and data for flowrate vs. time averaged for each subject and each resistance. The results from these experiments will be used directly to define the types and range of inspiratory maneuvers used by normal volunteers.

X. PLAN FOR CONTROL OF INVESTIGATIONAL DRUGS, BIOLOGICS, AND DEVICES.

Investigational drugs and biologics: IF Investigational Drug Pharmacy Service (IDS) is not being used, attach the IDS confirmation of receipt of the management plan.

Investigational and humanitarian use devices (HUDs): Describe your plans for the control of investigational devices and HUDs including:

- (1) how you will maintain records of the product’s delivery to the trial site, the inventory at the site, the use by each subject, and the return to the sponsor or alternative disposition of unused product(s);**
- (2) plan for storing the investigational product(s)/ HUD as specified by the sponsor (if any) and in accordance with applicable regulatory requirements;**
- (3) plan for ensuring that the investigational product(s)/HUDs are used only in accordance with the approved protocol; and**
- (4) how you will ensure that each subject understands the correct use of the investigational product(s)/HUDs (if applicable) and check that each subject is following the instructions properly**

(on an ongoing basis).

N/A. NO DRUGS, BIOLOGICS, AND DEVICES WILL BE USED IN THIS STUDY.

XI. DATA ANALYSIS PLAN

For investigator-initiated studies.

1. Individual profiles and the averages based on statistical analysis (below) will be analyzed in order to determine commonly used primary and secondary inhalation parameters as follows:

- Primary parameters
 - a) PIFR - Maximum volumetric flowrate value recorded in the recorded inhalation profile
 - b) V - Area under the curve of the inhalation profile,
 - c) T_{PIFR} - Time required to reach PIFR from the start of inhalation maneuver, T_{PIFR} ;
 - d) T_{total} - Total inhalation time
- Secondary parameters
 - a) Flow acceleration rate, FAR – $(PIFR/T_{PIFR})$
 - b) Mean inhalation flow rate, MIFR – (V/T_{total})
- % Change in the inhalation parameter after training will be calculated as below

$$\% \text{ Change} = \frac{\text{Inhalation parameter (after training)} - \text{Inhalation parameter (before training)}}{\text{Inhalation parameter (before training)}} \times 100$$

These analyses will enable profiles to be described in accord with terms used conventionally in pulmonology and in order to assist with manuscript preparation for academic journals

2. Selection of representative profiles for use in *in vitro* validation experiments

While representative inhalation profiles for volunteers and patients with different

demographics will ultimately be sought, this study is concerned with collection of data from normal volunteers only. After a statistical assessment of all the recorded profiles specific for each instruction and airflow resistance has been performed, three average inspiratory profiles will be generated for each resistance and instruction mode to represent the sample mean +/- 95% CI flowrate versus time curves for all normal volunteers.

XII. DATA AND SAFETY MONITORING

- **If the research involves greater than minimal risk and there is no provision made for data and safety monitoring by any sponsor, include a data and safety-monitoring plan that is suitable for the level of risk to be faced by subjects and the nature of the research involved.**
- **If the research involves greater than minimal risk, and there is a provision made for data and safety monitoring by any sponsor, describe the sponsor's plan.**
- **If you are serving as a Sponsor-Investigator, identify the Contract Research Organization (CRO) that you will be using and describe the provisions made for data and safety monitoring by the CRO. Guidance on additional requirements for Sponsor-Investigators is available at <http://www.research.vcu.edu/irb/wpp/flash/X-2.htm>**

The PI and Medical Monitor will be responsible for ensuring that inclusion/exclusion criteria and the protocol are adhered to; the PI will be responsible that all necessary reports to the IRB are submitted in a timely manner. Due to the absence of any drug exposure during this study, adverse events are extremely unlikely. Nevertheless, any unanticipated adverse events will be reported to the VCU IRB as required.

The inhalation profiles collected in this study will be stored as part of a human subjects' registry. Only those individuals directly involved with this research and named in this research synopsis will have access to the profiles, except where required by law. The PI will be responsible for the integrity of the registry as well as granting access to the registry.

XIII. MULTI-CENTER STUDIES

If VCU is the lead site in a multi-center project or the VCU PI is the lead investigator in a multi-center project, describe the plan for management of information that may be relevant to the protection of subjects, such as reporting of unexpected problems, project modifications, and interim results.

WRITTEN INSTRUCTIONS

AEROSOL RESEARCH LABORATORY, DEPT OF PHARMACEUTICS, VIRGINIA

COMMONWEALTH UNIVERSITY, RICHMOND VA 23298-0533

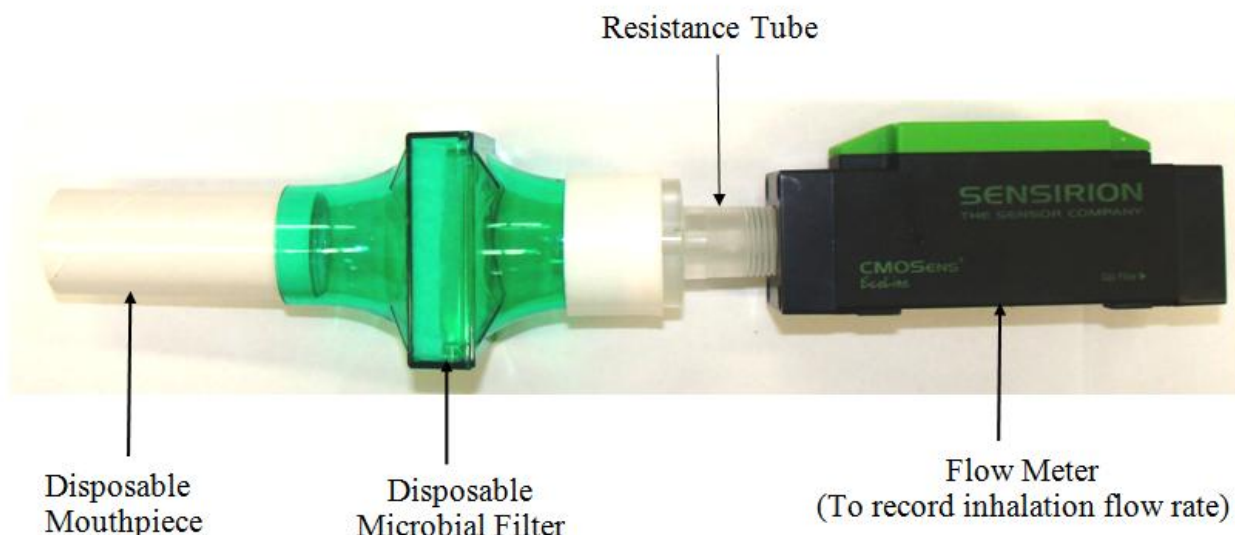
STUDY ID#

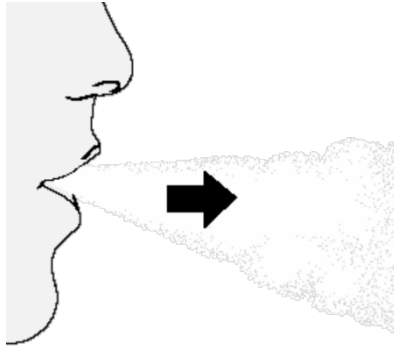
In this part of the study, we will determine how patients who receive a new inhaler, supplied only with written instructions, begin to use it. We would like you to inhale through the inhalation flow cell (IFC) shown below, as if it is an inhaler and you are the patient who will use it. You will not receive any drug during this procedure.

Please read these instructions carefully, and do your best to interpret them by yourself. Once you have read them, indicate to the investigator that you are ready to begin.

Look at the picture of the inhalation flow cell below. When you inhale through its mouthpiece, the cell will record the way in which you inhale. The instructions numbered **Step 1 – 4** below are taken from leaflets given to patients, to tell them how to use their inhalers. You should do your best to try to follow steps 1 to 4 when inhaling through the inhalation flow cell.

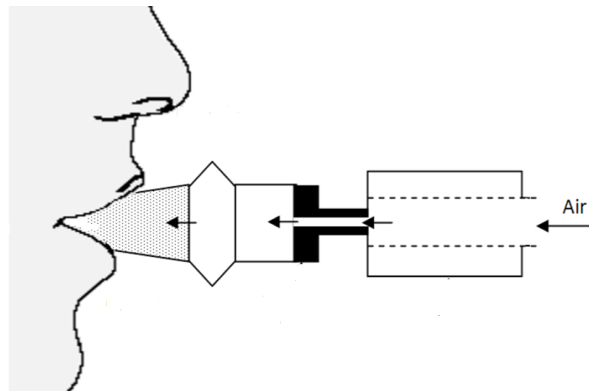
Inhalation Flow Cell (IFC)





Step 1

Breathe out completely. Do not breathe (exhale) into the mouthpiece of the Inhalation Flow cell (**IFC**) device.



Step 2

Hold the **Inhalation Flow Cell** and raise it to your mouth. Close your lips tightly around the mouthpiece. Keep your head **upright** and the device in a horizontal position.

Step 3

Breathe in **as quickly and as deeply** as you can

Step 4

Hold your breath for as long as you comfortably can while taking the IFC device out of your mouth. Then breathe normally

Ask the Study Monitor if you have questions. If you feel discomfort, tell the Study Monitor immediately.

VITA

Renishkumar Delvadia was born on June 12, 1982 in Gujarat, India and is Indian citizen. He received bachelor's degree in Pharmacy in 2003 and followed by Master's degree in Pharmaceutics and Pharmaceutical Technology from Gujarat University, India. After graduating in 2005, Renish worked as a research assistant for the division of inhaler formulation and device development, Sun Pharmaceuticals, for 2 years prior to coming to VCU. Renish joined Ph.D. program in Department of Pharmaceutics, Virginia Commonwealth University in Spring 2008. His multi-disciplinary research used pharmaceutical, engineering and clinical approaches. His progress in his research project resulted in four full papers (one published, two under review and one in preparation), three extended poster abstracts, two short abstracts, one of which was selected to receive an AAPS travel award for the annual meeting. He was also awarded a John Wood Award by the Department of Pharmaceutics in 2011 for his PhD work. Renish completed CITI based training for conducting biomedical and social/behavioral research on human subjects. He successfully completed and also passed the NIOSH certified training course for Spirometry. Renish also served as a Graduate Teaching Assistant for several Pharm. D. courses and one graduate course for 3 years. Renish is serving as an AAPS abstract reviewer since 2009. He also served as secretary/treasurer and webmaster for AAPS student chapter and School of Pharmacy Graduate Student Association.